METABOLIC CHANGES IN CELLULAR COMPONENTS OF THE VASCULATURE – EXAMINING THE LINK BETWEEN DIABETES AND CANCER

By

Adam Giebink

A DISSERTATION

Submitted to
Michigan State University
in partial fulfillment of the requirements
for the degree of

DOCTOR OF PHILOSOPHY

Chemistry

2012

ABSTRACT

METABOLIC CHANGES IN CELLULAR COMPONENTS OF THE VASCULATURE – EXAMINING THE LINK BETWEEN DIABETES AND CANCER

By

Adam Giebink

Currently, cancer and diabetes are two of the more devastating diseases worldwide, both in the number of people affected as well as the financial cost it takes to treat those with said conditions. While these two diseases are significantly different in their pathologies and physiological impacts, they both have characteristics of altered mechanisms by which they metabolize glucose when compared to healthy individuals. In fact, there is an increased risk that has been identified for people with diabetes to develop certain types of cancer. Motivated by the finding observed 90 years ago by Otto Warburg regarding the 'aerobic glycolytic' conditions exhibited by cancer cells and a study indicating a risk of developing cancer in non-obese persons with elevated fasting glucose levels, the presented work examines how the glucose metabolism of healthy cells is altered following exposure to biomolecules that are elevated in diabetes, drugs for the treatment of diabetes, and elevated glucose levels. The altered metabolism can then be compared to that of cancerous cells.

First, certain metabolic alterations in cultured bovine pulmonary artery endothelial cells following treatment with metal-activated C-peptide were monitored using liquid scintillation, platereader, and microfluidic techniques. As recent reports from the Spence group have identified C-peptide as a stimulator of glucose uptake and adenosine triphosphate (ATP) release from the red blood cell (RBC), similar *in vitro* experiments were performed on the endothelial cells lining the inner walls of the vasculature. Results indicate that C-peptide not only has a similar influence on the glucose uptake in endothelial cells as it does on the RBCs, but also

stimulates the production of a significant vasodilator in endothelial nitric oxide (NO) by a RBC mediated mechanism.

C-peptide is then administered to the RBCs and endothelial cells in the presence of the type 2 diabetes drug, metformin. The metabolism of the two cell types is monitored by measuring the glucose uptake and lactate release. The studies provide a hypothesis behind metformin's action by increasing the interaction of C-peptide with the RBCs while also increasing glucose uptake. In the endothelial cells, metformin alone causes a similar increase in glucose uptake. However, this uptake increase in both cell types results in the production of elevated levels of lactate, especially in hyperglycemic conditions, which can potentially lead to lactic acidosis. This increased lactate production from the endothelial cells following metformin administration led to an overall decrease in the intracellular pH hypothesized to be caused from the release of lactate from the cell through the monocarboxylate transporter (MCT1).

Lastly, the metabolic changes that occur in healthy endothelial cells in normal and elevated glucose environments are compared to those same changes in cancerous HeLa cells. The endothelial cells had an increased lactate release when they were incubated in the hyperglycemic buffers while the HeLa cells' metabolism remained relatively constant. This suggests a change in the healthy cells' metabolism depending on the sources of energy, namely glucose and pyruvate, available to it while the cancer cells' metabolism remains the same in any condition.

This research demonstrates some of the factors that alter the metabolism of normal, healthy cells. While the findings do not show that high glucose causes cancer directly, it does show that the metabolism can be altered by changes brought about by hyperglycemia, sometimes resembling many metabolic characteristics observed in cancer cells.

ACKNOWLEDGMENTS

I would fist like to acknowledge my High School Science teacher, Mrs. Karen Hammond, as one of the more influential figures I had in deciding to pursue a career in Chemistry. The dedication and devotion she put into our education to make sure we learned the material, coupled with the passion that she exhibited each and every class period, really motivated me to put everything I had into my education and science career and to not accept anything less than my best.

I want to express my appreciation for those responsible in stimulating my interest to pursue graduate level research, specifically Dr. Philip Whitefield and Dr. Nuran Ercal of the Chemistry Department at Missouri University of Science and Technology. These two academic mentors allowed me the opportunity to experience graduate research first hand under the supervision of established graduate students. Additionally, I want to thank the numerous faculty members in the Chemistry Department at the University of Missouri – Columbia who prepared me for my career after college, as well as encouraged, supported, and aided in my decision to attend graduate school at Michigan State University. Without the experience and guidance obtained from those individuals, I would not be where I am today.

I owe a significant amount of gratitude to my research advisor, Dr. Dana Spence, for his constant encouragement and dedication during my four and a half years at Michigan State. His confidence allowed me the freedom to work independently, while at the same time consistently challenging and motivating my drive to succeed. I have no doubt that his contributions to the field will one day change the way we view and treat many serious and devastating biological issues. To the Spence group lab members whom I have worked with, both past and present, I

want to thank each and every one for making my research experience here all the more enjoyable. I could not have asked for a better group atmosphere where everyone is more than willing to assist and support one another. I feel that the acquaintances that I made, particularly my colleagues John, Matt, and Steve who entered the Chemistry program at the same time I did, have turned into friendships that I hope will continue long after our time at Michigan State.

Finally, I want to each and every one of my family members who have encouraged me during all of the difficult endeavors in my life. Their constant encouragement during my pursuit of an advanced degree made pushing through the challenging times more manageable with the knowledge that I was supported by so many who care for me. Lastly, I want to express my gratitude and undying love to my wife Patty, who has been with me long before I decided to attend graduate school. You were the motivation that I called upon having witnessed your commitment and determination during your similar academic pursuit. I will never be able to completely express my appreciation for your love and patience exhibited each and every day. You are the most important person in my life and I feel blessed to share this experience with you at my side.

TABLE OF CONTENTS

LIST OF FIGURES

CHAPTER 1: INTRODUCTION

1.1 Introduction

Carbohydrate metabolism, more specifically glucose metabolism, refers to the processes by which glucose is transported into the cell and ultimately broken down into smaller molecules, such as pyruvate, while generating adenosine triphosphate (ATP), which is the primary energy molecule in living organisms. Abnormalities of this metabolism have been shown to be associated with many different diseases and conditions such as multiple sclerosis,[1, 2] cystic fibrosis,[3, 4] lactose intolerance[5] and galactosemia.[6] While the conditions mentioned have their unique pathologies and can result in death, there are two other diseases that have a larger impact throughout the world today.

Cancer (malignant) and diabetes are two of the more significant diseases worldwide. By definition, cancer refers to the large class of diseases where cells exhibit uncontrolled growth and reproduction. These cells have the ability to spread to surrounding tissue resulting in severe damage and even death. They are also able to spread (metastasize) to other locations throughout the body. Diabetes refers to the group of diseases where the basal blood sugar (glucose) levels are consistently uncontrolled. These glucose levels can be either high or low and have serious consequences on biological functions. While these two conditions have different biological behaviors, cancer and diabetes share the similarity of abnormal glucose metabolism and are two of the more deadly and devastating medical conditions/diseases in the world today.

According to the World Health Organization, in the year 2008, there were nearly 13 million newly diagnosed cases of cancer. In that same year, cancer was responsible for nearly 8

million deaths worldwide. This number accounts for roughly 13% of all deaths in that year. In the United States alone in 2010, it was estimated by the American Cancer Society that there were over 500,000 deaths caused by cancer, accounting for about 25% of the total deaths that year.[7] These numbers are associated with over 1.5 million newly diagnosed cases in the United States in that same year.

Similar numbers are observed for diabetes fatalities. The International Diabetes Federation estimated that in the year 2010, there were nearly 300 million adults, or about 7% of the global adult population who have diabetes. There were over 4 million deaths worldwide in 2010 that were caused by, or associated with diabetes. This accounts for slightly under 7% of the total fatalities. In the United States, diabetes accounted for over 100,000 deaths in 2010 or approximately 16% of the total fatalities reported.

In addition to the high number of persons affected by the two diseases, the cost required to treat these conditions is rising. The National Cancer Institute determined the cost of cancer care in the United States for the year 2010 to be 125 billion dollars. This number is inflated to 300 billion when considering global cancer treatment. The cost to treat diabetes is slightly higher on both levels. According to the American Diabetes Association, in the United States it cost roughly 175 billion dollars in 2007 for diabetes care. Globally, the cost rises to over 400 billion dollars in 2010 to treat diabetes.

While these two conditions are both very expensive to treat and have harmful and devastating effects, they are significantly different diseases in how they operate and behave metabolically. Both cancer and diabetes have different metabolic properties that cause their harmful effects. These distinct properties result in conditions that are difficult and challenging to treat and control. While they are two very different diseases, there are some metabolic

similarities between cancer and diabetes that can be evaluated using different analytical techniques. The research presented aims to examine how the glucose metabolism in healthy cells found in the vasculature is affected upon administration of molecules and drugs that are relevant to diabetes. These changes in the metabolism can then be compared with the altered metabolism already present in cancerous cells. The studies hopefully will further the understanding between the correlation/link that exists between cancer and diabetes.

1.2 A brief introduction to general cancer metabolism, treatments, and causes

As mentioned earlier, cancer is defined as an uncontrolled growth of cells within a living body. It has recently been described that nearly all forms of malignant cancer exhibit specific traits, or 'hallmarks'. In no particular order, those characteristics are; self-sufficiency in growth signals, insensitivity to anti-growth signals, tissue invasion and metastasis, limitless replicative potential, sustained angiogenesis, and evading apoptosis.[8] In short, cancer cells need to provide themselves with the nutrients required for limitless cell growth while ignoring any signals that may cease their growth or initiate programmed cell death (apoptosis). All of these cells require energy to perform and carry on each and every one of these listed hallmarks. The source of this energy is coming from an altering, or a reprogramming, of how these cells obtain and metabolize glucose. It is this reprogramming that might precede all of the aforementioned characteristics of cancer.[9]

1.2.1 General cancer metabolism

In most normal/healthy cells, the 6-carbon molecule glucose enters the intracellular matrix and is converted into two 3-carbon pyruvate molecules through a multistep pathway known as glycolysis (Figure 1.1). This pyruvate can then be transported into the mitochondria where it undergoes the aerobic process oxidative phorphorylation (Krebs Cycle, Citric Acid Cycle), ultimately generating approximately 38 molecules of ATP, the energy source for all cells, from each glucose molecule.[10, 11] In cancerous cells, this metabolism produces the majority of the energy needed through elevated glycolysis levels while bypassing the oxidative phorphorylation.[12] It is not the increased glycolytic rates that are unique to the glucose metabolism of cancer cells, but rather that the cells undergo higher rates of anaerobic glycolysis even in the presence of oxygen.[13, 14]

The relationship between aerobic (oxidative phosphorylation) and anaerobic (glycolysis) respiration (Figure 1.2) has been understood since the 1850s when Louis Pasteur observed changes in yeast metabolism upon aerobic and anaerobic conditions.[15] When higher oxygen levels were present, there was an increase in oxidative phosphorylation and a decrease in the rate of glycolysis. When oxygen levels were reduced, there was an increase in the glycolytic rate that was accompanied by an increase in glucose consumption.[16, 17] A similar finding was discovered in the 1920s by the German biochemist Otto Warburg. He discovered that even in 'oxygen rich' environments cancer cells utilized glycolysis rather than oxidative phosphorylation to fulfill their energetic requirements. This condition found in cancer cells where increased

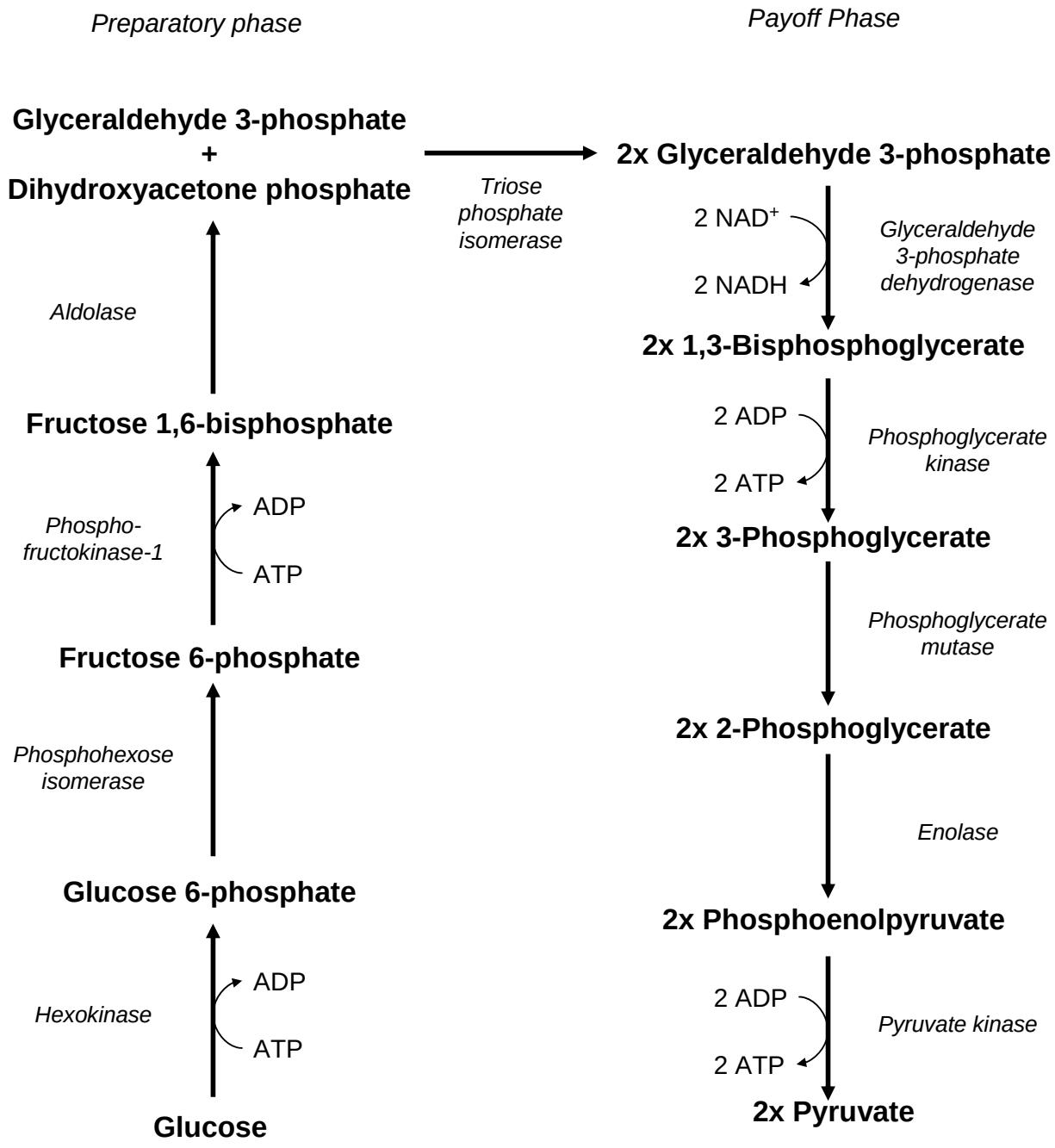

Figure 1.1 - The metabolic pathway of glycolysis where one molecule of glucose is converted enzymatically into two molecules of pyruvate. Glucose that is transported into the cell is immediately converted by the enzyme hexokinase to Glucose 6-phosphate (G6P). G6P is eventually converted into pyruvate, which can then be converted into lactate via anaerobic respiration or transported into the mitochondria and undergo aerobic respiration. The process is broken down into two phases, preparatory and payoff. In the preparatory state, 2 ATP molecules are consumed. In the payoff stage, 4 ATP molecules are generated. The reaction results in a net gain of 2 ATP molecules for each glucose molecule consumed.

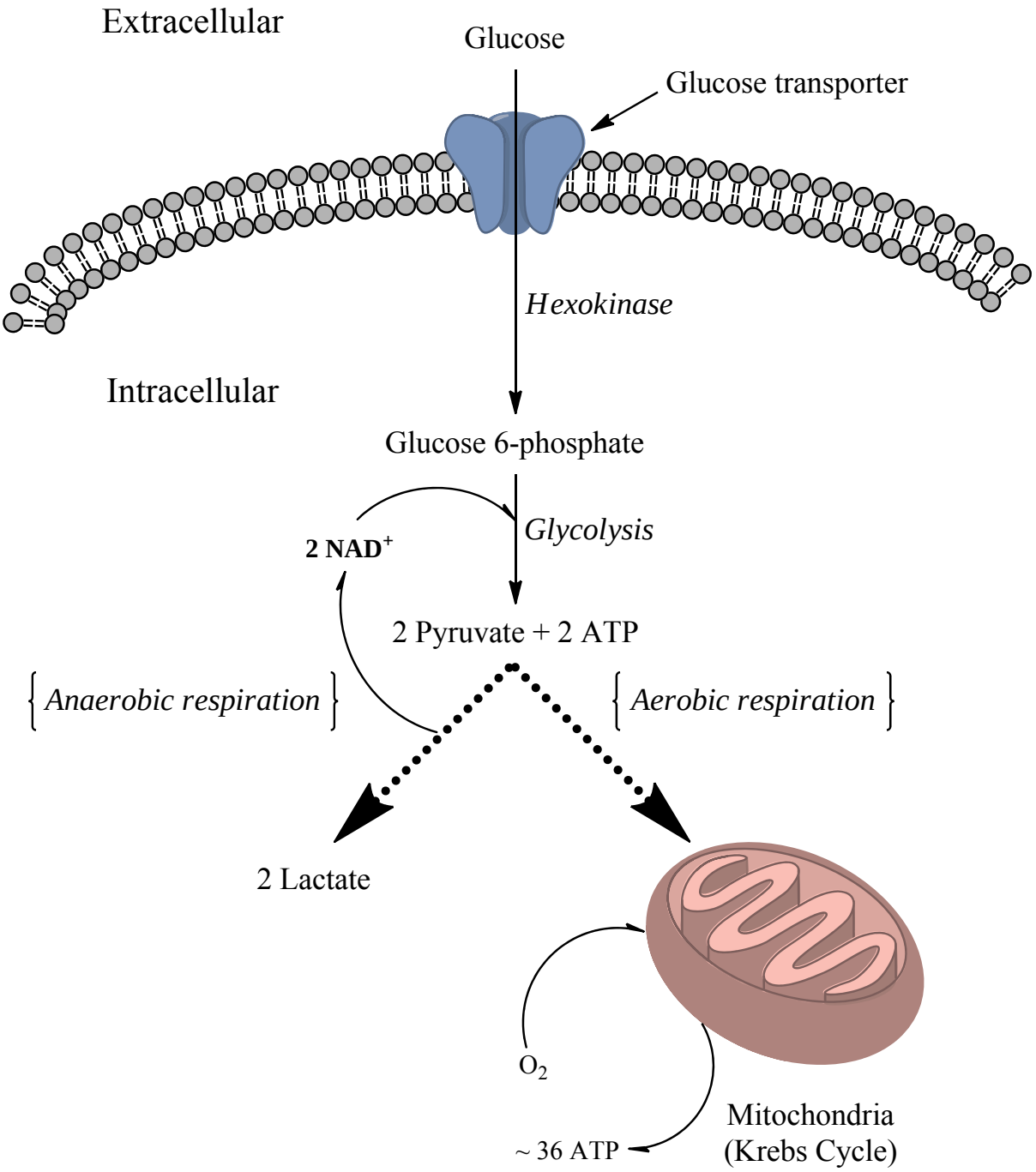

Figure 1.2 – Diagram illustrating the two primary mechanisms by which most cells generate ATP. Glucose is brought into the cell via glucose transporters and converted into pyruvate through glycolysis. In performing anaerobic respiration, or during aerobic glycolysis, the pyruvate is converted into lactate by lactate dehydrogenase, generating additional nicotinamide adenine dinucleotide (NAD^+) that can be subsequently used for increased rates of glycolysis. During aerobic respiration in the presence of oxygen, the pyruvate is shuttled into the mitochondria and sent through the Krebs Cycle, generating over 30 molecules of ATP for one molecule of glucose. For interpretation of the references to color in this and all other figures, the reader is referred to the electronic version of this dissertation.

glycolytic rates occur in oxygenated conditions (aerobic glycolysis) is given the term 'the Warburg effect'.[18-20] It is this increased glycolysis that favors and makes possible the cancer cell's abnormal growth and proliferation.

Cancer cells are able to survive in conditions that healthy cells utilizing oxidative phosphorylation could not survive in because they utilize aerobic glycolysis to meet their energy needs.[21] The increased rate of glycolysis results in an increased production of lactate and protons (H^+). This increased H^+ and decreased pH content could aid in the cancer invading other healthy cell tissues, causing acid induced apoptosis,[22-26] as well as inhibit certain immune responses.[27, 28] It has also been hypothesized that the lactate released from cancer cells can be taken in by stromal cells through the transmembrane monocarboxylate transporters (MCT) and converted into pyruvate.[27] This pyruvate can then be released and taken up again by the cancer cells and converted into lactate and NAD^+ (Figure 1.2), allowing for continued glycolysis and ATP generation. Interestingly, while this altered metabolism provides the cancer cells with the means to invade other tissues and proliferate rapidly, it also provides a target for potential treatment methods.

1.2.2 Cancer treatment

The treatment of cancer and tumor growths has been documented as far back as 4000 years ago. The practice of physically removing tumor growths was the generally accepted treatment for cancer until the development of chemotherapy agents in the 1940s. It was during

that time when the first documented cancer patient with lymphoma was treated with a nitrogen mustard compound that resulted in improved conditions and decreased tumor size.[29] Shortly after, Sidney Farber (known as the 'father' of modern chemotherapy) treated multiple children with acute leukemia with the synthetic compound, aminopterin. The treatment resulted in temporary remission of the disease in each case.[30] Shortly after, it was discovered that chemotherapy drugs, when treated in combination with one another, increased remission rates in patients with leukemia.[31] While the chemotherapy is able to help the reduction or remission of certain types of cancer, it still presents a significant risk to the patient with regards to their overall health. Because the chemotherapy agents are essentially poisons used to destroy the cancer cells, they can affect healthy tissue at the same time. To improve specificity to tumor cells, new compounds and molecules have been developed that aim to target the cancer cells more selectively, rendering the overall treatment less toxic.

Targeted therapy could take an indirect or direct approach in the method it attacks the cancer cell(s). An indirect method could involve the utilization of monoclonal antibodies.[32] Using antibodies that are specific for a certain antigen found selectively on the surface of the cancer cell, it is possible to either induce an immune response where the body will destroy the labeled cell, or deliver a specific agent such as a toxin or radioactive compound.[33-35] A direct approach that could be used to specifically target cancer cells could be the use of small molecules or drugs that interact/interfere with certain proteins that are essential for cellular function. One significant target for these small molecules has been specific protein kinases due to their importance in signal transduction.[36, 37] One of the initial kinase inhibitors used in

cancer treatment was Glivec, which terminated the cancer cells' proliferation both *in vitro* and *in vivo*.[38] While this instance illustrates the ability to develop an inhibitor for a specific enzyme, there are also instances that use existing molecules to target specific cellular components.

Recently, the small molecule dichloroacetate (DCA) has been shown to have potential as an anti-cancer treatment through past administration to patients with lactic acidosis.[39] In cancer cells, DCA has been shown to reduce glycolysis while stimulating oxidative phosphorylation (aerobic respiration).[40] It is able to reroute the metabolic pathways through inhibition of the pyruvate dehydrogenase kinase (PDK) enzyme. PDK inhibits the pyruvate dehydrogenase complex (PDH), decreasing the conversion of pyruvate to acetyl-CoA, which is the first step in oxidative phosphorylation (Figure 1.3).[41] In a recent trial on glioblastoma tumor samples, administration of DCA enhanced mitochondrial activity and stimulated apoptosis in cancer cells.[42] In a human trial, patients diagnosed with glioblastoma were treated with DCA after previous treatment options demonstrated little impact. Multiple patients experienced improved conditions, and reduced tumor size.[42] This overall effect of DCA on cancer cells is significant because healthy cells are not harmed by the introduction of the chemical, most likely due to the normal rates of occurring oxidative phosphorylation.

The mitochondria can also be stimulated directly to initiate increased rates of oxidative phosphorylation in cells.[43] When the mitochondrial protein frataxin is overexpressed in mammalian cells, there is an observed increase in cellular ATP production. This idea was then applied to cancer treatment with the intent of suppressing the growth of tumors following the induction of oxidative phosphorylation. Following over expression of frataxin in colon cancer

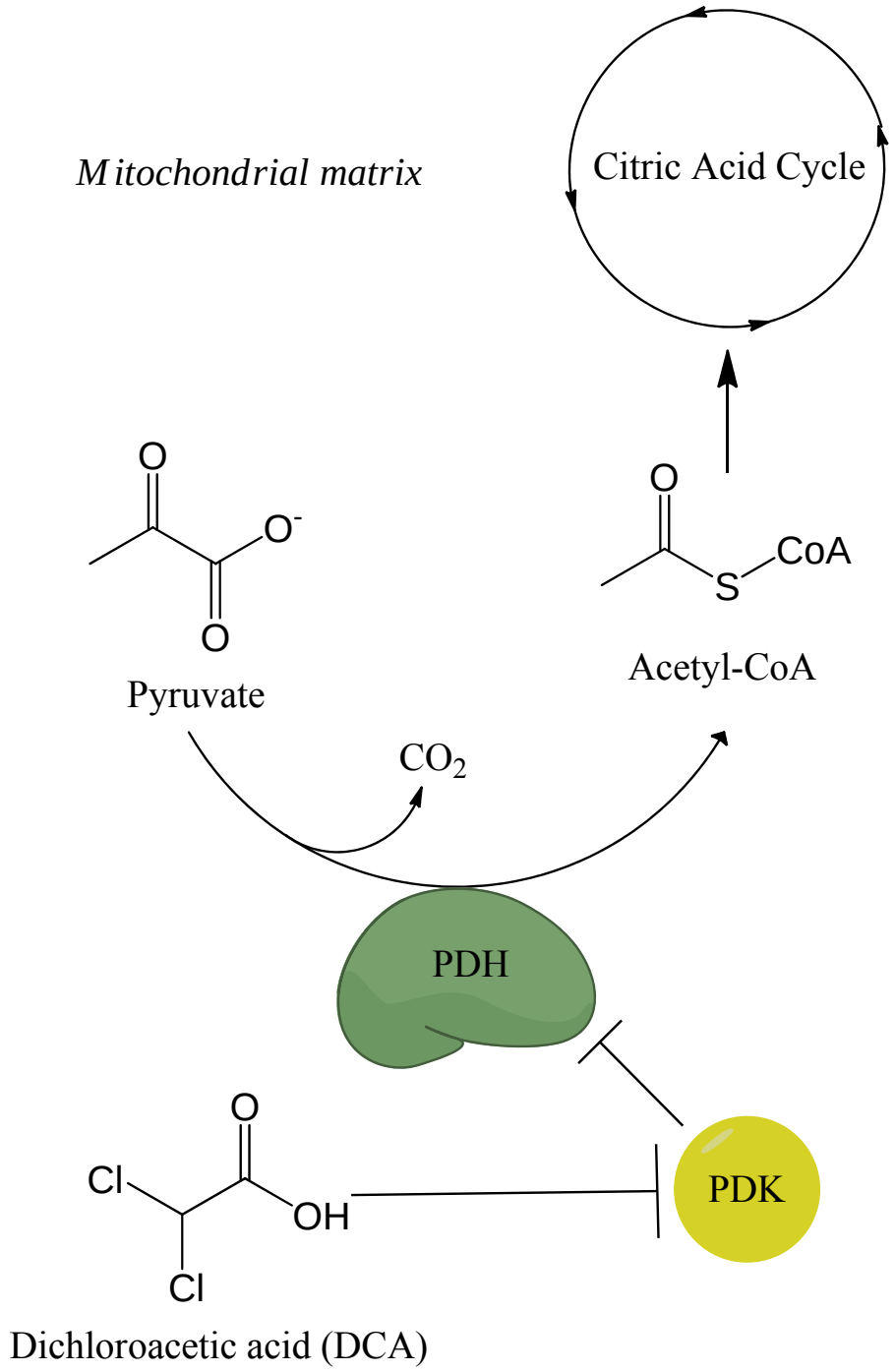

Figure 1.3 – Addition of dichloroacetic acid (DCA) as a potential treatment of cancer. The conversion of pyruvate into Acetyl-CoA is controlled by the pyruvate dehydrogenase complex (PDH). PDH is regulated by the enzyme pyruvate dehydrogenase kinase (PDK). Downregulation of PDH results in increased conversion of pyruvate to lactate in the cell. Inhibition of PDK, specifically with DCA, results in an increased conversion of pyruvate into acetyl-CoA, which can then be sent through the citric acid cycle. This increases the oxidative phosphorylation occurring within the cell and has been shown to suppress tumor growth.

cells, there were increased ATP levels indicative of oxidative phosphorylation as well as decreased growth rates of the tumors.[44] Overall, with more cancer treatments specifically aimed at targeting the metabolism of the disease, evidence suggests that altered metabolism may be a determinant in controlling the cancer cells' proliferation. The altered metabolism was hypothesized by Otto Warburg to be the cause of cancer back in the 1920s.

1.2.3 Causes of cancer

The search for a universal cause of cancer is one that has been going on since the disease was first being studied and will likely be debated for the next many years.[8] It has been widely accepted that cancer is initiated by changes in a healthy cell's ability to control its proliferation and homeostasis. However, the stimuli resulting in these changes are still undetermined. It is possible that there are numerous stimuli that lead to the onset of uncontrolled cell regulation. While there is evidence indicating that genetics does not play a significant role in cancer development (perhaps less than 10 %),[45] there are intracellular alterations that are shown to promote the misaligned metabolism previously described. There are also general environmental influences that have been shown to increase the risk of developing certain cancers.

1.2.3.1 Intracellular metabolic alterations

Oncogenes refer to specific genes that have the potential to cause cancer. Upregulation of these specific genes/proteins has been shown to initiate a switch in glucose metabolism, as well as promote angiogenesis (formation of new blood vessels) and cell growth. Not

surprisingly, these characteristics are two of the previously described 'hallmarks' of cancer. At the same time, the cell has built in tumor suppressing genes or anti-oncogenes which act to regulate the oncogenes' effects on the cell. Deletion or reduction in expression of the tumor suppressing genes or proteins may also lead to onset of cancer.

One transcription factor that could play a significant role in carcinogenesis is the hypoxia inducible factor 1 (HIF-1).[46] When activated, HIF-1 stimulates mechanisms to survive in hypoxic (low oxygen) conditions such as relying on anaerobic glycolysis for energy production.[47] This is accomplished through the activation of certain regulatory enzymes such as pyruvate dehydrogenase kinase 1 that inhibits pyruvate dehydrogenase, the glucose transporter GLUT1, hexokinase, and the monocarboxylate transporter 4.[21, 41, 48-50] The hexokinase increase is significant because it is the first step involved with glycolysis, and it is already over expressed in tumor cells.[51, 52] HIF-1 also promotes increased vascular endothelial growth factor (VEGF) levels.[53] VEGF is critical in stimulating cell growth, proliferation, and angiogenesis. While HIF-1 is important in stimulating glucose metabolism in a hypoxic environment, its upregulation in a normal environment can simulate Warburg's theory of increased aerobic glycolysis, while at the same time affect other essential cellular functions.

The previously described changes in metabolism may also hinder the activity of certain tumor suppressor proteins. The tumor suppressor p53 is one of the more important components in anti-tumor development. In a normal cell, it signals for damaged DNA repair, halts cell growth, or even initiates cellular apoptosis under conditions of stress.[54, 55] In cancerous cells, it has been shown that the increased glucose metabolism brought on by increased expression of

some previously mentioned enzymes (specifically GLUT1 and hexokinase) can decrease the activity of p53.[56] This inhibition of p53 through altered metabolism coupled with the changes in glucose metabolism and specific enzyme activities provide a relevant explanation of how small intracellular signaling changes can potentially promote and sustain cancerous properties.

1.2.3.2 Environmental influences

The changes that occur within cells resulting in altered metabolism and uncontrolled growth are primarily brought on by influences from the surrounding environment.[57] These influences can be as simple as something administered voluntarily into the body such as tobacco and alcohol. Some influences could be less distinguishable or recognizable such as certain infectious agents, pollution, or even unknown sources of radiation. Another influence that has recently become a major contributor to the growing list of risk factors in developing cancer is diet and obesity.

Of the materials shown to cause cancer that people knowingly put into their body, tobacco smoking is one of the more severe. The National Institute of Health has indicated that tobacco use can increase the risk of developing up to 14 different types of cancer, the most significant of which is lung cancer. In fact, tobacco smoking results in over 25% of all cancer related deaths. This increased risk of developing specific cancers arises from the 50 plus known carcinogens in tobacco, one of which (benzopyrenediol epoxide) has documented involvement in the development of lung cancer.[58] There is also evidence suggesting that the inflammatory marker NF-κB can be induced by cigarette smoke.[59]

While acting by slightly different means, alcohol also plays a significant role in the development of certain types of cancer. This effect was first noted back in 1910 when alcohol was shown to increase the risk of esophageal cancer.[60] Studies have now shown that most of the cancers caused by chronic alcohol consumption are of the upper respiratory and upper digestive systems. Few exceptions include liver and breast cancer, as they have been shown to have increased occurrences correlated with increased alcohol consumption.[61] While the cause of cancer from alcohol remains unknown, there are a few hypothesis associated with the breakdown of ethanol into acetaldehyde and free radicals that can cause DNA damage.[62] Alcohol can also act as a co-carcinogen when combined with smoking in esophageal cancer.[63]

Other sources of environmentally influenced cancer include certain infectious agents that are typically viruses. The most common examples of these are the human papillomavirus (HPV) and hepatitis B virus (HBV). HPV acts as a retrovirus that alters the DNA, while HBV promotes oxidative stress and chronic inflammation.[64, 65] Certain environmental pollutants from the air, water, or food have been shown to promote cancers.[66] Polycyclic aromatic hydrocarbons (PAH) from the atmosphere increase the risk for developing lung cancer. Environmental sources of radiation such as UV rays have been shown to promote skin cancers, while man-made sources of radiation or electric fields have also been linked to increased risks of leukemia or brain cancer.[66]

1.2.3.3 Diet and Obesity

The relationship between cancer occurrences and diet has been documented since the early 1980s, when it was estimated that around 30% of all cancer deaths were related to diet.[67] One link between diet and cancer is due to the carcinogenic material that comes directly from the food or as an additive. The nitrites used as preservatives have been linked to the development of certain cancer types.[68] Small molecules such as the bisphenol A from plastic food storage containers have also been linked to breast and prostate cancers as estrogenic tumor promotors.[69, 70] While there are numerous carcinogens that can be present in the food that is consumed, there is a growing global concern regarding the amount of food that is consumed and obesity's role in cancer development.

There have been numerous studies that have identified an increased risk for developing cancer in people who are overweight or obese.[71, 72] Obesity is a condition where fat in the body has accumulated to an extent that there might be observed detrimental health effects. This condition can lead to a resistance to the hormone insulin through inflammation or increased glycation of proteins. Insulin is produced in the pancreas and is released in response to elevated blood sugar levels. The insulin then causes certain cells to take in and store glucose in the form of glycogen. This resistance to insulin is also observed in diabetes, which is a medical condition that also has an altered metabolism as well as increased risks for developing certain cancers. A possible connection between these two conditions can be given after a more thorough evaluation of metabolic alterations in diabetes.

1.3 Diabetes Mellitus

As explained earlier, diabetes is a medical condition that is characterized by uncontrolled, elevated (greater than 6.5 mM) blood glucose levels. Classic symptoms of the disease include polyuria (frequent urination), polyphagia (increased hunger), polydipsia (increased thirst), and unexplained weight loss (type 1 diabetes). These symptoms and diabetic complications can be explained by either a decrease in insulin production, or a reduction in insulin efficiency. In determining whether or not diabetes is present, it is often the case to measure the plasma glucose levels 2 hours after consuming 1.75 grams of glucose per kilogram of body weight. This is often called an oral glucose tolerance test. Basal glucose levels can fluctuate between 5 and 6 mM. If the fasting blood glucose levels are above 7 mM, or if the glucose level is above 11 mM after the oral glucose tolerance test, the presence of diabetes is suggested.[73] Another test to confirm blood glucose levels, and potentially diabetes, is to measure the glycated hemoglobin levels (A1C). The hemoglobin becomes non-enzymatically glycated after a period of time, with the amount of glycation indicating the plasma glucose levels. If the A1C level is greater than 6.5%, the level at normal glucose concentrations, the presence of diabetes is also strongly suggested. While there are methods to universally diagnose the presence of diabetes, there are three main types of the condition, each with their own pathologies.

1.3.1 Types of diabetes

Insulin-dependent diabetes mellitus (IDDM) is commonly referred to as Type 1 diabetes. It can also be classified at juvenile diabetes. Type 1 diabetes constitutes between 5 and 10% of

all reported cases of diabetes. This type is specifically attributed to a lack of insulin production from the pancreas, which is essential for glucose uptake and storage (Figure 1.4).[74] The previously mentioned lack of insulin production is associated with the destruction of the beta cells (β-cells) in the islets of Langerhans, which are found in the pancreas. This destruction, though not well defined, is thought to be due to an autoimmune response. This response is hypothesized to come from viral infections that lead to increased inflammation, or possibly from antigens in specific food products.[75, 76] The gradual reduction of insulin production from the damaged β-cells leads to less glucose uptake into the muscle cells. This leads to the cells resorting to consuming fatty acids to generate the energy required to function. The break down of fatty acids leads to increased levels of ketone moieties, which in turn leads to ketoacidosis, a condition that can be fatal if not treated accordingly. Some of the symptoms of ketoacidosis normally are the first signs noticed by undiagnosed diabetics that result in required medical assistance.

In order to characterize the specific type of diabetes, it is possible to measure the amount of insulin present in the blood stream indirectly. This can be done by measuring the small biomolecule C-peptide.[77] C-peptide is a 31 amino acid chain that is produced in the pancreas due to the cleavage of proinsulin. It is used to hold the two insulin chains (A and B) together as they fold into proper alignment. The peptide is then cleaved off from the insulin and released into the bloodstream in equimolar amounts with insulin. C-peptide is preferred in measuring insulin levels due to the longer half-life of the peptide in vivo. In addition to type 1 diabetes, there are other types of diabetes where insulin is at normal levels, but blood glucose remains uncontrolled.

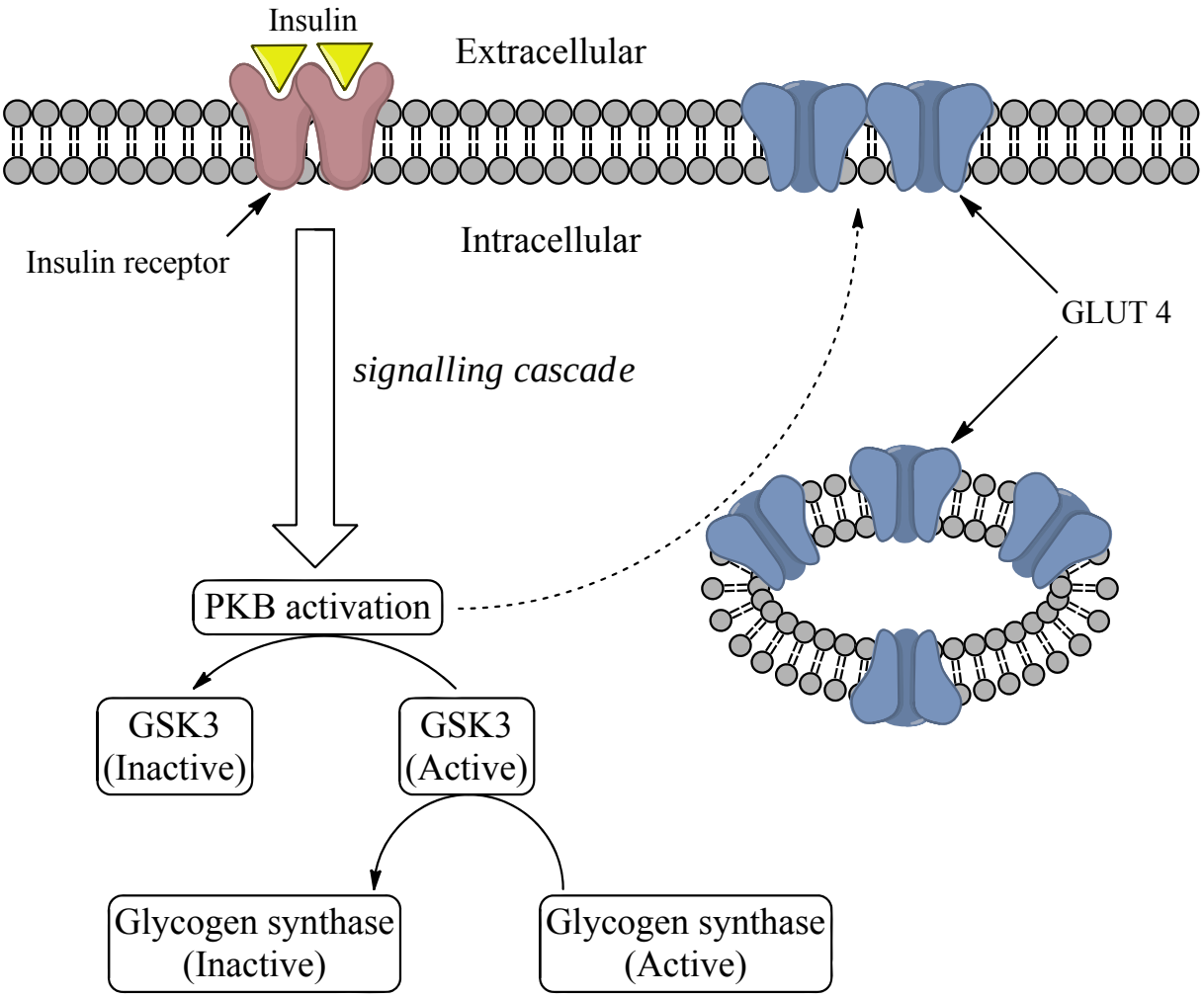

Figure 1.4 – Insulin signaling regulating glucose uptake and storage. Upon binding to the insulin receptor, the insulin initiates a signaling cascade that activates protein kinase B (PKB). PKB can phosphorylate and inactivate glycogen synthase kinase 3 (GSK3), which in its active form inactivates glycogen synthase. PKB can also stimulate the exocytosis of the glucose transporter 4 (GLUT4) to the plasma membrane, allowing for increased glucose uptake into the cell. The activated glycogen synthase is able to generate glycogen from the increased glucose presence. The glycogen can then be stored for future energetic demands.

Type 2 diabetes, or non-insulin dependent diabetes (NIDDM) is the form of diabetes classified by a resistance to the hormone insulin.[74] It can often be referred to as adult-onset diabetes and is the most common type of diabetes. Overall, it accounts for between 90 and 95% of all reported cases of diabetes. The resistance to insulin suggests that even though the insulin is constantly being produced and released by the pancreas, the cells that normally respond to the insulin by taking in and storing glucose are no longer stimulated by the hormone. This resistance results in increased blood glucose (hyperglycemia), higher A1C levels, and elevated glycation levels. The state of hyperglycemia has been shown to result in some β-cell dysfunction, leading to decreased insulin levels.[78] While β-cell dysfunction is not the hallmark condition of type 2 diabetes as it is with type 1, the number of β-cells found in the pancreas of a person with type 2 diabetes is significantly decreased when compared to a pancreas from a person who does not have diabetes.[79]

Insulin resistance is commonly associated with obesity. In fact, many of those diagnosed with type 2 diabetes are classified as obese or have elevated body fat. This resistance can be obtained through genetic means and/or lifestyle decisions. Some conditions that are associated with an increased risk of developing insulin resistance include age, a sedentary lifestyle, increased stress, tobacco, and alcohol consumption.[80] Some genetic sources of insulin resistance and type 2 diabetes development include hereditary components derived from ethnicity. In the United States, those ethnicities with an increased risk to develop type 2 diabetes include African American, Hispanic American, Native American, Asian American, or Pacific Islander.[80]

Another type of diabetes mellitus is referred to as gestational diabetes (GDM). GDM is defined as glucose intolerance to any noticeable degree upon the onset, or initial stages of

pregnancy. About 4% of pregnancies in the United States are affected by diabetes. Roughly 90% of those pregnancies are affected by GDM and the remaining 10% are from types 1 or 2 diabetes (pregestational diabetes). These conditions can prove to be fatal to the mother and unborn fetus if not treated properly.[81] Often states of hyperglycemia develop during the second half of the pregnancy following a gradual development of insulin resistance. This insulin resistance may arise from increased insulin levels during the first 20 weeks of the pregnancy due to an enhanced pancreatic response to blood glucose levels.[82] There are also observed increases in levels of hormones such as cortisol, estrogen, prolactin and human placental latogen that have been correlated with insulin resistance.[83]

GDM is diagnosed similarly to the other types of diabetes where an oral glucose tolerance test is administered. Initially, a lower amount of glucose (50 grams) is administered with the plasma glucose levels monitored after 1 hour. If the levels are above 140 mg/dL, further tests are performed. Women at high risk of developing GDM include those who are obese, have a personal or family history with type 2 diabetes or GDM, suffer from glucose intolerance, or glucosuria.[73] If GDM is diagnosed early in the pregnancy, it is possible to undergo strict treatments to control glucose levels in order to minimize the complications that may arise.

1.3.2 Complications associated with diabetes mellitus

Most people with diabetes will often be diagnosed with at least one or more complications that can arise from impaired insulin resistance or chronic hyperglycemia. These general complications include nerve damage, blindness, pregnancy complications, kidney and

renal damage, heart and cardiovascular disease, and stroke. The general complications listed result from the development of many other 'sub' complications that have their own pathologies and themselves result from conditions specific to types of diabetes mellitus. Conditions and the specific numbers are reported from the Centers for Disease Control and Prevention 2011 National Diabetes Fact Sheet.

In type 1 diabetes, it is possible for the body to achieve a state of hypoglycemia, or low blood glucose levels (< 3.4 mM). This state can occur if proper insulin levels are poorly regulated and the blood sugar levels are not monitored. This condition often triggers moderate autonomic warning symptoms such as hunger, anxiety, sweating, and nausea to such severe symptoms as blurred vision, slurred speech, or difficulty in concentrating depending on the extremity of the hypoglycemia.[84] If not corrected, diabetic ketoacidosis hypoglycemia will develop that can produce coma, seizures, permanent brain damage, or even death.

It is estimated that virtually 100% of all people with diabetes in the United States suffer from some form of neuropathy, or nerve damage. Up to 70% of those cases are diagnosed as peripheral neuropathy, which is a condition that affects the nerves of the extremities (hands/feet) and moves proximally. Some of the symptoms of the onset of peripheral neuropathy can include numbness, loss of dexterity, burning, hypersensitivity, and difficulty in rising from a seated position.[85] Multiple hypotheses for the cause of diabetic neuropathy have been provided; however it is most likely a combination of ideas that needs to be used to understand its pathogenesis. One hypothesis is that the conversion of glucose into sorbitol lowers myoinositol levels which decreases the velocity of nerve conduction.[86] Another idea suggests that the poor blood flow results in endoneurial hypoxia, decreasing nerve signaling.[87] Often the nerve

damage becomes so severe that the affected area requires amputation. In fact, over 60% of nontraumatic lower limb amputations occur in people with diabetes.

Pregnancy complications can result in severe birth defects in between 5 and 10% of all births from mothers who have type 1 diabetes. The number of spontaneous abortions caused by diabetes affects between 10 and 20% of all births. Newborns are subject to having low blood sugar, developing conditions such as jaundice, and have abnormal growth rates. Although most of these conditions develop due to pregestational diabetes during the first trimester of the pregnancy, GDM can result in certain congenital disorders that develop shortly after birth.

Diabetes, specifically diabetic retinopathy (DR), is the leading cause of new cases of blindness in adults between the ages of 20 and 74. Overall it accounts for about 12% of the new cases of blindness each year. It was reported that people with diabetes are about 30 times more likely than a healthy individual to become blind.[88] DR is caused by microvascular retinal changes. The hyperglycemic conditions in diabetes can lead to damaged blood vessels and poor oxygen circulation. The poor oxygen circulation causes retinal cells to produce the vascular endothelial growth factor (VEGF)[89] that contributes in the formation of new, fragile blood vessels that grow along the retina and into the fluid that fills the eye. The vessels can burst, cloud the vision, or in some severe cases completely destroy the retina.[85]

Currently, diabetes is the most significant cause of kidney/renal failure (nephropathy) in the United States. Over one third of the entire population having end stage renal failure are diagnosed with diabetes.[85] This condition is relatively evenly distributed between people with type 1 and type 2 diabetes. Renal problems can occur in those with diabetes via bladder diseases, arterial lesions and thrombosis, vascular problems, or a condition known as

glomerulosclerosis. Glomerulosclerosis refers to the hardening or scarring of the capillaries in the kidney that are used in the filtering of urine from the blood. The extent of damage can be determined by monitoring the concentrations of albumin and creatinine excreted in the urine.[90] The damaged capillaries, while they are able to be repaired, gradually worsen until kidney failure sets in. At this point, it is often necessary to undergo dialysis treatment or receive a kidney transplant. Risk factors for developing renal disease in diabetes include hyperglycemia, smoking, high protein intake, and hypertension (high blood pressure).

Hypertension is a condition where higher than normal blood pressure exists. Normal blood pressure has a systolic pressure (pressure during a heart beat) of below 120 mmHg and a diastolic (pressure between beats) of below 80 mmHg. Chronic values above both listed classify one as having hypertension. Greater than 65% of Americans who are diabetic either have, or will develop serious hypertension over their lifetime. This condition is a major risk factor for developing cardiovascular disease, coronary heart disease, or stroke. In fact, the diseases listed account for the major cause of mortality in people with diabetes.[91] People with diabetes also have a significantly greater chance to develop cardiovascular problems compared to healthy individuals.[92] It can also be a contributing factor in many of the complications previously discussed, such as blindness, kidney damage, and amputations. Hypertension can be brought on by the stiffening/hardening of the arteries. Over time, this allows for fatty deposits, plaque buildup, and/or cholesterol to narrow the artery diameter, resulting in the development of atherosclerosis. These blocked arteries are then able to lead to increased risks for stroke and heart attacks through thrombosis or arterial embolisms.

The main cause of most of the conditions described is not specifically the hyperglycemia present in diabetes. Many of the underlying mechanisms derive from the dysfunction that occurs at the interface between the blood stream and peripheral tissues, or the endothelial layer. Many of the previously mentioned complications, primarily the cardiovascular diseases, GDM, and atherosclerosis, are initiated through overexpressed inflammatory responses, oxidative stress, and general endothelial dysfunction.[93, 94]

1.3.3 Endothelial dysfunction in diabetes mellitus

Oxidative stress is explained by the loss of balance between the generation of reactive oxygen species (ROS) and the antioxidant defense that neutralizes excess reactive intermediates or repairs damage. ROS are chemically reactive species containing oxygen that under normal, healthy conditions have significant roles in cell homeostasis and signaling.[95] Some examples of the more common ROS molecules are superoxide (O_2^-), hydrogen peroxide (H_2O_2), peroxynitrite ($ONOO^-$), and the hydroxyl radical ($^{\bullet}OH$). In normal conditions, there are enzymes such as superoxide dismutase and catalase to convert the superoxide radical into hydrogen peroxide and subsequently hydrogen peroxide into water and oxygen, respectively. However, if there are increased levels of ROS and/or not enough antioxidants or defensive enzymes to neutralize most of the radicals, significant damaging effects could be done to the cell. Such effects include damage to the DNA, oxidation of amino acids in proteins, or inactivation of specific enzymes.

The source of the ROS in cells is derived primarily from the cell's own metabolism that occurs during oxidative phosphorylation and the electron transport chain.[96] The electron transport chain, or mitochondrial respiratory chain, is the energy (ATP) producing mechanism that is mediated by four complexes located on the inner mitochondrial membrane, cytochrome c, and ubiquinone (Figure 1.5). During the final steps of the mitochondrial respiratory chain, molecular oxygen is the terminal electron acceptor. When oxygen obtains these extra electrons, it is normally converted into water when combined with hydrogen. However, incomplete phosphorylation may result in the overproduction of the highly reactive superoxide radical or peroxide anions. This increase of ROS, potentially due to increased glucose metabolism, may lead to conditions of oxidative stress, which has been shown to be a side effect of chronic or acute hyperglycemia.[97] These hyperglycemic conditions, such as those in diabetes, are expected to play a significant role in the oxidative damage in the endothelium that can contribute to the pathogenesis of certain diabetic complications.[98-100]

1.3.3.1 Causes of endothelial dysfunction

It is hypothesized that endothelial dysfunction due to hyperglycemia can occur through enhanced cellular mechanisms to counteract the elevated glucose levels. One of these pathways/mechanisms is the polyol pathway.[101] In the polyol pathway (Figure 1.6) excess glucose is converted to sorbitol by the enzyme aldose reductase while oxidizing nicotinamide adenine dinucleotide phosphate (NADPH) to $NADP^+$. The sorbitol is then oxidized into fructose producing the reduced form of nicotinamide adenine dinucleotide (NADH). The decreased

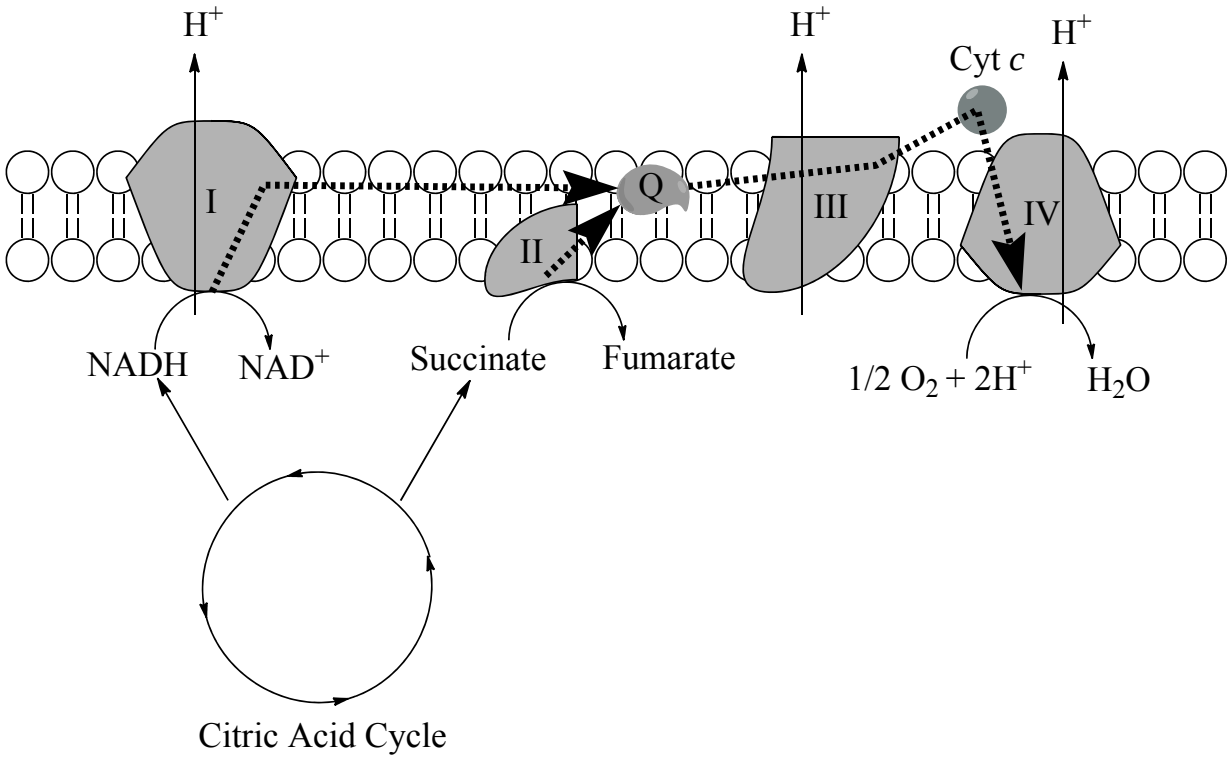

Figure 1.5 – Diagram illustrating the electron transport chain. Reduced nicotinamide adenine dinucleotide (NADH) and succinate that are generated during the citric acid cycle are used as electron donors in complex I and II, respectively. The electrons removed from the molecules in both complexes are transferred to ubiquinone (Q) where they are subsequently transported to cytochrome C via complex III. Electrons are then moved to complex IV, where oxygen is reduced into water. The protons 'pumped' out through the complexes are used to generate an electrochemical gradient, which is used to produce ATP via ATP synthase (not shown).

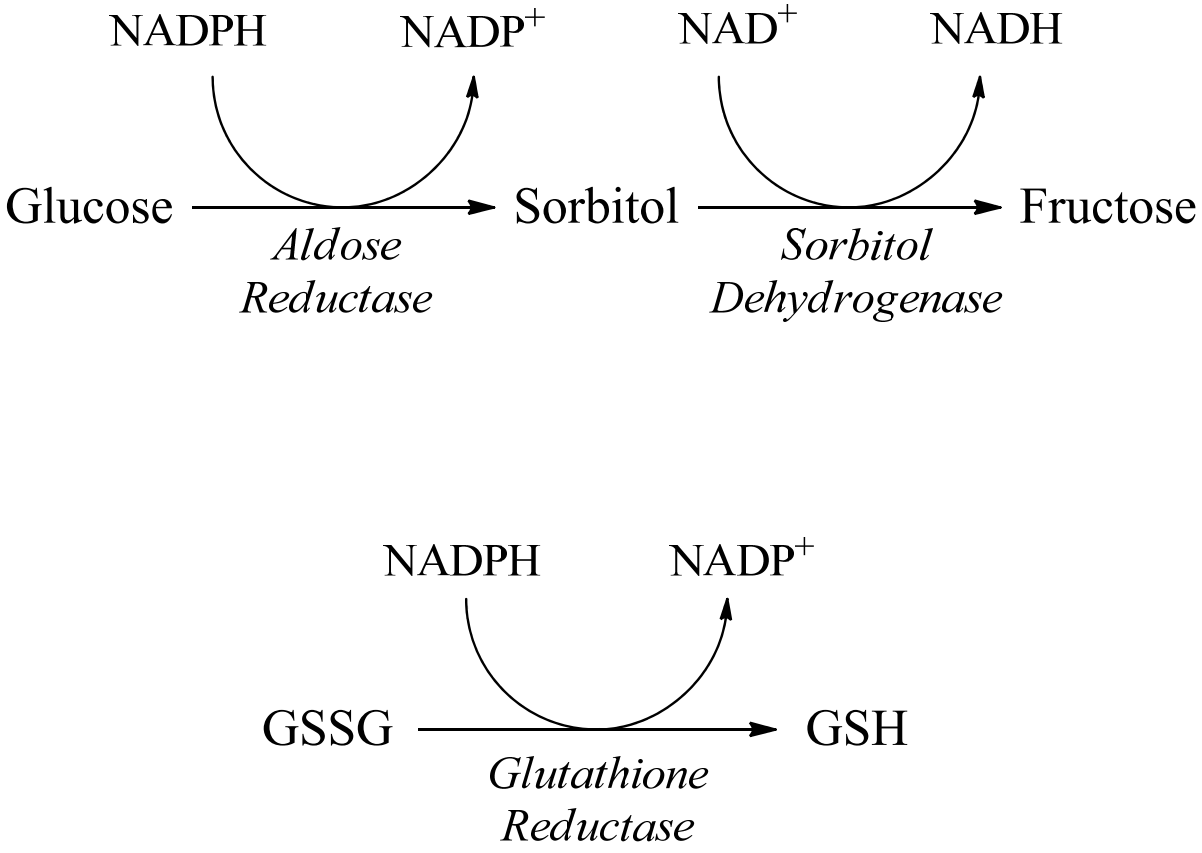

Figure 1.6 – Mechanisms of the polyol pathway (top) and the regeneration of the antioxidant glutathione (bottom). In the polyol (sorbitol-aldose reductase) pathway, excess glucose is converted into the sugar alcohol sorbitol by the enzyme aldose reductase while consuming NADPH. The sorbitol is then converted into fructose by sorbitol dehydrogenase, consuming NAD^+ and generating NADH. The regeneration of GSH from GSSG requires the presence of NADPH, which is decreased through increased rates of the sorbitol pathway. This results in an overall decrease in the presence of GSH. The increased NADH from the conversion of sorbitol to fructose can result in an inhibition of the glycolysis step that requires the conversion of NAD^+ to NADH (Figure 1.1) where glyceraldehyde 3-phosphate is converted into 1,3-bisphosphoglycerate.

NADPH can have direct effects on endothelial cell oxidative balance and vascular tone. NADPH is used to regenerate a primary antioxidant glutathione (GSH) (Figure 1.6) and is necessary for the generation of the vasodilator nitric oxide (NO) from the amino acid L-arginine (Figure 1.7). The decreased GSH levels can lead to lowered antioxidative defensive capabilities, while the decreased NO production leads to poorly regulated artery and capillary dilation that can result in vascular complications.

Another potential source of endothelial dysfunction can arise from the increased rate of the hexosamine pathway. One of the intermediates of glycolysis, fructose-1,6-bisphosphate, is accumulated due to inhibition of key enzymes in the glycolytic pathway by increased superoxide radicals. The fructose-1,6-bisphosphate is then converted by the enzyme glutamine:fructose-6-phosphate amidotransferase (GFAT) into glucosamine-6-phosphate, which is then able to be used in the synthesis of certain O-linked glycoproteins. Increased O-linked glycosylation can lead to increased activity of the transcription factor SP1, which in turn can promote increased activation of specific genes such as the plasminogen activator inhibitor (PAI-1) that inhibit the degradation of blood clots.[102] The alteration of insulin receptor/substrate metabolic signaling mechanisms, as well as decreased activation of eNOS and subsequent NO production are also observed under states of increased O-linked glycosylation.[103] These modifications can be directly attributed to altered glucose metabolism as well as the development of cardiovascular disease.

Just as the inhibition of specific proteins can lead to improper endothelial function, the activation of certain proteins has also been connected to endothelial dysfunction. Increased insulin presence due to hyperglycemia leads to the release of diacylglycerol (DAG). DAG activates specific isoforms of protein kinase C (PKC). Excessive PKC activation can lead to the

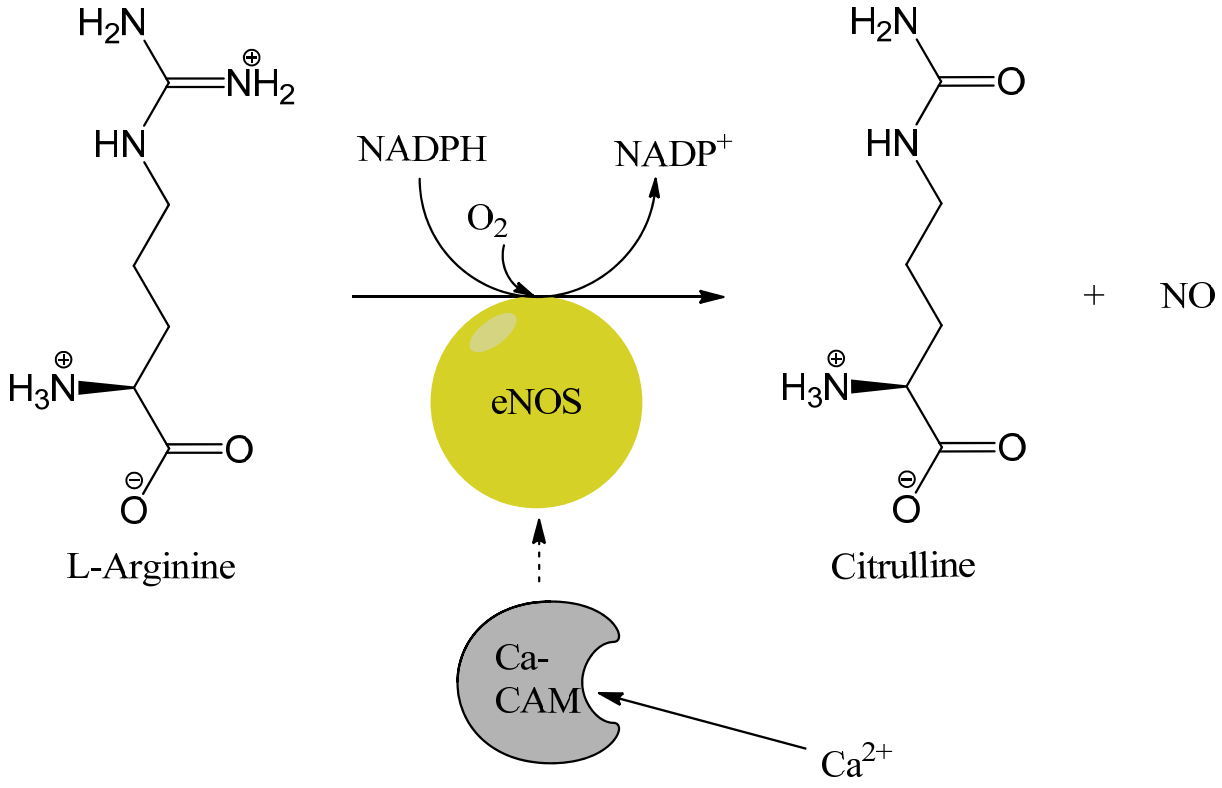

Figure 1.7 – Mechanism describing the production of nitric oxide (NO) in the endothelium. Free intracellular calcium activates the calcium calmodulin complex (Ca-CAM) that interacts with endothelial nitric oxide synthase (eNOS). Ca-CAM facilitates the electron transfer from the oxidation of NADPH to $NADP^+$. The electrons help to catalyze the reaction of oxygen with L-arginine to generate citrulline and NO.

presence of known inhibitors of the sodium-potassium pump, which are essential to maintain cell membrane potentials, transport molecules into and out of the cell, and control cell volume.[104] In addition to increased enzyme inhibitor production and release, PKC has been linked to activation of the proinflammatory transcription factor NF-κB. Similar to previously described causes of endothelial dysfunction, enhanced PKC activity also has been implicated in decreased NO production,[104] potentially resulting in improper vascular control.

In addition to up regulated metabolic pathways and protein activation, hyperglycemia can enhance the formation of advanced glycation end products (AGEs). Glycation refers to the non-enzymatic process where sugar molecules are bonded to lipids or proteins, potentially impairing the particular biomolecule's function. The rate of glycation can depend on the concentration of glucose (i.e. hyperglycemia) or the level of oxidative stress present inside the cell. AGEs can also modify proteins found on the extracellular surface of the plasma membrane, decreasing matrix to cell signaling. The increased levels of extracellular AGEs in those with diabetes also are able to bind at increased levels to cell surface receptors specific for the AGEs (RAGE).[105] When bound, these receptors are believed to promote an inflammatory response though activation of NF-κB.[106] In conditions of hyperglycemia, such as diabetes, the increased binding could lead to chronic inflammation.

1.3.3.2 Endothelial dysfunction in diabetic complications

As previously described, the potential causes for endothelial dysfunction have their own initiating mechanisms and damaging side effects. While the causes and effects of the endothelial

dysfunction may be different, there are often combinations of the side effects that contribute to the underlying pathology of many significant diabetic complications. For example, macroangiopathy refers to a condition in larger blood vessels where atherosclerosis and blood clots form to restrict the flow of blood. Microangiopathy focuses on the smaller capillaries found in the vasculature. The walls of the capillaries become thick and fragile. The walls can then break, allowing for circulatory proteins to leak out of the vessel, as well as decrease the overall blood flow. This restriction of blood supply, known as ischemia, restricts oxygen from reaching certain peripheral tissues. The lack of oxygen can lead to cell death and subsequent diseases such as gangrene that may require amputation. Microangiopathy is believed to be initiated by many of the previously mentioned precursors that lead to hyperglycemic-induced endothelial dysfunction such as increased oxidative stress, inflammation, and AGE formation.[107] Microangiopathy also contributes to many harmful conditions observed in diabetes mellitus, namely nephropathy, retinopathy, and neuropathy.

In diabetic nephropathy, one of the more significant effectors of glomerulosclerosis is the transforming growth factor (TGF). This growth factor is induced by specific transcriptional changes that originate from increased rates of the hexosamine pathway. Another growth factor that is implicated in nephropathy is VEGF. Hyperglycemia causes an upregulation of VEGF, which can eventually decrease the availability of the growth factor. Because VEGF is usually required for maintaining healthy systems of glomerular capillaries in the renal filtration barrier, a gradual decrease in the factor impairs the development of new vessels.[108]

Vasoregulation in nerve vessels and microvessels is significantly maintained by endothelial cell function. Therefore, dysfunction in the endothelium due to hyperglycemic conditions is hypothesized to play a crucial role in the development of diabetic neuropathy. It

was described earlier that poor blood flow can result in the hypoxia mediated nerve damage. This poor blood flow can arise from the oxidative stress in the endothelium initiated by hyperglycemia. The oxidative stress may lead to decreased endothelial NO production, allowing for abnormal or reduced vasodilation. The decrease in NO could also be attributed to hyperglycemia induced increased polyol pathway flux or AGE production.[109] AGEs have also been shown to activate NF-κB, which initiates inflammatory responses that are likely to promote endoneurial ischemia and subsequent nerve damage.[110]

1.3.4 Link between diabetes and cancer

As described earlier, there have been increased risks for developing certain cancers in people with diabetes, especially those with type 2. The risks are the greatest, nearly twice as high, for developing cancers of the liver, endometrium, and the pancreas.[111] Other slightly lower risks include breast, bladder, non-Hodgkin's lymphoma, and colon cancer.[111] In addition to the increased risk of developing cancer, there are also increased mortality rates associated with people who have diabetes and develop specific cancers compared to healthy individuals who develop the same malignancies.[112] While the pathophysiologies of both diabetes and cancer are not entirely understood, there are some potential risk factors and biological links between the two diseases.

Risk factors are characterized as a type of variable that is associated with an increased chance to develop certain illnesses or diseases. These risk factors can be classified as non-modifiable or modifiable when comparing common factors between diabetes and cancer. Some

of the non-modifiable include, but not limited to, age, gender, and race/ethnicity. About 80% of all newly diagnosed cancer occurs among people above 55 years in age, while the highest percentage of diabetics, at 24%, falls into the age range of 60 years or older.[113] Gender also can play a role as cancer occurs more frequently in males, who also have a higher age-adjusted risk for developing diabetes.[113] Lastly, race/ethnicity appears to play a role as African Americans in the United States are more likely to develop cancer compared to other ethnic groups. Diabetes also affects a disproportionate amount of African Americans, Native Americans, Hispanics, and Asian Americans compared to non-Hispanic whites.[113]

Modifiable risk factors refer to the variables that are more able to be altered or changed. The significant modifiable risk factors similar to cancer and diabetes include physical activity, tobacco and alcohol consumption, and obesity. Studies have demonstrated that elevated levels of physical activity can decrease the risk for developing cancers of the colon and possibly lung.[114] This same physical activity decreases the chances of developing type 2 diabetes by over 30%.[115] As previously described in the discussion of causes of cancer, tobacco smoking and alcohol consumption increase specific cancer risks. Smoking and excessive alcohol consumption also has been identified as a risk factor for developing diabetes.[116] Obesity has been discussed as a risk factor for cancer and diabetes in their respective discussions. However, obesity presents multiple biological conditions that provide certain links between the two diseases.

Obesity is traditionally measured by examining the body mass index (BMI) of an individual. The BMI of a 'normal' person usually falls between the ranges of 18.5 through 25, overweight is between 25 and 30, and obese is any value greater than 30. It is in the overweight

and obese categories where most of the increased risks are observed for developing type 2 diabetes, cardiovascular diseases, and certain types of cancer. Certain biological mechanisms that are promoted in obese and diabetic conditions such as chronic hyperinsulinemia, inflammation, and hyperglycemia can potentially promote cancer proliferation or carcinogenesis, the start of cancer growth.

Hyperinsulinemia, or excess insulin found in the blood stream, is correlated with the BMI and is often observed in type 2 diabetes where the individuals are more insulin resistant. The circulating insulin has been shown to have other influences on cell function in addition to its traditional role in glucose clearance. When insulin and insulin-like growth factors (IGF) bind to their respective receptors, certain signaling pathways are initiated that are similar to the previously described hallmarks of cancer. Not surprisingly, cancer cells have many of these receptors. Enhanced cell proliferation and protection from apoptosis are two of those pathways that are initiated.[117] In addition to promoting cancer growth, elevated insulin levels can also promote carcinogenesis by indirectly affecting IGF. In healthy individuals, insulin-like growth factor-binding proteins (IGFBP) binds to virtually all IGF, thus inhibiting the growth promoting effects. Elevated insulin levels decrease the presence of IGFBP,[118] allowing for increased interaction of IGF to various cells resulting in cellular environmental changes that may affect cancer development.

Obesity found in many type 2 diabetes cases is also associated with increased chronic inflammatory response pathways, some of which have been shown to promote cancer growth. Adipose tissue, or fat tissue, should be observed as its own endocrine organ that releases components into the blood stream such as interleukin-6 (IL-6) and PAI-1.[119] Both of these have

been implicated to cancer in different means. PAI-1 over expression has been connected to lower survival outcomes in patients with breast cancer, and the cytokine IL-6 activation of signaling pathways has been shown to enhance cancer cell proliferation, survival, and invasion.[120, 121]

Considering the previously described 'Warburg effect' where cancer cells perform aerobic glycolysis to achieve their energy demands, the same cancer cells consume glucose at a higher rate than normal cells. The idea that the hyperglycemia conditions found in type 2 diabetics can stimulate cancer cell growth needs to be considered. *In vivo* studies examining tumor growth in a hyperglycemic yet insulin deficient environment did not observe growth in the malignancies.[122] However, these studies did not evaluate whether hyperglycemia induced carcinogenesis. Another study was performed, evaluating the cancer risk associated with individuals who are not diabetic or obese, but have elevated fasting blood glucose levels.[123] While there were increased cancer mortality rates in those who were obese (BMI > 23) with high fasting blood glucose (FBG > 6.1 mM), there were also increased rates of mortality among normal weight (BMI < 20) individuals with elevated FBG (FBG > 6.1 mM) levels. These findings can support the idea that high blood glucose levels and/or hyperinsulinemia may have a more prominent role in cancer promoted by diabetes.

1.3.5 Current treatments and therapies for diabetes

In treating diabetes, the primary focus on the therapeutic methods applied is to maintain the blood glucose levels as close to normal as possible. While diabetes is often incurable, proper

glycemic control can have a significant impact on the progression of many of the diabetic complications previously discussed. Due to the fact that different types of diabetes have different mechanisms by which they alter blood glucose metabolism and affect biological systems, different treatments must be applied accordingly. While the actual treatments differ, they all are primarily focused on proper diet, regular exercise, and administration of specific medications.

The regulation and monitoring of a proper diet is essential for all types of diabetes. For those with type 1 diabetes, the amount of carbohydrates consumed must be strictly monitored in order to administer a proper amount of exogenous insulin. If too much insulin is administered, an eventual state of hypoglycemia can develop, while too little insulin may not allow for enough glucose to be metabolized by the body, maintaining a hyperglycemic state. Patients who develop GDM are suggested to monitor their carbohydrate consumption levels in order to reduce the chances of developing type 2 diabetes post-birth. At the same time, too few carbohydrates in their diet may result in lower birth weights for infants.[124] Type 2 diabetics adjust diet accordingly in order to achieve a healthy weight. Maintaining proper body weight is significant as obesity is a condition observed in over 80% of diagnosed cases of type 2 diabetes.[125] For most diabetic patients, the desired weight change is attained not only through the monitoring of one's diet, but in combination with exercise.

Exercise can serve as a major contributor of blood sugar uptake and consumption in the body, increasing consumption by up to 10 fold. While exercising, an insulin-independent mechanism increases the presence of GLUT4 on the outer surface of muscle membranes, allowing for an increased glucose uptake upon stimulation with insulin.[126] Patients with type 1

diabetes who take insulin and exercise regularly see increased glucose consumption and decreased blood glucose levels. The insulin levels must be strictly monitored, as regular insulin control is absent. Other studies have identified multiple health benefits of regular physical activity in patients with diabetes, particularly those with type 2. Those benefits include improved insulin sensitivity, decreased cholesterol and blood pressure, reduced chance of developing cardiovascular disease, and weight loss. In type 2 diabetics, weight loss is thought to contribute to the increased insulin sensitivity through changes in body composition, namely decreased fat levels and increased muscle levels allowing for more muscle blood flow.

In many cases of diabetes, diet and exercise need to be supplemented with the administration of medications that can have a more direct role in regulating blood glucose levels. For type 1 diabetics, the only current treatment is through insulin therapy. How and when this insulin is administered was unknown until the early 1990s. At that time, the Diabetes Control and Complications Trial (DCCT) examined the relationship between insulin administration, blood glucose control, and the development of diabetic complications.[127] The two groups, one that had more frequent insulin injections and another that had only two throughout the day, attempted to maintain their blood glucose levels to be as close to normal as possible. It was found that the group with a more strict insulin administration schedule had up to a 50% reduction in the development of diabetic complications (retinopathy, nephropathy, and neuropathy).

Type 2 diabetics may eventually resort to the administration of insulin to control blood glucose levels due to gradual pancreatic beta cell destruction. Before that event occurs, the medications often recommended to type 2 diabetics to maintain normal blood glucose levels work to compliment/support the insulin already present. Sulfonylureas (SU) act directly on the pancreatic beta cells by stimulating an influx of calcium, resulting in the secretion of more

insulin into the bloodstream.[128] Thiazolidinediones are able to bind to specific receptors that enhance the production of insulin sensitive enzymes.[129] The increase in enzymes ultimately leads to an improved utilization of glucose by adipocytes. Alpha glucosidase inhibitors (acarbose) reduce blood glucose levels by preventing the digestion of larger carbohydrate molecules, significantly lowering the absorption of glucose that occurs through the small intestine.[130]

While the mechanisms of action for sulfonylureas, thiazolidinediones, and alpha glucosidase inhibitors are well understood, other diabetic drugs are not entirely understood in how they work. One example of this is the widely used biguanide oral medication metformin. It is thought to increase sensitivity to insulin by pathways that are yet to be determined. In the UK Prospective Diabetes Study Group (UKPDS), studies were performed on overweight patients with type 2 diabetes. Those treated with metformin had a 42% lower diabetes related mortality compared to a 20% reduction in those treated without. Metformin also showed to be effective in lowering fasting blood glucose levels and AIC levels compared to other treatments.

There have also been recent findings that identify a potential treatment for diabetes not by a synthesized drug, but rather from a peptide that is produced naturally in the pancreas, C-peptide (Figure 1.8). As described earlier, C-peptide is produced with insulin and was believed to have only two functions: to hold the insulin chains together while they fold properly, and to indicate the levels of insulin circulating in the bloodstream. As recently as the early 1990s, C-peptide administration has been shown to alleviate certain complications in type 1 diabetics.[131-133] While the mechanism for C-peptide's action remains unknown and reproducibility of the *in vivo* studies is difficult to achieve, there are findings from the Spence group that identify the

Figure 1.8 – Amino acid sequence of C-peptide with the N-terminus at the top and the C-terminus at the bottom. The sequence illustrated is the 31 amino acid peptide that remains after cleavage from the proinsulin hormone. The 5 negatively charged acidic residues at indicated with an arrow.

presence and necessity of a metal to be with the peptide in order to see activity on human and rabbit red blood cells (RBCs), and bovine pulmonary artery endothelial cells.[134-136]

1.4 Thesis objective

The main goal of the dissertation and the research presented here has been to evaluate a potential connection or link between cancer and diabetes regarding glucose levels and metabolism. There have been numerous observations that type 2 diabetes can lead to increased risks of certain cancer developments. The other observation that obesity can lead to certain cancers provides a convincing argument connecting diabetes and cancer, as most type 2 diabetics are also classified as obese. However, the previously described studies that examine cancer prevalence as a function of fasting blood sugar levels suggests that it may be elevated glucose levels that play a role in cancer development in people with diabetes and not necessarily obesity. With the ideas that cancer utilizes abnormal glucose metabolism and diabetes is symbolized as having too much sugar (hyperglycemia) present, certain experiments evaluating the changes in energy metabolism in healthy cells found in the vasculature caused by changes in glucose concentrations were designed and performed.

The first chapter of this dissertation focuses on C-peptide, which has recently been given more attention based on its ability to improve vascular tone due to increased ATP release from the RBC as well as stimulating eNOS activity. The metal-activated C-peptide, that has multiple effects on the RBC, was applied to endothelial cells to observe whether similar changes in metabolism were stimulated. Stimulated glucose uptake as well as NO production in the endothelial cells upon metal-activated C-peptide administration was evaluated. As the presence

of C-peptide *in vivo* raise as glucose levels increase, any effects that the peptide has on glucose metabolism in normal glucose conditions may be enhanced in hyperglycemic states.

The second chapter looks again at metal-activated C-peptide, this time focusing on the drug metformin that is commonly administered to type 2 diabetics to aid in maintaining proper blood glucose levels. Metformin has been shown to reduce blood sugar levels, while improving certain diabetic complications. There are certain side effects with unknown originating mechanisms associated with the drug treatment, specifically lactic acidosis which is characterized as a buildup of lactate and lowering of basal pH. The potential mechanism by which metformin acts on the RBC in terms of glucose clearance and metabolism is evaluated by expanding on previous findings from the Spence group. The overall metabolism from the RBC is evaluated by measuring the glucose uptake as well as the lactate produced and released from the cells.

The first part of the final chapter expands the findings found in chapter 2, dealing with metformin, by applying the drug to endothelial cells in either normal or hyperglycemic conditions. Endothelial cells are examined due to the fact that they are also exposed to the drug *in vivo*, as they line the inner portion of blood vessels and arteries. The glucose metabolism of the endothelial cells is again measured by looking at the lactate produced and the glucose consumed. In addition to the direct glucose metabolism, other intracellular changes related to an altered metabolic state are monitored.

The later portion of the final chapter directly compares the metabolism that occurs in healthy endothelial cells and cancerous HeLa cells following exposure to different glucose concentrations. Application of specific inhibitors and controlling the extracellular sources of energy available to both types of cells identifies certain metabolic tendencies of cellular

metabolism in both normal and high glucose environments. The combination of observations for both the healthy and cancerous cells should provide some idea of how the metabolism, specifically glucose metabolism, of normal endothelial cells can be altered simply by changing the immediate surroundings, leading to a metabolic profile similar to that of cancerous cell.

REFERENCES

REFERENCES

1. Cerkez, C.; Chandler, J. H.; Chandler, D., Glucose metabolism in multiple sclerosis. *Dis. Nerv. Syst.* **1962,** 23, 377-82.

2. Roelcke, U.; Kappos, L.; Lechner-Scott, J.; Brunnschweiler, H.; Huber, S.; Ammann, W.; Plohmann, A.; Dellas, S.; Maguire, R. P.; Missimer, J.; Radu, E. W.; Steck, A.; Leenders, K. L., Reduced glucose metabolism in the frontal cortex and basal ganglia of multiple sclerosis patients with fatigue: a 18F-fluorodeoxyglucose positron emission tomography study. *Neurology* **1997,** 48, (6), 1566-71.

3. Couce, M.; O'Brien, T. D.; Moran, A.; Roche, P. C.; Butler, P. C., Diabetes mellitus in cystic fibrosis is characterized by islet amyloidosis. *J. Clin. Endocrinol. Metab.* **1996,** 81, (3), 1267-72.

4. Hardin, D. S.; Leblanc, A.; Lukenbaugh, S.; Seilheimer, D. K., Insulin resistance is associated with decreased clinical status in cystic fibrosis. *J. Pediatr.* **1997,** 130, (6), 948-956.

5. Swallow, D. M., Genetics of lactase persistence and lactose intolerance. *Annu. Rev. Genet.* **2003,** 37, 197-219.

6. Isselbacher, K. J.; Anderson, E. P.; Kurahashi, K.; Kalckar, H. M., Congenital galactosemia, a single enzymatic block in galactose metabolism. *Science (New York, N.Y.)* **1956,** 123, (3198), 635-6.

7. Jemal, A.; Siegel, R.; Xu, J.; Ward, E., Cancer statistics, 2010. *CA Cancer J. Clin.* **2010,** 60, (5), 277-300.

8. Hanahan, D.; Weinberg, R. A., The hallmarks of cancer. *Cell* **2000,** 100, (1), 57-70.

9. Hanahan, D.; Weinberg, R. A., Hallmarks of cancer: the next generation. *Cell* **2011,** 144, (5), 646-74.

10. Lehninger, A. L.; Nelson, D. L.; Cox, M. M., *Lehninger principles of biochemistry*. 4th ed.; W.H. Freeman: New York, 2005.

11. Pfeiffer, T.; Schuster, S.; Bonhoeffer, S., Cooperation and competition in the evolution of ATP-producing pathways. *Science (New York, N.Y.)* **2001,** 292, (5516), 504-7.

12. Baggetto, L. G., Deviant energetic metabolism of glycolytic cancer cells. *Biochimie.* **1992,** 74, (11), 959-74.

13. Brahimi-Horn, M. C.; Chiche, J.; Pouyssegur, J., Hypoxia signalling controls metabolic demand. *Curr. Opin. Cell Biol.* **2007,** 19, (2), 223-9.

14. Bustamante, E.; Morris, H. P.; Pedersen, P. L., Energy metabolism of tumor cells. Requirement for a form of hexokinase with a propensity for mitochondrial binding. *J. Biol. Chem.* **1981,** 256, (16), 8699-704.

15. Shaw, R. J., Glucose metabolism and cancer. *Curr. Opin. Cell Biol.* **2006,** 18, (6), 598-608.

16. Baierlein, J. L.; Foster, J. M., Studies on the energy metabolism of human leukocytes. II. Mechanism of the Pasteur effect in human leukocytes. *Blood* **1968,** 32, (3), 412-22.

17. Barker, J.; Khan, M. A.; Solomos, T., Mechanism of the Pasteur effect. *Nature* **1966,** 211, (5048), 547-8.

18. Warburg, O., On the origin of cancer cells. *Science (New York, N.Y.)* **1956,** 123, (3191), 309-14.

19. Warburg, O.; Posener, K.; Negelein, E., Metabolism of carcinoma cells. *Biochemische Zeitschrift* **1924,** 152, 309-44.

20. Warburg, O.; Wind, F.; Negelein, E., The Metabolism of Tumors in the Body. *J. Gen. Physiol.* **1927,** 8, (6), 519-30.

21. Pouyssegur, J.; Dayan, F.; Mazure, N. M., Hypoxia signalling in cancer and approaches to enforce tumour regression. *Nature* **2006,** 441, (7092), 437-43.

22. Gatenby, R. A., The potential role of transformation-induced metabolic changes in tumor-host interaction. *Cancer Res.* **1995,** 55, (18), 4151-6.

23. Gatenby, R. A.; Gawlinski, E. T., A reaction-diffusion model of cancer invasion. *Cancer Res.* **1996,** 56, (24), 5745-53.

24. Gatenby, R. A.; Gawlinski, E. T., The glycolytic phenotype in carcinogenesis and tumor invasion: insights through mathematical models. *Cancer Res.* **2003,** 63, (14), 3847-54.

25. Williams, A. C.; Collard, T. J.; Paraskeva, C., An acidic environment leads to p53 dependent induction of apoptosis in human adenoma and carcinoma cell lines: implications for clonal selection during colorectal carcinogenesis. *Oncogene* **1999,** 18, (21), 3199-204.

26. Park, H. J.; Lyons, J. C.; Ohtsubo, T.; Song, C. W., Acidic environment causes apoptosis by increasing caspase activity. *Br. J. Cancer* **1999,** 80, (12), 1892-7.

27. Koukourakis, M. I.; Giatromanolaki, A.; Harris, A. L.; Sivridis, E., Comparison of metabolic pathways between cancer cells and stromal cells in colorectal carcinomas: a metabolic survival role for tumor-associated stroma. *Cancer Res.* **2006,** 66, (2), 632-7.

28. Lardner, A., The effects of extracellular pH on immune function. *J. Leukoc. Biol.* **2001,** 69, (4), 522-30.

29. Goodman, L. S.; Wintrobe, M. M.; et al., Nitrogen mustard therapy; use of methyl-bis (beta-chloroethyl) amine hydrochloride and tris (beta-chloroethyl) amine hydrochloride for Hodgkin's disease, lymphosarcoma, leukemia and certain allied and miscellaneous disorders. *J. Am. Med. Assoc.* **1946,** 132, 126-32.

30. Farber, S.; Diamond, L. K., Temporary remissions in acute leukemia in children produced by folic acid antagonist, 4-aminopteroyl-glutamic acid. *New Engl. J. Med.* **1948,** 238, (23), 787-93.

31. Frei, E., 3rd; Karon, M.; Levin, R. H.; Freireich, E. J.; Taylor, R. J.; Hananian, J.; Selawry, O.; Holland, J. F.; Hoogstraten, B.; Wolman, I. J.; Abir, E.; Sawitsky, A.; Lee, S.; Mills, S. D.; Burgert, E. O., Jr.; Spurr, C. L.; Patterson, R. B.; Ebaugh, F. G.; James, G. W., 3rd; Moon, J. H., The effectiveness of combinations of antileukemic agents in inducing and maintaining remission in children with acute leukemia. *Blood* **1965,** 26, (5), 642-56.

32. Harris, M., Monoclonal antibodies as therapeutic agents for cancer. *Lancet Oncol.* **2004,** 5, (5), 292-302.

33. Goldenberg, D. M.; Gaffar, S. A.; Bennett, S. J.; Beach, J. L., Experimental radioimmunotherapy of a xenografted human colonic tumor (GW-39) producing carcinoembryonic antigen. *Cancer Res.* **1981,** 41, (11 Pt 1), 4354-60.

34. Witzig, T. E.; White, C. A.; Gordon, L. I.; Wiseman, G. A.; Emmanouilides, C.; Murray, J. L.; Lister, J.; Multani, P. S., Safety of yttrium-90 ibritumomab tiuxetan radioimmunotherapy for relapsed low-grade, follicular, or transformed non-hodgkin's lymphoma. *J. Clin. Oncol.* **2003,** 21, (7), 1263-70.

35. Kreitman, R. J.; Wilson, W. H.; Bergeron, K.; Raggio, M.; Stetler-Stevenson, M.; FitzGerald, D. J.; Pastan, I., Efficacy of the anti-CD22 recombinant immunotoxin BL22 in chemotherapy-resistant hairy-cell leukemia. *New Engl. J. Med.* **2001,** 345, (4), 241-7.

36. Knight, Z. A.; Shokat, K. M., Features of selective kinase inhibitors. *Chem Biol* **2005,** 12, (6), 621-37.

37. Cohen, P., The development and therapeutic potential of protein kinase inhibitors. *Curr. Opin. Chem. Biol.* **1999,** 3, (4), 459-65.

38. Capdeville, R.; Buchdunger, E.; Zimmermann, J.; Matter, A., Glivec (STI571, imatinib), a rationally developed, targeted anticancer drug. *Nat. Rev. Drug Discov.* **2002,** 1, (7), 493-502.

39. Stacpoole, P. W.; Lorenz, A. C.; Thomas, R. G.; Harman, E. M., Dichloroacetate in the treatment of lactic acidosis. *Ann. Intern. Med.* **1988,** 108, (1), 58-63.

40. Bonnet, S.; Archer, S. L.; Allalunis-Turner, J.; Haromy, A.; Beaulieu, C.; Thompson, R.; Lee, C. T.; Lopaschuk, G. D.; Puttagunta, L.; Harry, G.; Hashimoto, K.; Porter, C. J.; Andrade, M. A.; Thebaud, B.; Michelakis, E. D., A mitochondria-K+ channel axis is

suppressed in cancer and its normalization promotes apoptosis and inhibits cancer growth. *Cancer Cell* **2007,** 11, (1), 37-51.

41. Koukourakis, M. I.; Giatromanolaki, A.; Sivridis, E.; Gatter, K. C.; Harris, A. L., Pyruvate dehydrogenase and pyruvate dehydrogenase kinase expression in non small cell lung cancer and tumor-associated stroma. *Neoplasia* **2005,** 7, (1), 1-6.

42. Michelakis, E. D.; Sutendra, G.; Dromparis, P.; Webster, L.; Haromy, A.; Niven, E.; Maguire, C.; Gammer, T. L.; Mackey, J. R.; Fulton, D.; Abdulkarim, B.; McMurtry, M. S.; Petruk, K. C., Metabolic modulation of glioblastoma with dichloroacetate. *Sci. Transl Med* **2010,** 2, (31), 31ra34.

43. Ristow, M.; Pfister, M. F.; Yee, A. J.; Schubert, M.; Michael, L.; Zhang, C. Y.; Ueki, K.; Michael, M. D., 2nd; Lowell, B. B.; Kahn, C. R., Frataxin activates mitochondrial energy conversion and oxidative phosphorylation. *P. Natl. Acad. Sci. USA* **2000,** 97, (22), 12239-43.

44. Schulz, T. J.; Thierbach, R.; Voigt, A.; Drewes, G.; Mietzner, B.; Steinberg, P.; Pfeiffer, A. F.; Ristow, M., Induction of oxidative metabolism by mitochondrial frataxin inhibits cancer growth: Otto Warburg revisited. *J. Biol. Chem.* **2006,** 281, (2), 977-81.

45. Hamilton, A. S.; Mack, T. M., Puberty and genetic susceptibility to breast cancer in a case-control study in twins. *New Engl. J. Med.* **2003,** 348, (23), 2313-22.

46. Harris, A. L., Hypoxia--a key regulatory factor in tumour growth. *Nat. Rev. Cancer* **2002,** 2, (1), 38-47.

47. Semenza, G. L., Hypoxia-inducible factor 1 (HIF-1) pathway. *Sci. STKE* **2007,** 2007, (407), cm8.

48. Kim, J. W.; Tchernyshyov, I.; Semenza, G. L.; Dang, C. V., HIF-1-mediated expression of pyruvate dehydrogenase kinase: a metabolic switch required for cellular adaptation to hypoxia. *Cell Metab.* **2006,** 3, (3), 177-85.

49. Papandreou, I.; Cairns, R. A.; Fontana, L.; Lim, A. L.; Denko, N. C., HIF-1 mediates adaptation to hypoxia by actively downregulating mitochondrial oxygen consumption. *Cell Metab.* **2006,** 3, (3), 187-97.

50. Flier, J. S.; Mueckler, M. M.; Usher, P.; Lodish, H. F., Elevated levels of glucose transport and transporter messenger RNA are induced by ras or src oncogenes. *Science (New York, N.Y.)* **1987,** 235, (4795), 1492-5.

51. Mathupala, S. P.; Rempel, A.; Pedersen, P. L., Glucose catabolism in cancer cells. Isolation, sequence, and activity of the promoter for type II hexokinase. *J. Biol. Chem.* **1995,** 270, (28), 16918-25.

52. Rempel, A.; Bannasch, P.; Mayer, D., Differences in expression and intracellular distribution of hexokinase isoenzymes in rat liver cells of different transformation stages. *Biochim. Biophys. Acta* **1994,** 1219, (3), 660-8.

53. Kim, J. W.; Gao, P.; Liu, Y. C.; Semenza, G. L.; Dang, C. V., Hypoxia-inducible factor 1 and dysregulated c-Myc cooperatively induce vascular endothelial growth factor and metabolic switches hexokinase 2 and pyruvate dehydrogenase kinase 1. *Mol. Cell. Biol.* **2007,** 27, (21), 7381-93.

54. Horn, H. F.; Vousden, K. H., Coping with stress: multiple ways to activate p53. *Oncogene* **2007,** 26, (9), 1306-16.

55. Schwartz, D.; Rotter, V., p53-dependent cell cycle control: response to genotoxic stress. *Semin. Cancer Biol.* **1998,** 8, (5), 325-36.

56. Zhao, Y.; Coloff, J. L.; Ferguson, E. C.; Jacobs, S. R.; Cui, K.; Rathmell, J. C., Glucose metabolism attenuates p53 and Puma-dependent cell death upon growth factor deprivation. *J. Biol. Chem.* **2008,** 283, (52), 36344-53.

57. Mucci, L. A.; Wedren, S.; Tamimi, R. M.; Trichopoulos, D.; Adami, H. O., The role of gene-environment interaction in the aetiology of human cancer: examples from cancers of the large bowel, lung and breast. *J. Intern. Med.* **2001,** 249, (6), 477-93.

58. Denissenko, M. F.; Pao, A.; Tang, M.; Pfeifer, G. P., Preferential formation of benzo[a]pyrene adducts at lung cancer mutational hotspots in P53. *Science (New York, N.Y.)* **1996,** 274, (5286), 430-2.

59. Anto, R. J.; Mukhopadhyay, A.; Shishodia, S.; Gairola, C. G.; Aggarwal, B. B., Cigarette smoke condensate activates nuclear transcription factor-kappaB through phosphorylation and degradation of IkappaB(alpha): correlation with induction of cyclooxygenase-2. *Carcinogenesis* **2002,** 23, (9), 1511-8.

60. Tuyns, A. J.; Pequignot, G.; Abbatucci, J. S., Oesophageal cancer and alcohol consumption; importance of type of beverage. *Int. J. Cancer* **1979,** 23, (4), 443-7.

61. Longnecker, M. P.; Newcomb, P. A.; Mittendorf, R.; Greenberg, E. R.; Clapp, R. W.; Bogdan, G. F.; Baron, J.; MacMahon, B.; Willett, W. C., Risk of breast cancer in relation to lifetime alcohol consumption. *J. Natl. Cancer Inst.* **1995,** 87, (12), 923-9.

62. Poschl, G.; Stickel, F.; Wang, X. D.; Seitz, H. K., Alcohol and cancer: genetic and nutritional aspects. *Proc. Nutr. Soc.* **2004,** 63, (1), 65-71.

63. Kuratsune, M.; Kohchi, S.; Horie, A., Carcinogenesis in the Esophagus. I. Penetration of Benzo(a) Pyrene and Other Hydrocarbons into the Esophageal Mucosa. *Gann* **1965,** 56, 177-87.

64. Song, S.; Pitot, H. C.; Lambert, P. F., The human papillomavirus type 16 E6 gene alone is sufficient to induce carcinomas in transgenic animals. *J. Virol.* **1999,** 73, (7), 5887-93.

65. Hagen, T. M.; Huang, S.; Curnutte, J.; Fowler, P.; Martinez, V.; Wehr, C. M.; Ames, B. N.; Chisari, F. V., Extensive oxidative DNA damage in hepatocytes of transgenic mice with chronic active hepatitis destined to develop hepatocellular carcinoma. *P. Natl. Acad. Sci. USA* **1994,** 91, (26), 12808-12.

66. Belpomme, D.; Irigaray, P.; Hardell, L.; Clapp, R.; Montagnier, L.; Epstein, S.; Sasco, A. J., The multitude and diversity of environmental carcinogens. *Environ. Res.* **2007,** 105, (3), 414-29.

67. Doll, R.; Peto, R., The causes of cancer: quantitative estimates of avoidable risks of cancer in the United States today. *J. Natl. Cancer Inst.* **1981,** 66, (6), 1191-308.

68. Sasaki, Y. F.; Kawaguchi, S.; Kamaya, A.; Ohshita, M.; Kabasawa, K.; Iwama, K.; Taniguchi, K.; Tsuda, S., The comet assay with 8 mouse organs: results with 39 currently used food additives. *Mutat. Res.* **2002,** 519, (1-2), 103-19.

69. Durando, M.; Kass, L.; Piva, J.; Sonnenschein, C.; Soto, A. M.; Luque, E. H.; Munoz-de-Toro, M., Prenatal bisphenol A exposure induces preneoplastic lesions in the mammary gland in Wistar rats. *Environ. Health Perspect.* **2007,** 115, (1), 80-6.

70. Ho, S. M.; Tang, W. Y.; Belmonte de Frausto, J.; Prins, G. S., Developmental exposure to estradiol and bisphenol A increases susceptibility to prostate carcinogenesis and epigenetically regulates phosphodiesterase type 4 variant 4. *Cancer Res.* **2006,** 66, (11), 5624-32.

71. Calle Eugenia, E.; Rodriguez, C.; Walker-Thurmond, K.; Thun Michael, J., Overweight, obesity, and mortality from cancer in a prospectively studied cohort of U.S. adults. *The New England journal of medicine* **2003,** 348, (17), 1625-38.

72. Irigaray, P.; Newby, J. A.; Lacomme, S.; Belpomme, D., Overweight/obesity and cancer genesis: More than a biological link. *Biomed. Pharmacother.* **2007,** 61, (10), 665-678.

73. Standards of medical care in diabetes--2010. *Diabetes Care* **2010,** 33 Suppl 1, S11-61.

74. Diagnosis and classification of diabetes mellitus. *Diabetes Care* **2010,** 33 Suppl 1, S62-9.

75. Filippi, C. M.; von Herrath, M. G., Viral trigger for type 1 diabetes: pros and cons. *Diabetes* **2008,** 57, (11), 2863-71.

76. Karjalainen, J.; Martin, J. M.; Knip, M.; Ilonen, J.; Robinson, B. H.; Savilahti, E.; Akerblom, H. K.; Dosch, H. M., A bovine albumin peptide as a possible trigger of insulin-dependent diabetes mellitus. *New Engl. J. Med.* **1992,** 327, (5), 302-7.

77. Tillil, H.; Shapiro, E. T.; Given, B. D.; Rue, P.; Rubenstein, A. H.; Galloway, J. A.; Polonsky, K. S., Reevaluation of urine C-peptide as measure of insulin secretion. *Diabetes* **1988,** 37, (9), 1195-201.

78. Nathan, D. M., Clinical practice. Initial management of glycemia in type 2 diabetes mellitus. *New Engl. J. Med.* **2002,** 347, (17), 1342-9.

79. Bonner-Weir, S.; O'Brien, T. D., Islets in type 2 diabetes: in honor of Dr. Robert C. Turner. *Diabetes* **2008,** 57, (11), 2899-904.

80. Johnson, K. H.; Bazargan, M.; Cherpitel, C. J., Alcohol, tobacco, and drug use and the onset of type 2 diabetes among inner-city minority patients. *J. Am. Board Fam. Pract.* **2001,** 14, (6), 430-6.

81. Engelgau, M. M.; Herman, W. H.; Smith, P. J.; German, R. R.; Aubert, R. E., The epidemiology of diabetes and pregnancy in the U.S., 1988. *Diabetes Care* **1995,** 18, (7), 1029-33.

82. Boden, G., Fuel metabolism in pregnancy and in gestational diabetes mellitus. *Obstet. Gynecol. Clin. North Am.* **1996,** 23, (1), 1-10.

83. Ryan, E. A., Pregnancy in diabetes. *Med. Clin. North Am.* **1998,** 82, (4), 823-45.

84. Hepburn, D. A.; Deary, I. J.; Frier, B. M.; Patrick, A. W.; Quinn, J. D.; Fisher, B. M., Symptoms of acute insulin-induced hypoglycemia in humans with and without IDDM. Factor-analysis approach. *Diabetes Care* **1991,** 14, (11), 949-57.

85. Poretsky, L., *Principles of diabetes mellitus*. Kluwer Academic Publishers: Boston, 2002; p 784 p.

86. Airey, M.; Bennett, C.; Nicolucci, A.; Williams, R., Aldose reductase inhibitors for the prevention and treatment of diabetic peripheral neuropathy. *Cochrane Database Syst. Rev.* **2000**, (2), CD002182.

87. Low, P. A.; Schmelzer, J. D.; Ward, K. K.; Curran, G. L.; Poduslo, J. F., Effect of hyperbaric oxygenation on normal and chronic streptozotocin diabetic peripheral nerves. *Exp. Neurol.* **1988,** 99, (1), 201-12.

88. Scott, I. U.; Flynn, H. W.; Smiddy, W. E.; American Academy of Ophthalmology., *Diabetes and ocular disease : past, present, and future therapies*. 2nd ed.; Oxford University Press in cooperation with the American Academy of Ophthalmology: Oxford ; New York, 2010; p xv, 496 p.

89. Pierce, E. A.; Avery, R. L.; Foley, E. D.; Aiello, L. P.; Smith, L. E., Vascular endothelial growth factor/vascular permeability factor expression in a mouse model of retinal neovascularization. *P. Natl. Acad. Sci. USA* **1995,** 92, (3), 905-9.

90. Bennett, P. H.; Haffner, S.; Kasiske, B. L.; Keane, W. F.; Mogensen, C. E.; Parving, H. H.; Steffes, M. W.; Striker, G. E., Screening and management of microalbuminuria in patients with diabetes mellitus: recommendations to the Scientific Advisory Board of the National Kidney Foundation from an ad hoc committee of the Council on Diabetes Mellitus of the National Kidney Foundation. *Am. J. Kidney Dis.* **1995,** 25, (1), 107-12.

91. McFarlane, S. I.; Banerji, M.; Sowers, J. R., Insulin resistance and cardiovascular disease. *J. Clin. Endocrinol. Metab.* **2001,** 86, (2), 713-8.

92. Stephens, J. W.; Khanolkar, M. P.; Bain, S. C., The biological relevance and measurement of plasma markers of oxidative stress in diabetes and cardiovascular disease. *Atherosclerosis* **2009,** 202, (2), 321-9.

93. Carpenter, M. W., Gestational diabetes, pregnancy hypertension, and late vascular disease. *Diabetes Care* **2007,** 30 Suppl 2, S246-50.

94. Richardson, A. C.; Carpenter, M. W., Inflammatory mediators in gestational diabetes mellitus. *Obstet. Gynecol. Clin. North Am.* **2007,** 34, (2), 213-24, viii.

95. Devasagayam, T. P.; Tilak, J. C.; Boloor, K. K.; Sane, K. S.; Ghaskadbi, S. S.; Lele, R. D., Free radicals and antioxidants in human health: current status and future prospects. *J. Assoc. Physicians India* **2004,** 52, 794-804.

96. Davies, K. J., Oxidative stress: the paradox of aerobic life. *Biochem. Soc. Symp.* **1995,** 61, 1-31.

97. Quijano, C.; Castro, L.; Peluffo, G.; Valez, V.; Radi, R., Enhanced mitochondrial superoxide in hyperglycemic endothelial cells: direct measurements and formation of hydrogen peroxide and peroxynitrite. *Am. J. Physiol. Heart Circ. Physiol.* **2007,** 293, (6), H3404-14.

98. Brownlee, M., Biochemistry and molecular cell biology of diabetic complications. *Nature* **2001,** 414, (6865), 813-20.

99. Evans, J. L.; Goldfine, I. D.; Maddux, B. A.; Grodsky, G. M., Oxidative stress and stress-activated signaling pathways: a unifying hypothesis of type 2 diabetes. *Endocr. Rev.* **2002,** 23, (5), 599-622.

100. Lipinski, B., Pathophysiology of oxidative stress in diabetes mellitus. *J. Diabet. Complications* **2001,** 15, (4), 203-10.

101. Hwang, Y. C.; Kaneko, M.; Bakr, S.; Liao, H.; Lu, Y.; Lewis, E. R.; Yan, S.; Ii, S.; Itakura, M.; Rui, L.; Skopicki, H.; Homma, S.; Schmidt, A. M.; Oates, P. J.; Szabolcs, M.; Ramasamy, R., Central role for aldose reductase pathway in myocardial ischemic injury. *FASEB J.* **2004,** 18, (11), 1192-9.

102. Du, X. L.; Edelstein, D.; Rossetti, L.; Fantus, I. G.; Goldberg, H.; Ziyadeh, F.; Wu, J.; Brownlee, M., Hyperglycemia-induced mitochondrial superoxide overproduction activates the hexosamine pathway and induces plasminogen activator inhibitor-1 expression by increasing Sp1 glycosylation. *P. Natl. Acad. Sci. USA* **2000,** 97, (22), 12222-6.

103. Federici, M.; Menghini, R.; Mauriello, A.; Hribal, M. L.; Ferrelli, F.; Lauro, D.; Sbraccia, P.; Spagnoli, L. G.; Sesti, G.; Lauro, R., Insulin-dependent activation of endothelial nitric

oxide synthase is impaired by O-linked glycosylation modification of signaling proteins in human coronary endothelial cells. *Circulation* **2002,** 106, (4), 466-72.

104. Way, K. J.; Katai, N.; King, G. L., Protein kinase C and the development of diabetic vascular complications. *Diabetic Med.* **2001,** 18, (12), 945-59.

105. Neeper, M.; Schmidt, A. M.; Brett, J.; Yan, S. D.; Wang, F.; Pan, Y. C.; Elliston, K.; Stern, D.; Shaw, A., Cloning and expression of a cell surface receptor for advanced glycosylation end products of proteins. *J. Biol. Chem.* **1992,** 267, (21), 14998-5004.

106. Bierhaus, A.; Schiekofer, S.; Schwaninger, M.; Andrassy, M.; Humpert, P. M.; Chen, J.; Hong, M.; Luther, T.; Henle, T.; Kloting, I.; Morcos, M.; Hofmann, M.; Tritschler, H.; Weigle, B.; Kasper, M.; Smith, M.; Perry, G.; Schmidt, A. M.; Stern, D. M.; Haring, H. U.; Schleicher, E.; Nawroth, P. P., Diabetes-associated sustained activation of the transcription factor nuclear factor-kappaB. *Diabetes* **2001,** 50, (12), 2792-808.

107. Hunt, B. J., The endothelium in atherogenesis. *Lupus* **2000,** 9, (3), 189-93.

108. Aird, W. C., *Endothelial biomedicine*. Cambridge University Press: Cambridge ; New York, 2007; p xl, 1856 p., 24 p. of plates.

109. Cameron, N. E.; Eaton, S. E.; Cotter, M. A.; Tesfaye, S., Vascular factors and metabolic interactions in the pathogenesis of diabetic neuropathy. *Diabetologia* **2001,** 44, (11), 1973-88.

110. Bierhaus, A.; Haslbeck, K. M.; Humpert, P. M.; Liliensiek, B.; Dehmer, T.; Morcos, M.; Sayed, A. A.; Andrassy, M.; Schiekofer, S.; Schneider, J. G.; Schulz, J. B.; Heuss, D.; Neundorfer, B.; Dierl, S.; Huber, J.; Tritschler, H.; Schmidt, A. M.; Schwaninger, M.; Haering, H. U.; Schleicher, E.; Kasper, M.; Stern, D. M.; Arnold, B.; Nawroth, P. P., Loss of pain perception in diabetes is dependent on a receptor of the immunoglobulin superfamily. *J. Clin. Invest.* **2004,** 114, (12), 1741-51.

111. Vigneri, P.; Frasca, F.; Sciacca, L.; Pandini, G.; Vigneri, R., Diabetes and cancer. *Endocr. Relat. Cancer* **2009,** 16, (4), 1103-23.

112. Larsson, S. C.; Mantzoros, C. S.; Wolk, A., Diabetes mellitus and risk of breast cancer: a meta-analysis. *Int. J. Cancer* **2007,** 121, (4), 856-62.

113. Giovannucci, E.; Harlan, D. M.; Archer, M. C.; Bergenstal, R. M.; Gapstur, S. M.; Habel, L. A.; Pollak, M.; Regensteiner, J. G.; Yee, D., Diabetes and cancer: a consensus report. *Diabetes Care* **2010,** 33, (7), 1674-85.

114. Physical activity decreases cancer risk. Exercise may help prevent the development of certain cancers, notably colon and breast, numerous studies show. *Duke Med. Health News* **2008,** 14, (5), 9-10.

115. Charatan, F., Exercise and diet reduce risk of diabetes, US study shows. *BMJ (Clinical research ed.)* **2001,** 323, (7309), 359.

116. Foy, C. G.; Bell, R. A.; Farmer, D. F.; Goff, D. C., Jr.; Wagenknecht, L. E., Smoking and incidence of diabetes among U.S. adults: findings from the Insulin Resistance Atherosclerosis Study. *Diabetes Care* **2005,** 28, (10), 2501-7.

117. Mardilovich, K.; Pankratz, S. L.; Shaw, L. M., Expression and function of the insulin receptor substrate proteins in cancer. *Cell Commun. Signal* **2009,** 7, 14.

118. Powell, D. R.; Suwanichkul, A.; Cubbage, M. L.; DePaolis, L. A.; Snuggs, M. B.; Lee, P. D., Insulin inhibits transcription of the human gene for insulin-like growth factor-binding protein-1. *J. Biol. Chem.* **1991,** 266, (28), 18868-76.

119. van Kruijsdijk, R. C.; van der Wall, E.; Visseren, F. L., Obesity and cancer: the role of dysfunctional adipose tissue. *Cancer Epidemiol. Biomarkers Prev.* **2009,** 18, (10), 2569-78.

120. Ulisse, S.; Baldini, E.; Sorrenti, S.; D'Armiento, M., The urokinase plasminogen activator system: a target for anti-cancer therapy. *Curr. Cancer Drug Targets* **2009,** 9, (1), 32-71.

121. Yu, H.; Pardoll, D.; Jove, R., STATs in cancer inflammation and immunity: a leading role for STAT3. *Nat. Rev. Cancer* **2009,** 9, (11), 798-809.

122. Heuson, J. C.; Legros, N., Influence of insulin deprivation on growth of the 7,12-dimethylbenz(a)anthracene-induced mammary carcinoma in rats subjected to alloxan diabetes and food restriction. *Cancer Res.* **1972,** 32, (2), 226-32.

123. Jee, S. H.; Ohrr, H.; Sull, J. W.; Yun, J. E.; Ji, M.; Samet, J. M., Fasting serum glucose level and cancer risk in Korean men and women. *JAMA* **2005,** 293, (2), 194-202.

124. Major, C. A.; Henry, M. J.; De Veciana, M.; Morgan, M. A., The effects of carbohydrate restriction in patients with diet-controlled gestational diabetes. *Obstet. Gynecol.* **1998,** 91, (4), 600-4.

125. Kuczmarski, R. J.; Flegal, K. M.; Campbell, S. M.; Johnson, C. L., Increasing prevalence of overweight among US adults. The National Health and Nutrition Examination Surveys, 1960 to 1991. *JAMA* **1994,** 272, (3), 205-11.

126. Goodyear, L. J.; King, P. A.; Hirshman, M. F.; Thompson, C. M.; Horton, E. D.; Horton, E. S., Contractile activity increases plasma membrane glucose transporters in absence of insulin. *Am. J. Physiol.* **1990,** 258, (4 Pt 1), E667-72.

127. The effect of intensive treatment of diabetes on the development and progression of long-term complications in insulin-dependent diabetes mellitus. The Diabetes Control and Complications Trial Research Group. *New Engl. J. Med.* **1993,** 329, (14), 977-86.

128. Aguilar-Bryan, L.; Nichols, C. G.; Wechsler, S. W.; Clement, J. P. t.; Boyd, A. E., 3rd; Gonzalez, G.; Herrera-Sosa, H.; Nguy, K.; Bryan, J.; Nelson, D. A., Cloning of the beta cell high-affinity sulfonylurea receptor: a regulator of insulin secretion. *Science (New York, N.Y.)* **1995,** 268, (5209), 423-6.

129. Petrie, J.; Small, M.; Connell, J., "Glitazones", a prospect for non-insulin-dependent diabetes. *Lancet* **1997,** 349, (9045), 70-1.

130. Acarbose for diabetes mellitus. *Med. Lett. Drugs Ther.* **1996,** 38, (967), 9-10.

131. Johansson, B. L.; Sjoeberg, S.; Wahren, J., The influence of human C-peptide on renal function and glucose utilization in type 1 (insulin-dependent) diabetic patients. *Diabetologia* **1992,** 35, (2), 121-8.

132. Wahren, J.; Ekberg, K.; Samnegard, B.; Johansson, B. L., C-peptide: a new potential in the treatment of diabetic nephropathy. *Curr. Diab. Rep.* **2001,** 1, (3), 261-6.

133. Hansen, A.; Johansson, B. L.; Wahren, J.; von Bibra, H., C-peptide exerts beneficial effects on myocardial blood flow and function in patients with type 1 diabetes. *Diabetes* **2002,** 51, (10), 3077-82.

134. Meyer, J. A.; Subasinghe, W.; Sima, A. A.; Keltner, Z.; Reid, G. E.; Daleke, D.; Spence, D. M., Zinc-activated C-peptide resistance to the type 2 diabetic erythrocyte is associated with hyperglycemia-induced phosphatidylserine externalization and reversed by metformin. *Mol. Biosyst.* **2009,** 5, (10), 1157-62.

135. Meyer, J. A.; Froelich, J. M.; Reid, G. E.; Karunarathne, W. K.; Spence, D. M., Metal-activated C-peptide facilitates glucose clearance and the release of a nitric oxide stimulus via the GLUT1 transporter. *Diabetologia* **2008,** 51, (1), 175-82.

136. Medawala, W.; McCahill, P.; Giebink, A.; Meyer, J.; Ku, C. J.; Spence, D. M., A Molecular Level Understanding of Zinc Activation of C-peptide and its Effects on Cellular Communication in the Bloodstream. *Rev. Diabet. Stud.* **2009,** 6, (3), 148-58.

CHAPTER 2: DIRECT AND INDIRECT EFFECTS OF METAL-ACTIVATED C-PEPTIDE ON ENDOTHELIAL CELL METABOLISM

2.1 C-peptide and diabetes

C-peptide is a 31 amino acid peptide that is produced in the beta cells of the pancreas and released into the bloodstream in equimolar amounts with the hormone insulin.[1, 2] In the beta cells that are specifically located on the Islets of Langerhans, C-peptide is part of the proinsulin prohormone molecule and is responsible for facilitating the folding of the insulin molecule by connecting the A and B chains.[3-5] Upon completion of the folding process, C-peptide is enzymatically cleaved from the proinsulin molecule and secreted with insulin from the pancreas. After the discovery of the C-peptide molecule in the 1960s, subsequent research suggested that the peptide had no biological significance following its release into the bloodstream.[6] In fact, C-peptide's only significant role was that of a 'biomarker' for insulin, used as a determinant for the concentration of circulating insulin in the blood due to the longer half-life *in vivo*, and because it is released in equimolar quantities.[7-9] However, since the 1990s studies have identified C-peptide as a significant bioactive peptide that shows important beneficial effects on different tissues, blood flow, organs, and vascular cells in people with diabetic complications.

C-peptide replacement therapy in people with type 1 diabetes has been shown to improve certain conditions that are hallmarks of early and advanced stage diabetes. Renal function and glucose utilization have been shown to be improved in people with type 1 diabetes when C-peptide therapy is administered.[10-15] Improvements in nerve function and diabetic neuropathy

in rat models have been observed following C-peptide administration.[16-18] It is proposed that the improvements in nerve function are a direct result of improved vascular function and blood flow. These improvements in blood flow have been studied and observed specifically in the forearm and skin.[19-23] While the exact mechanism of C-peptide's ability to improve blood flow and specific diabetic conditions remains unknown, there have been recent findings that identify certain effects that the peptide has on two significant cell types found in the vasculature; the red blood cell (RBC) and the endothelium.

2.2 Interaction between the endothelium and the RBC

The RBC is believed to play a significant role in maintaining proper blood flow/circulation through its ability to release ATP and stimulate NO production in the endothelium. The endothelium is the layer of cells that line the innermost portion of blood vessels, thus exposing the cells to any stimuli that may be released by the RBC. The ATP stimulates eNOS activity upon binding to specific purinergic receptors on the endothelial cell's surface, subsequently generating NO that is able to diffuse to the smooth muscle cells. Once the NO reaches the smooth muscle cells, it activates the enzyme soluble guanylyl cyclase (sGC), generates increased guanosine monophosphate (cGMP) levels through conversion from guanosine triphosphate (GTP), leading to the observed relaxation and dilation.[24] The possible interaction between the two cell types and subsequent vasodilation is illustrated in Figure 2.1. This hypothesis of RBC mediated NO production is supported by the findings that the RBCs

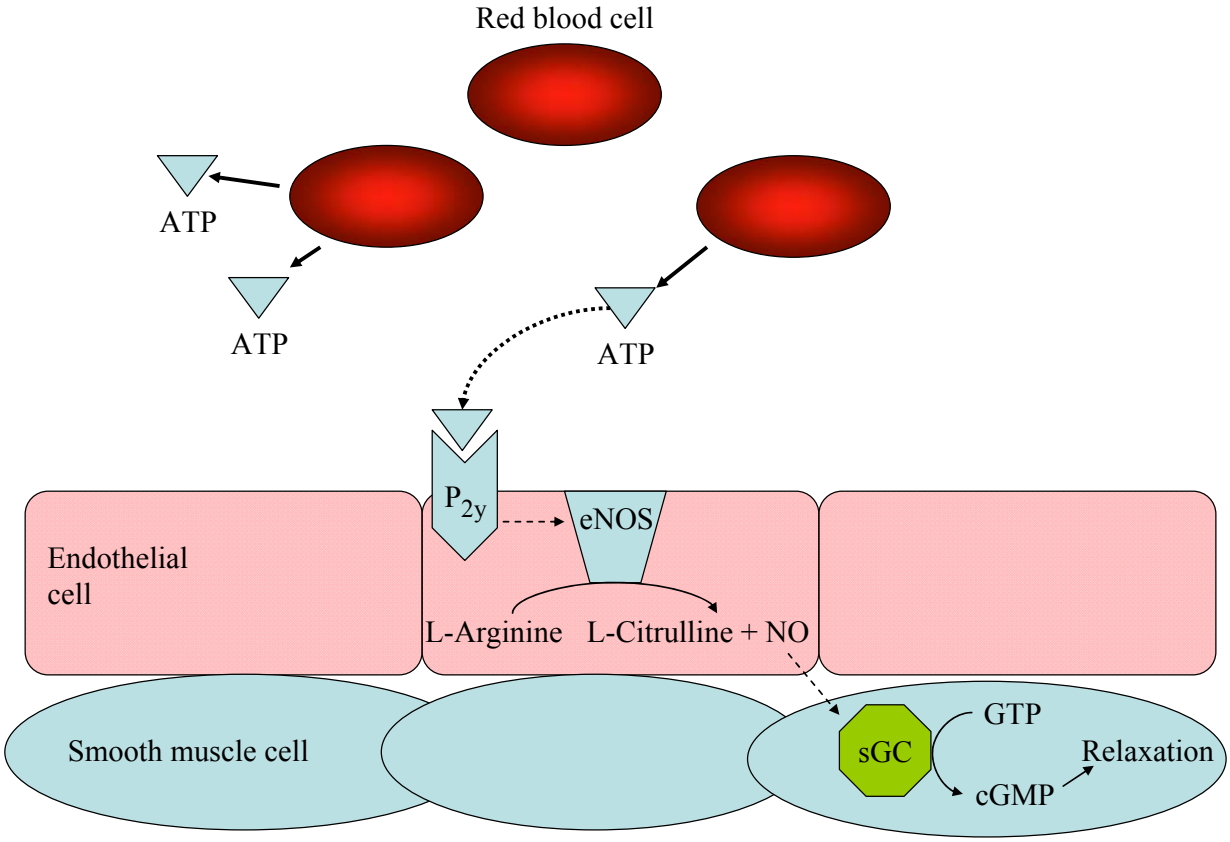

Figure 2.1 – Diagram illustrating RBC stimulated vasorelaxation. ATP released from the RBC is able to diffuse and bind to the P_{2y} purinergic receptors on the endothelial cells. The binding of ATP to the receptors activate endothelial nitric oxide synthase (eNOS), converting L-arginine into L-Citrulline and nitric oxide (NO). NO is able to diffuse to the smooth muscle cells, and activate soluble guanylyl cyclase (sGC). Guanosine triphosphate (GTP) is converted into cyclic guanosine monophosphate (cGMP), which causes the relaxation of the muscle and facilitates dilation.

have high intracellular concentrations of ATP[25, 26] which is released under certain conditions such as hypoxia[27-29] or deformability arising from mechanical deformation in resistance vessels.[30]

It has been shown that people with both type 1 and 2 diabetes have RBCs with reduced deformability, one cause possibly arising from reduced Na^+,K^+-ATPase activity.[31, 32] These diabetic RBCs have been shown to release less ATP due to their lack of deformability.[33] Following administration of C-peptide, the impaired deformability of the diabetic RBCs is reversed and the Na^+,K^+-ATPase is partially repaired.[16, 17, 34] This increased deformability can lead to an increased ATP release from the diabetic RBCs.[35, 36] In fact, those same reports from Meyer et al. indicate that C-peptide requires the presence of a metal in order to produce the increased ATP release levels from healthy and RBCs from people who have diabetes.[35, 36] While it does appear possible that the increased ATP release from the RBCs following C-peptide administration will lead to eNOS activation and subsequent NO production, there have been reports indicating that C-peptide acts directly on the endothelium.

Specific *in vitro* studies have recently examined both a direct and indirect means by which C-peptide is able to stimulate NO production in immobilized bovine aortic endothelial cells (BAECs). One study examined how C-peptide directly stimulates NO production via an increased calcium influx immediately following exposure to physiological concentrations of the peptide.[37] An additional study identified C-peptide's ability to increase the eNOS gene transcription, thereby increasing the expression of the eNOS protein.[38] This is believed to

happen through the activation of an extracellular signal-regulated mitogen activated protein kinase (ERK).[38]

2.3 Endothelial cell glucose uptake

In addition to generating the NO that participates in the regulation of vascular tone and blood flow, the endothelium also contributes to the glucose clearance from the bloodstream. Endothelial cells primarily utilize the GLUT1 isoform of the glucose transport proteins to transfer the glucose from the extracellular space to the cytosol through passive diffusion.[39-41] In fact, GLUT1 is the glucose transporter used by the RBCs to transport glucose. The prevalence of GLUT1 in vascular components leads the specific isoform to be responsible for transporting the majority of glucose that is adsorbed by tissues in body.[42] While glucose transport through GLUT1 is insulin independent, some endothelial cells do express specific insulin receptors.[43, 44] As previously described, insulin receptors stimulate GLUT4 externalization and glycogen synthase. It is believed that insulin does not stimulate glucose uptake into endothelial cells under normal glycemic conditions. However, there are mixed reports whether or not initiates glucose uptake into endothelial cells in hyperglycemic conditions.[44, 45] The same hyperglycemic conditions have been shown to downregulate the expression of GLUT1 in vascular endothelial cells as a means to maintain intracellular glucose levels.[39, 40, 46]

The work presented here aims to identify some novel roles that C-peptide, specifically metal-activated C-peptide, has on the endothelium in both glucose uptake and NO production.

Motivated by previous results showing increased glucose uptake into RBCs upon metal-activated C-peptide administration,[35, 36] and that GLUT1 is the primary glucose transporter in both the RBC and endothelial cell, it was hypothesized that the glucose uptake in the endothelium can be stimulated by C-peptide. In addition, the past work demonstrating C-peptide's direct stimulation of eNOS activity and increased ATP release from the RBC led to the idea that the metal-activated form of C-peptide could stimulate eNOS activity by means of an RBC mediated mechanism.

2.4 Experimental

2.4.1 Preparation of reagents

Unless stated otherwise, all aqueous stock and working solutions were prepared using purified (18.2 MΩ) double-distilled water (DDW). All reagents that were prepared in volumetric glassware were transferred to polypropylene tubes immediately to reduce the metal contamination.

Crude human C-peptide (Genscript, Piscataway, NJ) was purified using a reverse phase high performance liquid chromatography (RP-HPLC) system.[47] Briefly, 20 mg of the crude C-peptide were dissolved in minimal DDW, followed by dropwise addition of acetonitrile to completely dissolve the solid. The separation was then performed using a non-linear gradient with 5 mL fractions collected manually at different time points within the gradient. The fractions were then analyzed for purity using matrix assisted laser desorption ionization (MALDI) coupled to an ion-trap detection scheme. Fractions containing the purest form of the peptide were

collected and freeze dried (lyophilized) overnight in polypropylene tubes. The dried peptide was then weighed and dissolved in enough DDW to have a concentration of 1000 μg/mL. The solution was then aliquotted into microfuge vials, each containing 250 μL of the C-peptide solution (250 μg C-peptide), and vacuum dried, leaving the solid peptide behind. Vials were stored dry at -20°C until needed. Stock solutions of C-peptide were prepared by dissolving 250 μg in 10 mL of DDW for a final concentration of 8.3 μM.

Zinc (Zn^{2+}) solutions were prepared by dissolving 10.0 mg zinc chloride (Jade Scientific, Canton, MI) in 500 mL DDW to achieve a stock concentration of 147 μM. That stock solution is then diluted to working concentrations of 8.3 μM.

A radiolabeled analogue of glucose, D-glucose $^{14}C(U)$ (Moravek Biochemicals and Radiochemicals, Brea, CA) was used for the glucose uptake studies. The concentration of the ^{14}C-glucose was 0.1 millicuries (mCi)/mL, with a specific activity of 200 mCi/mmol. A 10 mg/mL (1.72 mM) insulin solution (Sigma Aldrich, St. Louis, MO) buffered with 25 mM HEPES that had no zinc was used to prepare 1 mL working solutions of 20 and 1000 μM. Phloretin (Enzo Life Sciences, Farmingdale, NY) was prepared by dissolving 200 mg in 5 mL of ethanol to achieve a 146 mM stock concentration.

ATP (Sigma Aldrich) for the calcium uptake and NO production studies was prepared by dissolving 20 mg in 1 mL of DDW, resulting in a 36.3 mM concentration. The calcium ionophore A23187 (Sigma Aldrich) stock solution was made by dissolving the entire vial (1 mg) with 500 mL of dimethyl sulfoxide (DMSO), resulting in a 3.8 mM concentration.

To measure the endothelial intracellular NO production and calcium influx, 4-amino-5-methylamino-2',7'-difluorofluorescein diacetate (DAF-FM DA – Invitrogen, Carlsbad, CA) and

Fluo-4 AM (Invitrogen) were used, respectively. Both stock solutions of DAF-FM DA and Fluo-4 AM were prepared by dissolving a 50 μg aliquot in 20 μL of high quality anhydrous DMSO, resulting in stock concentrations of 5 and 2.2 mM, respectively. In the calcium studies, Pluronic F-127 was used to help facilitate the transport of the Fluo-4 AM into the cell. 200 mg of the Pluronic F-127 were dissolved in 1 mL of anhydrous DMSO to make a 20% (w/v) stock solution.

The buffers used for experiments involving endothelial cells and RBCs were Locke's solution and a physiological salt solution (PSS). The composition of the Locke's solution was as follows (in mM); NaCl – 154.0, KCl – 5.6, $CaCl_2$ – 2.0, $MgCl_2$ – 1.0, $NaHCO_3$ – 3.6, glucose – 5.6, HEPES – 10.0. The resulting buffer was adjusted to a pH of 7.4 by dropwise addition of concentrated sodium hydroxide or hydrochloric acid. The PSS consists of (mM); KCl – 4.7, $CaCl_2$ – 2.0, NaCl – 140.5, $MgSO_4$ – 12.0, tris(hydroxymethyl)aminomethane – 21.0, glucose – 5.6, 5% bovine serum albumin. The pH was adjusted to 7.4 by dropwise addition of concentrated hydrochloric acid.

2.4.2 Collection and purification of RBCs

For the studies examining RBC-mediated endothelial NO production, human blood was obtained from willing volunteers at the antecubital fossa and collected into heparinized tubes (BD Biosciences, Sparks, MD). The whole blood was then combined into larger tubes and centrifuged at 500 x g for 10 minutes. The plasma and buffy coat removed by aspiration and the packed RBCs were resuspended/rinsed with PSS. The RBCs were centrifuged again and rinsed with PSS two additional times. The hematocrit of the packed RBC sample was determined using

a hematocrit measurement device (CritSpin®, Iris sample processing, Westwood, MA). Experiments were always performed the day of obtaining the human blood.

2.4.3 Endothelial cell culture

Bovine pulmonary artery endothelial cells (bPAECs) were purchased as frozen cryovials (Lonza, Walkersville, MD). The vials were thawed in a water bath at 37°C, and the cells immediately transferred to a 75 cm^2 filtered tissue culture flask (TPP brand - MIDSCI, St. Louis, MO) containing ~ 15 mL of endothelial growth media (EGM). EGM consists of a low glucose (5.5 mM) Dulbecco's Modified Eagles Medium (DMEM – MIDSCI, St. Louis, MO) supplemented with 2.5% v/v adult bovine serum (Sigma Aldrich), 7.5% fetal bovine serum (Lonza), penicillin, streptomycin, and amphotericin B (MIDSCI). The cells were allowed to grow in a humidified incubator at 37°C and 5% CO_2. The EGM was changed every three days while the cells were allowed to proliferate until they cover 80 to 100 % of the flask surface.

When the cells reach the point when they create a confluent layer, they were ready to be subcultured. The EGM was aspirated and the cells were rinsed with 5 to 6 mL of a HEPES buffered saline solution for approximately 30 seconds. The HEPES was removed and 4 mL of a 0.25% trypsin/EDTA solution were introduced to the cells. After two or three minutes in the incubator, the trypsin was aspirated off and the cells detached by tapping the back of the flask. The cells were rinsed repeatedly with 5 to 10 mL of warm EGM to neutralize any remaining trypsin. The cell suspension was then divided into other flasks, tissue culture plates, or seeded on microfluidic devices depending on what experiment the cells will be utilized for.

2.4.4 Microfluidic device production

Soft lithography techniques were used to produce poly(dimethylsiloxane) (PDMS) slabs from silicon masters.[48] Briefly, silicon masters were spin coated with four mL of SU8-50 photoresist (MicroChem Corp., Newton, MA) at 500 rpm for 15 seconds, then 1000 rpm for 30 seconds. A transparency mask used to form the features was then placed over the wafer, and exposed to UV light (340 nm) for one minute for a 100 μm thick feature, and then developed.

PDMS slabs were prepared by mixing Sylgard 184 (Ellsworth Adhesives, Germantown, WI) bulk polymer with curing agent in a 20:1 ratio was used where increased sealing was desired, whereas a more rigid 5:1 mixture was utilized on edges. Each layer of PDMS was subsequently cured by heating for 10 minutes at 75° C. Outlets and wells were punched using 1/8 in. to 1/16 in. hole punches. A luer stub adapter was employed to punch inlets, and then plumbed using 20 gauge stainless steel tubing used to deliver the RBCs.

Assembly of the microfluidic device has been described in previous studies,[49, 50] and consists of two PDMS slabs. Briefly, a lower PDMS slab contains channels whose dimensions were 200 μm wide by 100 μm tall, which were prepared using the lithographic techniques described above. A second upper PDMS slab has two columns of 1/8 in. wells that overlay the channels of the other slab of PDMS. The columns of wells in the upper PDMS slab were separated from the channels in the underlying PDMS slab by a polycarbonate membrane with a pore size of 0.6 μm. After the microfluidic device was constructed, it was irreversibly sealed by heating for 30 minutes at 75°C.

2.4.5 Enzyme-Linked Immunosorbent Assay (ELISA) used to examine the interaction of C-peptide with the endothelium

In order to confirm that metal-activated C-peptide was indeed interacting with the endothelium, either by internalization or interacting with a surface receptor, bPAECs were cultured on 12-well tissue culture plates and allowed to grow to confluence. When the cells were confluent, the EGM was replaced with serum free DMEM with either low (5.5 mM, DMEM) or high (25 mM, HG DMEM) glucose and allowed to incubate for 24 hours. After the 24 hour incubation, the cells were rinsed and allowed to incubate for one hour in 10 nM metal-activated C-peptide in either DMEM or HG DMEM. The samples were prepared by combining 20 μL of a 250 nM C-peptide solution with 5 μL of a 1000 nM Zn^{2+} solution, followed by the addition of 475 μL of DMEM. The DMEM/C-peptide solutions were immediately transferred to the cells, after which they were allowed to incubate at 37°C for 60 minutes.

Following the one hour incubation, the supernatant was removed from the cells and diluted 10 fold by taking 100 μL of the DMEM and adding 900 μL of DDW. These diluted samples were then analyzed with the C-peptide amounts quantified using a commercially available ELISA kit (Millipore, Bellerica, MA). Standards ranging from 0.1 through 1 nM were prepared from the previously described 250 nM working C-peptide solution diluted in a 1:10 solution of DMEM:DDW to compensate for any matrix interferences. Using the generated standard curve, the amount of C-peptide in the supernatant can be subtracted from the known amount of C-peptide placed on the cells, which should provide the amount that interacted with the cell. The reaction scheme for the ELISA used to detect the C-peptide in the supernatant is shown in Figure 2.2.

2.4.6 Measuring the glucose uptake of the endothelium following C-peptide and/or insulin administration

The glucose uptake and utilization by the bPAECs was monitored using a radioactive form of ^{14}C-glucose combined with liquid scintillation counting (Figure 2.3). In this form of glucose, any of the carbon atoms in the molecule can be labeled. bPAECs were subcultured from the flasks and loaded into 6-well tissue culture plates. When the cells had grown to near confluence, the EGM was replaced with low serum (< 1%) DMEM (low or high glucose) and allowed to incubate for 24 hours. Following the incubation, the cells were rinsed with warm (37°C) PSS containing glucose concentrations of 0, 0.550, or 5.5 mM. 1 mL of PSS containing the ^{14}C-glucose and various concentrations of either C-peptide, metal-activated C-peptide, insulin, or phloretin was added to the wells and allowed to incubate for up to one hour. The working radiolabeled glucose PSS solution was prepared by adding 60 µL of the 0.1 mCi/mL ^{14}C-glucose stock solution to 6000 µL of PSS. 30, 120 or 300 µL were also added to 6000 µL of PSS to prepare a 0.5, 2 or 5 mCi/mL working solution, respectively.

In the initial studies, PSS different ^{14}C-glucose amounts were added to cells and allowed to incubate between for periods 30 and 60 minutes (Figure 2.4). Following the desired incubation time, the experimental PSS was removed from the wells, and the cells were rinsed multiple times with cold (4°C) PSS to remove any residual ^{14}C-glucose. The rinsed cells were then lysed with 1 mL of an alkaline sodium dodecyl sulfate (SDS) solution. The lysis solution contains 1% w/v SDS in a 0.2 M sodium hydroxide mixture. Following heating at 37°C for 60

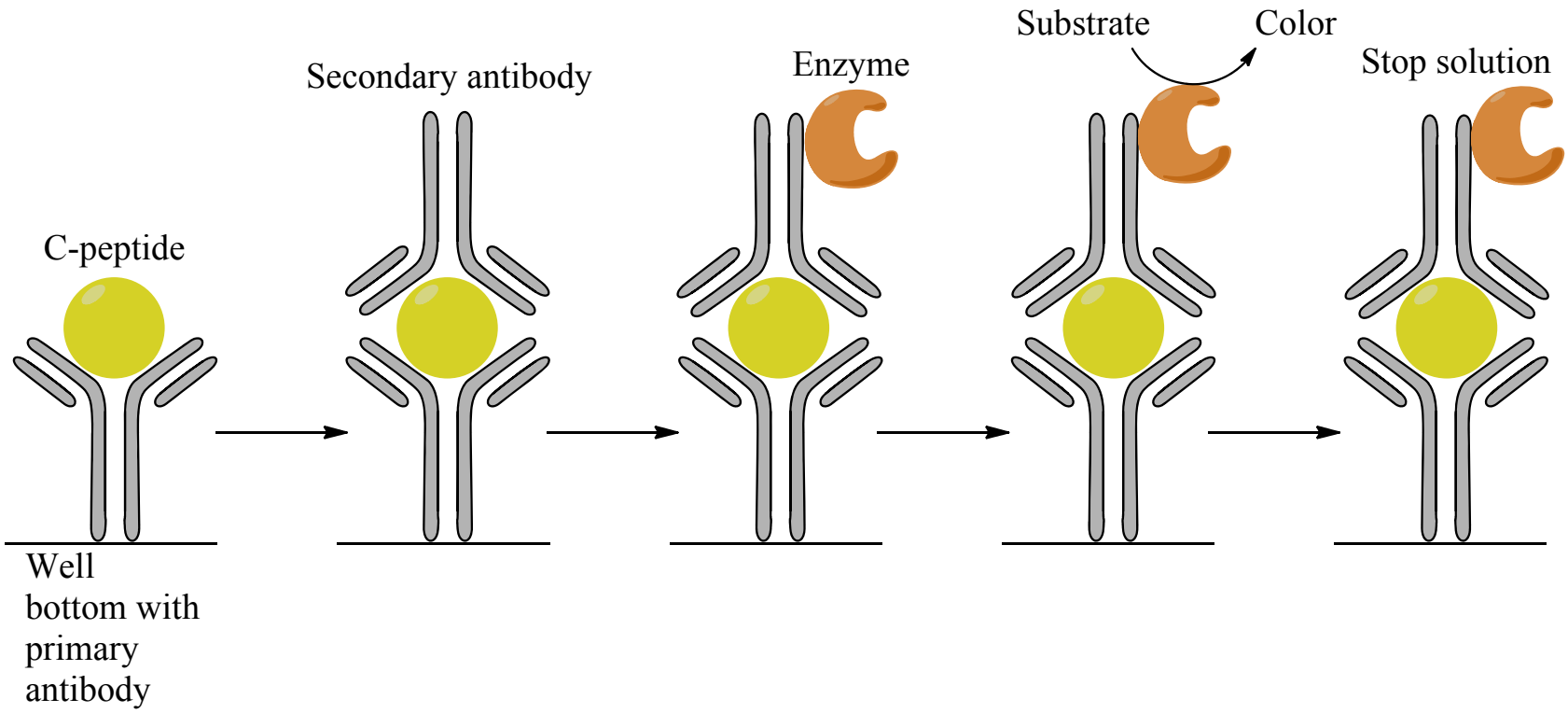

Figure 2.2 – Diagram showing the ELISA setup used to measure C-peptide interacting with the bPAECs. The diluted C-peptide samples are loaded into the 96-well plate setup that has a primary antibody coated along the bottom. The C-peptide is allowed to bind to the antibody, after which a biotinylated secondary antibody is added to the solution. Following incubation, the wells are washed multiple times and an enzyme (pre-titered streptavidin-horseradish peroxidase) that binds to the secondary antibody through biotinylation is added. After another incubation, the wells are again rinsed and a substrate is added that produces a product upon reacting with the enzyme. This reaction produces an overall color to in sample that is stopped after the addition of the 'Stop Solution'. The absorbance of the solution at 450 nm using a multiwell plate reader is used to determine that concentration of C-peptide in the original sample by comparing to a standard curve. The absorbance is proportional to the amount of C-peptide in the samples.

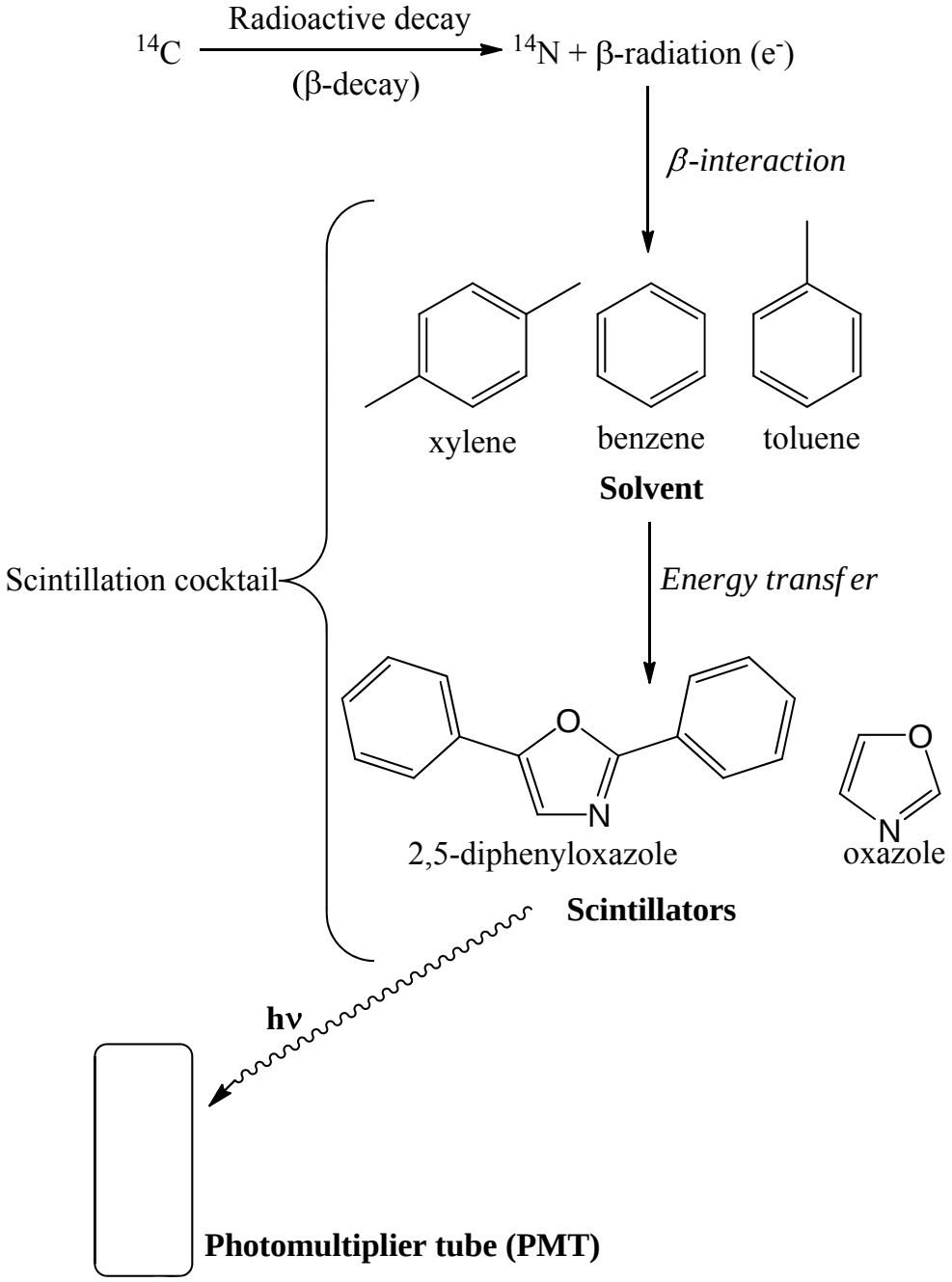

Figure 2.3 – Mechanism by which liquid scintillation counting (LSC) generally occurs. The radioactive material, in this case carbon-14, decays via beta-decay that releases an electron. This electron is able to transfer energy to the solvent molecules of the scintillation cocktail, which subsequently transfers that energy to specific scintillators/fluors. The energy transferred to the sctintillators is eventually released by means of emitting light. The light is then detected by photomultiplier tubes and quantified. The light intensity, often reported as counts per minute (CPM), is proportional to the amount of radioactive material in the sample.

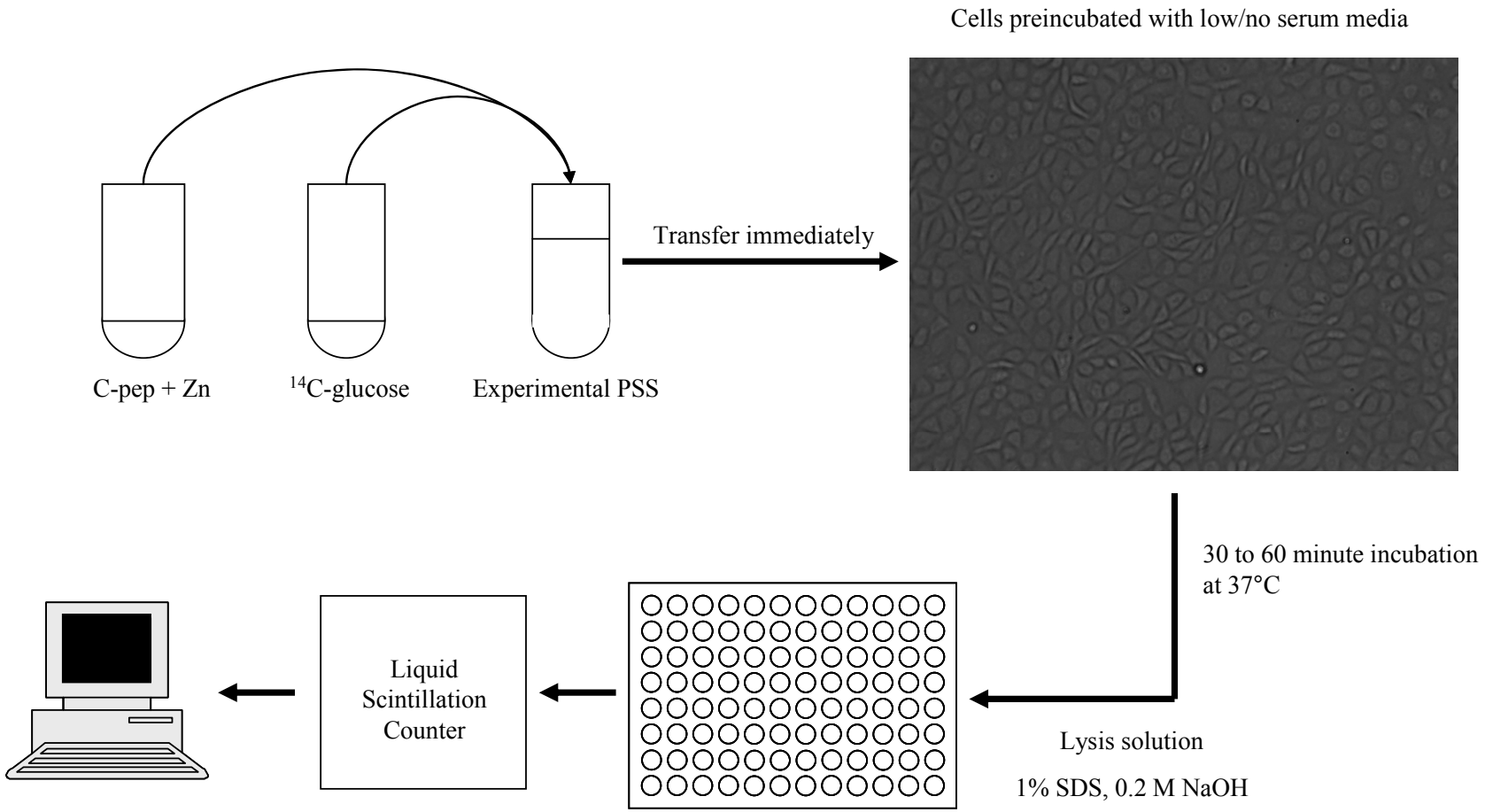

Figure 2.4 – Diagram illustrating the procedure to measure glucose uptake in immobilized bPAECs. The radiolabeled glucose and the desired stimulant (metal-activated C-peptide in this case) are combined into the experimental PSS. To avoid any metal exchanges with the peptide, the PSS is immediately transferred to the cells pre-incubated 24 hours with high or low glucose DMEM. Following an incubation period, the cells are rinsed and lysed with an alkaline lysis solution. The lystate is added to a 96-well microplate, followed by the scintillation cocktail. The plate is then placed in a liquid scintillation counter, where the quantity of radiolabeled glucose is expressed as counts per minute (CPM).

minutes, 200 μL of the lystate were removed and loaded into white, 96-well clear-bottom microplates (Perkin Elmer, Waltham, MA). 100 μL of a liquid scintillation cocktail (Perkin Elmer) were added to each well containing lysate. The microplate was then placed in a Microbeta PLUS liquid scintillation counter (Perkin Elmer), and the amount of ^{14}C-glucose present in the lystate was quantified by luminescence and expressed in terms of CPM (counts per minute).

For the phloretin inhibition studies, appropriate volumes of the 200 mM working solution of phloretin were added to the ^{14}C-glucose PSS to make 1 mL of a 0.1 and 0.5 mM final concentration solution (0.5 and 2.5 μL respectively). To check the effect of the solvent, PSS containing 2.5 μL of ethanol was used as a control. The samples were then put on the rinsed cells and allowed to incubate for 60 minutes, followed by the rinsing, lysis, and quantification as described earlier.

To prepare the C-peptide solutions, equal volumes of the 8.3 μM solutions of C-peptide and Zn^{2+} were combined. For the 1 mL samples at a final concentration of 10 nM metal-activated C-peptide, 1.2 μL of both the C-peptide and Zn^{2+} solutions were mixed. 998 μL of the ^{14}C-glucose PSS were added to the metal-activated C-peptide. The PSS was immediately transferred to the cells to avoid any metal ion exchanging with the peptide and allowed to incubate at 37°C for up to 60 minutes. Following the incubation, the procedures for rinsing, lysing the cells, and quantifying the ^{14}C-glucose were identical to that described in Figure 2.4.

In the experiments evaluating the effect of insulin administration, 1 μL of the 20 or 1000 μM working insulin solutions was added to 1 mL of PSS and added to the cells 30 minutes prior

to introduction of the radiolabeled glucose. The experimental setup was similar to that of the C-peptide studies, only that 1 μL of the 20 or 1000 μM working insulin solutions was added to the1 mL samples containing metal-activated C-peptide and ^{14}C-glucose immediately before addition to the cells. After the cells incubated for 60 minutes, they were rinsed, lysed, and the lysate radioactivity was quantified by liquid scintillation.

2.4.7 C-peptide stimulated endothelial calcium influx and NO production

Monitoring the influence that metal-activated C-peptide has on stimulating intracellular NO production and calcium influx in immobilized endothelial cells utilized the application of intracellular probes that are specific for free radicals and free calcium within the cell. The probes for NO and calcium that were used were DAF-FM DA and Fluo-4 AM. These probes were allowed to cross the plasma membrane where esterases cleave certain moieties off the molecule so the probe is not allowed to leave the cell (Figure 2.5). In order to ensure that the probes were functioning adequately, known stimulants of NO production and calcium influx were administered, ATP and the calcium ionophore A23187.

To utilize the high throughput capabilities of a microplate reader, the experiments were performed in multiwell tissue culture plates. bPAECs were cultured and grown in 75 cm^2 tissue culture flasks until they were confluent. The cells were subcultured onto 24-well tissue culture plates and allowed to grow until full. 24 hours prior to the experiment, the cells were incubated in serum free DMEM. Following the incubation, the cells were rinsed multiple times with warm Locke's solution, and the specific probes were added. Figure 2.6 diagrams the procedure that was used to measure the intracellular calcium and NO production.

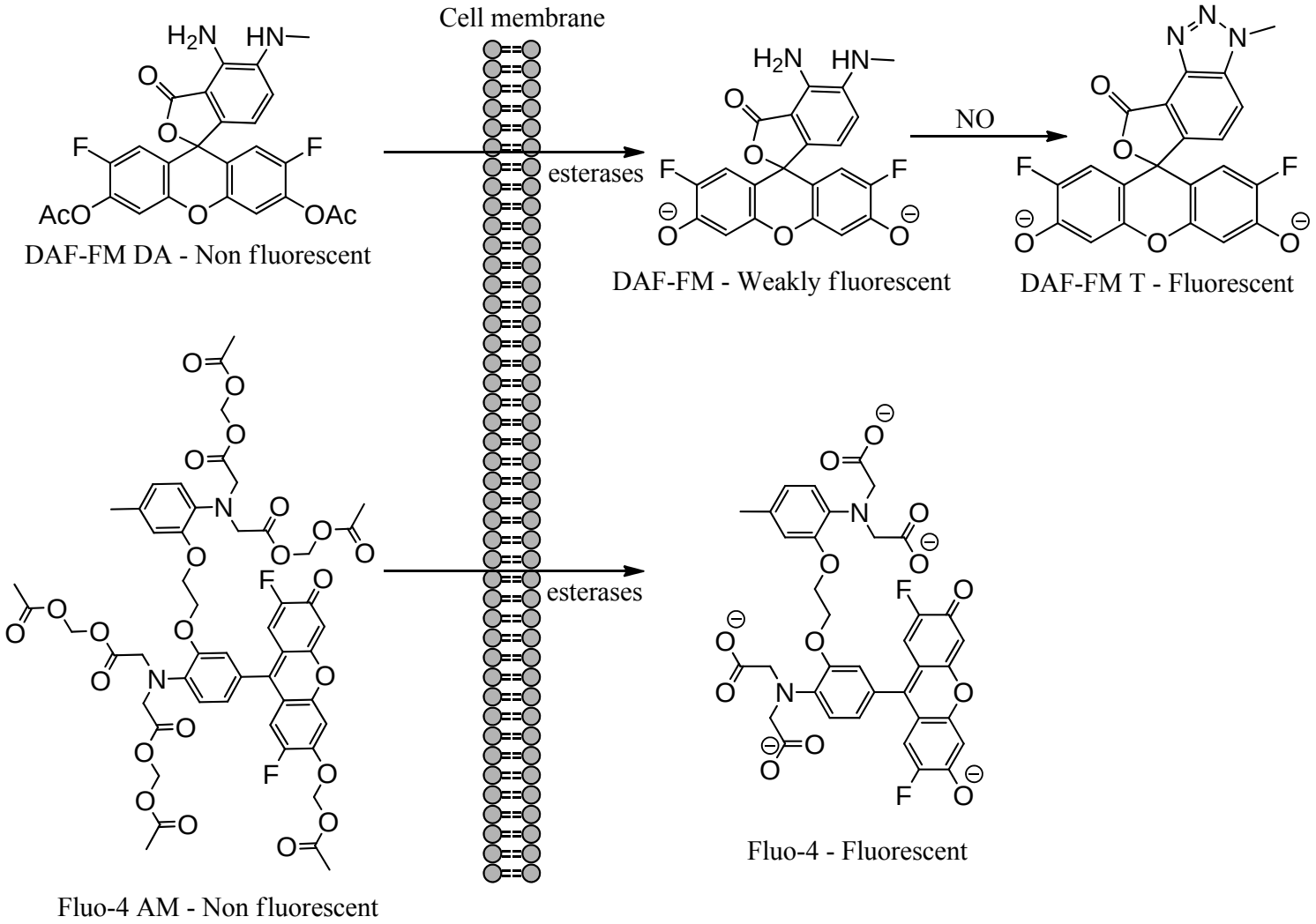

Figure 2.5 – Illustration showing the structures of DAF-FM DA (top) and Fluo-4 AM (bottom) for measuring intracellular NO production and calcium influx respectively. When the non-fluorescent probes are brought into the cell, esterases cleave off the acetate moieties on the DAF-FM DA and the acetomethylester moieties on the Fluo-4 AM. This leaves the probes DAF-FM and Fluo-4 to interact with their specific targets molecules/atoms.

2.4.7.1 Intracellular NO measurements

Following the rinse with the Locke's solution, the cells were incubated with 250 μL of 5 μM DAF-FM DA. This working solution was achieved by diluting 5 μL of the stock into 5000 μL of Locke's. The cells were incubated for approximately 30 minutes at 37°C, after which the probe was removed and the wells were rinsed with warm (37°C) Locke's. Following multiple rinses, 300 μL of a 1 mM L-arginine solution was allowed to incubate on the cells for an additional 20 minutes at 37°C. After the incubation, the basal fluorescence intensity (ex. 488 nm – em. 520 nm) was measured on a multifunction plate reader (Molecular Devices, Sunnyvale, CA) in order to determine a baseline that will be used to identify any change in NO production.

Once a baseline was established, 60 μL of the supernatant were removed and immediately replaced by 60 μL of Locke's solution containing stimuli of intracellular NO production that were at a concentration 5 times higher than the experimental concentration to account for dilution. The stimuli and final concentrations of the controls were ATP (50, 100, 500, and 1000 μM) and the calcium ionophore A23187 (0.1 and 0.5 μM). The C-peptide samples were prepared by adding equal volume amounts of 8.3 μM C-peptide and Zn^{2+} followed by the addition of Locke's that resulted in concentrations ranging from 500 nM down to 33 nM. The C-peptide samples were then immediately transferred to the cells by the method previously described, resulting in experimental concentrations between 6.6 and 100 nM.

Following addition of the stimuli, a fluorescence measurement was obtained (ex. 488 nm – em. 520 nm) once every minute over the span of 1 hour. The changes observed in the fluorescence were normalized to the baseline fluorescence obtained earlier.

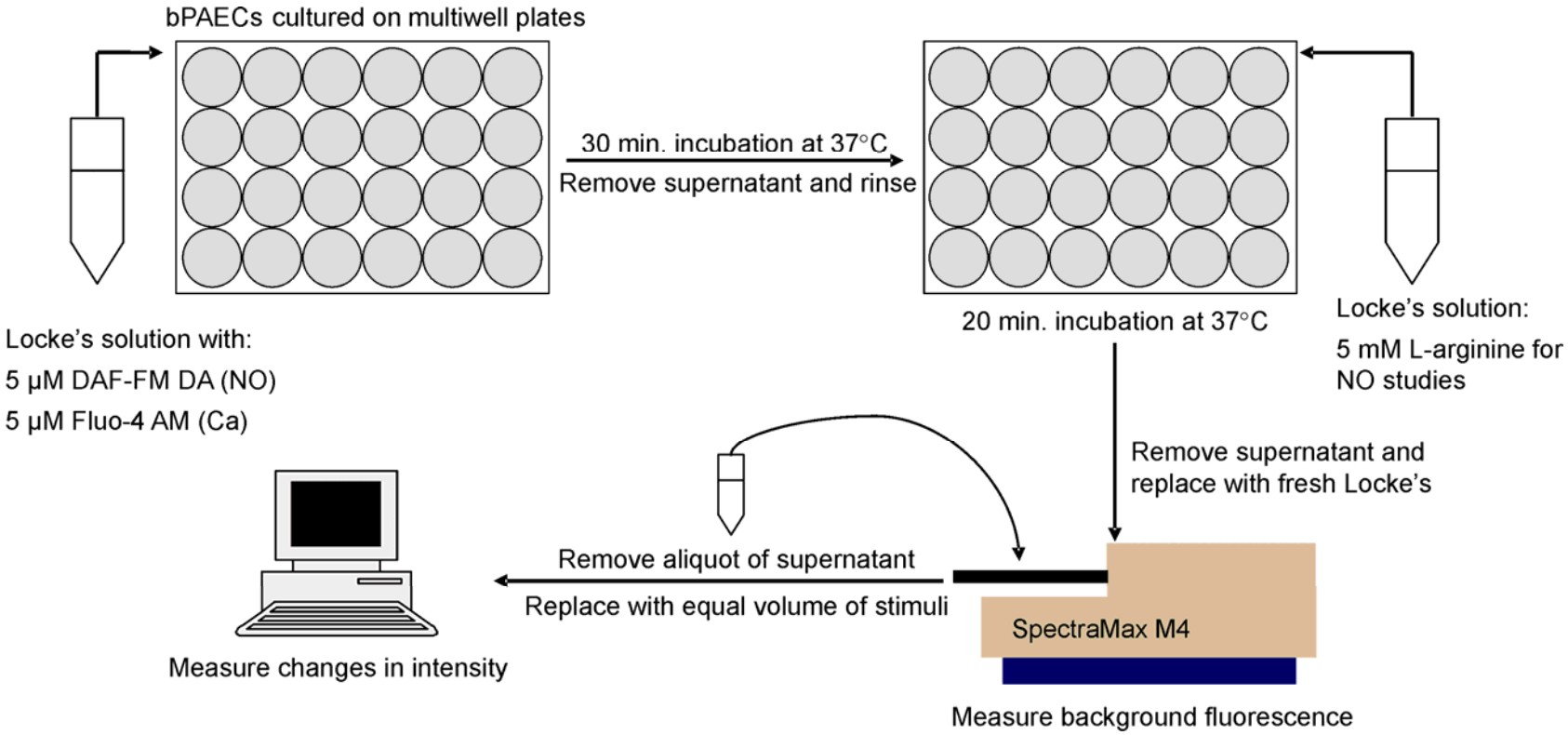

Figure 2.6 – Diagram showing the procedures for observing changes in intracellular NO production or calcium influx upon the addition of specific stimuli. Locke's solution containing the probe of interest is loaded onto bPAECs and incubated for 30 minutes. Following multiple rinses, fresh Locke's is put on the cells and allowed to sit an additional 20 minutes to allow for the probes to completely be internalized and have their specific moieties cleaved. In the NO studies, L-arginine is added to the Locke's. After the incubation, the Locke's is again changed and the background fluorescence is obtained. A volume of supernatant is removed and immediately replaced with an equal volume of the stimuli. The fluorescence is immediately obtained at fixed time intervals, depending on the specific probe in use.

2.4.7.2 Intracellular calcium measurements

Following the multiple rinses with the Locke's solution, the cells were incubated for 30 minutes at 37°C in 250 µL of a 2.2 µM Fluo-4 AM solution. The experimental probe solution was prepared by first combining 5 µL of the Fluo-4 AM with 5 µL Pluronic F-127. This mixture was then diluted in 5000 µL of Locke's solution. Following the loading step, the probe was removed and the cells were washed multiple times with Locke's and allowed to incubate an additional 20 minutes. The solution was changed once more and replaced with 300 µL of warm Locke's. The basal fluorescence (ex. 494 nm – em. 520 nm) was measured at intervals of 3 seconds over a span of 30 seconds in order to obtain a baseline with regards to intracellular free calcium present.

Using a multichannel pipettor, 60 µL of the supernatant were removed and immediately replaced with 60 µL of Locke's containing C-peptide and known calcium influx stimuli ATP and the calcium ionophore A23187 at concentrations 5 fold higher than the desired experimental concentrations. Final concentrations for ATP ranged from 500 to 50 µM, calcium ionophore from 5 to 0.5 µM, and C-peptide from 100 to 6.6 nM. The C-peptide solutions were prepared as described in the previous section.

Immediately following the addition of one round of the stimuli, the fluorescence (ex. 494 nm – em. 520 nm) was again measured at 3 second intervals over the span of 3 minutes. Due to the rapid change in fluorescence, a smaller time frame was required. The fluorescence measured at different time points after addition of the stimuli was normalized to the baseline obtained earlier.

2.4.8 Microfluidic observation of endothelial NO production via C-peptide treated RBCs

Before the NO production can be measured on the microfluidic device, bPAECs must be immobilized on the membrane. In order for the bPAECs to adhere to the polycarbonate membrane, 10 μL of a 100 mg/μL solution of fibronectin were pipetted into the wells of the PDMS device and allowed to air dry. Meanwhile, confluent endothelial cells in a 75 cm^2 tissue culture flask were subcultured with the resulting cell suspension centrifuged at 1500 rpm for 5 minutes. The media was then aspirated off and the cell pellet was resuspended with 1 mL of warm EGM. This concentrated cell suspension was then divided into 10 μL aliquots and pipetted into the fibronectin coated wells of the microfluidic device. Following a 1 hour incubation at 37°C, the media was carefully replaced with fresh EGM and allowed to incubate overnight.

Following the overnight incubation, the media was removed and replaced with 10 μL of Hank's balanced salt solution (HBSS) containing 5 mM L-arginine and incubated for an additional 30 minutes. The L-arginine/HBSS solution was removed and replaced with 10 μL of an HBSS solution containing 133 μM DAF-FM DA. The probe was allowed to incubate with the cells for another 30 minutes, after which the DAF-FM DA solution was removed and 10 μL of phosphate buffered saline was added to each well. Fluorescence images were obtained of each well using an Olympus MVX10 microscope setup (Olympus America, Center Valley, PA). The setup consisted of a mercury arc lamp light source sent through a Green Fluorescent Protein (GFPA) filter cube that allows for an excitation wavelength of around 475 nm and emission wavelength around 509 nm. The images of the fluorescence intensities were used to obtain a baseline for intracellular NO production.

After the baseline fluorescence was established, human RBC samples that had been incubated with metal-activated C-peptide, only C-peptide, only zinc, or nothing were introduced to the device. The RBC samples were prepared as a 7% hematocrit from a packed RBC solution with a hematocrit usually around 70%. To prepare a 5 mL 7% RBC sample with 20 nM metal-activated C-peptide, 200 μL of a 500 nM C-peptide solution and 100 μL of a 1000 nM Zn^{2+} solution were combined. 4200 μL of PSS were then added to the metal-activated C-peptide, which was immediately followed by 500 μL of the packed (~ 70% hematocrit) RBCs. To prepare the other samples, such as only the metal or only the C-peptide, the unwanted additives were replaced with equal volumes of DDW. Following a 2 hour incubation, the treated RBC samples were flowed by syringe pumps at a rate of 1.0 μL/min through the device under the immobilized endothelial cells.

After 30 minutes of the RBCs flowing under the bPAECs, fluorescent images of the wells were obtained by the Olympus microscope setup. The fluorescent images before and after the flow of the treated and untreated RBCs were measured by taking the mean gray value at random regions in the image. The difference in the mean gray values in the same regions before and after the flow of RBCs was used to identify a change in the NO production of the immobilized bPAECs. Figure 2.7 shows the microfluidic device setup and how the experiment was performed.

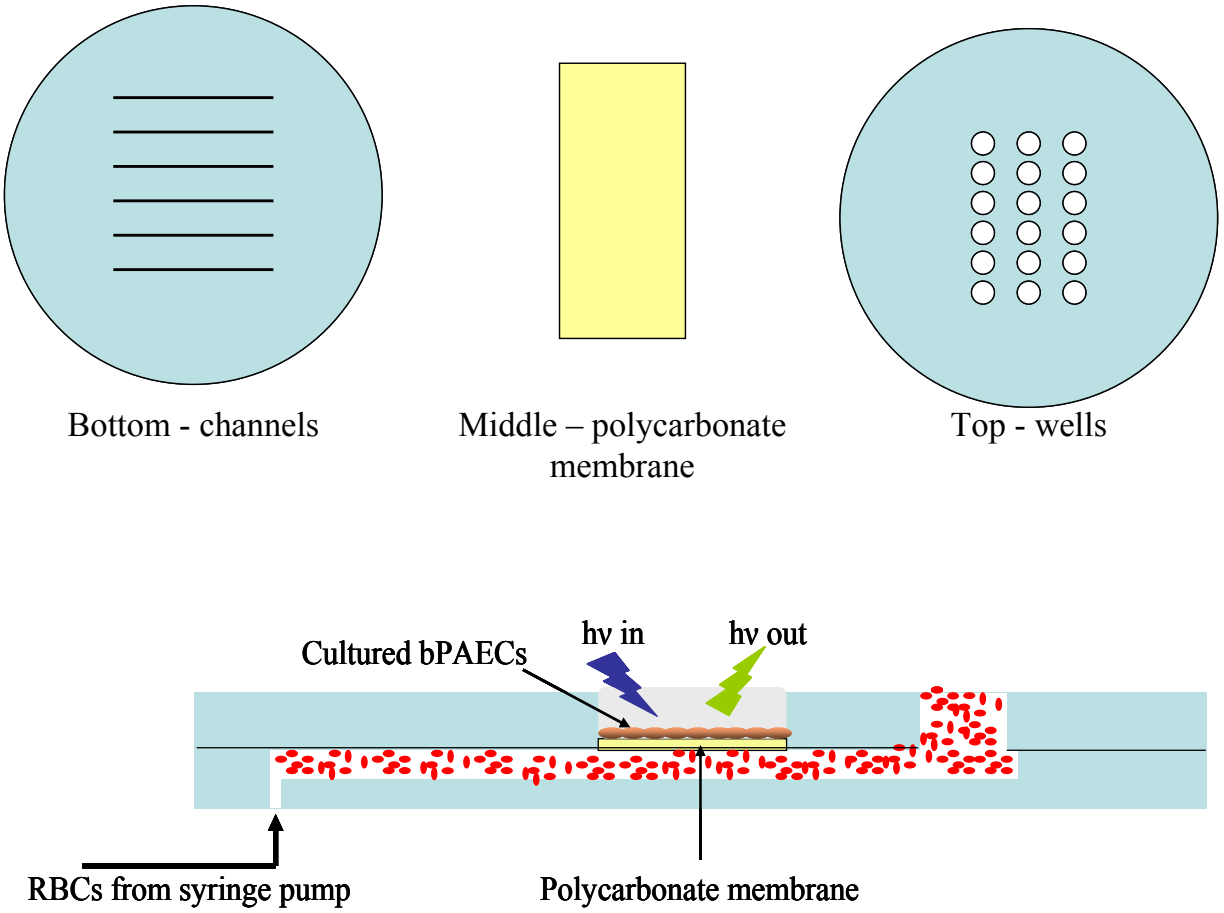

Figure 2.7 – Illustration showing the microfluidic device preparation and setup for experimental measurements. The top diagram shows the three layers to the device, while the bottom picture shows a cross section of the completed chip. The bottom of the device is a PDMS slab with channels imprinted along the surface. The polycarbonate membrane is the middle layer and covers most of the channel area. The top PDMS slab has multiple wells punched into it. It is set on top of the membrane allowing for transport of materials from the channels. Once the device is prepared, the basal NO production images are obtained from the bPAECs loaded with the DAF-FM DA probe. Next, RBCs are flowed through the channels underneath the membrane. Periodically, fluorescence images of the cells are obtained to observe changes in intensity.

2.5 Results

2.5.1 Glucose uptake into the endothelium

2.5.1.1 Radiolabeled glucose concentration and incubation time dependence

To demonstrate as a proof of concept that the amount of ^{14}C-glucose that enters the bPAECs is regulated by the amount of the extracellular glucose present as well as the length of time that the cells were exposed to the radiolabeled material, bPAECs in multiple plates were exposed to differing amounts of radioactive glucose and for different amounts of time. Immobilized bPAECs were incubated with PSS containing 0.5 or 1.0 μCi/ml for either 30, 45 or 60 minutes, after which the cells were rinsed, lysed, and measured using liquid scintillation counting. The CPM values reported were background subtracted to wells containing only buffer and scintillation cocktail. Figure 2.8 represents the results obtained from the varying incubation times and ^{14}C-glucose concentrations. After 30 minutes incubation, the lysate containing 0.5 mCi/mL ^{14}C-glucose gave an average CPM of 195 ± 16, while the 1.0 mCi/mL gave a higher signal at 345 ± 7 CPM. At each incubation time, the CPM values were statistically different ($p < 0.05$) from each other at both radiolabeled glucose concentrations. A 45 minute incubation gave averages of 258 ± 12 and 445 ± 15 CPM, respectively, for the 0.5 and 1.0 μCi/mL solutions. As expected, the longest incubation times of the three, 60 minutes, resulted in the highest CPM values for the 0.5 and 1.0 μCi/mL samples at 341 ± 8 and 599 ± 29, respectively.

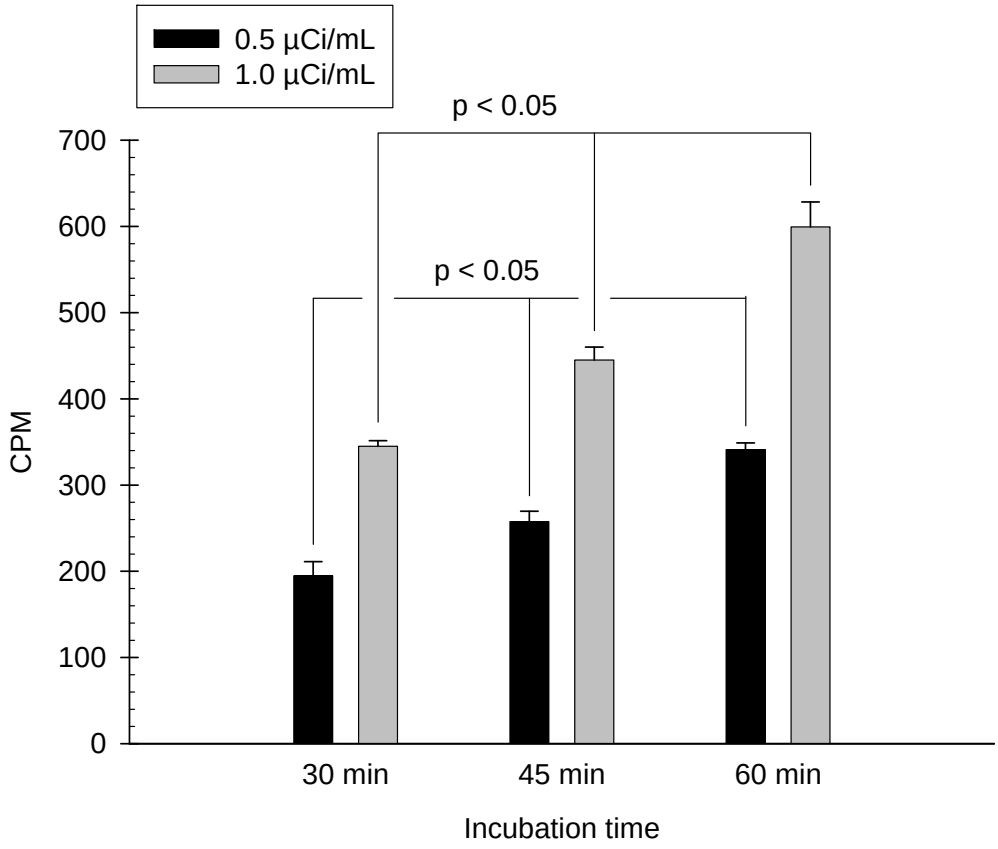

Figure 2.8 – Glucose transport observed in plated bPAECs with different ^{14}C-glucose concentrations and incubation times. The higher amount of radiolabeled material (gray bars – 1.0 µCi/mL) resulted in higher signals than the 0.5 µCi/mL samples, indicating more intracellular material. The longer the incubation time went, the higher the signal became. The bars represent the average (n = 3) with the error bars represent the standard error of the mean.

2.5.1.2 GLUT1 inhibitor phloretin affecting endothelial cell glucose uptake

In order to indicate the significance the membrane protein GLUT1 has on basal endothelial cell glucose uptake, bPAECs were incubated in varying phloretin concentrations for 60 minutes. Following the desired time, the lysates were measured using liquid scintillation counting with the CPM values of the different phloretin solutions normalized to the values of the cells incubated with no phloretin. As shown in Figure 2.9, there were statistically significant ($p < 0.001$) decreases in the glucose uptake by cells incubated with 0.1 and 0.5 mM phloretin. bPAECs incubated for 60 minutes with 0.1 mM phloretin had a glucose uptake that was approximately 18 ± 3% of that compared to the total uptake of untreated cells. The higher concentration of phloretin, 0.5 mM, resulted in an uptake that was 2.6 ± 0.6% that of the untreated cells. Incubation of bPAECs with equal volumes of ethanol (EtOH), the solvent used to dissolve the phloretin, showed no significant change in the overall glucose uptake after 60 minutes incubation. The glucose uptake by the cells following incubation with ethanol was increased by 4 ± 9% compared to the cells with no added stimuli.

2.5.2 C-peptide interaction and stimulated glucose uptake in the endothelium

2.5.2.1 Metal-activated C-peptide interaction

Prior to determining how metal-activated C-peptide affects glucose transport or calcium influx/NO production, the previously described C-peptide ELISA was utilized to determine whether the peptide was being internalized or interactive with the cells in any way. By measuring the amount of C-peptide in the supernatant after a 60 minute incubation, the amount

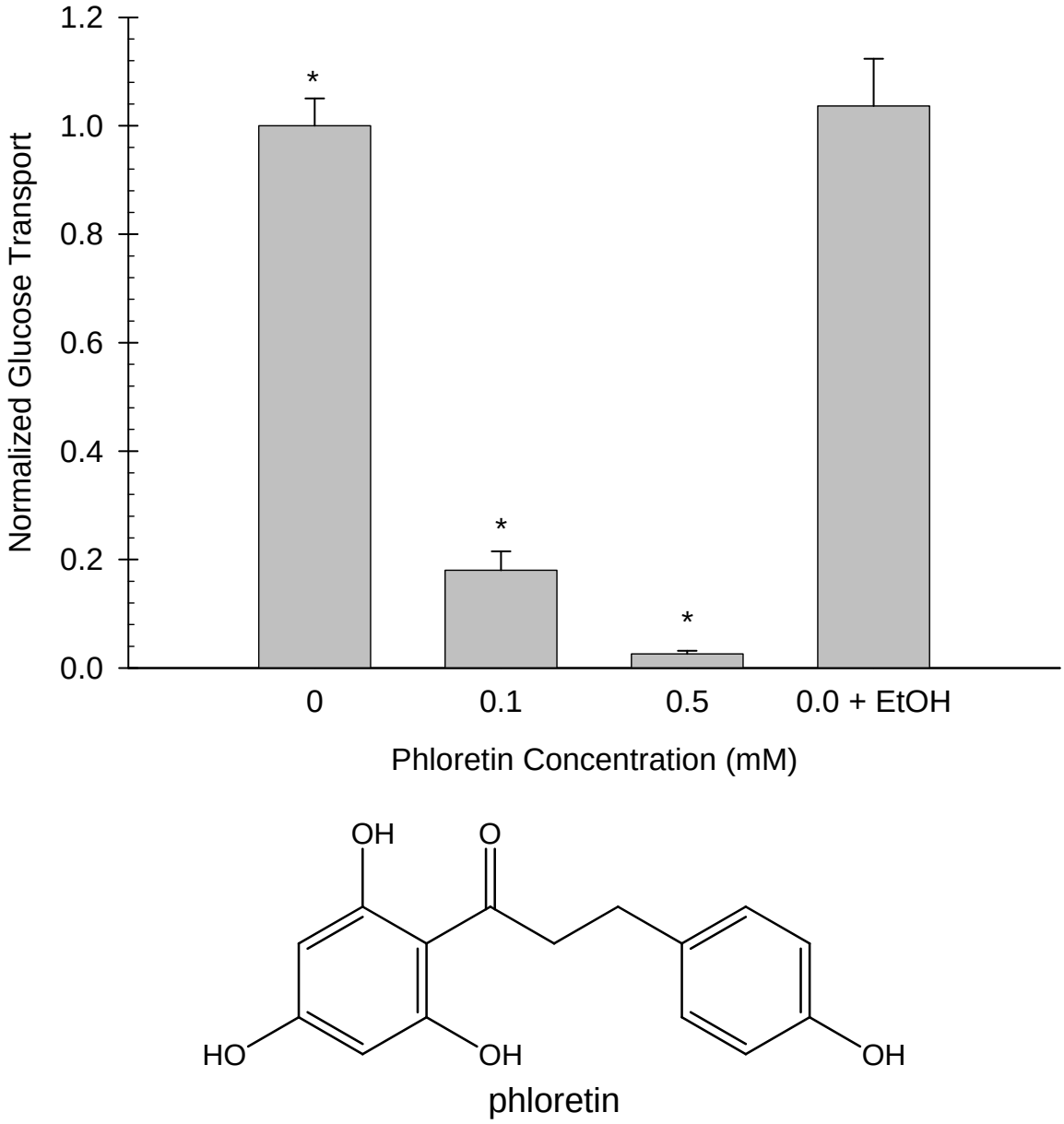

Figure 2.9 – Inhibition of glucose uptake in bPAECs by the molecule phloretin. The grey bars represent the CPM values that have been normalized to the sample with 0 mM phloretin added. In both instances (0.1 and 0.5 mM), phloretin caused a significant decrease (*$p < 0.001$) in ^{14}C-glucose uptake. With the addition of ethanol (solvent used to dissolve phloretin) there was no observed change in the glucose uptake by the bPAECs. The error bars represent the standard error of the mean with $n = 3$.

that interacted with the cells can be determined. Figure 2.10 shows the amount of C-peptide that is bound/internalized in the cell. As indicated, the bPAECs incubated in normal glucose DMEM with a concentration of 10 nM metal-activated C-peptide resulted in approximately 2.0 ± 0.1 attomoles (amol) of C-peptide binding on each cell, while the bPAECs incubated in high glucose DMEM resulted in about half of that value with 0.9 ± 0.1 amol/cell.

2.5.2.2 Metal-activated C-peptide stimulated glucose uptake

In order to determine whether metal-activated C-peptide stimulated glucose uptake into immobilized bPAECs, procedures similar to the general glucose transport methods described were performed. The only difference being the presence of the metal-activated peptide during the incubation. Initial studies examined the effect that metal-activated C-peptide, normal C-peptide, and a metal (Zn^{2+}) had on glucose uptake. Figure 2.11 illustrates the results. All averages were normalized to the CPM values from the cells treated with no stimulants. There were no statistical changes in the normalized glucose uptake of the cells following incubation with either 100 nM Zn^{2+} or 100 nM C-peptide when compared to the untreated cells. However, there was a significant increase in glucose uptake of 21 ± 2% in the cells following the addition of 100 nM metal-activated C-peptide.

2.5.2.3 Extracellular glucose concentration affecting glucose uptake

To generate less competition for the ^{14}C-glucose in the uptake studies, the PSS that was used for the initial 60 minute incubations with C-peptide contained less than 5.5 mM ^{12}C-glucose. To ensure that the experimental extracellular glucose concentrations did not have an

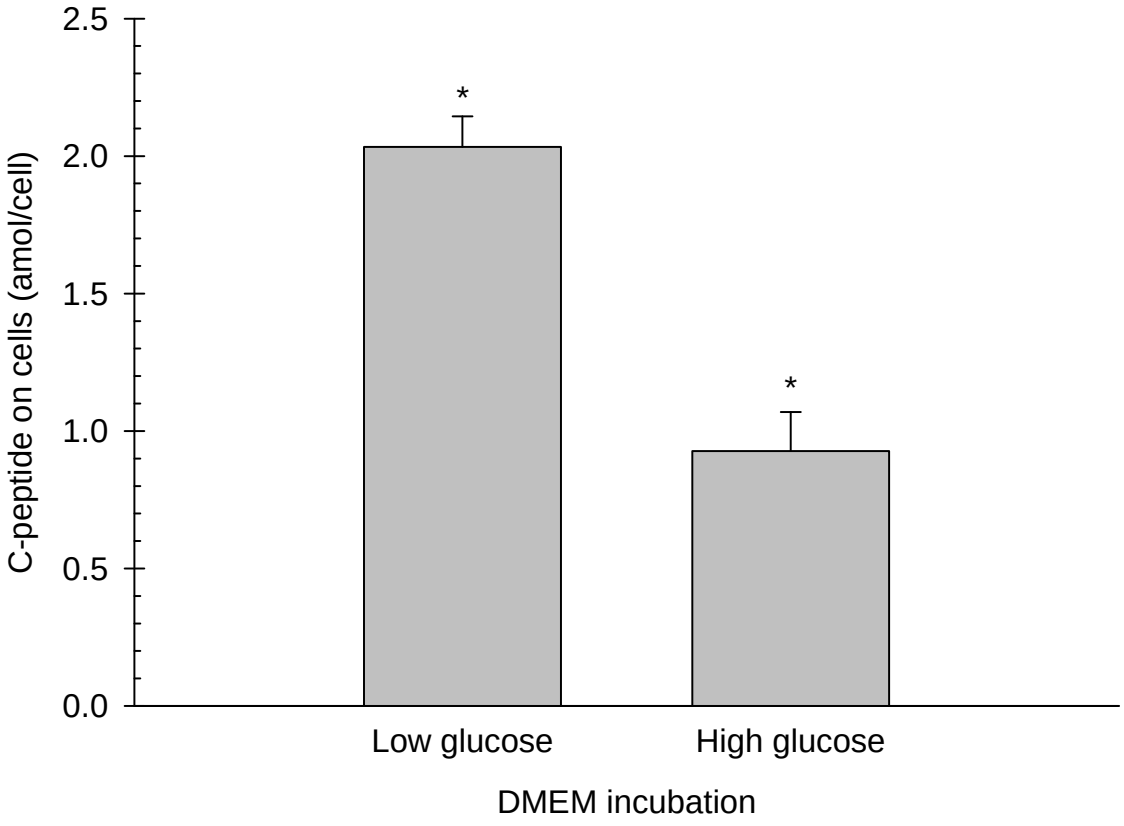

Figure 2.10 – C-peptide interacting with bPAECs following incubation with either normal (low) or high glucose DMEM. The bPAECs incubated with high glucose for 24 hours had about half (*$p < 0.001$) of the C-peptide interacting with it compared to the cells incubated in normal glucose conditions. The bars represent the average amount of C-peptide in nmol quantities ($n = 4$) that were unaccounted for in the ELISA. The error bars represent the standard error of the mean. The number of cells was approximately 45,000 in ach well.

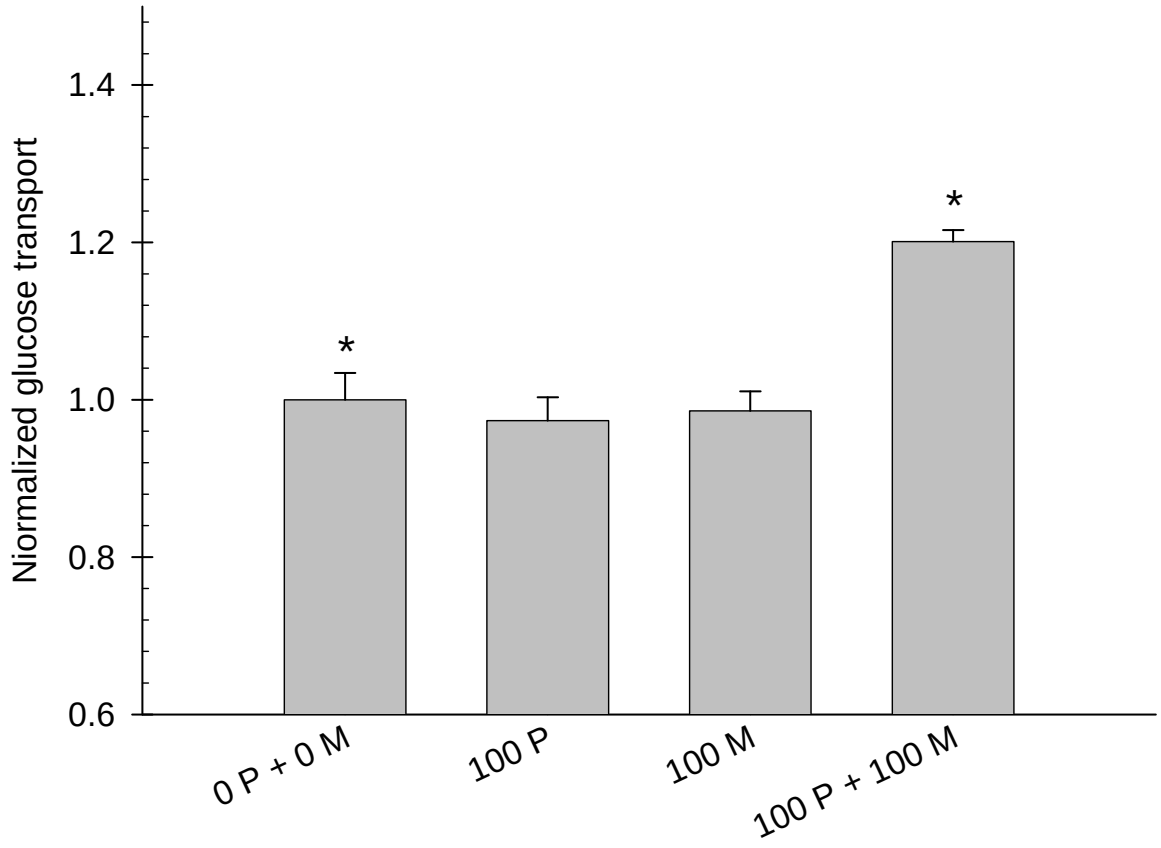

Figure 2.11 – Metal-activated C-peptide stimulated glucose uptake in bPAECs. The bars represent the average CPM values (n = 4) of intracellular glucose from cells treated with 100 nM of only the peptide (100 P), metal/zinc (100 M) or metal-activated C-peptide (100 P + 100 M) that have been normalized to the values from the cells that were incubated without any added stimuli (0 P + 0 M). The only significant increase (*$p < 0.001$) in intracellular glucose was observed following incubation with metal-activated C-peptide. The error bars represent the standard error of the mean.

effect on normalized ^{14}C-glucose uptake values, similar experiments were performed with cells incubated with both forms of C-peptide in different extracellular glucose PSS. Figure 2.12 suggests that regardless of the ^{12}C-glucose concentrations, the normalized increase in glucose uptake stimulated by metal-activated C-peptide remained the same. In 0.0, 0.550, and 5.5 mM ^{12}C-glucose physiological salt solutions, 100 nM metal-activated C-peptide stimulated normalized increases of 18 ± 2%, 21.0 ± 0.9%, and 18.4 ± 0.8%, respectively, compared to untreated cells. Also similar to before, the C-peptide without the metal activation did not stimulate an increase in glucose uptake.

2.5.2.4 Varying metal-activated C-peptide concentration affecting glucose uptake

In evaluating whether the cultured bPAECs would be affected differently by different quantities of metal-activated C-peptide, concentrations ranging from 10 to 100 nM were applied in similar 60 minute incubations as previously described. Each concentration tested had similar outcomes with the metal-activated peptide causing a statistically significant ($p < 0.001$) increase in normalized glucose uptake compared to the untreated cells, while the metal free peptide showed no increase. Figure 2.13 indicates the glucose uptake increases of 23 ± 1%, 20 ± 1%, and 21 ± 2% for metal-activated C-peptide concentrations of 10, 50, and 100 nM.

2.5.2.5 Hyperglycemic environment affecting C-peptide stimulate glucose uptake

24 hours prior to administering metal-activated C-peptide, immobilized bPAECs were incubated in either DMEM or HG DMEM. Metal-activated C-peptide at a concentration of 100 nM was added to the cells as described earlier and incubated for 60 minutes. The lysate was

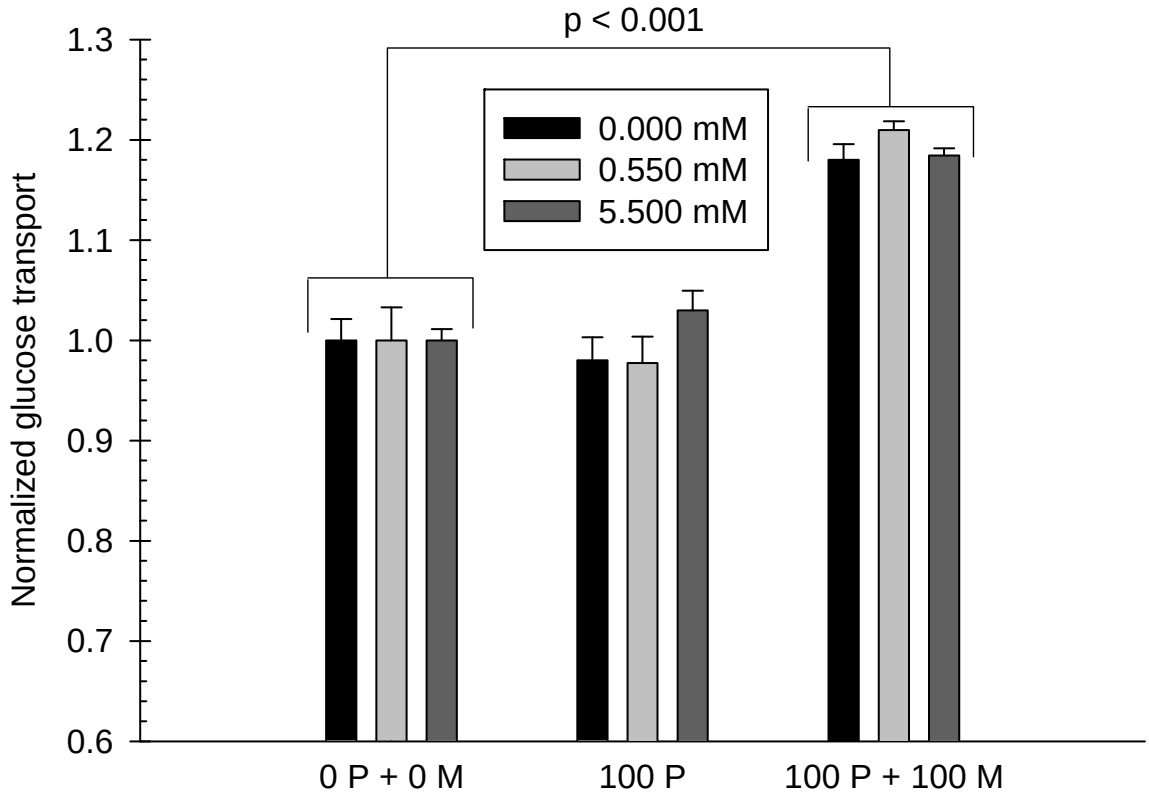

Figure 2.12 – Extracellular ^{12}C-glucose effects on metal-activated C-peptide's ability to stimulate bPAEC glucose uptake. The experimental PSS contained either 0.0 mM, 0.55 mM, or 5.5 mM ^{12}C-glucose along with the radiolabeled glucose and 100 nM of the peptide (100 P) or metal-activated C-peptide (P + M). The bars represent the average (n = 3) CPM values that have been normalized to their respective samples that contain no peptide. The error bars represent the standard error of the mean.

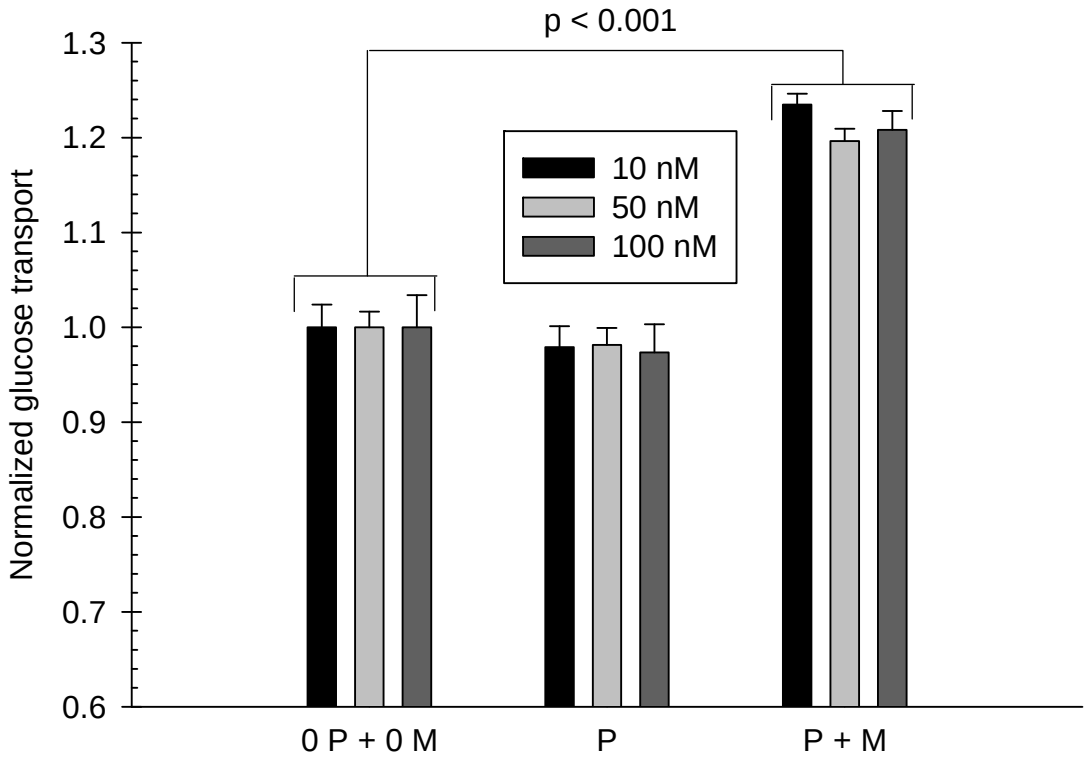

Figure 2.13 – The effects of increasing C-peptide's (P) and metal-activated C-peptide's (P + M) concentrations on bPAEC glucose uptake. Cells were incubated with physiological (10 nM – black bars) up to 100 nM (dark grey bars) C-peptide (P) and metal-activated C-peptide (P + M). Each series is normalized to their respective samples that contain no C-peptide or metal (0 P + 0 M). For each concentration of metal-activated C-peptide applied, a similar significant ($p < 0.001$) increase in intracellular glucose was observed. The bars are the average normalized values of $n = 5$ for each concentration. The error bars represent the standard error of the mean.

collected and measured with the CPM values of the C-peptide samples normalized to the 'blank' samples with no peptide (Figure 2.14). The normalized glucose uptake change for the normal glucose DMEM was similar to what was obtained before at a 21 ± 1% increase compared to untreated cells. The bPAECs incubated in the high glucose DMEM for 24 hours also produced a significant increase when treated with metal-activated C-peptide at 15 ± 1%. However, this increase was statistically lower than the increase observed with the cells incubated prior in the normal glucose media.

2.5.2.6 C-peptide stimulated glucose uptake in the presence of insulin

Following incubation in either normal or high glucose DMEM for 24 hours, insulin at final concentrations of 20 or 1000 nM was added to cultured bPAECs for a further 30 minutes. The solutions were then removed and replaced with PSS containing different combinations of insulin and C-peptide and allowed to incubate for 60 minutes. The results of the normalized glucose uptake into the cells are shown in Figure 2.15. The cells with 20 nM insulin did not have a change in glucose uptake regardless of whether or not the metal-activated peptide was present. In the presence of 100 nM metal-activated C-peptide and 20 nM insulin, there was an observed increase of 21 ± 1% and 16 ± 3% in the cells pre-incubated in the normal and high glucose DMEM respectively compared to the untreated cells. With the 1000 nM insulin alone, there was a slight glucose uptake increase of 7 ± 3% observed in the cells pre-incubated with the high glucose DMEM while no increase was observed in the normal glucose samples. The metal-activated C-peptide and 1000 nM insulin resulted in a 20 ± 2% increase in glucose uptake with the cells incubated in the normal glucose DMEM and a 27 ± 3% glucose uptake with the cells incubated in the high glucose DMEM.

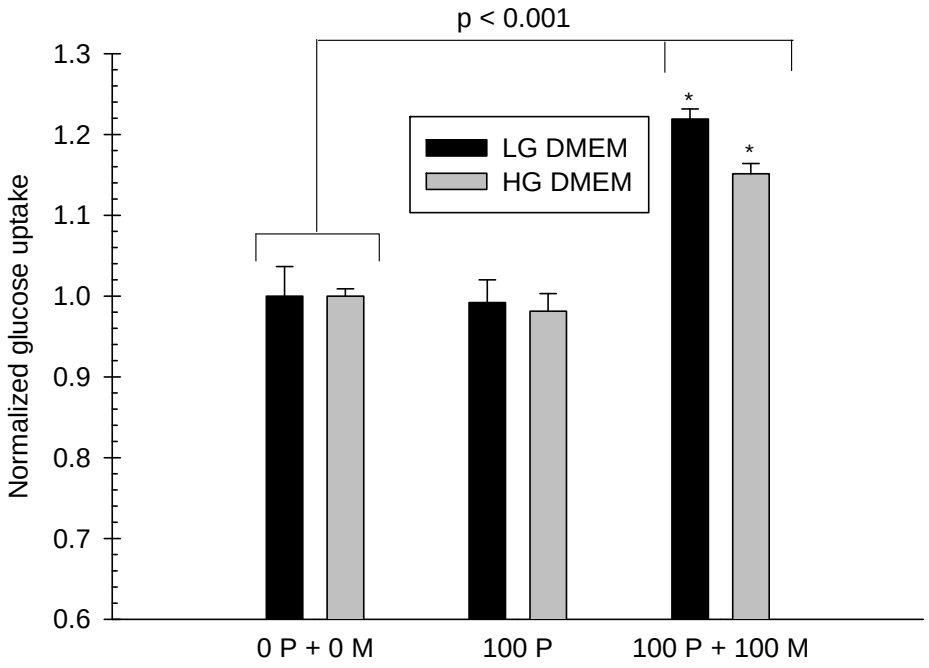

Figure 2.14 – Preincubation in different glucose environments affecting metal-activated C-peptide's ability to stimulate glucose uptake. The bPAECs incubated in a high glucose environment (grey bar) 24 hours prior to the addition of C-peptide had a significantly lower (*$p < 0.02$) normalized intracellular glucose uptake than the cells incubated in normal glucose conditions (black bar), even though in both instances the metal-activated C-peptide did stimulate an increase in overall glucose uptake. Both series are the average CPM values ($n = 4$) that are normalized to the cells that did not have C-peptide added to them. The error bars represent the standard error of the mean.

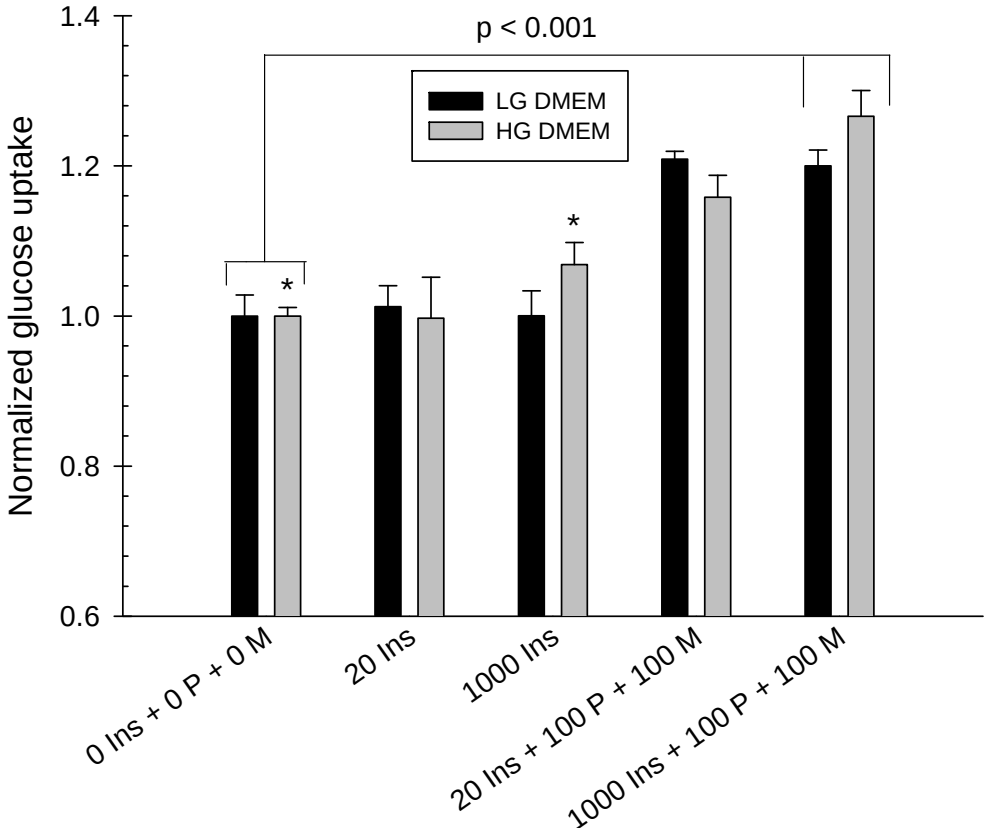

Figure 2.15 – Insulin and C-peptide combination stimulating glucose uptake. bPAECs were incubated in either normal glucose (LG DMEM) or high glucose (HG DMEM) conditions 24 hours prior to experimentation. The glucose uptake is reported here as the average (n = 5) CPM values that have been normalized to the cells containing no insulin or C-peptide. The numerical values indicate the concentration of either insulin (Ins) or metal-activated C-peptide (P + M) that is added to the cells in nM. In every instance, metal activated C-peptide resulted in a significant ($p < 0.001$) increase in glucose uptake. Insulin alone only had a slight increase at 1000 μM by itself (*$p < 0.02$). All insulin used had no zinc present. Error bars represent the standard error of the mean.

2.5.3 Endothelial NO production and calcium influx

2.5.3.1 ATP stimulated calcium influx and intracellular NO production

In order to ensure that intracellular calcium and NO production were monitored fluorescently, certain stimuli were used as controls. The first of which was ATP. Utilizing the previously described methods for measuring calcium influx and NO production, ATP was added to the supernatant above the bPAECs to produce final concentrations ranging from 50 to 1000 μM and the fluorescence monitored. The fluorescence intensities are shown in Figure 2.16. In examining the calcium influx upon ATP addition, final concentrations of 50, 100, and 500 μM resulted in a rapid increase of intracellular calcium with the maximum fluorescence intensity measured at 2.3 ± 0.2, 2.8 ± 0.3, and 3.5 ± 0.2 fold, respectively, to that of the intensity measured before the addition of ATP. The addition of only buffer resulted in no change in fluorescence intensity when looking at intracellular calcium. Upon addition of 50, 100, 500, and 1000 μM ATP to the cells to measure intracellular NO production, there was a steady increase of fluorescence intensity that eventually leveled off at 1.47 ± 0.06, 1.67 ± 0.05, 2.00 ± 0.05, and 2.45 ± 0.05 fold, respectively. The addition of a volume of Locke's solution equal to the volume of ATP added resulted in a slight increase of 13 ± 2% ($p < 0.001$) in the fluorescence intensity over the same time frame. The leveling off values of the NO production upon ATP addition suggests and supports the purinergic receptor mechanism of action of ATP stimulated NO production.

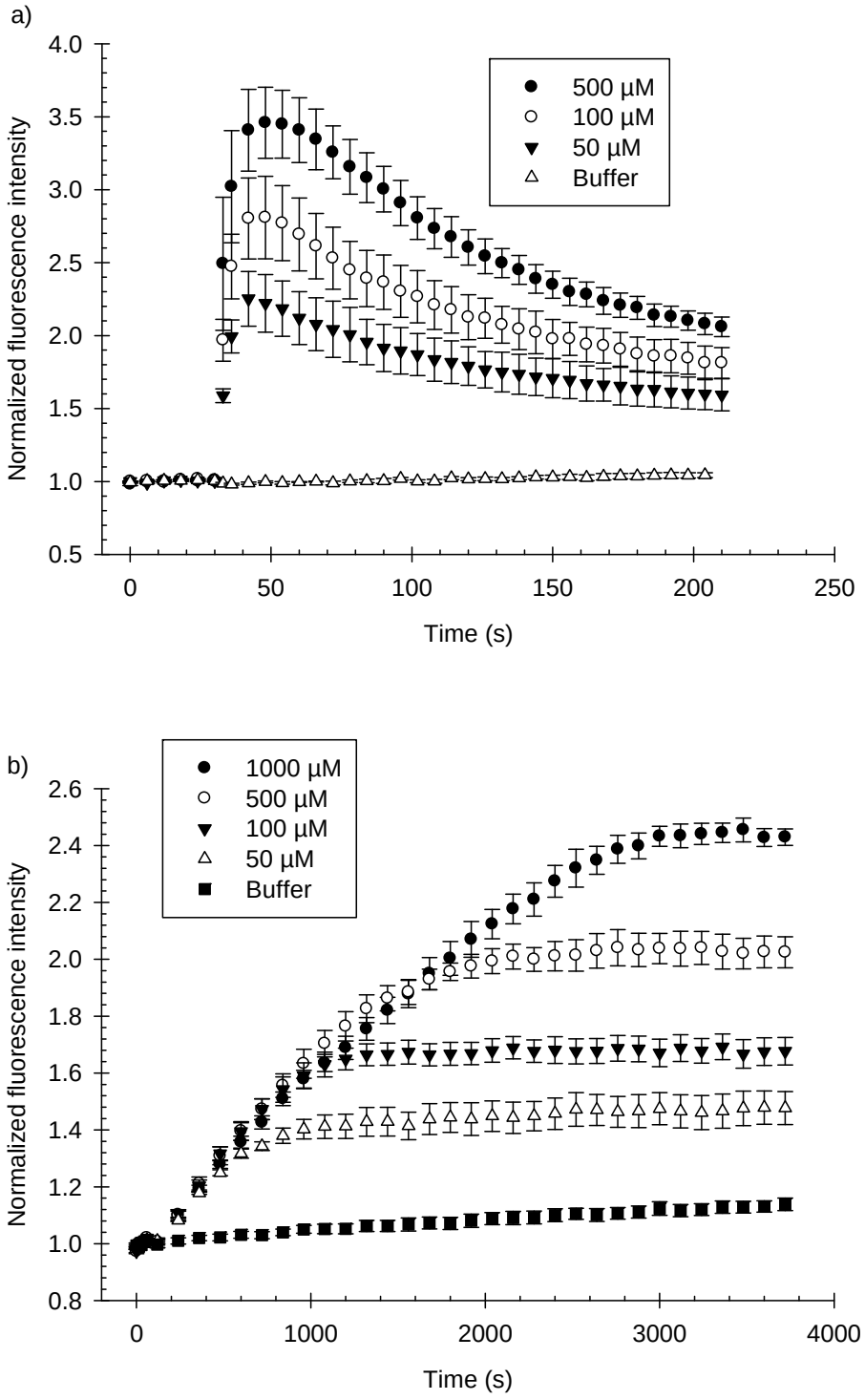

Figure 2.16 – Data showing the ATP stimulated a) calcium influx and b) NO production in immobilized bPAECs. Basal fluorescence is obtained during the first 30 seconds, followed by administration of ATP at the indicated concentrations. Each point is normalized to their respective baseline fluorescence intensity. The error bars represent the standard error of the mean with n = 4.

2.5.3.2 Calcium ionophore A23187 stimulated calcium influx and intracellular NO production

The other stimulus that was used as a control for increasing calcium influx and NO production in the cultured bPAECs was the calcium ionophore A23187. Addition of increasing concentrations of the ionophore resulted in a rapid increase in fluorescence intensities representing intracellular free calcium levels as shown in Figure 2.17. Each concentration of ionophore added had a maximum fluorescence intensity value that was 2.7 ± 0.2, 3.4 ± 0.2, and 4.0 ± 0.1 fold higher than the respective baseline signal that was obtained before the addition of 0.5, 1.0, and 5.0 μM respectively. Similar to the ATP studies, addition of equal volume quantities of Locke's solution resulted in no increase in the fluorescence intensity, indicating that the stimuli are causing the change in signal.

The increase in intracellular calcium by addition of the calcium ionophore was accompanied with an increase in DAF-FM DA fluorescence intensity, which is indicative of an increase in intracellular NO production. When bPAECs were incubated with different concentrations of the ionophore at 0.5 and 0.1 μM, there was an observed increase in fluorescence intensity of 4.1 ± 0.2 and 2.51 ± 0.09 fold respectively at the end of the measurement time. Addition of the solvent used with the ionophore, DMSO, as well as equal volume quantities of the Locke's solution did not stimulate an increase in the fluorescence intensity. The intensities were normalized to the basal fluorescence obtained before the addition of the ionophore, DMSO, or Locke's.

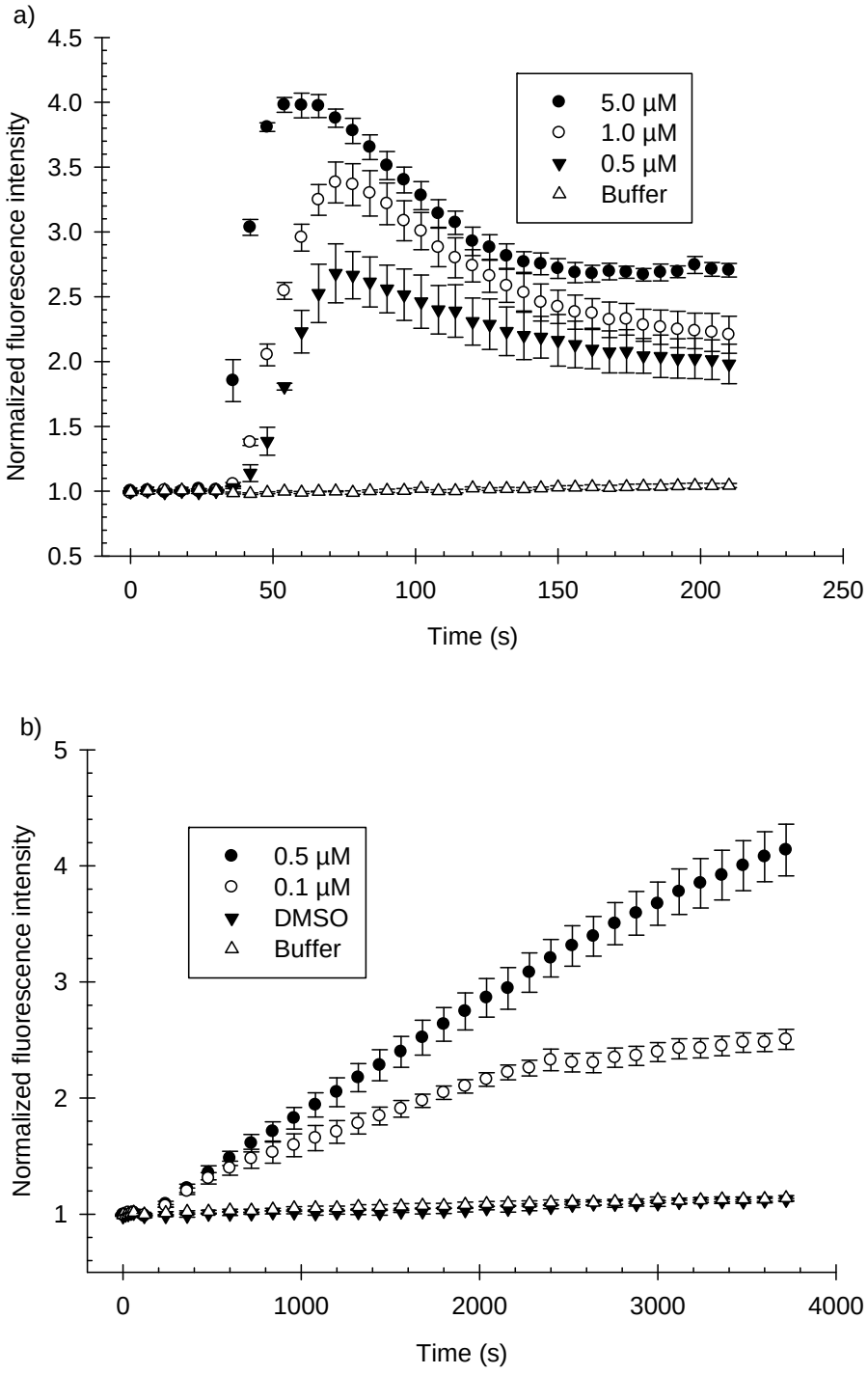

Figure 2.17 – Data showing the influence calcium ionophore has on a) calcium influx and b) intracellular NO production. The individual points represent the fluorescence intensities that are normalized to the baseline obtained 30 seconds before the addition of the stimuli. The final concentrations of the ionophore are indicated on the figure. The error bars represent the standard error of the mean with n = 4.

2.5.3.3 Metal-activated C-peptide stimulated calcium influx and intracellular NO production

After the different controls were performed to verify that the calcium uptake and subsequent NO production could be measured, different forms (metal-activated and metal-free) of C-peptide in various concentrations were added to the bPAECs. Concentrations of C-peptide and metal-activated C-peptide ranged from physiological (6.6 nM) to above physiological conditions (100 nM). The fluorescence intensities of both the calcium uptake and NO production studies are summarized in Figure 2.18. Regardless of the concentration of the regular and metal-activated form of the peptide, whether it be 6.6, 10, 50, or 100 nM, there were no changes in the fluorescence intensity representing either calcium influx or intracellular NO production, suggesting that C-peptide is not directly stimulating NO production in the pulmonary artery endothelial cells.

2.5.3.4 RBC stimulated endothelial NO production on microfluidic device

After the administration of flowed RBCs treated with metal-activated C-peptide, C-peptide, or Zn^{2+} under the immobilized bPAECs, images of the fluorescent DAF-FM DA using the macroscope setup described earlier were obtained. After comparing the fluorescence intensities before and after the administration of the treated and untreated RBCs, a change in intensity representing NO production was identified. The data represented in Figure 2.19 were normalized to the immobilized bPAECs that had untreated RBCs flowed underneath. bPAECs that had RBCs treated with only the peptide or only the Zn^{2+} flowed underneath showed no increase in fluorescence intensity indicating a change in NO production. However, RBCs that

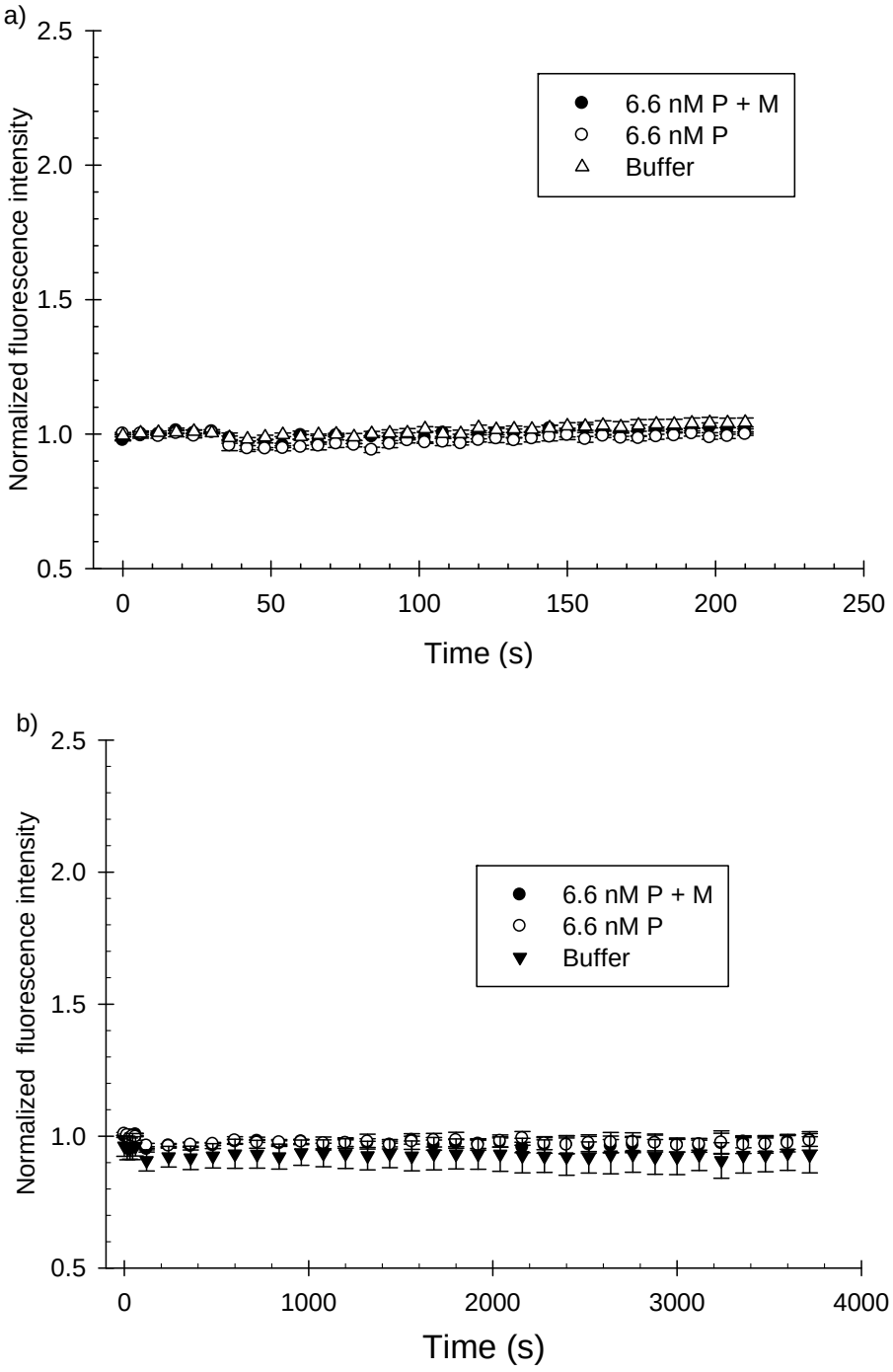

Figure 2.18 – C-peptide's influence on bPAEC a) calcium influx and b) intracellular NO production. The basal fluorescence was obtained during the first 30 seconds, after which C-peptide (P) or metal-activated C-peptide (P + M) were added to achieve a final concentration that is indicated in the figure. The following concentrations were also tested, but not shown: 10, 50, 100 nM. The fluorescence intensities after the addition of the peptide were normalized to the basal fluorescence. The error bars represent the standard error of the mean for n = 4.

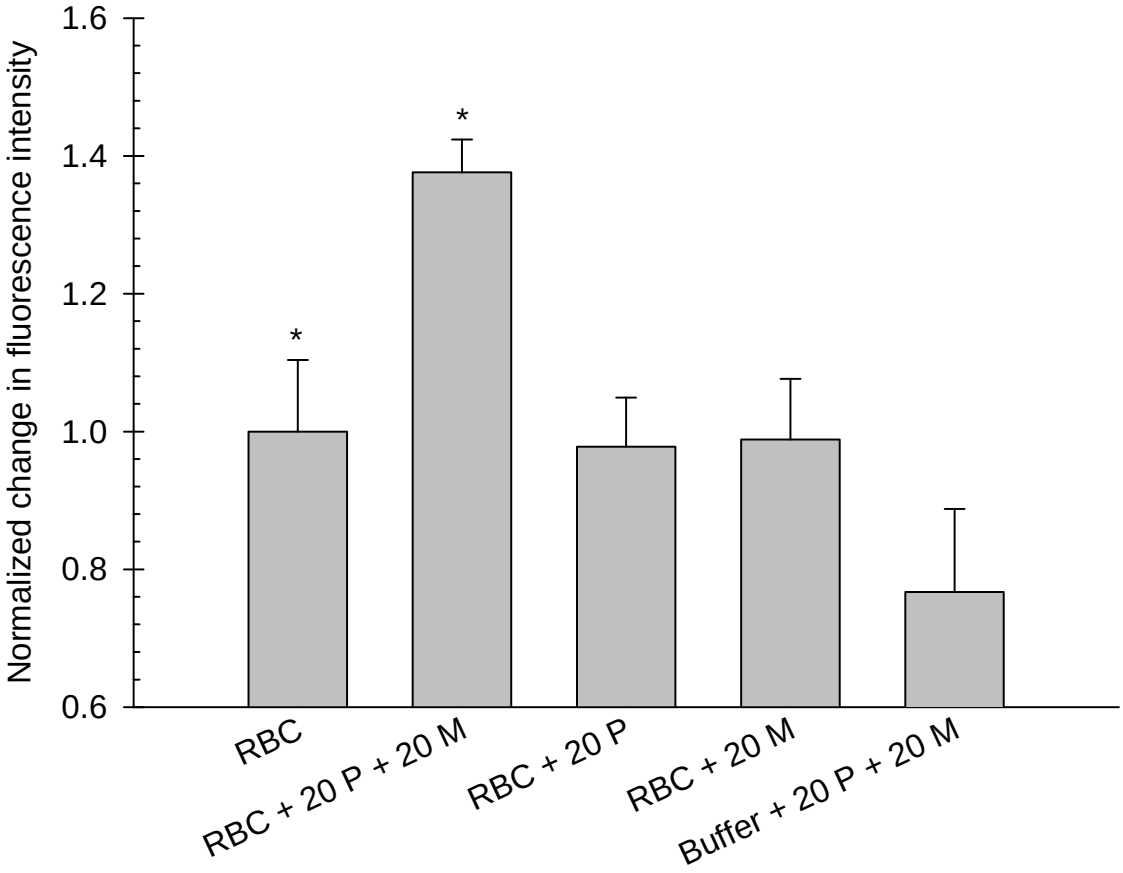

Figure 2.19 – Data illustrating the fluorescence intensity of NO measurements obtained from bPAECs immobilized on the microfluidic device. The values (n = 3 devices) were normalized to the change in fluorescence intensity measured from the bPAECs with only an untreated 7% RBC solution flowed underneath. With the solutions of treated RBCs flowed under the bPAECs, only the RBCs incubated with metal-activated C-peptide resulted in a significant (*$p < 0.05$) increase in observed fluorescence intensity, indicating an increase in NO production. Error bars represent the standard error of the mean.

had been treated with metal-activated C-peptide and flowed underneath the bPAECs resulted in a significant ($p < 0.05$) increase of 38 ± 5% in fluorescence intensity.

2.6 Discussion

C-peptide stimulated glucose uptake

After allowing for the proper alignment and folding of the insulin hormone in the pancreatic beta cells by connecting the two chains (A and B) together, C-peptide is cleaved from the proinsulin molecule and released into the bloodstream. Until recently, it was believed that there was no biological relevance or significance to C-peptide other than to facilitate the folding of insulin. However, recent *in vivo* studies have demonstrated C-peptide's ability to reduce specific complications and improve other conditions in type 1 diabetes.[10-14, 16-23] While these improvements in diabetics were observed, there was no clear explanation of how the once thought inactive biomolecule initiated the changes.

Since the aforementioned improvements in diabetics were monitored and observed, recent studies have emerged that proposed ideas and hypothesis on how mechanisms of C-peptide's activity may contribute to the alleviation of certain complications, many of which derive from improved blood flow. Studies involving healthy and RBCs obtained from people with diabetes have demonstrated C-peptide's ability to increase glucose uptake as well as improve cell deformability that is accompanied by an increased release of ATP, an activator of eNOS which produces the well known vasodilator NO.[31-36] Studies have also linked C-peptide with an increased eNOS activity in endothelial cells directly.[37, 38] With the studies involving

ATP release described by Meyer et al., the significance of a metal-activated peptide was demonstrated. This present group of studies aimed to determine whether metal-activated C-peptide can have similar effects on the endothelium to what was observed previously such as cell interaction, glucose uptake, and NO production.

In order for C-peptide to affect the endothelium in such ways as previously described, it must be interacting with the cell in some way either through internalization or a receptor based mechanism. Previous studies have utilized fluorescently labeled C-peptide molecules to track internalization into Swiss 3T3, HEK-293, human endothelial and smooth muscle cells.[51, 52] Some of the studies incubated the cells with concentrations orders of magnitude higher than the physiologically relevant concentration of 10 nM to compare with previous peptide uptake studies. Some concentrations used in the studies were as high as 10 or 1000 μM. These experiments were also not performed in hyperglycemic conditions that might be observed in diabetes. In the present study, while not using fluorescent techniques to image the internalization of C-peptide, ELISA results did support the previous findings that C-peptide was indeed binding on the cells or being internalized. Studies where the cells were pre-incubated in a high glucose environment resulted in around a 50% decrease in the amount of C-peptide binding to the cell compared to the normal glucose samples. This can explain why some of the complications that are shown to be ameliorated by C-peptide in people with type 1 diabetes, where C-peptide levels are decreased, still exist in people with type 2 diabetes even though normal or elevated levels of the peptide are present.

The observation by Meyer et al. that metal-activated C-peptide can stimulate glucose clearance via the RBC by increasing glucose uptake through GLUT1 was significant because the endothelium also uses that same transporter for the majority of its glucose uptake. The discussed

phloretin experiments where the glucose uptake was reduced by more than 50%, without the presence of GLUT4 stimulating insulin, support the significance that GLUT1 has in basal glucose uptake observed in the endothelium. Motivated from the findings dealing with RBC glucose uptake[35] and previous *in vivo* C-peptide/insulin glucose utilization studies,[15] it was observed and reported for the first time that incubation with the same metal-activated C-peptide that was able to cause an increase in intracellular glucose levels in RBCs also stimulated increased glucose levels in the bPAECs, presumably through GLUT1. As expected, this C-peptide stimulated glucose uptake required the presence of Zn^{2+}, further supporting the metal-activation hypothesis.[53] The controls involving the metal-free peptide and only Zn^{2+} indicate that zinc or C-peptide stimulate glucose uptake by itself. In fact, following incubation with levels of C-peptide that begin at physiologically relevant concentrations and elevated to supraphysiological levels all resulted in similar 20% increases in intracellular glucose.

Earlier it was discussed that bPAECs incubated in hyperglycemic conditions prior to the addition of metal-activated C-peptide resulted in a decreased interaction with the cell through the use of an immunoassay. Previous studies reported that hyperglycemia increased the amount of Annexin V binding to the surface of aortic endothelial cells.[54] The Annexin results suggest increased amounts of phosphatidylserine, a negatively charged phospholipid, on the outer surface of the cell. As C-peptide is negatively charged, there is likely a repulsion between the peptide and the cell surface. This would result in the decreased C-peptide binding measured with the ELISA.

This lowered binding of C-peptide to the bPAECs was also suggested by observing the glucose uptake in bPAECs incubated in hyperglycemic conditions that had been stimulated by

the metal-activated peptide. While there was still an increase in glucose uptake following administration of C-peptide on the cells in a hyperglycemic environment, the relative increase was lowered from 21% down to 15%. These findings evaluating the binding of C-peptide to the endothelial cells and the resulting glucose uptake identifies how the elevated glucose levels such as those in type 2 diabetes can result in the body's decreased ability to maintain proper blood sugar levels.

In many of the initial studies examining the beneficial effects that C-peptide has upon administration to type 1 diabetics, insulin needed to be administered simultaneously in order for these effects to be observed.[14] It is likely in these experiments that the insulin contained trace levels of zinc above 1% according to Sigma Aldrich. This insulin presence with zinc has been shown to cause the metal-activation of C-peptide upon combining the two *in vitro*, allowing for the observed effects of increased glucose uptake and ATP release.[53] The studies presented here combining metal-free insulin and metal-activated C-peptide demonstrate that it is only the C-peptide resulting in the increased glucose transport, especially since GLUT1 is insulin independent and is the primary glucose transporter in the RBCs and bPAECs. Because the insulin used in the described experiments did not contain zinc, according to the manufacturer's information, there was no activation of the metal-free C-peptide.

The addition of insulin alone in physiological concentrations to bPAECs pre-incubated in hyperglycemic conditions did not impact the glucose uptake levels, while the maximally effective concentrations increased intracellular glucose by 6%. There are conflicting reports from Gosmanov et al.[45] that identify insulin-stimulated glucose uptake in endothelial cells and Artwohl et al.[44] that states insulin does not have any glucose uptake effects. The results

discussed here tend to support the findings of Gosmanov et al., as there was an increase in glucose uptake following insulin administration. The 6% increase is not as significant as the 15 fold increase that was reported in the literature, but the studies here did not utilize the 2-deoxy-glucose analog that was applied.

C-peptide stimulated NO production

One of the earlier observations connecting C-peptide and NO production was made when an eNOS inhibitor administered to type 1 diabetic rats affected C-peptide's influence glucose utilization.[15] Additional studies that were more specific to C-peptide induced NO production observed that when combined with insulin, C-peptide could stimulate the dilation of skeletal muscle arterioles.[55] More recent studies have focused on impaired blood flow observed in diabetic neuropathy due to decreased eNOS expressions.[18, 56] Upon C-peptide treatment/administration, the blood flow was at least partially improved. In many of these aforementioned *in vivo* studies, it is well-believed that the improved blood flow derives from increased NO release from the endothelium following C-peptide interaction.

Previous studies that have specifically looked at the C-peptide endothelium interaction have utilized bovine aortic endothelial cells (bAECs). One specific study observed that there was an increase in NO release from the bAECs following incubation with physiological (6.6 nM) and elevated levels (66 nM) of C-peptide.[37] It was thought that this NO increase was due to an increased calcium influx, leading to increased eNOS activation. Another study found increased eNOS protein expression following the addition and incubation with C-peptide.[38] The increase of eNOS alone could allow for more generation of NO. With these two findings of C-peptide

stimulated endothelial NO production, combined with the previous findings in the Spence group that suggests metal-activation is required for activity, the previously discussed studies were performed to observe whether the metal-activation is also required for calcium influx and NO production.

Upon the administration of C-peptide and metal-activated C-peptide to immobilized bPAECs, there was no detectable increase or change of any kind in the endothelial NO production or calcium influx. This finding is somewhat unexpected, considering the past studies discussed, and that the addition of certain control molecules (calcium ionophore, ATP) did produce a change (increase) in the NO production and intracellular calcium. The calcium ionophore caused a constant increase in NO production from the constant influx of calcium, while the addition of ATP caused a leveling off of the NO production as the purinergic receptors became activated at a rate depending on ATP concentration. The C-peptide studies utilizing the ELISA confirmed that the peptide is indeed binding with the cells. Based on the null findings of the C-peptide administration regarding NO production and calcium influx, it was further hypothesized that C-peptide does play a significant role in regulating blood flow, due to the recent findings that when incubated with metal-activated C-peptide, RBCs release increased levels of ATP.[35, 36, 53] This potential interaction between the ATP released from the RBCs and the endothelial cells lining the innermost layer of the vessel walls is examined using microfluidics.

In a separate study performed by Paul Vogel in the Spence lab, human RBCs treated with metal-activated C-peptide or other controls were flowed under immobilized bPAECs in a microfluidic device similar to previous reports.[49, 50] The change in fluorescence intensity, which is indicative of intracellular NO production, was increased by 40% in the bPAECs where

RBCs incubated with metal-activated C-peptide were flowed underneath. This finding suggests that the RBCs, specifically in the presence of metal-activated C-peptide, do play a significant role in regulating blood flow through purinergic signaling mechanisms with the endothelium. The results also support the suggestion that the metal-activation is required to observe these effects, as the other controls did not alter the bPAEC intracellular NO production.

Summarily, the findings regarding the endothelial glucose uptake stimulated by metal-activated C-peptide agreed with the hypothesis. The metal-activation was required for activity and the glucose uptake was increased. The direct C-peptide stimulated endothelial NO production was nonexistent. However, the microfluidic evaluation revealed that endothelial NO production is stimulated and enhanced by RBCs that had been treated with metal-activated C-peptide.

REFERENCES

REFERENCES

1. Rubenstein, A. H.; Block, M. B.; Starr, J.; Melani, F.; Steiner, D. F., Proinsulin and C-peptide in blood. *Diabetes* **1972,** 21, (2 Suppl), 661-72.

2. Steiner, D. F.; Cunningham, D.; Spigelman, L.; Aten, B., Insulin biosynthesis: evidence for a precursor. *Science (New York, N.Y.)* **1967,** 157, (789), 697-700.

3. Steiner, D. F.; Clark, J. L.; Nolan, C.; Rubenstein, A. H.; Margoliash, E.; Aten, B.; Oyer, P. E., Proinsulin and the biosynthesis of insulin. *Recent Prog. Horm. Res.* **1969,** 25, 207-82.

4. Melani, F.; Ryan, W. G.; Rubenstein, A. H.; Steiner, D. F., Proinsulin secretion by a pancreatic beta-cell adenoma. Proinsulin and C-peptide secretion. *New Engl. J. Med.* **1970,** 283, (14), 713-9.

5. Steiner, D. F., On the role of the proinsulin C-peptide. *Diabetes* **1978,** 27 Suppl 1, 145-8.

6. Hoogwerf, B. J.; Bantle, J. P.; Gaenslen, H. E.; Greenberg, B. Z.; Senske, B. J.; Francis, R.; Goetz, F. C., Infusion of synthetic human C-peptide does not affect plasma glucose, serum insulin, or plasma glucagon in healthy subjects. *Metabolism* **1986,** 35, (2), 122-5.

7. Faber, O. K.; Binder, C., C-peptide response to glucagon. A test for the residual beta-cell function in diabetes mellitus. *Diabetes* **1977,** 26, (7), 605-10.

8. Kuzuya, H.; Blix, P. M.; Horwitz, D. L.; Rubenstein, A. H.; Steiner, D. F.; Binder, C.; Faber, O. K., Heterogeneity of circulating C-peptide. *J. Clin. Endocrinol. Metab.* **1977,** 44, (5), 952-62.

9. Samnegard, B.; Brundin, T., Renal extraction of insulin and C-peptide in man before and after a glucose meal. *Clin. Physiol.* **2001,** 21, (2), 164-71.

10. Johansson, B. L.; Borg, K.; Fernqvist-Forbes, E.; Kernell, A.; Odergren, T.; Wahren, J., Beneficial effects of C-peptide on incipient nephropathy and neuropathy in patients with Type 1 diabetes mellitus. *Diabetic Med.* **2000,** 17, (3), 181-9.

11. Ekberg, K.; Brismar, T.; Johansson, B. L.; Lindstrom, P.; Juntti-Berggren, L.; Norrby, A.; Berne, C.; Arnqvist, H. J.; Bolinder, J.; Wahren, J., C-Peptide replacement therapy and sensory nerve function in type 1 diabetic neuropathy. *Diabetes Care* **2007,** 30, (1), 71-6.

12. Samnegard, B.; Jacobson, S. H.; Jaremko, G.; Johansson, B. L.; Sjoquist, M., Effects of C-peptide on glomerular and renal size and renal function in diabetic rats. *Kidney Int.* **2001,** 60, (4), 1258-65.

13. Johansson, B. L.; Sjoeberg, S.; Wahren, J., The influence of human C-peptide on renal function and glucose utilization in type 1 (insulin-dependent) diabetic patients. *Diabetologia* **1992,** 35, (2), 121-8.

14. Johansson, B. L.; Kernell, A.; Sjoberg, S.; Wahren, J., Influence of combined C-peptide and insulin administration on renal function and metabolic control in diabetes type 1. *J. Clin. Endocrinol. Metab.* **1993,** 77, (4), 976-81.

15. Li, L.; Oshida, Y.; Kusunoki, M.; Yamanouchi, K.; Johansson, B. L.; Wahren, J.; Sato, Y., Rat C peptide I and II stimulate glucose utilization in STZ-induced diabetic rats. *Diabetologia* **1999,** 42, (8), 958-64.

16. Ido, Y.; Vindigni, A.; Chang, K.; Stramm, L.; Chance, R.; Heath, W. F.; DiMarchi, R. D.; Di Cera, E.; Williamson, J. R., Prevention of vascular and neural dysfunction in diabetic rats by C-peptide. *Science (Washington, D. C.)* **1997,** 277, (5325), 563-566.

17. Sima, A. A. F.; Zhang, W.; Sugimoto, K.; Henry, D.; Li, Z.; Wahren, J.; Grunberger, G., C-peptide prevents and improves chronic Type I diabetic polyneuropathy in the BB/Wor rat. *Diabetologia* **2001,** 44, (7), 889-897.

18. Cotter, M. A.; Ekberg, K.; Wahren, J.; Cameron, N. E., Effects of proinsulin C-peptide in experimental diabetic neuropathy: vascular actions and modulation by nitric oxide synthase inhibition. *Diabetes* **2003,** 52, (7), 1812-7.

19. Forst, T.; Kunt, T.; Pohlmann, T.; Goitom, K.; Engelbach, M.; Beyer, J.; Pfutzner, A., Biological activity of C-peptide on the skin microcirculation in patients with insulin-dependent diabetes mellitus. *J. Clin. Invest.* **1998,** 101, (10), 2036-41.

20. Hansen, A.; Johansson, B. L.; Wahren, J.; von Bibra, H., C-peptide exerts beneficial effects on myocardial blood flow and function in patients with type 1 diabetes. *Diabetes* **2002,** 51, (10), 3077-82.

21. Johansson, B. L.; Sundell, J.; Ekberg, K.; Jonsson, C.; Seppanen, M.; Raitakari, O.; Luotolahti, M.; Nuutila, P.; Wahren, J.; Knuuti, J., C-peptide improves adenosine-induced myocardial vasodilation in type 1 diabetes patients. *Am. J. Physiol. Endocrinol. Metab.* **2004,** 286, (1), E14-9.

22. Johansson, B. L.; Wahren, J.; Pernow, J., C-peptide increases forearm blood flow in patients with type 1 diabetes via a nitric oxide-dependent mechanism. *Am. J. Physiol. Endocrinol. Metab.* **2003,** 285, (4), E864-70.

23. Johansson, B. L.; Linde, B.; Wahren, J., Effects of C-peptide on blood flow, capillary diffusion capacity and glucose utilization in the exercising forearm of type 1 (insulin-dependent) diabetic patients. *Diabetologia* **1992,** 35, (12), 1151-8.

24. Palmer, R. M. J.; Ferrige, A. G.; Moncada, S., Nitric oxide release accounts for the biological activity of endothelium-derived relaxing factor. *Nature (London, United Kingdom)* **1987,** 327, (6122), 524-6.

25. Dean, B. M.; Perrett, D., Studies on adenine and adenosine metabolism by intact human erythrocytes using high performance liquid chromatography. *Biochim. Biophys. Acta* **1976,** 437, (1), 1-5.

26. Miseta, A.; Bogner, P.; Berenyi, E.; Kellermayer, M.; Galambos, C.; Wheatley, D. N.; Cameron, I. L., Relationship between cellular ATP, potassium, sodium and magnesium concentrations in mammalian and avian erythrocytes. *Biochim. Biophys. Acta* **1993,** 1175, (2), 133-9.

27. Faris, A.; Spence, D. M., Measuring the simultaneous effects of hypoxia and deformation on ATP release from erythrocytes. *Analyst* **2008,** 133, (5), 678-82.

28. Bergfeld, G. R.; Forrester, T., Release of ATP from human erythrocytes in response to a brief period of hypoxia and hypercapnia. *Cardiovasc. Res.* **1992,** 26, (1), 40-7.

29. Ellsworth, M. L.; Forrester, T.; Ellis, C. G.; Dietrich, H. H., The erythrocyte as a regulator of vascular tone. *Am. J. Physiol.* **1995,** 269, (6 Pt 2), H2155-61.

30. Sprague, R. S.; Ellsworth, M. L.; Stephenson, A. H.; Lonigro, A. J., ATP: the red blood cell link to NO and local control of the pulmonary circulation. *Am. J. Physiol.* **1996,** 271, (6 Pt 2), H2717-22.

31. Vague, P.; Coste, T. C.; Jannot, M. F.; Raccah, D.; Tsimaratos, M., C-peptide, Na+,K(+)-ATPase, and diabetes. *Exp. Diabesity Res.* **2004,** 5, (1), 37-50.

32. De La Tour, D. D.; Raccah, D.; Jannot, M. F.; Coste, T.; Rougerie, C.; Vague, P., Erythrocyte Na/K ATPase activity and diabetes: relationship with C-peptide level. *Diabetologia* **1998,** 41, (9), 1080-4.

33. Subasinghe, W.; Spence, D. M., Simultaneous determination of cell aging and ATP release from erythrocytes and its implications in type 2 diabetes. *Anal. Chim. Acta* **2008,** 618, (2), 227-33.

34. Kunt, T.; Schneider, S.; Pfutzner, A.; Goitum, K.; Engelbach, M.; Schauf, B.; Beyer, J.; Forst, T., The effect of human proinsulin C-peptide on erythrocyte deformability in patients with type I diabetes mellitus. *Diabetologia* **1999,** 42, (4), 465-471.

35. Meyer, J. A.; Froelich, J. M.; Reid, G. E.; Karunarathne, W. K.; Spence, D. M., Metal-activated C-peptide facilitates glucose clearance and the release of a nitric oxide stimulus via the GLUT1 transporter. *Diabetologia* **2008,** 51, (1), 175-82.

36. Meyer, J. A.; Subasinghe, W.; Sima, A. A.; Keltner, Z.; Reid, G. E.; Daleke, D.; Spence, D. M., Zinc-activated C-peptide resistance to the type 2 diabetic erythrocyte is associated with hyperglycemia-induced phosphatidylserine externalization and reversed by metformin. *Mol. Biosyst.* **2009,** 5, (10), 1157-62.

37. Wallerath, T.; Kunt, T.; Forst, T.; Closs, E. I.; Lehmann, R.; Flohr, T.; Gabriel, M.; Schafer, D.; Gopfert, A.; Pfutzner, A.; Beyer, J.; Forstermann, U., Stimulation of

endothelial nitric oxide synthase by proinsulin C-peptide. *Nitric Oxide* **2003,** 9, (2), 95-102.

38. Kitamura, T.; Kimura, K.; Makondo, K.; Furuya, D. T.; Suzuki, M.; Yoshida, T.; Saito, M., Proinsulin C-peptide increases nitric oxide production by enhancing mitogen-activated protein-kinase-dependent transcription of endothelial nitric oxide synthase in aortic endothelial cells of Wistar rats. *Diabetologia* **2003,** 46, (12), 1698-705.

39. Alpert, E.; Gruzman, A.; Riahi, Y.; Blejter, R.; Aharoni, P.; Weisinger, G.; Eckel, J.; Kaiser, N.; Sasson, S., Delayed autoregulation of glucose transport in vascular endothelial cells. *Diabetologia* **2005,** 48, (4), 752-5.

40. Kaiser, N.; Sasson, S.; Feener, E. P.; Boukobza-Vardi, N.; Higashi, S.; Moller, D. E.; Davidheiser, S.; Przybylski, R. J.; King, G. L., Differential regulation of glucose transport and transporters by glucose in vascular endothelial and smooth muscle cells. *Diabetes* **1993,** 42, (1), 80-9.

41. Regina, A.; Roux, F.; Revest, P. A., Glucose transport in immortalized rat brain capillary endothelial cells in vitro: transport activity and GLUT1 expression. *Biochim. Biophys. Acta* **1997,** 1335, (1-2), 135-43.

42. Wiernsperger, N. F., Is non-insulin dependent glucose uptake a therapeutic alternative? part 2: do such mechanisms fulfill the required combination of power and tolerability? *Diabetes Metab.* **2005,** 31, (6), 521-525.

43. Noyman, I.; Marikovsky, M.; Sasson, S.; Stark, A. H.; Bernath, K.; Seger, R.; Madar, Z., Hyperglycemia reduces nitric oxide synthase and glycogen synthase activity in endothelial cells. *Nitric Oxide* **2002,** 7, (3), 187-93.

44. Artwohl, M.; Brunmair, B.; Fuernsinn, C.; Hoelzenbein, T.; Rainer, G.; Freudenthaler, A.; Porod, E. M.; Huttary, N.; Baumgartner-Parzer, S. M., Insulin does not regulate glucose transport and metabolism in human endothelium. *Eur. J. Clin. Invest.* **2007,** 37, (8), 643-650.

45. Gosmanov Aidar, R.; Stentz Frankie, B.; Kitabchi Abbas, E., De novo emergence of insulin-stimulated glucose uptake in human aortic endothelial cells incubated with high glucose. *Am. J. Physiol. Endocrinol. Metab.* **2006,** 290, (3), E516-22.

46. Alpert, E.; Gruzman, A.; Totary, H.; Kaiser, N.; Reich, R.; Sasson, S., A natural protective mechanism against hyperglycaemia in vascular endothelial and smooth-muscle cells: role of glucose and 12-hydroxyeicosatetraenoic acid. *Biochem. J.* **2002,** 362, (Pt 2), 413-22.

47. Keltner, Z.; Meyer, J. A.; Johnson, E. M.; Palumbo, A. M.; Spence, D. M.; Reid, G. E., Mass spectrometric characterization and activity of zinc-activated proinsulin C-peptide and C-peptide mutants. *Analyst* **2010,** 135, (2), 278-88.

48. McDonald, J. C.; Duffy, D. C.; Anderson, J. R.; Chiu, D. T.; Wu, H.; Schueller, O. J.; Whitesides, G. M., Fabrication of microfluidic systems in poly(dimethylsiloxane). *Electrophoresis* **2000,** 21, (1), 27-40.

49. Letourneau, S.; Hernandez, L.; Faris, A. N.; Spence, D. M., Evaluating the effects of estradiol on endothelial nitric oxide stimulated by erythrocyte-derived ATP using a microfluidic approach. *Anal. Bioanal. Chem.* **2010,** 397, (8), 3369-75.

50. Genes, L. I.; N, V. T.; Hulvey, M. K.; Martin, R. S.; Spence, D. M., Addressing a vascular endothelium array with blood components using underlying microfluidic channels. *Lab Chip* **2007,** 7, (10), 1256-9.

51. Lindahl, E.; Nyman, U.; Melles, E.; Sigmundsson, K.; Stahlberg, M.; Wahren, J.; Obrink, B.; Shafqat, J.; Joseph, B.; Jornvall, H., Cellular internalization of proinsulin C-peptide. *Cell Mol. Life Sci.* **2007,** 64, (4), 479-86.

52. Luppi, P.; Geng, X.; Cifarelli, V.; Drain, P.; Trucco, M., C-peptide is internalised in human endothelial and vascular smooth muscle cells via early endosomes. *Diabetologia* **2009,** 52, (10), 2218-28.

53. Medawala, W.; McCahill, P.; Giebink, A.; Meyer, J.; Ku, C. J.; Spence, D. M., A Molecular Level Understanding of Zinc Activation of C-peptide and its Effects on Cellular Communication in the Bloodstream. *Rev. Diabet. Stud.* **2009,** 6, (3), 148-58.

54. Recchioni, R.; Marcheselli, F.; Moroni, F.; Pieri, C., Apoptosis in human aortic endothelial cells induced by hyperglycemic condition involves mitochondrial depolarization and is prevented by N-acetyl-L-cysteine. *Metabolism clinical and experimental* **2002,** 51, (11), 1384-8.

55. Jensen, M. E.; Messina, E. J., C-peptide induces a concentration-dependent dilation of skeletal muscle arterioles only in presence of insulin. *Am. J. Physiol.* **1999,** 276, (4 Pt 2), H1223-8.

56. Stevens, M. J.; Zhang, W.; Li, F.; Sima, A. A., C-peptide corrects endoneurial blood flow but not oxidative stress in type 1 BB/Wor rats. *Am. J. Physiol. Endocrinol. Metab.* **2004,** 287, (3), E497-505.

CHAPTER 3: METFORMIN ENHANCES METAL-ACTIVATED C-PEPTIDE'S EFFECTS ON VASCULAR COMPONENTS UNDER HYPERGLYCEMIC CONDITIONS

3.1 RBC metabolism

The red blood cell (RBC) is the most common cell found in the blood stream. The most well known purpose of the RBC is to carry hemoglobin-bound oxygen to various tissues and organs throughout the body and releasing it as needed. As the RBC matures, certain organelles found in most eukaryotic cells begin to disappear. These organelles that are void in a mature RBC include, but are not limited to, a nucleus, Golgi apparatus, endoplasmic reticulum, and the mitochondria. The lack of a nucleus is significant because there is no ability to regulate/control gene and subsequent protein expression. The lack of mitochondria limits the mechanisms by which the RBC is able to metabolize glucose. Because the mitochondria are required for the oxidative phosphorylation of glucose and the production of higher amounts of ATP, the RBC must rely solely on glycolysis to maintain their ATP supplies.

Glucose is brought into the RBC through the insulin-independent GLUT1, passively transporting the carbohydrate through the membrane. Once internalized, the glucose is first converted into glucose-6-phosphate (G6P) by the enzyme hexokinase. From here, the G6P can then be sent through glycolysis (Figure 1.1) producing pyruvate, or the pentose phosphate pathway (Figure 3.1). In a healthy RBC, the majority of the glucose is sent through the glycolytic pathway with only a small fraction being shuttled through the pentose phosphate pathway ($1/60^{th}$ of its potential).[1] However, in states of increased oxidative stress, the overall glucose metabolism is shifted towards the pentose phosphate pathway.[1, 2] The regular flux of

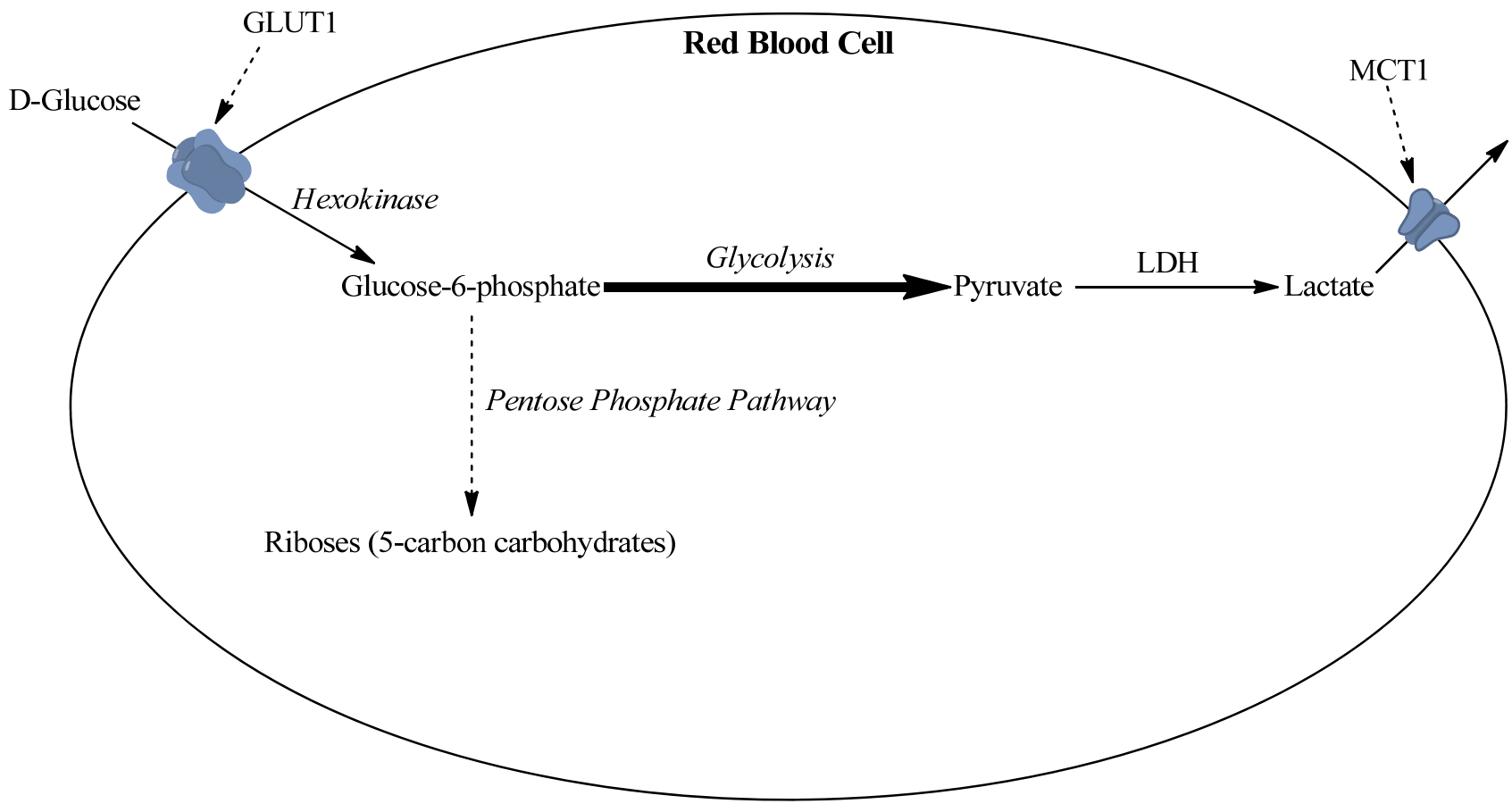

Figure 3.1 – Illustration showing the main pathways used by the red blood cell (RBC) to metabolize glucose. After being transported into the cell by GLUT1, hexokinase phosphorylates glucose into glucose-6-phosphate (G6P). The majority of the G6P is sent through glycolysis (bold arrow) where it is converted into pyruvate. Lactate dehydrogenase (LDH) then converts the pyruvate into lactate. The metabolic byproduct is then removed from the cell through the monocarboxylate transporter isoform (MCT1). Depending on the cell's energy requirements, oxidative stress, etc., the G6P can be sent through the pentose phosphate pathway (PPP – dashed arrow). The production of the 5-carbon ribose molecules generates NADPH, which can be used to reduce glutathione, regenerating the cell's antioxidant capabilities.

glucose metabolism through the glycolytic pathway results in the eventual conversion of pyruvate into lactate (Figure 3.1), which is ultimately transported out of the cell via the monocarboxylate transporter 1 (MCT1) and into the bloodstream where it is removed by the liver and kidney.[3-5]

Under conditions of chronic hyperglycemia, such as those found in diabetes, the RBC functionality, and structure to some extent, are altered. The decreased deformability of the RBC due to reduced Na^+,K^+-ATPase activity that has been discussed previously in Chapter 2.2, results in the lowered release of the NO stimulating purinergic signaling molecule ATP.[6, 7] Another observed characteristic of the RBC structure during conditions of chronic hyperglycemia is externalization of certain lipids on the plasma membrane. In a typical RBC membrane, the phospholipids phosphatidylcholine (PC) and sphingomyelin (SM) are usually located on the outer portion of the lipid bilayer, while other amine containing phospholipids such as phosphatidylserine (PS) and phosphatidylethanolamine (PE) are found on the inner portion of the membrane (Figure 3.2).[8-10] However, in diabetic conditions with chronic hyperglycemia, RBCs have increased PS levels on the outer portion of the membrane that can lead to increased aggregation.[11-13] In fact, incubation of normal human RBCs in hyperglycemic environments has been shown to increase externalized PS exposure.[14, 15]

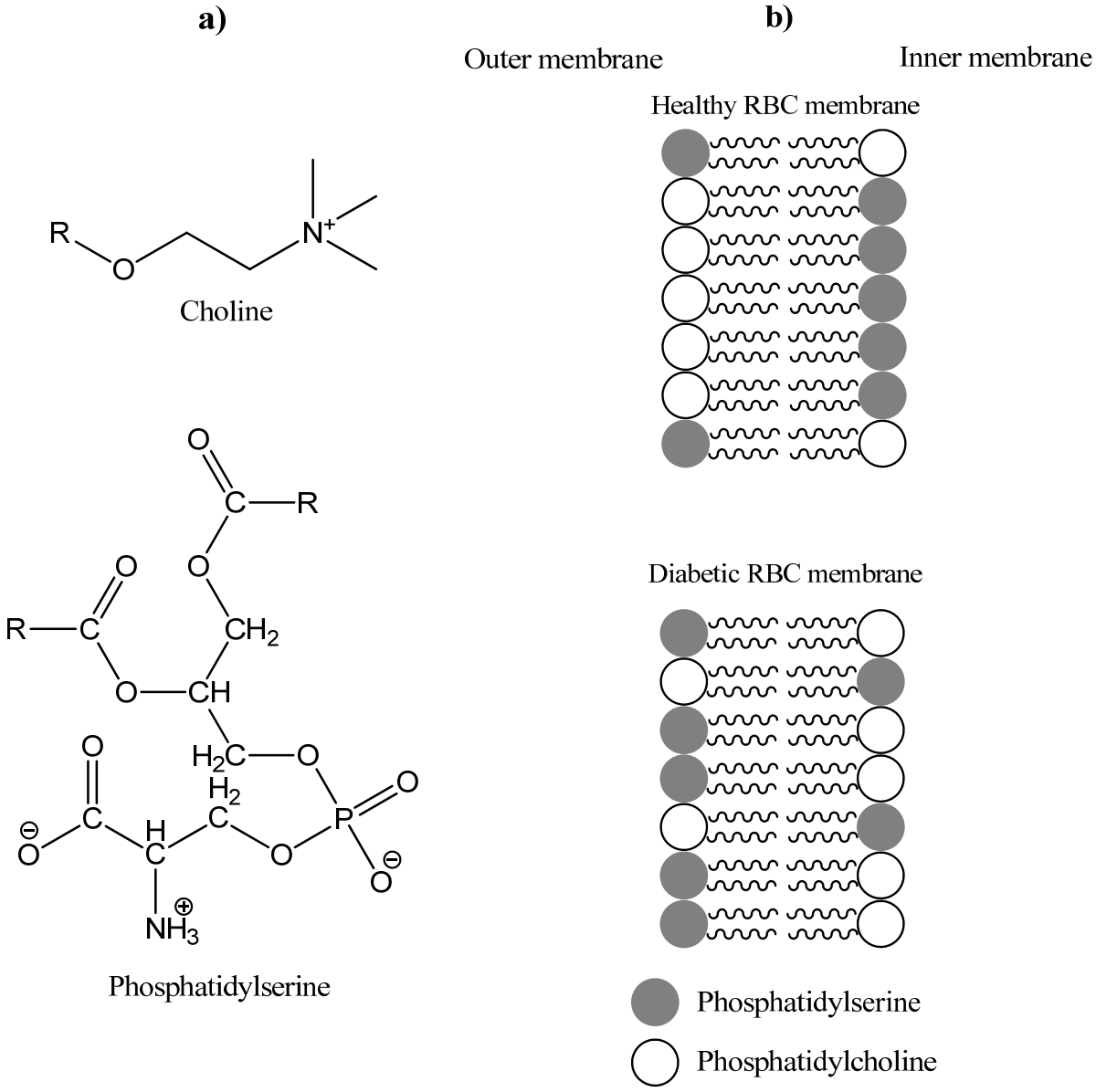

Figure 3.2 – a) Structural information of the different phospholipids head groups that comprise the majority of the RBC membrane surfaces. In a normal RBC cell membrane (b – top), the outer membrane is comprised primarily of phospholipids with the choline head group (a – top) with the negatively charged phosphatidylserine (a – bottom) comprising the majority of the inner portion. However, in RBCs exposed to hyperglycemic conditions or times of increased oxidative stress, there are increased PS levels on the outer surface of the membrane (b – bottom).

3.2 Metformin and diabetes

Today, the biguanide drug metformin (Figure 3.3) is one of only two drugs approved by the World Health Organization used to treat patients with type 2 diabetes. Since its introduction in 1957, metformin was shown to decrease the elevated plasma glucose levels found in people with type 2 diabetes.[16-19] This effect is believed to occur through increased insulin sensitivity, decreased insulin presence, and decreased hepatic glucose production in the liver (gluconeogenesis).[20] There have also been observed improvements in the vascular function of insulin-resistant rats.[21] While there are many beneficial characteristics of the treatment of type 2 diabetes with metformin, there are also specific side effects.

Some of the side effects deriving from metformin therapy are considered minor such as gastrointestinal upset and decreased testosterone levels in men.[22, 23] One of the more serious side effects (fatality rate of 50%) from metformin therapy is lactic acidosis.[24, 25] This condition, while rare,[26] occurs when the metabolic byproduct lactic acid (lactate) levels in the vasculature increase. Increasing the lactate levels can result in an overall decrease in blood pH that can prove to be fatal if left untreated. While it is essential for people to be cautions when taking metformin, the risk of developing lactic acidosis is due primarily to improper dosing of the drug, or decreased liver and/or renal function and the body's inability to efficiently remove the increased lactate.

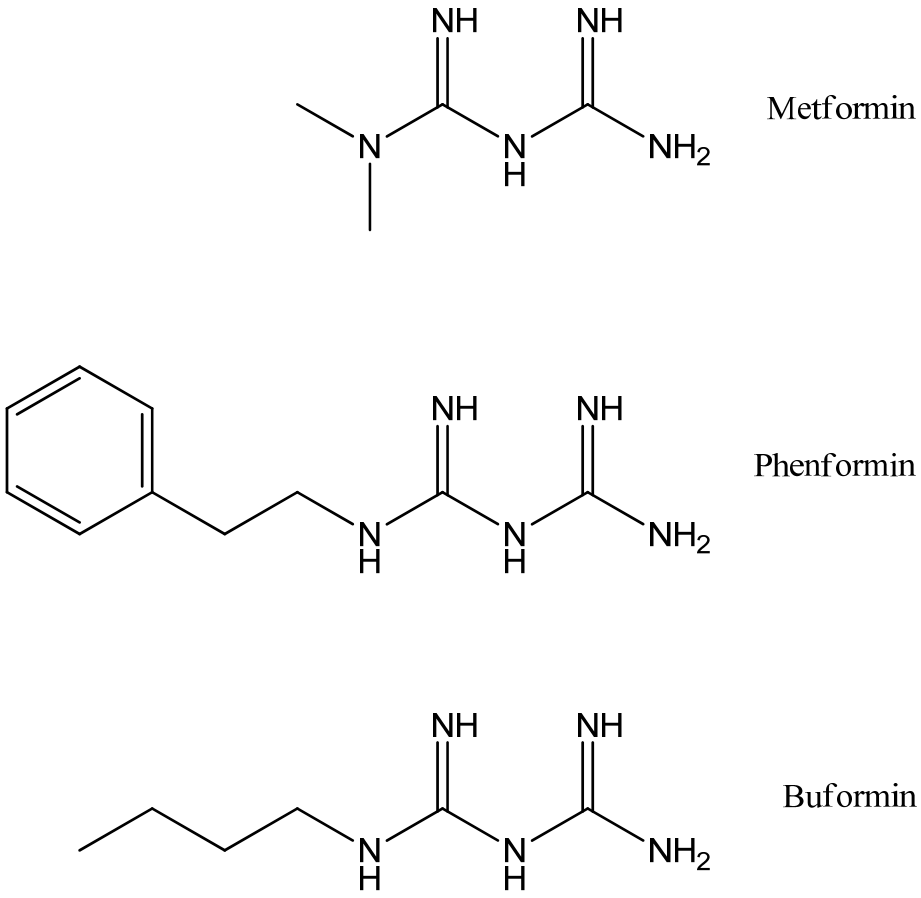

Figure 3.3 – Molecular structures of the different biguanide molecules that are used as anti-diabetic drugs. All drugs have identical base structures with phenformin containing an extra phenol group and buformin having an extra butyl group. Currently, metformin is the only one of the three drugs used for the treatment of diabetes. It is administered as an oral medication. There have been minimal side effects reported, such as gastrointestinal discomfort and lactic acidosis. The other two medications listed are no longer in use as anti-diabetic treatments in the United States due to their toxic effects. Phenformin was removed from the market in the late 1970s and buformin was withdrawn from nearly all countries shortly after.

3.3 C-peptide and metformin

There have been recent findings from the Spence lab that have identified C-peptide, specifically metal-activated C-peptide, as a stimulus that increases glucose uptake into the RBC and cultured endothelial cells.[27-29] C-peptide also increases ATP release from the RBCs of both normal and diabetic subjects. When metformin was administered to the same RBC samples (normal and diabetic) in the presence of metal-activated C-peptide, the ATP levels and glucose uptake were both increased in the RBCs of people with diabetes while the normal RBCs' glucose uptake and ATP release remained unchanged.[28] Metformin by itself did not have a significant effect on the ATP release or glucose uptake. In the same study, it was reported that the addition of metformin to diabetic RBCs decreased the amount of PS on the outer membrane by measuring the presence of annexin that bound to the externalized PS.

Although it has been shown that metformin increases the glucose uptake and ATP release from RBCs obtained from subjects with diabetes in the presence of metal-activated C-peptide when compared to C-peptide alone, the mechanisms of the metformin influence remain unknown. The work presented here aims to identify an increased metal-activated C-peptide interaction with RBCs incubated with metformin in a simulated diabetic environment and follow the metabolism occurring within the cell. Some of the previous findings regarding metformin and C-peptide are also applied to endothelial cells, as they have been shown to be stimulated by the same metal-activated C-peptide.

3.4 Experimental

3.4.1 Preparation of reagents

Unless stated otherwise, all aqueous stock and working solutions were prepared using purified (18.2 MΩ) double-distilled water (DDW). All reagents that were prepared in volumetric glassware were transferred to polypropylene tubes immediately to reduce any unwanted metal contamination.

Human C-peptide (Genscript, Piscataway, NJ) was obtained and purified as described in Chapter 2.4.1. C-peptide stock solutions of 8.3 μM were prepared by dissolving 250 μg of the purified peptide previously stored at -20°C in 10 mL of DDW and aliquotted into smaller vials to prevent any additional contamination from being introduced from repeated pipetting. Further working solutions of 500 nM were prepared by diluting 60.2 μL stock C-peptide into 1 mL of DDW.

Zinc (Zn^{2+}) solutions were prepared by dissolving 10.0 mg zinc chloride (Jade Scientific, Canton, MI) in 500 mL of DDW to achieve a stock concentration of 147 μM. The stock solution was then diluted to working concentrations of 1.0 μM by diluting 6.8 μL of the stock into 1 mL of DDW. For use in different experiments, two different metformin solutions had to be prepared. For the experiments involving metformin and the RBCs, a metformin working solution of 35.2 mM was prepared by dissolving 5.85 mg metformin (Sigma Aldrich) in 1 mL of DDW. For the experiments involving metformin and bPAECs, a working metformin solution of 239 mM was prepared by dissolving 20 mg of metformin in 505 μL of DMEM.

For the lactate assay, a 6.66 mM L-lactic acid stock solution was prepared by dissolving 15 mg L-lactic acid (Sigma Aldrich) in 25 mL of DDW. From the stock solution, a working solution of 50 μM was prepared by diluting 75 μL of stock into 10 mL of DDW to be used in the standard addition experiments. For experiments utilizing the preparation of standards, a working solution of 1 mM was made by diluting 150 μL of the stock into 1 mL of DDW. Standards of L-lactic acid ranging from 10 – 100 μM were prepared from the 1 mM working solution by diluting the appropriate volume up to 1 mL with DDW. The stock solution of nicotinamide adenine dinucleotide (NAD^+) was made by dissolving the vial containing 50 mg (Sigma Aldrich) of the solid with 1 mL of DDW, resulting in a final concentration of 50.2 mM. The L-lactic dehydrogenase enzyme (Sigma Aldrich) used in the assay was supplied already prepared in an ammonium sulfate suspension at ~ 6.7 units/μL.

For quantification in the glucose assay, a 6.66 mM D-glucose (Sigma Aldrich) stock solution was prepared by dissolving 30 mg in 25 mL of DDW. Standards were then prepared from the stock solution at concentrations between 10 and 100 μM by adding the appropriate volume from the stock and diluting with DDW up to 1 mL. Nicotinamide adenine dinucleotide phosphate ($NADP^+$ - Sigma Aldrich) was prepared at a final working concentration of 12.5 mM by dissolving 100 mg in 10.76 mL of DDW and aliquotted into single use volumes of 320 μL. A 20 mM ATP stock solution was prepared by dissolving 5.5 mg in 500 μL of DDW. The magnesium chloride ($MgCl_2$ – Columbus Chemical Industries, Columbus, WI) stock solution was prepared at 100 mM by dissolving 203 mg in 10 mL of DDW. Of the two enzymes used, the glucose-6-phosphate dehydrogenase (G6PDH, Sigma Aldrich) was supplied in an ammonium sulfate suspension at ~ 3.75 units/μL. The other enzyme, hexokinase (Sigma Aldrich), was

prepared as a stock solution with a concentration of 57 units/mL by dissolving 10 mg of the lyophilized enzyme in 10 mL of DDW.

The physiological salt solution (PSS) used to prepare RBC solutions was prepared in DDW from the following materials (all from Sigma Aldrich) with the numerical values indicating the final concentration (mM); KCl – 4.7, $CaCl_2$ – 2.0, NaCl – 140.5, $MgSO_4$ – 12.0, tris(hydroxymethyl)aminomethane – 21.0, glucose – 5.6, 5% bovine serum albumin. The pH was adjusted to 7.4 by adding concentrated hydrochloric acid dropwise. In order to simulate the hyperglycemic environment observed in diabetes, a 15 mM glucose PSS (HG PSS) solution was prepared by adding 25.6 mg D-glucose to 15 mL of the 5.5 mM glucose PSS.

3.4.2 Collection and purification of RBCs

The RBCs used in the studies were obtained from male New Zealand White rabbits following the protocols that were approved by Michigan State University. The procedures for obtaining the blood are previously described.[28-31] Rabbits were first sedated with ketamine (8 mL/kg, i.m.) and xylazine (1 mg/kg, i.m.) and then anesthetized with pentobarbital sodium (15 mg/kg, i.v.). A cannula was inserted into the trachea, allowing the rabbit to be ventilated with room air at a rate of 20 breaths per minute. A catheter was then inserted into the carotid artery allowing for the administration of the anticoagulant heparin (500 units, i.v.), followed by exsanguination.

Approximately 70 to 80 mL of whole blood were obtained from the rabbit and divided into multiple tubes. The blood was then centrifuged at 500 x g at 25°C for 10 minutes, after which the plasma layer and buffy coat were removed via aspiration. The remaining RBC layer

was rinsed with PSS and centrifuged an additional three times. Following the multiple rinses, the washed RBC hematocrit was determined. The RBCs were always used the day they were obtained.

Human RBCs that were used in experimentation were obtained via venipuncture from healthy volunteers, both male and female. The collection vacuum vials were centrifuged for 10 minutes at 500 x g, after which the plasma and buffy coat were removed. The final preparation/washing of the human RBCs was the same as that used for the rabbit RBCs.

3.4.3 Endothelial cell culture

The protocols for culturing the bovine pulmonary artery endothelial cells (bPAECs) (Lonza) were explained in chapter 2.4.3. Briefly, the cells were cultured and grown on 75 cm^2 tissue culture flasks with the endothelial growth media (EGM) until full. The cells were then subcultured and removed following treatment with trypsin, and transferred into 6-well or 12-well tissue culture plates. Once the cells proliferate to fill the wells, and 24 hours before the experiments, the EGM was replaced with serum free DMEM with different concentrations of glucose, either 5.5 mM (DMEM) or 25 mM (HG DMEM).

3.4.4 RBC preparation for C-peptide/metformin studies

The process for preparing the samples for experimentation is provided in Figure 3.4. In order to evaluate how metformin can affect the ability of metal-activated C-peptide to interact with the RBC and stimulate glucose uptake and subsequent lactate production in normal and

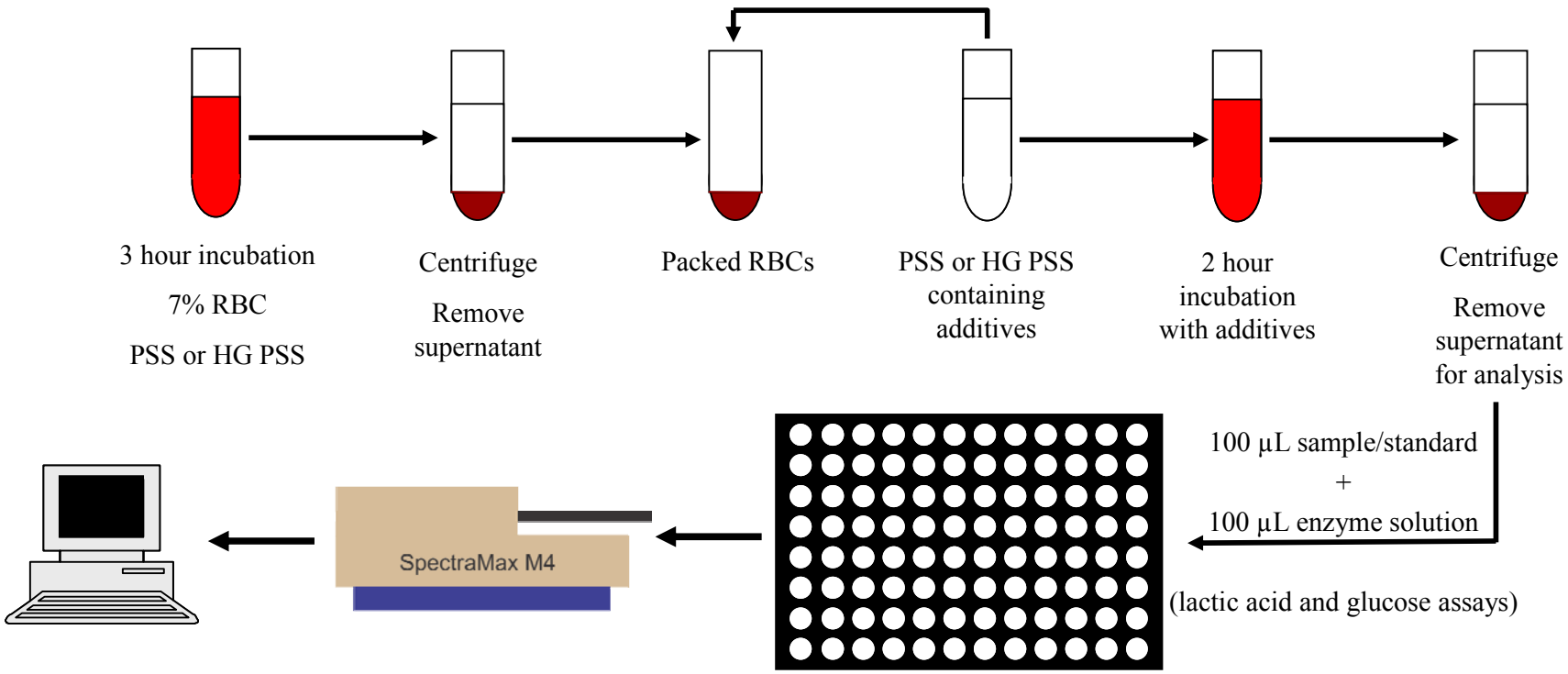

Figure 3.4 – Diagram describing the preparation of the RBC samples for use in the metformin/C-peptide experiments. The lactate and glucose measurements are described here with the supernatant arranged in a 96-well plate followed by the appropriate enzyme solution. The C-peptide ELISA (not shown) uses the same supernatant that is described after the second centrifugation step. Following the appropriate incubation in the 96-well plate with either the enzyme solutions or ELISA reagents, the fluorescence is obtained using a microplate reader to determine the lactate and glucose content. The ELISA is performed by measuring the absorbance using the same microplate reader.

hyperglycemic environments, multiple 1 mL solutions using human/rabbit RBCs at a 7% hematocrit were initially incubated at 37°C for 3 hours. Half of the RBC solutions were prepared in PSS containing 5.5 mM glucose to simulate a normoglycemic environment, while the other half was prepared in HG PSS containing 15 mM glucose to simulate the glucose conditions of a diabetic environment. Following the 3 hour incubation, the vials were centrifuged, and 850 μL of the supernatant were removed. 850 mL of either PSS or HG PSS containing 20 nM metal-activated C-peptide with/without 30 μM metformin, or metformin by itself were added to the vials and allowed to incubate an additional 2 hours at 37°C. At the same time, a 7% RBC solution to be used as a blank was prepared in PSS with DDW replaced for the C-peptide and metformin and allowed to incubate the same amount of time as the samples.

The experimental solutions containing the C-peptide and/or metformin were prepared as 1 mL volumes using the following method. 40 μL of the 500 nM C-peptide solution (20 picomoles) were combined with 20 μL of a 1000 nM Zn^{2+} solution (20 picomoles) to prepare the metal-activated C-peptide. In the C-peptide solutions containing metformin, 1 μL of the 35.2 mM metformin stock solution was then added. In the solutions without C-peptide, 1 mL of metformin stock was added followed by 60 μL of DDW. The C-peptide solutions containing no metformin had 1 μL of DDW added to maintain similar volumes between samples. The samples then were diluted into 789 μL of either PSS or HG PSS and immediately transferred to the centrifuged RBC pellet. For the RBC blank sample, 789 μL PSS were added to 61 μL of DDW. All samples were incubated for 2 hours at 37°C, after which the supernatant was removed and measured for C-peptide, lactate, or glucose content.

3.4.5 Enzyme Linked Immunosorbent Assay (ELISA) used to examine the interaction of C-peptide with the RBC when treated with metformin

Only the samples containing metal-activated C-peptide with/without metformin were used when measuring the amount of C-peptide that interacted with the RBC. Following the final 2 hour incubation at 37°C, the RBC samples were centrifuged for 5 minutes at 500 x g. The supernatant was removed and diluted by a factor of 20 by taking a 50 µL aliquot of the supernatant and adding to 950 µL of DDW.

In order to reduce the potential matrix interferences, multiple 'blank' samples were prepared to contain the same ratio of supernatant to water that is present in the samples. The blank RBC sample containing no C-peptide or metformin was also diluted by a factor of 20 by diluting 95 µL of the supernatant into 1805 µL of DDW. Using this supernatant solution, C-peptide standards at concentrations 0, 0.1, 0.5, and 1.0 nM were prepared by diluting 2 µL of the 500 nM C-peptide stock solution in 998 µL of the diluted supernatant. The other 2 standards were prepared from the 1 nM standard using serial dilutions. Standards with the same concentrations of C-peptide were also prepared with 1.5 µM metformin to compensate for any matrix interferences the molecule may have.

With the samples and standards prepared, a C-peptide ELISA (Millipore) was utilized (Figure 2.2) and the protocol provided by the company was followed. Briefly, the wells in the ELISA were washed multiple times with the provided rinse solution, followed by the addition of 50 µL of an assay buffer, 10 µL of the sample/standard, and 20 µL of the secondary C-peptide detection antibody. The plate was allowed to sit and incubate at room temperature for 90 minutes. The contents of the well were discarded, and the wells were rinsed three times. 80 µL

of an enzyme solution were added to the wells, followed by a 30 minute incubation at room temperature. The wells were again washed three times and 80 μL of a substrate that reacts with the enzyme to produce a color change were added and incubated for 12 minutes. The addition of 80 μL of a 0.3 M HCl solution stops the conversion of the substrate and the absorbance of the solution was measured at 450 nm in a plate reader. Using the generated standard curve and the dilution factor, the amount of C-peptide in the supernatants of the samples was determined and subtracted from the known amount of peptide that was in the sample. This difference indicates the amount of C-peptide that bound to the RBCs.

3.4.6 Measurement of lactate released from RBCs in hyperglycemic and normal conditions after administration of metal-activated C-peptide/metformin

The determination of the metabolic product lactate uses the same samples that were described earlier in Figure 3.4. Following the final 2 hour incubation, the samples containing metal-activated C-peptide with/without metformin or metformin alone were centrifuged and the supernatant removed. The supernatants were prepared in a 96-well plate in a series of standard addition samples (Figure 3.5). Briefly, 5 μL of the supernatant were added into 4 wells also containing 45 μL of DDW. To those 4 wells, lactic acid (50 μM) was added in volumes of 0, 10, 25, and 50 μL. DDW was then added to each well to bring the final volume to 100 μL.

Once the samples were arranged, 100 μL of an enzyme solution containing 5 mM NAD^+ and 5 U/mL lactate dehydrogenase (LDH) in a 0.1 M Trizma base buffer (pH ~ 8.9) were added to each well. The protocol was modified from a previously described assay.[32] The buffer was prepared by dissolving 1.21 g Trisma base (Sigma Aldrich) in 100 mL of DDW and adjusting the

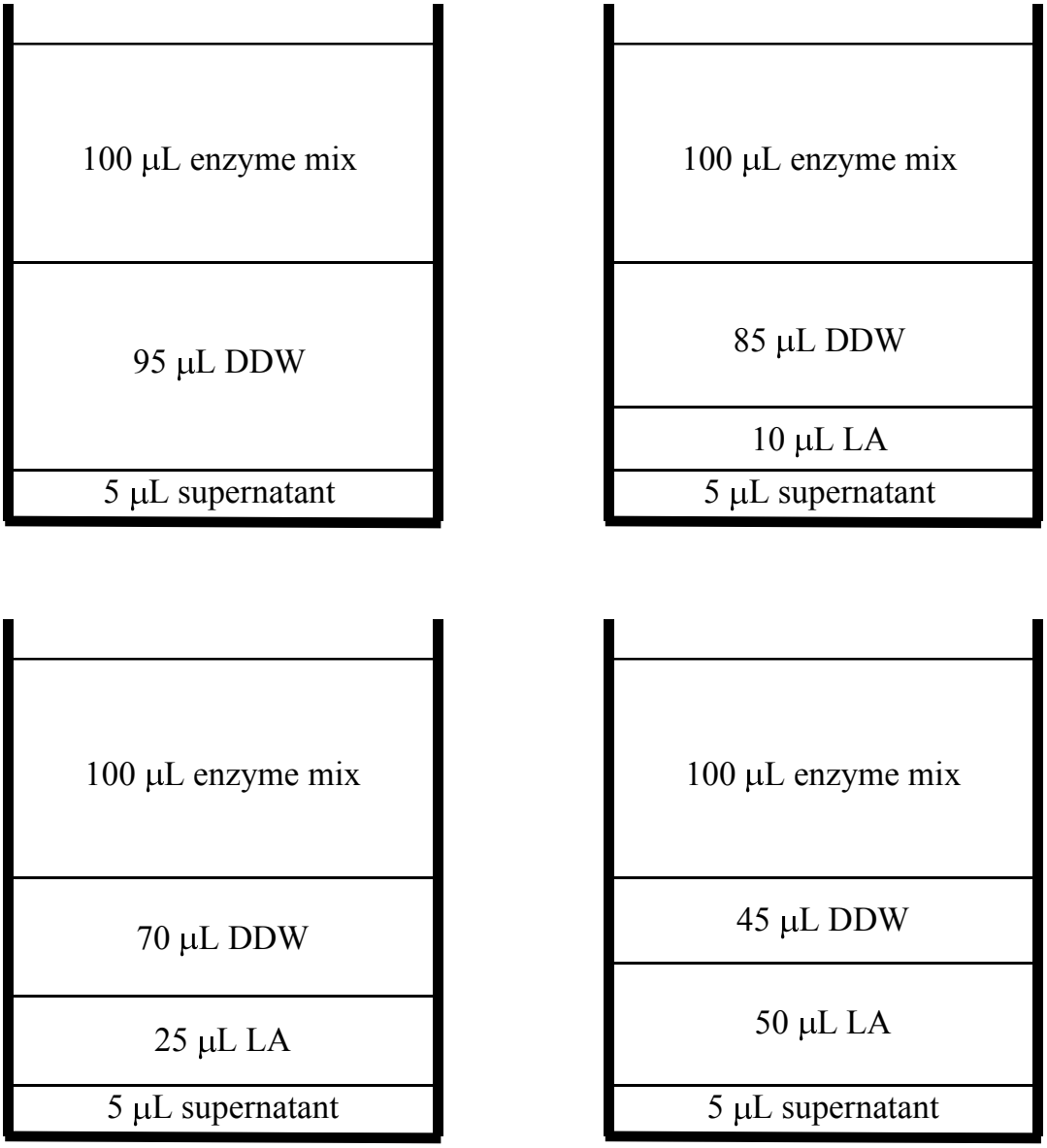

$$C_x = \frac{bC_s}{mV_x}$$

Figure 3.5 – Standard addition method used to determine the lactate content in the supernatant of RBC samples incubated with either normal or high glucose PSS and treated with metformin, metal-activated C-peptide, or both. Using the equation (y = mx + b) of the line generated by plotting the fluorescence intensity (y – axis) vs. the volume of standard added (x – axis), the concentration (C_X) of the lactic acid in the supernatant can be determined. The variables (b) and (m) are obtained from the linear equation, C_S represents the lactic acid (LA) standard concentration (50 μM), and V_X refers to the volume of the supernatant (5 μL).

pH to 8.9 by adding 2 M sodium hydroxide (NaOH) drop wise. The enzyme reaction utilizes the oxidation of lactate to pyruvate while reducing NAD^+ to NADH. The reaction mechanism and standard curve are described in Figure 3.6. Following a 15 minute incubation, the fluorescence of NADH was measured at an emission at 460 nm after excitation at 340 nm. The fluorescence intensity is proportional to the amount of NADH present, and subsequently the lactate present. The approximate concentration of the sample added can be determined using the fluorescence values.

3.4.7 Validation of the lactic acid assay

Two different experiments were designed to evaluate the capability and reproducibility of the previously described lactic acid assay, prior to the administration of the assay to the C-peptide based studies. The first was designed to determine whether the lactic acid assay could be applied by measuring the lactate released by RBCs stored in PSS at different temperatures. Two, 1 mL RBC samples at 7% hematocrit were prepared in PSS to determine temperature effects on RBC metabolism. One of the samples was stored at 4°C while the other one stored at 37°C, both for 2 hours. Following the appropriate incubation time, the samples were centrifuged at 500 x g for 5 minutes. The supernatant was removed (5 μL) and arranged in the standard addition series as described in Figure 3.5. 100 μL of the lactic acid assay enzyme solution were added to each well with the fluorescence (ex. 340 nm, em. 460 nm) measured after 15 minutes at 37°C.

The other experiment examined whether different glucose concentration storage solutions had an effect on the RBC glucose metabolism when stored at 4°C, multiple different human RBC samples were prepared at around a 50% hematocrit in buffers containing either 5.55 mM

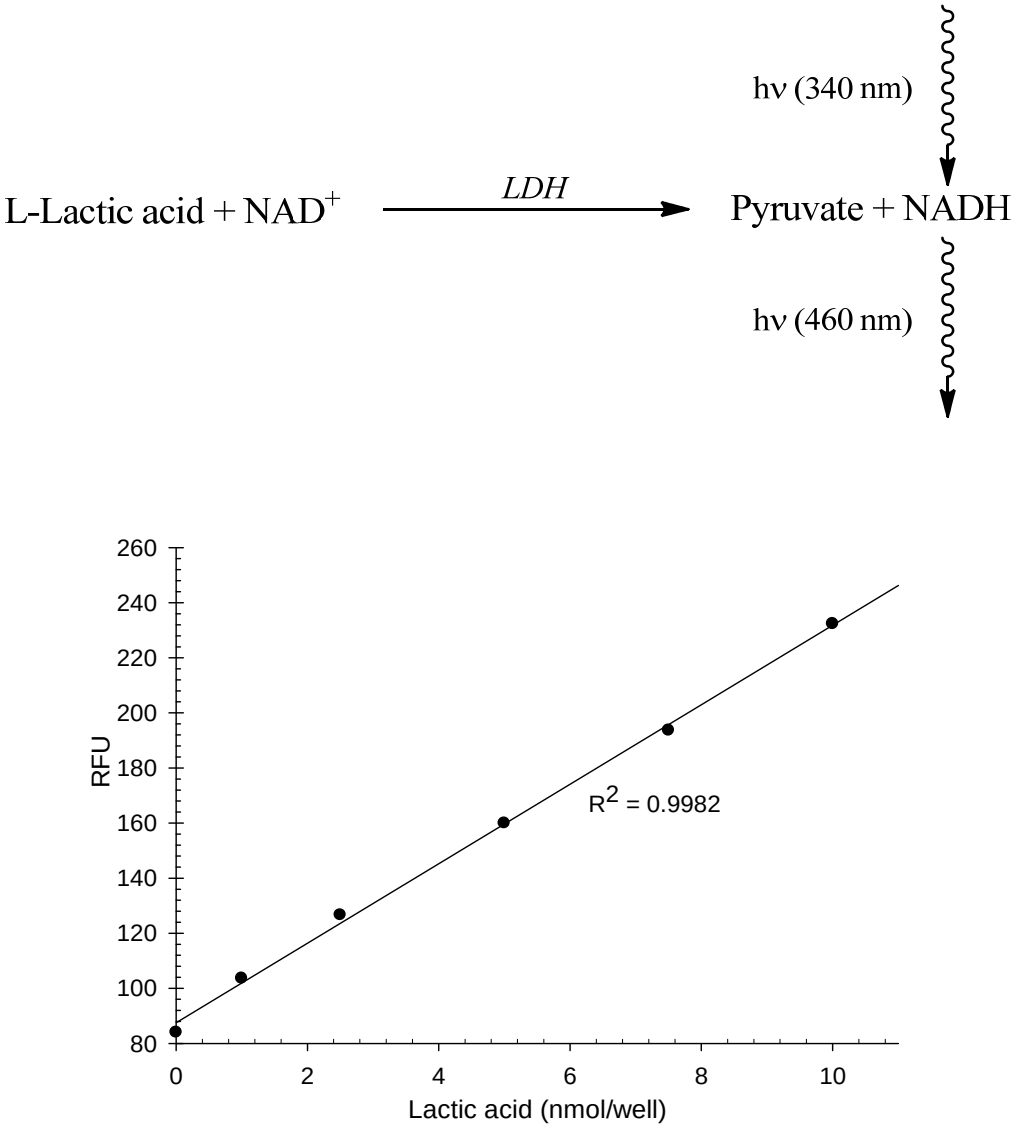

Figure 3.6 – Reaction mechanism behind the fluorescent lactic acid assay. The lactate in the sample is oxidized to pyruvate by the enzyme lactate dehydrogenase (LDH). The fluorescence is obtained at an emission of 460 nm after excitation of 340 nm, which is indicative of the amount of NADH present. The amount of lactate originally present is proportional to the NADH intensity, and can be quantified by using a standard curve generated from known concentrations of L-lactic acid. The y-axis values are given in relative fluorescence units (RFU).

(LG) or 111 mM glucose (HG). The aqueous buffer consisted of 1.8 mM adenine, 41.2 mM mannitol, 154.0 mM sodium chloride, and glucose. After a set number of days of being stored 4°C (1, 4, 8, 11, 16 days) an aliquot of the RBC sample was diluted to a 7% hematocrit solution in the same buffer that the RBCs were stored in, either the 5.55 or 111 mM glucose solution. The cells were immediately centrifuged and the supernatant was arranged into the standard addition series (Figure 3.5). Similar to before, 100 μL of the lactic acid assay enzyme solution were added to each well with the fluorescence measured.

3.4.8 Measurement of the glucose consumed by the RBC following administration of metal-activated C-peptide/metformin

The same initial preparation protocols apply in preparing the samples when determining the amount of glucose taken in by the RBCs following incubation with metal-activated C-peptide, metformin, or both. After the final 2 hour incubation, the RBC samples were centrifuged and the supernatant was collected. 1 μL of the supernatant of the PSS samples and the PSS itself was diluted into 99 μL of DDW, and 0.5 μL of the supernatant from the HG PSS samples and the buffer was diluted into 99.5 μL of DDW. 100 μL of D-glucose standards ranging from 0 to 100 μM were added to the plate. These samples and standards were prepared in the same 96-well microplates that were used in the lactate measurements.

Once the samples were loaded, 100 μL of an enzyme solution described in an earlier report were added to each of the samples.[32] The solution consisted of 2 mM ATP, 1.25 mM $NADP^+$, 2 mM $MgCl_2$, 1.66 U/mL hexokinase, and 0.89 U/mL G6PDH in a 0.3 M triethanolamine (TEA) buffer at a pH of 7.6. The assay utilizes the conversion of glucose to 6-

phospho-gluconate, reducing $NADP^+$ into the fluorescent NADPH (Figure 3.7). Following a 30 minute incubation at room temperature, the fluorescence (ex. 340, em. 460) was obtained for both the standards and samples.

3.4.9 Measurement of lactate released from the endothelium after C-peptide/metformin administration

The lactate released from immobilized bPAECs in 12-well plates was measured in the plate reader using the same methods to that of the previously described glucose measurements of the RBC samples. Following a 24 hour incubation in either serum free normal glucose or high glucose DMEM, the media was replaced with DMEM containing 100 nM metal-activated C-peptide and/or 2 mM metformin. In order to prepare the samples containing 100 nM metal-activated C-peptide, 18 μL each of the 4.15 μM working solutions of C-peptide and Zn^{2+} were combined, followed by 714 μL of DMEM. The 2 mM metformin samples were prepared by the addition of 6.3 μL of the 239 mM working solution to 742.7 μL of DMEM. For the samples containing both C-peptide and metformin, 18 μL each of the C-peptide and Zn^{2+} solution were combined, followed by 6.3 μL of metformin and 707.7 μL of DMEM. The solutions were immediately transferred onto the cells and allowed to incubate at 37°C for 24 hours (Figure 3.8).

Following the incubation, 1 μL of the supernatant of each of the samples was diluted into 99 μL of DDW in a 96-well microplate. Similar to the glucose studies, a series of L-lactic acid standards (0 – 100 μM) was prepared with 99 μL of each standard loaded into the plate. In order to compensate for any effects the phenol red in the DMEM might have on the fluorescence

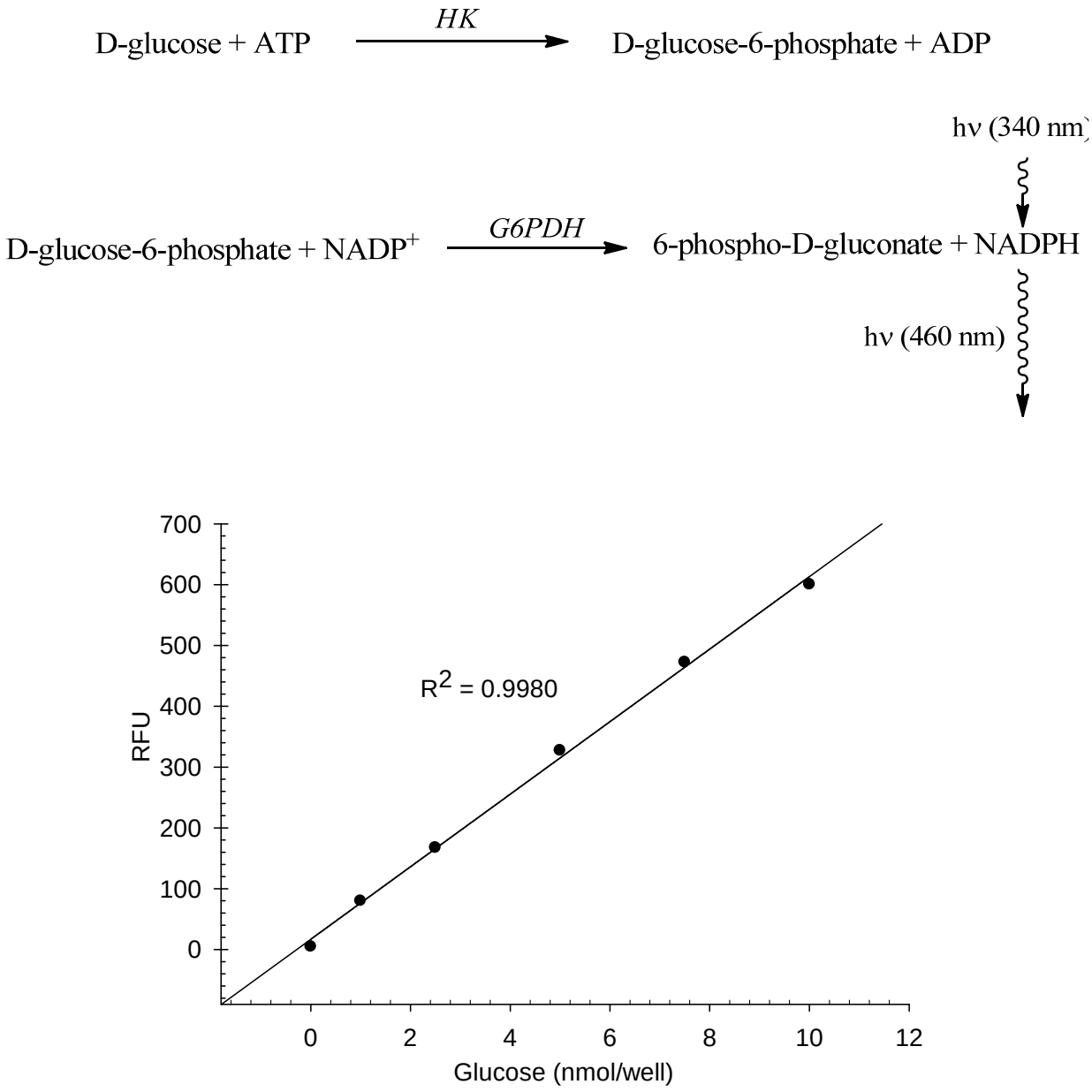

Figure 3.7 – Reaction mechanisms behind the extracellular glucose assay. Extracellular glucose from the supernatant is first converted into glucose-6-phosphate (G6P) by hexokinase (HK). G6P is subsequently converted into 6-phospho-gluconate by glucose-6-phosphate dehydrogenase (G6PDH) while reducing $NADP^+$ into NADPH. The fluorescence intensity of the NADPH is representative of the amount of glucose that was in the sample and can be quantified by using a standard curve generated from known D-glucose solutions. The y-axis values are given in relative fluorescence units (RFU).

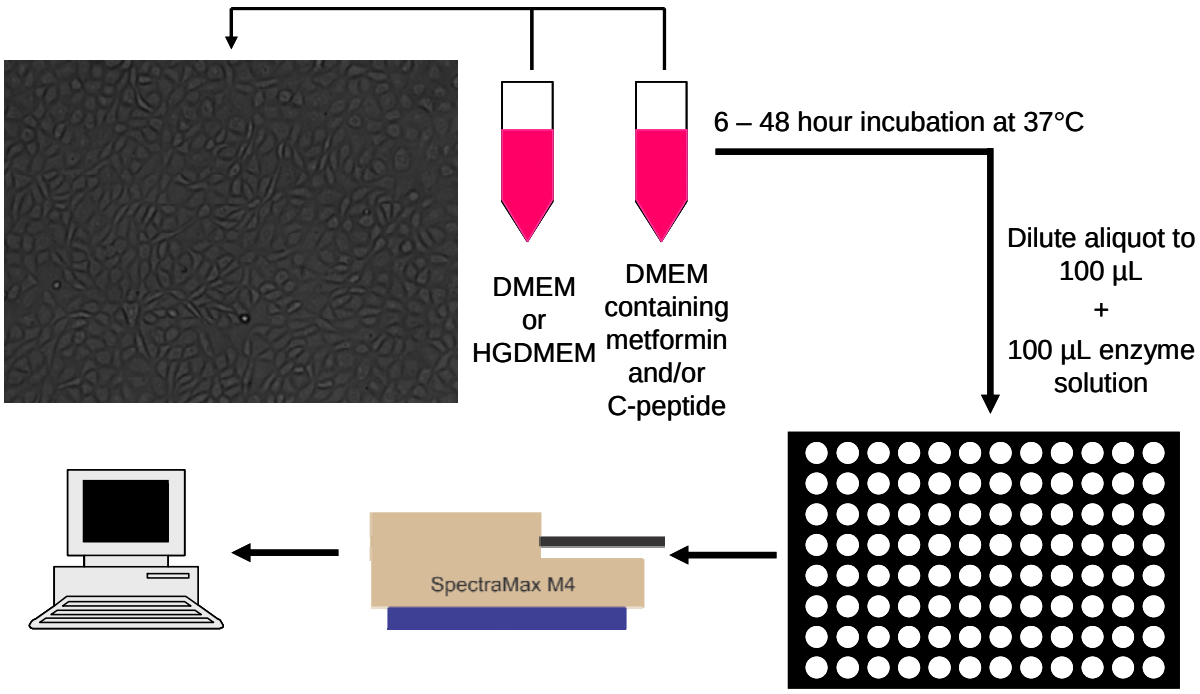

Figure 3.8 – Diagram describing the procedures used to measure the lactate from cultured bPAECs. Following a 24 hour incubation in either DMEM or HG DMEM, the media was replaced with DMEM containing metformin, C-peptide, or both. The cells were then allowed to incubate for longer times, after which the supernatant was removed and diluted into multiwell plates. The enzyme solution was added, and the fluorescence measured in a plate reader after incubation at 37°C for 20 minutes.

measurements, 1 μL of DMEM containing no glucose or sodium pyruvate was added to each standard to bring the final volume of each well to 100 μL. Similar to the standard addition methods described earlier, 100 μL of the lactic acid assay enzyme solution were added to each well. After a 15 minute incubation at 37°C, the fluorescence of NADH (ex. 340, em. 460) was measured, indicating the amount of lactate present in the sample.

3.4.10 Observations whether metformin affects the lactic acid assay

Two different experiments were performed to ensure that metformin was not having any direct influence in the fluorescence measurements. First, a time study was performed with bPAECs grown in 12-well plates in either normal or high glucose environments and incubated with concentrations of metformin ranging from 0 to 7.5 mM. The lactate content was measured every 6, 12, 24, and 48 hours. Appropriate dilutions were prepared that resulted in a final volume of 750 μL in each well using the 239 mM working solution of metformin in either DMEM or HG DMEM. After the appropriate incubation time, 1 μL of each supernatant was removed and measured for lactate using the standard curve method described earlier in section 3.4.9.

There was another experiment performed that examined whether the metformin has a direct effect on the fluorescence measurements. To examine this potential effect of metformin on the assay, bPAECs in a 12-well plate were incubated with either DMEM or HG DMEM for 24 hours. Following that incubation, the DMEM was removed and replaced by the metformin samples. The samples were prepared by diluting 6.3 μL of the 239 mM metformin stock in 742.7 μL of DMEM and adding to the cells. The final concentration of metformin was 2 mM.

Following the incubation with metformin, the solution was removed and replaced with DMEM or HG DMEM containing no metformin. The cells were then allowed to incubate an additional 24 hours, after which 1 μL of the supernatant was measured for lactate using the standard curve protocol as described earlier.

3.5 Results

3.5.1 ELISA determination of C-peptide interaction with the RBC in normal and hyperglycemic conditions following metformin administration

Utilizing the ELISA techniques, the C-peptide content in the supernatant of RBCs incubated in normal or hyperglycemic conditions and then treated with C-peptide with/without metformin was able to be determined. The amount of C-peptide that interacted with, or bound to the cell membrane, was then determined by subtracting the supernatant content from the original amount introduced to the cells. These C-peptide results are summarized in Figure 3.9. Each sample consisted of approximately 8.2×10^8 RBCs. Following incubation in the normal glucose PSS (LG), the RBCs treated with 20 nM or 20 picomoles (pmol) of metal-activated C-peptide had a total of 4.80 ± 0.06 pmol unaccounted for that had bound with the RBCs. Following incubation of the RBCs with the HG PSS (HG), there was a significantly ($p < 0.005$) lower quantity of C-peptide that bound with the cells at a value of 3.4 ± 0.1 pmol. In the samples that contained 30 μM metformin with the 20 nM metal-activated C-peptide, there was a significant increase ($p < 0.005$) in the amount of C-peptide that bound with the RBCs in HG PSS

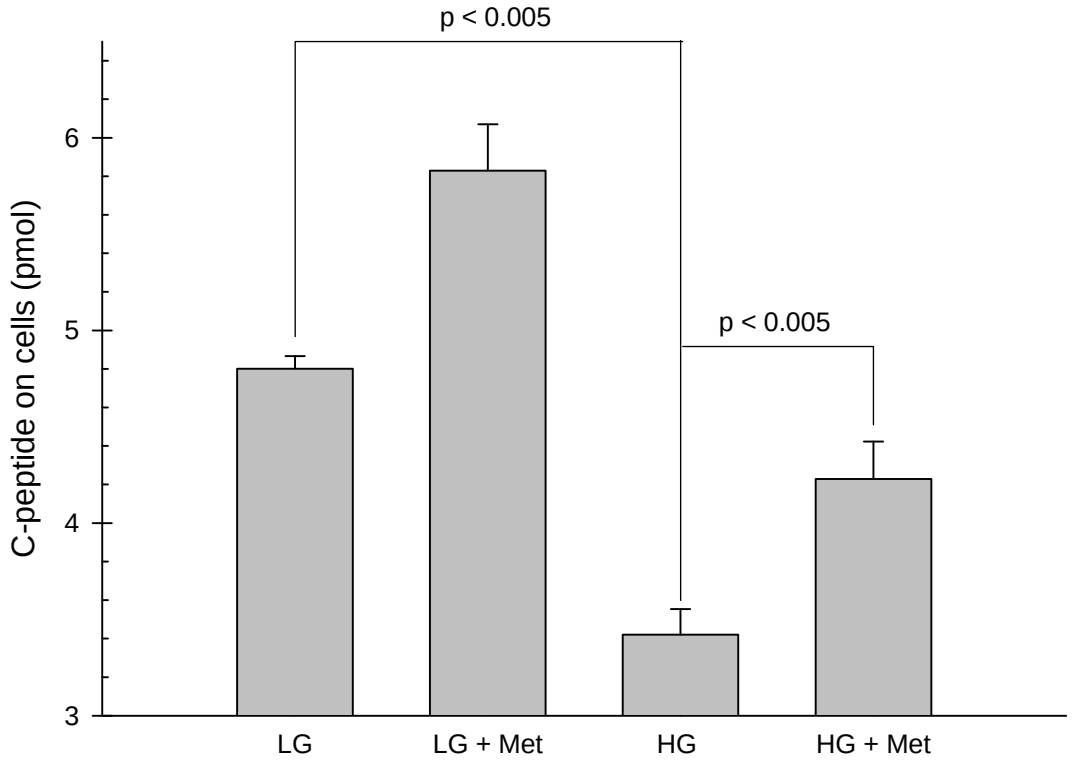

Figure 3.9 – The amount of metal-activated C-peptide that interacts with the RBC samples. All samples were incubated with 20 pmol of metal-activated C-peptide in either normal glucose (LG) or high glucose (HG) PSS. Some samples were treated with 30 μM metformin simultaneously (+ Met) with the C-peptide and incubated for 2 hours. The bars represent the average amount of C-peptide (pmol) that was unaccounted for following the measurement of the supernatants using the ELISA. The error bars represent the standard error of the mean for n = 6 blood draws. The differences in the C-peptide interacting with the cells are provided with the individual p-values indicating significance.

(HG + Met) when compared to the metformin-free HG samples. HG + Met samples had 4.2 ± 0.2 pmol.

3.5.2 Lactic acid assay on stored blood samples

The first experiment described with the stored blood samples in validating the lactic acid assay examined how temperature affected lactate production/release from 7% hematocrit RBC solutions. The results are shown in Figure 3.10. The lactate released from the two different temperature samples was normalized to the lactate values of the samples incubated at 37°C. With the normalized value of the lactate produced from the 37°C sample at 1.00 ± 0.06, the lactate release from the 4°C samples after 2 hours was decreased significantly ($p < 0.001$) to 50 ± 4% that of the 37°C sample.

For the other portion of the stored blood/assay validation experiment, multiple RBC samples were stored in different glucose containing buffers for up to 16 days at 4°C. Using the lactic acid assay, the amount of lactate released from the RBCs on each day was measured and compared to the day 1 values of each sample, as well as the previous experimental values as shown in Figure 3.11. With a concentration of extracellular lactate of 145 ± 13 μM for the HG sample at day 1, the LG sample measured at an extracellular concentration of 143 ± 9 μM on the same day. Day 4 values for both the LG and HG samples had significant increases ($p < 0.001$) in lactate production compared to the day 1 samples at 260 ± 20 and 265 ± 8 μM respectively. Day 8 values for both samples (LG and HG) increased significantly ($p < 0.001$) once again from day 4 values to 444 ± 12 and 446 ± 6 μM respectively.

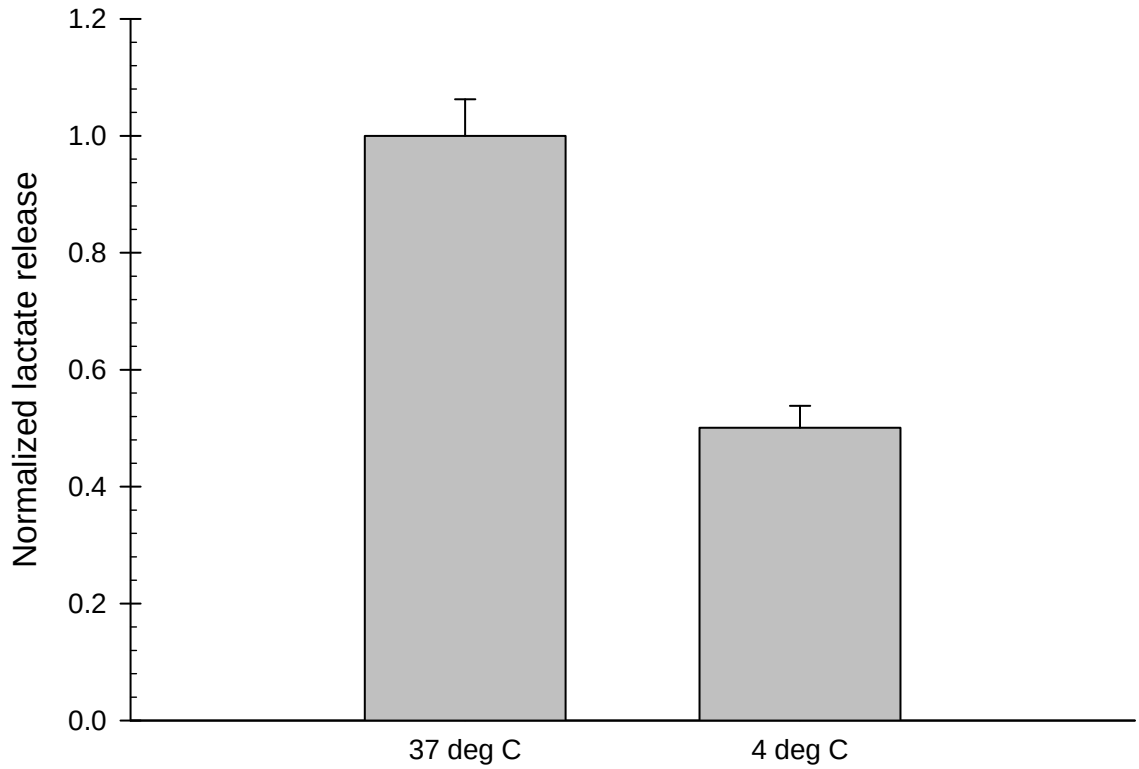

Figure 3.10 – Lactate released from 7% hematocrit RBC samples after 2 hours incubated at either 37°C or 4°C. The lactate released from both samples was normalized to the sample incubated at 37°C. The error bars represent the standard error of the mean for n = 4 blood draws. The difference in lactate release after the two hours is considered significant (*$p < 0.001$).

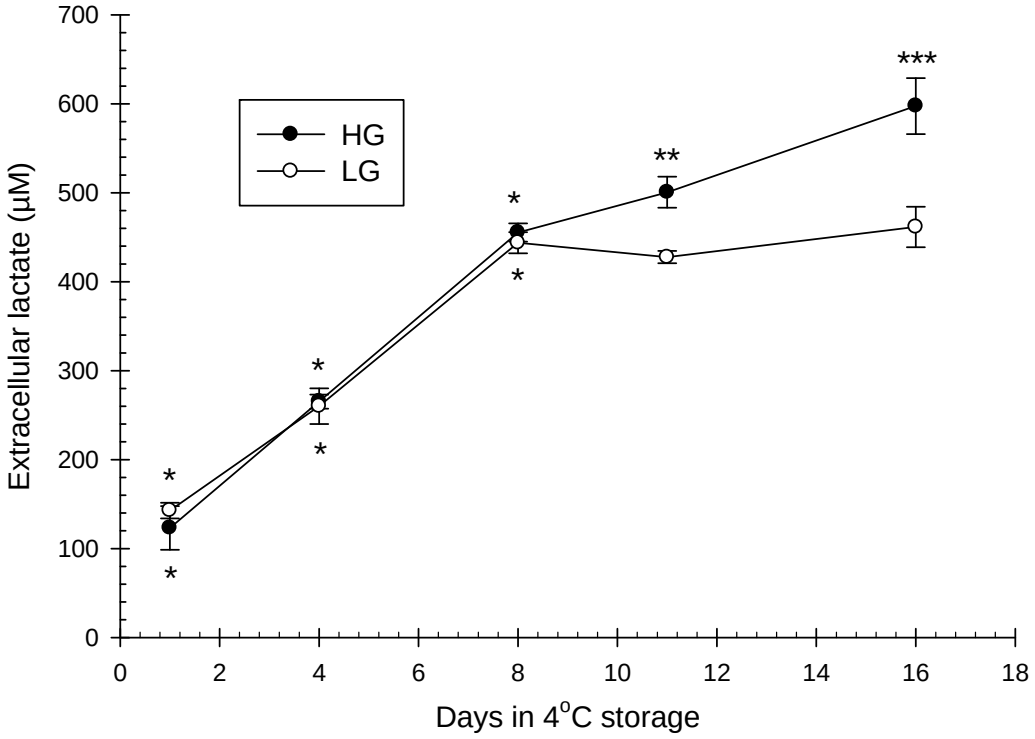

Figure 3.11 – Extracellular lactate in RBC samples kept in differing glucose buffers, either 5.5 mM (LG) or 111 mM (HG), for long term storage. The points indicate the average (n = 4 blood draws) extracellular lactate concentration (y-axis) after the specified number of days kept refrigerated (x-axis). Day 1 refers to the day that the sample was obtained and stored in the buffer, meaning there was no storage at 4°C for this data point. The error bars on each point represent the standard error of the mean. Significant increases in the lactate concentration from the previous measured point are indicated: *$p < 0.001$, **$p < 0.05$, ***$p < 0.06$.

The measurements made in day 11 resulted in certain changes in the previous trends. The samples in the HG environment had an increase in lactate release that was statistically higher ($p < 0.05$) than the day 8 measurements. The lactate increased to 500 ± 17 μM. While the HG sample increased from day 8 to 11, the LG sample lactate measurement remained statistically the same between the same days at 428 ± 7 μM. Once again on day 16 measurements, the HG samples increased ($p = 0.056$) in lactate concentration to 597 ± 32 μM. At the same time, the LG samples remained the same at 442 ± 16 μM.

3.5.3 Lactate release from RBCs treated with metformin and/or C-peptide

Following the stored blood experiments suggesting that the lactate released from the RBCs was measured using the previously described method, the influence that metal-activated C-peptide and/or metformin has on RBC lactate release was observed. Using the steps illustrated in Figure 3.4, the lactate content of the supernatants from the samples was obtained. Initially, samples containing no C-peptide or metformin were measured to observe whether the extracellular glucose concentration has an effect on lactate release (Figure 3.12). Following a total of 5 hours in either PSS or HG PSS, RBC solutions at a 7% hematocrit in PSS were assigned a normalized lactate value of 1.00 ± 0.02. RBC samples incubated with HG PSS resulted in an increase of 31 ± 7% ($p < 0.001$) in the extracellular lactate content. While the two solutions resulted in different lactate contents, the samples with metformin, metal-activated C-peptide, or both were normalized to their respective samples containing only PSS or HG PSS (Figure 3.13).

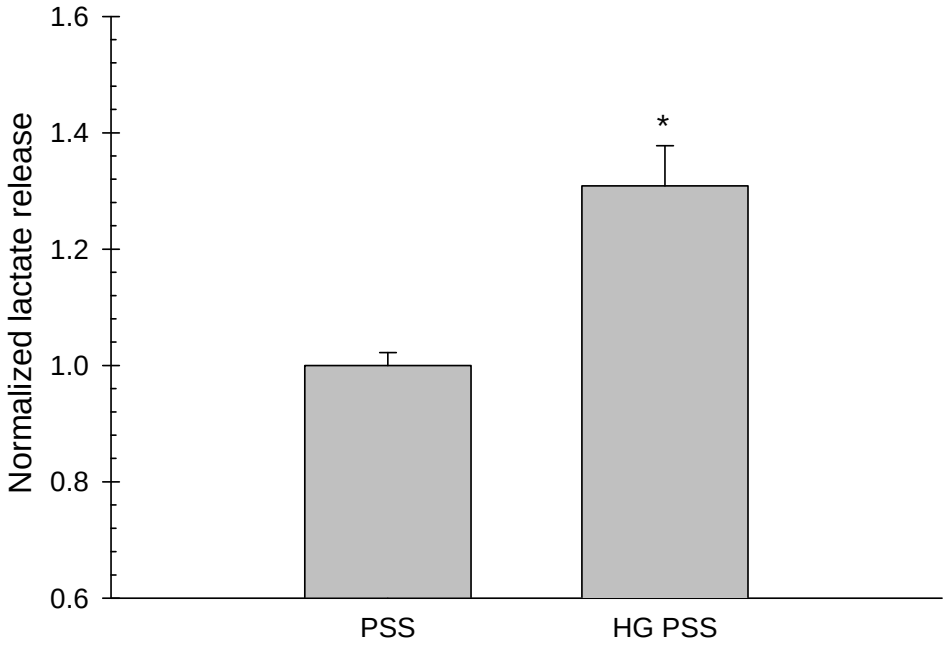

Figure 3.12 – Normalized lactate release from 7% hematocrit RBC solutions after 5 hours in either normal glucose (PSS) or high glucose (HG PSS) conditions. The bars represent the average (n = 4 blood draws) of the amount of extracellular lactate that has been normalized to the PSS sample. The error bars represent the standard error of the mean. The 31% increase in lactate from the HG PSS sample compared to the PSS is considered significant with *$p < 0.001$.

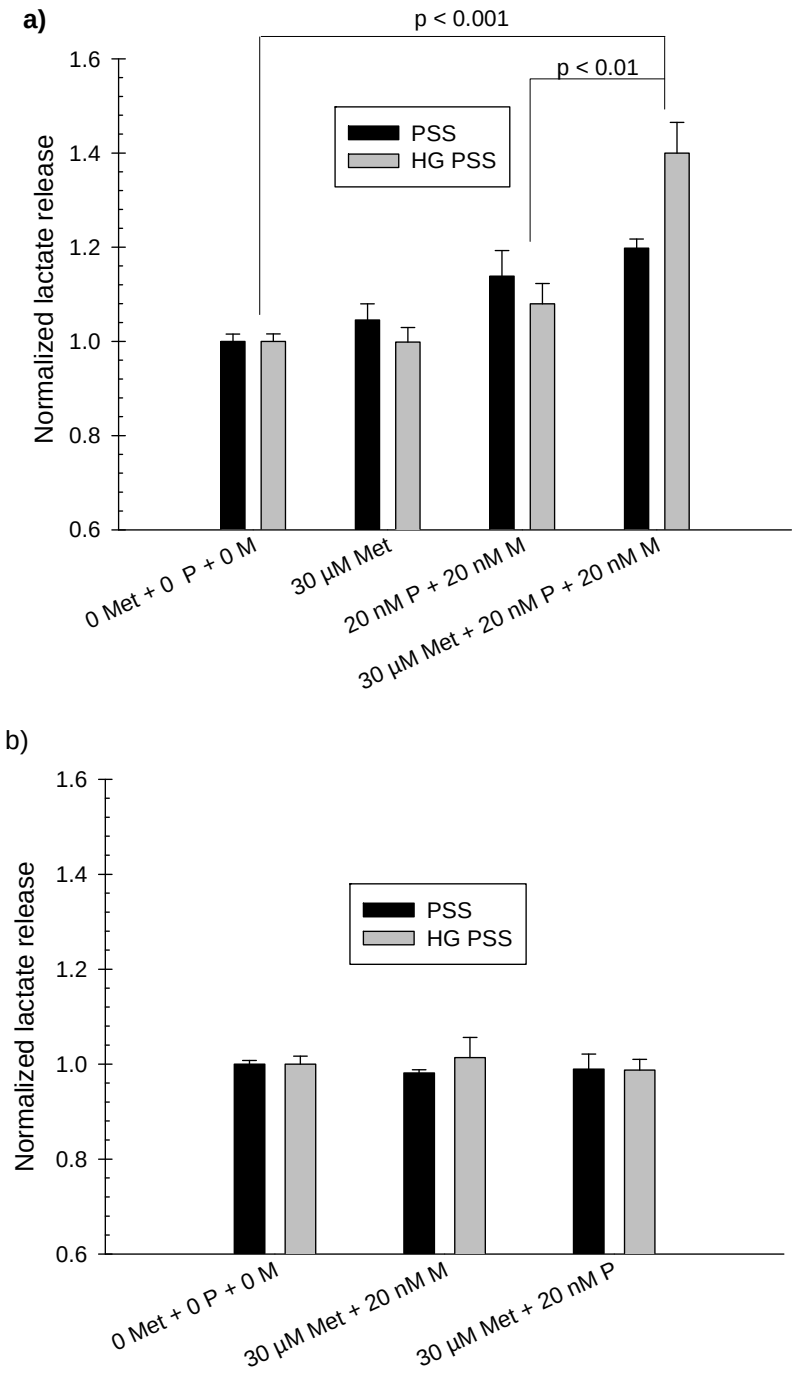

Figure 3.13 – **a)** Normalized extracellular lactate release from 7% hematocrit RBC samples that have been incubated with either metformin (Met), metal-activated C-peptide (P + M), or both (Met + P + M). Each individual series has been normalized to their respective sample that contains neither C-peptide nor metformin. The relevant statistically significant changes in the lactic acid released have been identified with their respective p-values. **b)** Control experiments containing metformin with either the peptide or the Zn^{2+}. The bars have again been normalized to their respective samples containing no metformin or C-peptide. The error bars in both figures represent the standard error of the mean for n = 6 draws.

In the RBC samples containing only 30 μM metformin (30 μM Met) for the final 2 hour incubation, there was no change in the normalized lactate values at 1.04 ± 0.03 and 1.00 ± 0.03 for the PSS and HG PSS samples, respectively. When the samples were incubated with only metal-activated C-peptide (20 nM P + 20 nM M), there was an increase ($p < 0.03$) in lactate release of 14 ± 5% from the RBCs incubated with the PSS, while the RBCs incubated in the HG PSS did not increase the lactate production or release. When metformin and metal-activated C-peptide were combined (30 μM Met + 20 nM P + 20 nM M) and allowed to incubate with RBCs in different glucose environments, there were significant increases ($p < 0.001$) observed in both cases when compared to the untreated RBCs. The PSS samples incubated with both metformin and metal-activated C-peptide produced a 20 ± 2% increase in extracellular lactate while the HG PSS samples had a 40 ± 7% increase. When compared to the lactate produced from the samples containing only metal-activated C-peptide, the lactate production from samples with both metformin and C-peptide were not statistically different between the PSS samples. However, the difference between the same two samples incubated in the hyperglycemic environment provided by the HG PSS was statistically different ($p < 0.01$).

Multiple controls were performed and analyzed to identify that the metal-activation property is required to observe the lactate increase (Figure 3.13-**b**). All controls with the metformin combined with either the peptide (30 μM Met + 20 nM P) or the Zn^{2+} (30 μM Met + 20 nM M) resulted in no increase in lactate release when normalized to the untreated RBC samples.

3.5.4 RBC glucose uptake following metformin/C-peptide administration

To measure the amount of D-glucose consumed by the 1 mL RBC solutions, the fluorescence of the samples and standards, combined with an enzyme solution, were measured and compared to a generated standard curve. After determining the amount of glucose in the supernatant, that value was subtracted from the amount in the PSS or HG PSS to determine the amount of glucose consumed by the RBCs.

The amount of glucose consumed by each sample is shown in Figure 3.14. The RBCs incubated in PSS alone (0 Met + 0 P + 0 M) consumed 0.47 ± 0.04 micromoles (μmol) of glucose. That quantity of glucose remains statistically unchanged (0.46 ± 0.05 μmol) when the RBCs were incubated with 30 μM metformin (30 μM Met). There were significant increases ($p < 0.05$) in the amount of glucose consumed when the RBCs were treated with either metal-activated C-peptide (20 nM P + 20 nM M) or metal-activated C-peptide combined with metformin (30 μM + 20 nM P + 20 nM M) with values of 0.62 ± 0.05 and 0.65 ± 0.05 μmol, respectively.

Following incubation with the HG PSS, the glucose consumption values were generally higher than the PSS incubation. RBCs incubated with no C-peptide or metformin (0 Met + 0 P + 0 M) consumed 1.5 ± 0.2 μmol of glucose. Similar to the PSS samples, the RBCs incubated with metformin (30 μM Met) remained statistically the same with 1.5 ± 0.6 μmol of glucose consumed. Unlike the PSS solutions, RBC samples containing metal-activated C-peptide (20 nM P + 20 nM M) did not have a significant change in glucose consumption, 1.6 ± 0.4 μmol. However, when the RBC samples were treated with both metal-activated C-peptide and

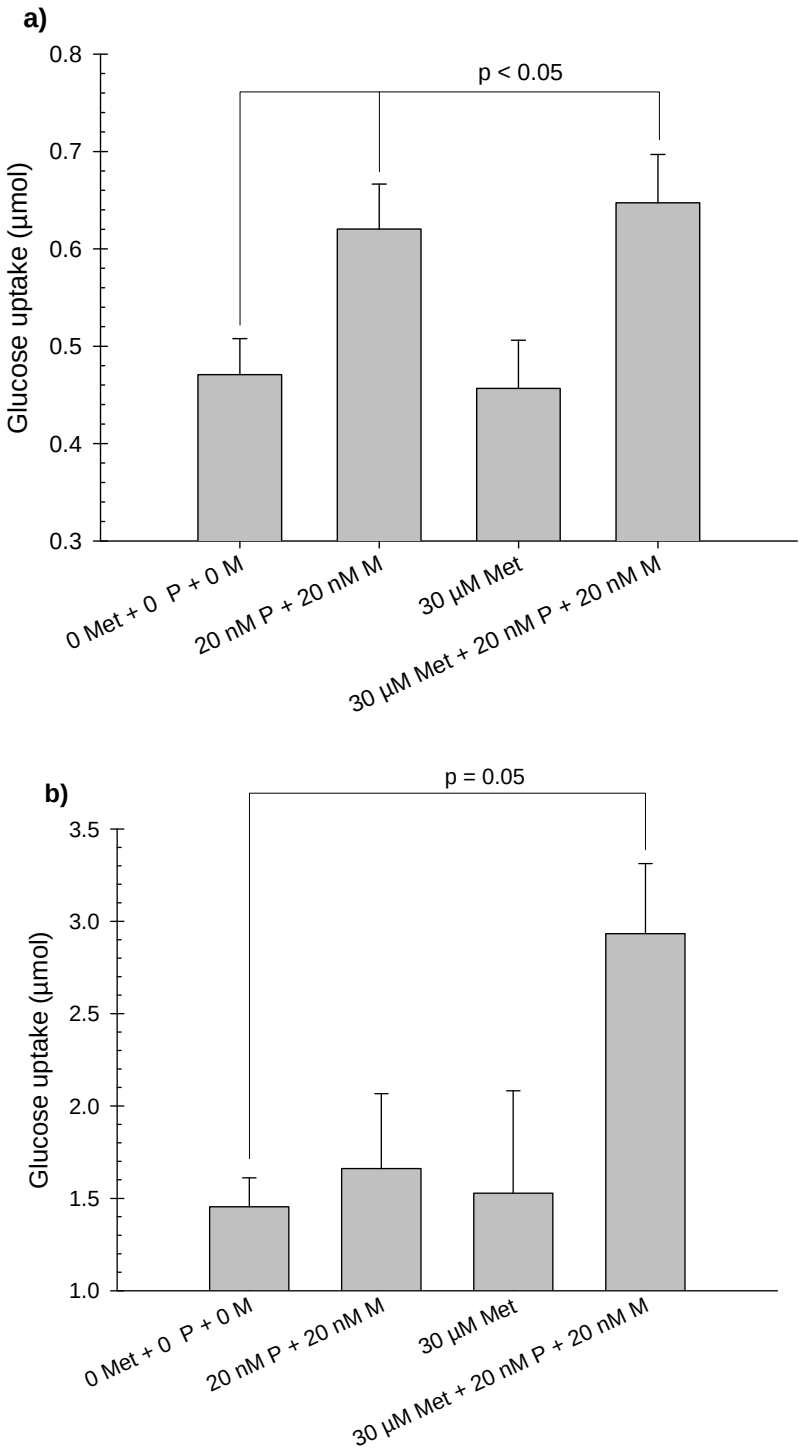

Figure 3.14 – Data showing the C-peptide/metformin induced glucose uptake in 7% hematocrit RBC solutions incubated in either PSS (a) or HG PSS (b) while containing metformin (Met), metal-activated C-peptide (P + M), or both (Met + P + M). The glucose uptake (y-axis) represents the average value (n = 5 draws) of the total quantity of glucose taken up by the entire 1 mL sample of RBCs. The significant changes in glucose uptake are indicated in the figure with their respective p-values. The error bars in both figures represent the standard error of the mean.

metformin (30 μM + 20 nM P + 20 nM M), they did consume a significantly higher ($p < 0.05$) amount of glucose compared to the untreated RBC samples with an amount of 2.9 ± 0.4 μmol.

3.5.5 bPAEC lactate production after the addition of metformin/C-peptide

The lactate released from the bPAECs stimulated with metformin and metal-activated C-peptide was significantly different than the results from the RBCs alone. These results are shown in Figure 3.15. bPAECs incubated in only DMEM and HG DMEM for 24 hours (0 MAP + 0 Met) resulted in different ($p < 0.01$) extracellular lactate concentrations of 2.7 ± 0.2 and 4.3 ± 0.3 mM, respectively. When incubated with 100 nM metal-activated C-peptide (100 nM P + M), there were no significant changes in the amount of lactate present in either the DMEM or HG DMEM samples. The concentrations for the two samples were 3.2 ± 0.3 mM for the cells incubated in DMEM and 5.0 ± 0.7 in the HG DMEM samples. When the bPAECs were incubated for 24 hours with only the 2 mM metformin (2 mM Met), the lactate concentration in the DMEM increased significantly ($p = 0.001$) to 8.7 ± 1.4 mM and the HG DMEM lactate increased to 11.7 ± 1.0 mM. While the lactate levels increased in the RBC samples following administration of both metal-activated C-peptide and metformin, the bPAEC samples incubated with C-peptide and metformin (100 nM P + M + 2 mM Met) remained the same compared to incubation with metformin alone.

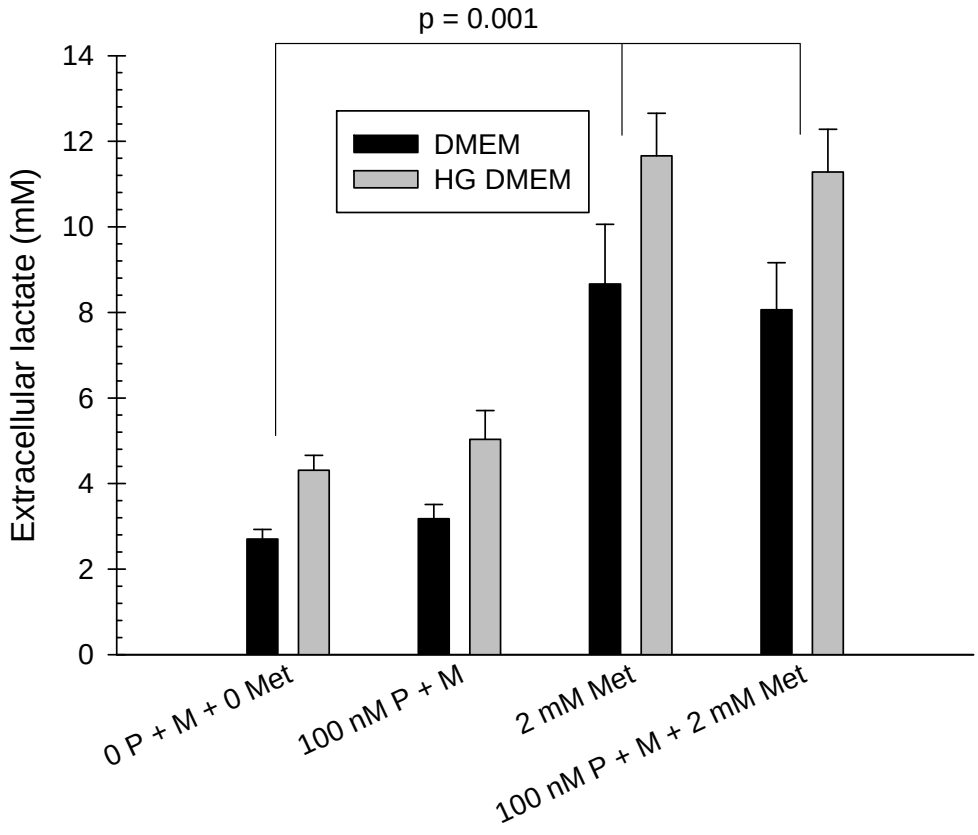

Figure 3.15 – Extracellular lactate content above bPAECs incubated in either normal glucose (DMEM) or high glucose (HG DMEM) conditions for 24 hours with metal-activated C-peptide (P + M) or metformin (Met). The extracellular lactate content is quantified using a generated standard curve with the lactic acid assay. The significant increases in lactate content are indicated with their respective p-values. The error bars represent the standard error of the mean for n = 4.

3.5.6 Metformin affecting lactic acid assay

To verify that metformin does not affect the fluorescent enzymatic lactic acid assay, the extracellular lactate content above the bPAEC samples incubated with DMEM and metformin concentrations ranging from 0 through 7.5 mM was measured at 6, 12, 24, and 48 hours (Figure 3.16). After 6 hours, the basal lactate concentration was 0.77 ± 0.02 mM and the highest metformin concentration resulted in a lactate concentration of 2.2 ± 0.2 mM. At 12 hours, the lactate concentrations increased linearly from 1.6 ± 0.1 through 4.9 ± 0.6 mM. After 24 hours, the concentrations of lactate started at 3.2 ± 0.2 mM and increased to 10.1 ± 0.4 mM while leveling off at metformin concentrations above 2 mM. Finally, after 48 hours, the basal lactate concentration was 6.4 ± 0.8 mM with the highest concentration at 13.9 ± 0.9 mM while leveling off after 1 mM metformin this time.

In the study to determine whether metformin directly facilitates the production of lactate, bPAECs in DMEM were incubated with 2 mM metformin for 24 hours. The media was replaced with new containing either metformin or no metformin, and the lactate content was measured 24 hours later. The results are shown in Figure 3.17. For the bPAECs incubated with no metformin either time (0 Met), the extracellular lactate content was measured at 3.3 ± 0.5 mM. The bPAECs incubated with 2 mM metformin followed by another 24 hours incubation with 2 mM metformin (2 mM Met + 2 mM Met) resulted in an expected increase ($p < 0.001$) in the extracellular lactate concentration to 10.8 ± 0.6 mM. In the samples incubated with 2 mM metformin and then incubated with no metformin (2 mM Met + 0 Met), the lactate level remained elevated at 10.3 ± 0.4 mM. These findings suggest that metformin is causing a

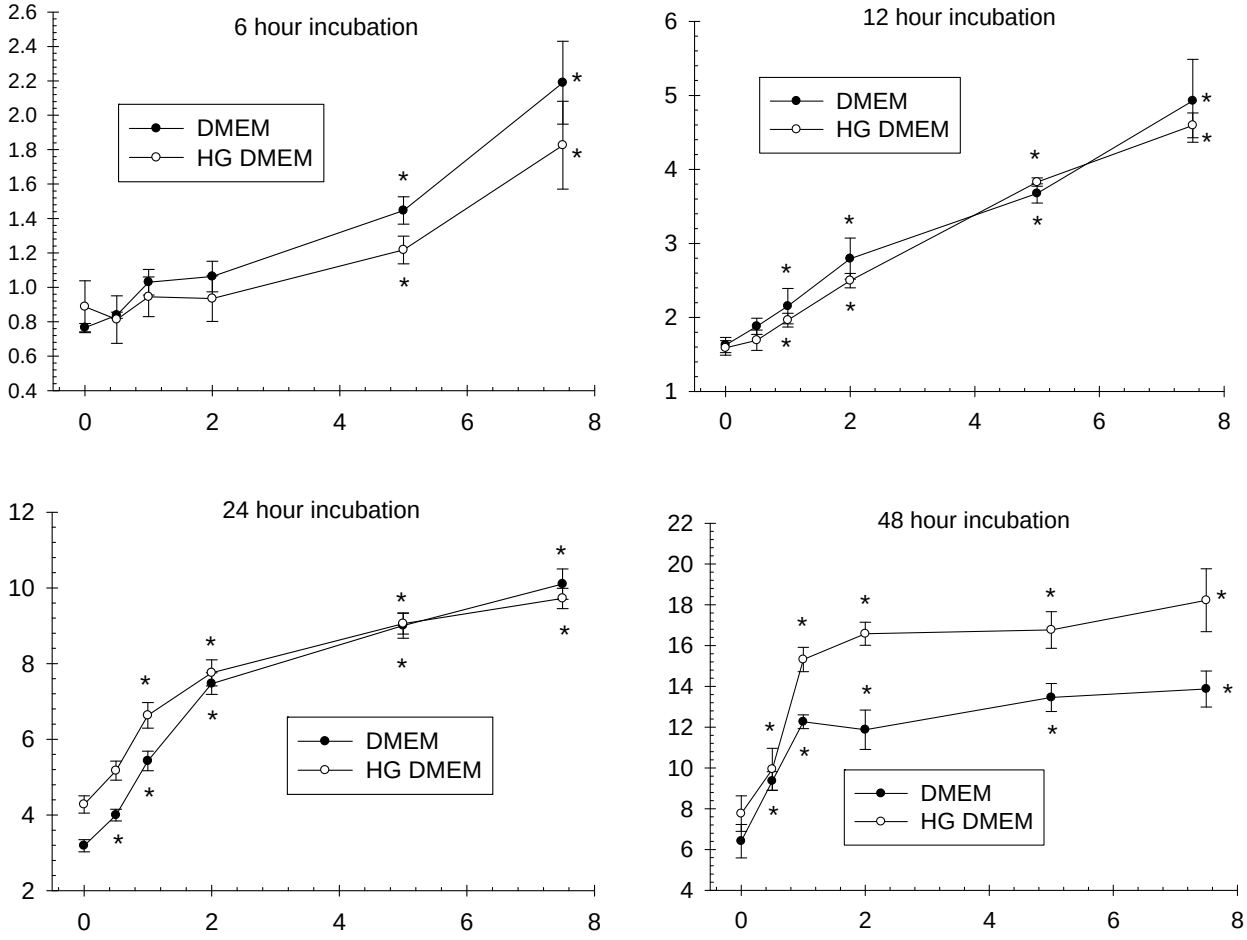

Figure 3.16 – Data showing the effect of metformin on bPAEC lactate production/release. The extracellular lactate concentration in mM is represented by the y-axis, while the concentration of metformin on the cells is shown on the x-axis. After the indicated time, the supernatant is measured for the lactate content using the previously described lactic acid assay. The error bars on each point represent the standard error of the mean (n = 3) for each incubation time. Points at different metformin concentrations indicated with an (*) are considered significantly different ($p < 0.05$) when compared to their respective point containing no metformin.

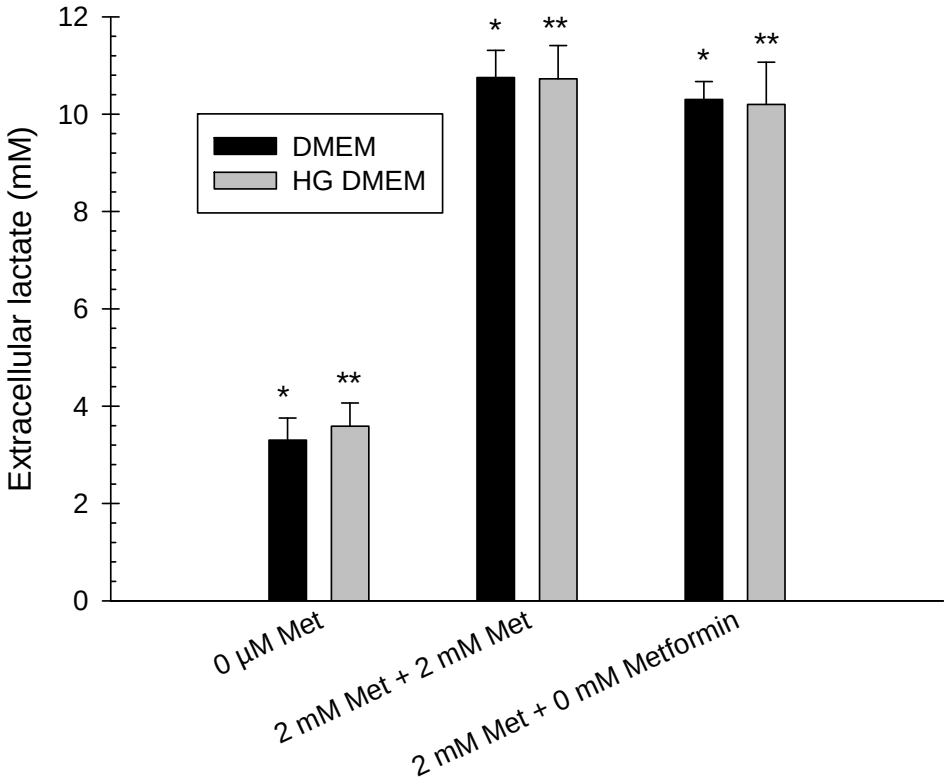

Figure 3.17 – Data illustrating a change the metabolism caused by metformin in bPAECs to allow for increased lactate release, even without the presence of the molecule. The bars represent the average lactate release (n = 4) following incubation with 2 mM metformin for 24 hours and then an additional 24 hours in either metformin (2 mM Met + 2 mM Met) or no metformin (2 mM Met + 0 mM Met). The error bars over the average values represent the standard error of the mean. Significant changes in extracellular lactate content compared to the samples containing no metformin is indicated with *$p < 0.001$ for the DMEM samples or **$p < 0.001$ for the HG DMEM samples.

metabolic change within the cell rather than directly facilitating glucose into the cell, resulting in increased lactate production.

3.6 Discussion

Metformin enhances the activity of metal-activated C-peptide on diabetic RBC characteristics such as glucose uptake and ATP release,[28] through a hypothesized increased binding of the peptide. Utilizing multiple analytical measurement techniques, the results presented here indicate an increased C-peptide interaction with the RBCs incubated in hyperglycemic conditions following simultaneous incubation with metformin. Glucose uptake and subsequent lactate release from the RBCs in high glucose conditions were also observed.

The ELISA results, showing that less C-peptide interacts with RBCs incubated in elevated glucose conditions, identify a reason for decreased C-peptide activity/interaction found from diabetic studies *in vivo* and *in vitro*, i.e. less ATP release, more vascular complications, etc. The externalization of higher amounts of the negatively charged phosphatidylserine (PS) to the outer portion of the lipid bilayer results in an overall negatively charged characteristic of the membrane.[33, 34] Previous findings in the Spence group indicate that there are higher levels of PS exposure on the outer membrane of RBCs obtained from type 2 diabetic subjects when compared to healthy controls.[28] Other reports have suggested that normal RBCs incubated in hyperglycemic conditions increase the extracellular PS levels on the membrane.[14] A hypothesized mechanism of action can be generated by combining the two findings. With C-peptide existing as an acidic peptide at physiological pH (5 negatively charged side chains), the

negatively charged peptide can be repelled by the negatively charged membrane. This repulsion would lead to the decreased interaction of the C-peptide to the RBC, thereby decreasing the beneficial effects that have been demonstrated in past findings.[35-41]

According to the ELISA results, the addition of metformin enabled more C-peptide to interact with the RBCs that were incubated in the hyperglycemic buffer. When examining the structure of the metformin molecule (Figure 3.3), there are multiple amine groups that could become positively charged. The positively charged molecule can mask the negative charges on the membrane, allowing for the acidic peptide to interact with the cell and possibly be internalized if that is the mechanism of action.[42]

A more likely explanation for the increased interaction following the administration of metformin could be the internalization into erythrocytes, followed by the antioxidant capabilities of metformin.[43] Increased oxidative stress decreases the transfer of PS from the outer leaflet to the inner portion of the membrane.[44] Metformin decreases oxidative stress and improves the radical/antioxidant imbalance that occurs in that state.[45, 46] This improvement leads to the cell transferring the PS from the outer to the inner membrane and allow for the C-peptide to bind with reduced repulsion from charge interaction.

In conjunction with the increased interaction of C-peptide with the RBCs when combined with metformin, there were observed changes in the glucose that was brought into the cell. Previous reports from Meyer et al. utilized ^{14}C-glucose transport studies to monitor the metal-activated C-peptide stimulated glucose transport into the RBCs of healthy and diabetic subjects following treatment with/without metformin.[28] The findings reported here suggest similar

increases in glucose uptake from the normal RBCs treated with metal-activated C-peptide with/without metformin without using the radiolabeled material. While the published studies used RBCs from people who have been diagnosed clinically with diabetes, the RBCs incubated in high glucose conditions used in the experiments presented here had increased glucose uptake when treated with both metformin and metal-activated C-peptide.

The studies performed by Meyer et al. reported a 60% and a 2.4 fold increase in glucose uptake in the control and diabetic RBCs, respectively, following the administration of metformin and metal-activated C-peptide. Those measurements were taken after 4 hours incubation with the stimuli. The findings reported here indicated a 40% and 2 fold increase in glucose uptake from the control RBCs and RBCs incubated in hyperglycemic conditions, respectively, after a 2 hour incubation with the stimuli. The decreased glucose uptake from the control RBCs in these studies are likely due to the halved incubation time while the RBCs incubated in hyperglycemic conditions cannot be compared to the RBCs from a diabetic subject. Nonetheless, the application of two different glucose uptake assays, the previous study using radiolabeled material and this study using a fluorescent glucose assay, the outcomes were still similar in that increased glucose uptake was measured in cells incubated with metformin and metal-activated C-peptide.

With the increased glucose uptake in the RBCs incubated with high glucose PSS, it was anticipated that there would be increased levels of lactate released from the cells, as there are no other means by which ATP can be generated in the RBC. There are no mitochondria present. The RBCs incubated in normal glucose conditions and metal-activated C-peptide released a lactate amount that was half of the glucose uptake increase, suggesting that not all of the glucose was metabolized via anaerobic respiration. Other pathways such as the pentose phosphate pathway also can utilize glucose. The increase in lactate production from the RBCs incubated in

hyperglycemic conditions with metformin and metal-activated C-peptide corresponded with the glucose uptake results. However, the 40% increase in lactate production was under half of the 100% increase in glucose uptake that was observed. This 'shuttling' of glucose to other pathways in hyperglycemic conditions was examined in a recent report from the Spence group where the polyol pathway in RBCs from type 2 diabetics was evaluated.[47]

With metformin allowing for increased C-peptide levels to interact with the RBC, glucose uptake was increased, indicating the plasma glucose lowering capabilities of metformin that have already been reported.[16-19] The plasma glucose lowering capabilities results in the glucose needing to be metabolized which is done primarily through glycolysis, generating the lactate as the final step. If the increased lactate levels are not able to completely be removed by the liver or kidney, lactic acidosis could set in. Future studies need to be performed *in vivo* to determine whether this increase is enough to cause lactic acidosis.

The results from the bPAEC lactate production following administration of metal-activated C-peptide were not what had initially been hypothesized. Following the finding that C-peptide was able to stimulate glucose uptake into the bPAECs,[27] it was initially expected that this increase would lead to more lactate being produced. However, because the endothelial cells have other means by which they can metabolize glucose, such as oxidative phosphorylation,[48] the glucose increase could be metabolized through those pathways. This could be examined by future studies that measure the mitochondrial activity after C-peptide administration.

Influenced by previous reports of metformin causing an increase of glucose uptake in bovine aortic endothelial cells (bAECs),[49] it was assumed that similar results would occur with the bPAECs. While no glucose measurements were performed in these studies, the lactate curve

at 24 hours (Figure 3.16) resembles the glucose uptake curve that was previously reported.[49] The glucose uptake doubled from 0 through 2 mM and then leveled off.[49] The same increase was observed in the lactate production from the endothelial cells over the same metformin concentration range. The studies performed by Sasson et al. utilized the non-metabolized glucose analog 2-deoxy-glucose for the glucose uptake measurements, so they were not able to measure over as long as a time frame. The 2-deoxy-glucose, because it is not metabolized, could accumulate and essentially 'halt' the overall metabolism and not allow more glucose to enter, potentially explaining why the glucose uptake curve levels off at 2 mM metformin and the lactate presented in these studies slightly increased above 2 mM metformin.

Summarily, the objective of the experiments presented here was to identify how the diabetic medication metformin controls and regulates plasma glucose levels via the RBC through *in vitro* studies. It was shown that metformin by itself has no impact on glucose uptake of the RBC by monitoring the extracellular glucose as well as the lactate released. Metformin is shown to work together with metal-activated C-peptide to increase the glucose uptake in RBCs that have been incubated in a hyperglycemic diabetic environment, resulting in the increased extracellular lactate levels. The findings from the bPAEC lactate production after metformin treatment suggest that the drug interacts differently with the endothelial cells than it does with the RBC. Further glucose uptake studies needed to be performed, which they were and reported in Chapter 4. At the time of the reported findings by Sasson et al., there was no clear explanation of why metformin had the effects that were observed. Shortly after, there were reports that metformin may act on cellular metabolism by inhibiting Complex I in the mitochondria, or by activating AMP-activated protein kinase (AMPK), which is a key regulator in cell metabolism

and may play significant roles in both type 2 diabetes and possibly some cancers by altering intracellular conditions.[50-54]

REFERENCES

REFERENCES

1. Bossi, D.; Giardina, B., Red cell physiology. *Mol. Aspects Med.* **1996,** 17, (2), 117-28.

2. Messana, I.; Orlando, M.; Cassiano, L.; Pennacchietti, L.; Zuppi, C.; Castagnola, M.; Giardina, B., Human erythrocyte metabolism is modulated by the O2-linked transition of hemoglobin. *FEBS Lett* **1996,** 390, (1), 25-8.

3. Poole, R. C.; Halestrap, A. P., Interaction of the erythrocyte lactate transporter (monocarboxylate transporter 1) with an integral 70-kDa membrane glycoprotein of the immunoglobulin superfamily. *J. Biol. Chem.* **1997,** 272, (23), 14624-8.

4. Bartlett, S.; Espinal, J.; Janssens, P.; Ross, B. D., The influence of renal function on lactate and glucose metabolism. *Biochem. J.* **1984,** 219, (1), 73-8.

5. Bellomo, R., Bench-to-bedside review: lactate and the kidney. *Crit. Care* **2002,** 6, (4), 322-6.

6. Vague, P.; Coste, T. C.; Jannot, M. F.; Raccah, D.; Tsimaratos, M., C-peptide, Na+,K(+)-ATPase, and diabetes. *Exp. Diabesity Res.* **2004,** 5, (1), 37-50.

7. De La Tour, D. D.; Raccah, D.; Jannot, M. F.; Coste, T.; Rougerie, C.; Vague, P., Erythrocyte Na/K ATPase activity and diabetes: relationship with C-peptide level. *Diabetologia* **1998,** 41, (9), 1080-4.

8. Bretscher, M. S., Membrane structure: some general principles. *Science (New York, N.Y.)* **1973,** 181, (100), 622-9.

9. Verkleij, A. J.; Zwaal, R. F.; Roelofsen, B.; Comfurius, P.; Kastelijn, D.; van Deenen, L. L., The asymmetric distribution of phospholipids in the human red cell membrane. A combined study using phospholipases and freeze-etch electron microscopy. *Biochim. Biophys. Acta* **1973,** 323, (2), 178-93.

10. Rothman, J. E.; Lenard, J., Membrane asymmetry. *Science (New York, N.Y.)* **1977,** 195, (4280), 743-53.

11. Martinez, M.; Vaya, A.; Server, R.; Gilsanz, A.; Aznar, J., Alterations in erythrocyte aggregability in diabetics: the influence of plasmatic fibrinogen and phospholipids of the red blood cell membrane. *Clin. Hemorheol. Microcirc.* **1998,** 18, (4), 253-8.

12. Zwaal, R. F.; Schroit, A. J., Pathophysiologic implications of membrane phospholipid asymmetry in blood cells. *Blood* **1997,** 89, (4), 1121-32.

13. Wali, R. K.; Jaffe, S.; Kumar, D.; Sorgente, N.; Kalra, V. K., Increased adherence of oxidant-treated human and bovine erythrocytes to cultured endothelial cells. *J. Cell Physiol.* **1987,** 133, (1), 25-36.

14. Wilson, M. J.; Richter-Lowney, K.; Daleke, D. L., Hyperglycemia induces a loss of phospholipid asymmetry in human erythrocytes. *Biochemistry* **1993,** 32, (42), 11302-10.

15. Jain, S. K.; Palmer, M.; Chen, Y., Effect of vitamin E and N-acetylcysteine on phosphatidylserine externalization and induction of coagulation by high-glucose-treated human erythrocytes. *Metabolism* **1999,** 48, (8), 957-9.

16. Effect of intensive blood-glucose control with metformin on complications in overweight patients with type 2 diabetes (UKPDS 34). UK Prospective Diabetes Study (UKPDS) Group. *Lancet* **1998,** 352, (9131), 854-65.

17. Bailey, C. J., Biguanides and NIDDM. *Diabetes Care* **1992,** 15, (6), 755-72.

18. Stumvoll, M.; Nurjhan, N.; Perriello, G.; Dailey, G.; Gerich, J. E., Metabolic effects of metformin in non-insulin-dependent diabetes mellitus. *New Engl. J. Med.* **1995,** 333, (9), 550-4.

19. Abbasi, F.; Chu, J. W.; McLaughlin, T.; Lamendola, C.; Leary, E. T.; Reaven, G. M., Effect of metformin treatment on multiple cardiovascular disease risk factors in patients with type 2 diabetes mellitus. *Metabolism* **2004,** 53, (2), 159-64.

20. Hundal, R. S.; Krssak, M.; Dufour, S.; Laurent, D.; Lebon, V.; Chandramouli, V.; Inzucchi, S. E.; Schumann, W. C.; Petersen, K. F.; Landau, B. R.; Shulman, G. I., Mechanism by which metformin reduces glucose production in type 2 diabetes. *Diabetes* **2000,** 49, (12), 2063-9.

21. Katakam, P. V.; Ujhelyi, M. R.; Hoenig, M.; Miller, A. W., Metformin improves vascular function in insulin-resistant rats. *Hypertension* **2000,** 35, (1 Pt 1), 108-12.

22. Bolen, S.; Feldman, L.; Vassy, J.; Wilson, L.; Yeh, H. C.; Marinopoulos, S.; Wiley, C.; Selvin, E.; Wilson, R.; Bass, E. B.; Brancati, F. L., Systematic review: comparative effectiveness and safety of oral medications for type 2 diabetes mellitus. *Ann. Intern. Med.* **2007,** 147, (6), 386-99.

23. Ozata, M.; Oktenli, C.; Bingol, N.; Ozdemir, I. C., The effects of metformin and diet on plasma testosterone and leptin levels in obese men. *Obes. Res.* **2001,** 9, (11), 662-7.

24. Silvestre, J.; Carvalho, S.; Mendes, V.; Coelho, L.; Tapadinhas, C.; Ferreira, P.; Povoa, P.; Ceia, F., Metformin-induced lactic acidosis: a case series. *J. Med. Case Reports* **2007,** 1, 126.

25. McGuinness, M. E.; Talbert, R. L., Phenformin-induced lactic acidosis: a forgotten adverse drug reaction. *Ann. Pharmacother.* **1993,** 27, (10), 1183-7.

26. Gan, S. C.; Barr, J.; Arieff, A. I.; Pearl, R. G., Biguanide-associated lactic acidosis. Case report and review of the literature. *Arch. Intern. Med.* **1992,** 152, (11), 2333-6.

27. Medawala, W.; McCahill, P.; Giebink, A.; Meyer, J.; Ku, C. J.; Spence, D. M., A Molecular Level Understanding of Zinc Activation of C-peptide and its Effects on Cellular Communication in the Bloodstream. *Rev. Diabet. Stud.* **2009,** 6, (3), 148-58.

28. Meyer, J. A.; Subasinghe, W.; Sima, A. A.; Keltner, Z.; Reid, G. E.; Daleke, D.; Spence, D. M., Zinc-activated C-peptide resistance to the type 2 diabetic erythrocyte is associated with hyperglycemia-induced phosphatidylserine externalization and reversed by metformin. *Mol. Biosyst.* **2009,** 5, (10), 1157-62.

29. Meyer, J. A.; Froelich, J. M.; Reid, G. E.; Karunarathne, W. K.; Spence, D. M., Metal-activated C-peptide facilitates glucose clearance and the release of a nitric oxide stimulus via the GLUT1 transporter. *Diabetologia* **2008,** 51, (1), 175-82.

30. Sprague, R. S.; Stephenson, A. H.; Dimmitt, R. A.; Weintraub, N. L.; Branch, C. A.; McMurdo, L.; Lonigro, A. J., Effect of L-NAME on pressure-flow relationships in isolated rabbit lungs: role of red blood cells. *Am. J. Physiol.* **1995,** 269, (6 Pt 2), H1941-8.

31. Edwards, J.; Sprung, R.; Sprague, R.; Spence, D., Chemiluminescence detection of ATP release from red blood cells upon passage through microbore tubing. *Analyst* **2001,** 126, (8), 1257-60.

32. Liddell, J. R.; Zwingmann, C.; Schmidt, M. M.; Thiessen, A.; Leibfritz, D.; Robinson, S. R.; Dringen, R., Sustained hydrogen peroxide stress decreases lactate production by cultured astrocytes. *J. Neurosci. Res.* **2009,** 87, (12), 2696-708.

33. Yeung, T.; Heit, B.; Dubuisson, J. F.; Fairn, G. D.; Chiu, B.; Inman, R.; Kapus, A.; Swanson, M.; Grinstein, S., Contribution of phosphatidylserine to membrane surface charge and protein targeting during phagosome maturation. *J. Cell. Biol.* **2009,** 185, (5), 917-28.

34. Yeung, T.; Gilbert, G. E.; Shi, J.; Silvius, J.; Kapus, A.; Grinstein, S., Membrane phosphatidylserine regulates surface charge and protein localization. *Science (New York, N.Y.)* **2008,** 319, (5860), 210-3.

35. Ekberg, K.; Brismar, T.; Johansson, B. L.; Jonsson, B.; Lindstrom, P.; Wahren, J., Amelioration of sensory nerve dysfunction by C-Peptide in patients with type 1 diabetes. *Diabetes* **2003,** 52, (2), 536-41.

36. Ekberg, K.; Brismar, T.; Johansson, B. L.; Lindstrom, P.; Juntti-Berggren, L.; Norrby, A.; Berne, C.; Arnqvist, H. J.; Bolinder, J.; Wahren, J., C-Peptide replacement therapy and sensory nerve function in type 1 diabetic neuropathy. *Diabetes Care* **2007,** 30, (1), 71-6.

37. Johansson, B. L.; Linde, B.; Wahren, J., Effects of C-peptide on blood flow, capillary diffusion capacity and glucose utilization in the exercising forearm of type 1 (insulin-dependent) diabetic patients. *Diabetologia* **1992,** 35, (12), 1151-8.

38. Johansson, B. L.; Sjoberg, S.; Wahren, J., The influence of human C-peptide on renal function and glucose utilization in type 1 (insulin-dependent) diabetic patients. *Diabetologia* **1992,** 35, (2), 121-8.

39. Johansson, B. L.; Sundell, J.; Ekberg, K.; Jonsson, C.; Seppanen, M.; Raitakari, O.; Luotolahti, M.; Nuutila, P.; Wahren, J.; Knuuti, J., C-peptide improves adenosine-induced myocardial vasodilation in type 1 diabetes patients. *Am. J. Physiol. Endocrinol. Metab.* **2004,** 286, (1), E14-9.

40. Johansson, B. L.; Wahren, J.; Pernow, J., C-peptide increases forearm blood flow in patients with type 1 diabetes via a nitric oxide-dependent mechanism. *Am. J. Physiol. Endocrinol. Metab.* **2003,** 285, (4), E864-70.

41. Sima, A. A. F.; Zhang, W.; Sugimoto, K.; Henry, D.; Li, Z.; Wahren, J.; Grunberger, G., C-peptide prevents and improves chronic Type I diabetic polyneuropathy in the BB/Wor rat. *Diabetologia* **2001,** 44, (7), 889-897.

42. Lindahl, E.; Nyman, U.; Melles, E.; Sigmundsson, K.; Stahlberg, M.; Wahren, J.; Obrink, B.; Shafqat, J.; Joseph, B.; Jornvall, H., Cellular internalization of proinsulin C-peptide. *Cell Mol. Life Sci.* **2007,** 64, (4), 479-86.

43. Lalau, J. D.; Lacroix, C., Measurement of metformin concentration in erythrocytes: clinical implications. *Diabetes Obes. Metab.* **2003,** 5, (2), 93-8.

44. Brunauer, L. S.; Moxness, M. S.; Huestis, W. H., Hydrogen peroxide oxidation induces the transfer of phospholipids from the membrane into the cytosol of human erythrocytes. *Biochemistry* **1994,** 33, (15), 4527-32.

45. Pavlovic, D.; Kocic, R.; Kocic, G.; Jevtovic, T.; Radenkovic, S.; Mikic, D.; Stojanovic, M.; Djordjevic, P. B., Effect of four-week metformin treatment on plasma and erythrocyte antioxidative defense enzymes in newly diagnosed obese patients with type 2 diabetes. *Diabetes Obes. Metab.* **2000,** 2, (4), 251-6.

46. Chakraborty, A.; Chowdhury, S.; Bhattacharyya, M., Effect of metformin on oxidative stress, nitrosative stress and inflammatory biomarkers in type 2 diabetes patients. *Diabetes Res. Clin. Pract.* **2011,** 93, (1), 56-62.

47. Tolan, N. V.; Genes, L. I.; Subasinghe, W.; Raththagala, M.; Spence, D. M., Personalized metabolic assessment of erythrocytes using microfluidic delivery to an array of luminescent wells. *Anal. Chem.* **2009,** 81, (8), 3102-8.

48. Quijano, C.; Castro, L.; Peluffo, G.; Valez, V.; Radi, R., Enhanced mitochondrial superoxide in hyperglycemic endothelial cells: direct measurements and formation of hydrogen peroxide and peroxynitrite. *Am. J. Physiol. Heart Circ. Physiol.* **2007,** 293, (6), H3404-14.

49. Sasson, S.; Gorowits, N.; Joost, H. G.; King, G. L.; Cerasi, E.; Kaiser, N., Regulation by metformin of the hexose transport system in vascular endothelial and smooth muscle cells. *Br. J. Pharmacol.* **1996,** 117, (6), 1318-24.

50. Guigas, B.; Detaille, D.; Chauvin, C.; Batandier, C.; De Oliveira, F.; Fontaine, E.; Leverve, X., Metformin inhibits mitochondrial permeability transition and cell death: a pharmacological in vitro study. *Biochem. J.* **2004,** 382, (Pt 3), 877-84.

51. Zhou, G.; Myers, R.; Li, Y.; Chen, Y.; Shen, X.; Fenyk-Melody, J.; Wu, M.; Ventre, J.; Doebber, T.; Fujii, N.; Musi, N.; Hirshman, M. F.; Goodyear, L. J.; Moller, D. E., Role of AMP-activated protein kinase in mechanism of metformin action. *J. Clin. Invest.* **2001,** 108, (8), 1167-74.

52. Hardie, D. G., The AMP-activated protein kinase cascade: the key sensor of cellular energy status. *Endocrinology* **2003,** 144, (12), 5179-5183.

53. Winder, W. W.; Hardie, D. G., AMP-activated protein kinase, a metabolic master switch: possible roles in type 2 diabetes. *Am. J. Physiol.* **1999,** 277, (1 Pt 1), E1-10.

54. Luo, Z.; Saha, A. K.; Xiang, X.; Ruderman, N. B., AMPK, the metabolic syndrome and cancer. *Trends Pharmacol. Sci.* **2005,** 26, (2), 69-76.

CHAPTER 4: INTRACELLULAR CHANGES IN THE ENDOTHELIUM UPON AMPK ACTIVATION – GLUCOSE METABOLIC COMPARISON BETWEEN HEALTHY AND CANCEROUS CELL LINES IN NORMAL AND HYPERGLYCEMIC CONDITIONS

4.1 AMP-activated protein kinase activation and effects

AMP-activated protein kinase (AMPK) is one of the more significant regulators of cellular energy. Structurally, it is described as a phylogenetically conserved heterotrimer protein that contains three subunits denoted as α, β, and γ, each of which has a minimum of two isoforms.[1-3] The (α) is considered the catalytic subunit, while the (β and γ) are classified as the regulatory subunits.[1, 4] It is widely believed that AMPK is one of the key regulatory proteins when cells are subjected to such energy stresses as exercise, adiponectin, leptin, glucose deprivation, hypoxia, and oxidant stress.[1, 3-6] AMPK is activated with increasing adenosine monophosphate (AMP)/ATP ratios, either through decreased ATP production or increased ATP consumption.[7, 8] AMP levels alone do not determine the extent of AMPK activation, as ATP antagonizes all of the effects exhibited by AMP on the activation of AMPK.[9]

The (α) subunit of AMPK must become phosphorylated for activation to occur.[10, 11] This activation can be initiated directly via AMP promoted phosphorylation, or by inhibiting the dephosphorylation of the subunit.[9, 12] Upon activation, AMPK generally turns on pathways that generate ATP (catabolic), and turn off pathways that consume ATP (anabolic).[13] The activation of AMPK stimulates an increase in glucose uptake in muscles, fatty acid oxidation in the muscle

tissue and liver, and inhibits hepatic glucose production from the liver.[3] AMPK activation also inhibits acetyl CoA carboxylase (ACC), which is used to generate the intermediates to produce fatty acids.[14] While this described activation occurs naturally under conditions of energetic stress, there are chemical compounds that can be used to activate AMPK.

Two of the compounds regularly used to stimulate AMPK activity are 5-aminoimidazole-4-carboxamide ribotide (AICAR) and the biguanide molecule metformin. AICAR is taken in by the cell and converted by an adenosine kinase into 5-aminoimidazole-4-carboxamide-1-D-ribofuranosyl-5'-monophosphate (ZMP), which has similar effects as AMP, activating AMPK in the same manner as AMP does.[15] The ZMP is able to increase the AMP/ATP ratio, thereby activating AMPK. In contrast to the aforementioned effects of AICAR on muscle tissue and liver cells, studies involving human umbilical vein endothelial cells (HUVEC) incubated with AICAR resulted in decreases in both glucose uptake and glycolytic rates, even during periods of increased AMPK activation.[16] Therefore, the activation of AMPK via AICAR administration appears to have different effects on different cell types.

While metformin has been shown to activate AMPK in multiple cell types and *in vivo* conditions,[17-21] the general mechanism for the activation remains uncertain. There have been reports demonstrating AMPK activation with metformin in muscle cells, Chinese hamster ovary fibroblasts, and rat hepatoma cells without observing any change in the AMP/ATP intracellular ratio.[22, 23] However, studies evaluating rat heart samples revealed increased cytosolic AMP levels and subsequent AMPK activation following metformin administration.[18] Results from other studies suggested an increased amount of lactate released from cardiomyocytes that had

been incubated with varying metformin concentrations.[24] While the studies presented here do not examine the AMPK activation directly, metabolic changes in healthy bovine pulmonary endothelial cells (bPAECs), that had been incubated with metformin and AICAR, were determined by measuring lactate release, glucose uptake and consumption, as well as intracellular pH.

4.2 Lactate clearance from cells

When catabolic metabolic reactions generate ATP, particularly anaerobic respiration that converts the monocarboxylic acid pyruvate into lactate following the last steps of glycolysis, the waste byproducts need to be removed from the cell. The removal of lactate from the cytosol of the cell is essential to maintain a metabolic equilibrium, as well as to prevent potential cell damage.[25, 26] In some instances, certain cells are able to metabolize the lactate or pyruvate that is released from other cells for their own cellular energy. These monocarboxylic acids, pyruvate and lactate in particular, are transported out of and into these cells through a transporter family known as monocarboxylate transporters (MCTs).[26, 27]

The MCTs in the studies reported here are proton-coupled MCTs. While there are multiple isoforms of MCTs,[28] the isoform of interest here is the MCT isoform 1, or MCT1. The label as a proton-coupled transporter explains the kinetics of how the substrate, namely lactate, is transported either in or out of the cell. The MCT1 isoform works by simply exchanging a substrate molecule for a proton (H^+) (Figure 4.1).[29, 30] While the MCTs remove lactate from the intracellular to the extracellular space, many of the studies performed on these transport

proteins focus on the influx of lactate and pyruvate through the MCT, rather than the efflux. These studies are performed through the inhibition of the transporters using molecules such as α-cyano-4-hydroxycinnamic Acid (ACCA) and monitoring the influx of the molecules through the use of radiolabeled lactate and pyruvate compounds.[31-33]

Although they are important in regulating cellular metabolism in normal cells and tissues, MCTs have also been implicated with cancer cells and their metabolism for their ability to regulate intracellular pH.[34] It is hypothesized that the acidic microenvironment of most tumors is due to increased rates of glycolysis and lactate release from cancer cells.[35, 36] As described in prior studies, it is this acidic environment that provides the tumor its aggressive and invasive features.[37, 38] The MCTs can also play a critical role in the tumor's ability to transport pyruvate from the extracellular to the intracellular space, as findings have suggested that some cancerous cells obtain pyruvate for energy production from surrounding stromal cells, or surrounding connective tissue cells.[39]

The present studies focus on some of the intracellular changes, such as intracellular pH, that occur in healthy cells that are stimulated to metabolize glucose in different means. The studies also utilize ACCA to inhibit the MCTs on the bPAECs and cancerous HeLa cells to determine how MCTs affect endothelial cell and cancerous cell transport and metabolism of glucose. The glucose uptake rates and extracellular lactate levels were measured to observe the metabolic rates and functions of bPAEC and cancerous HeLa cell cultures following the transporter inhibition.

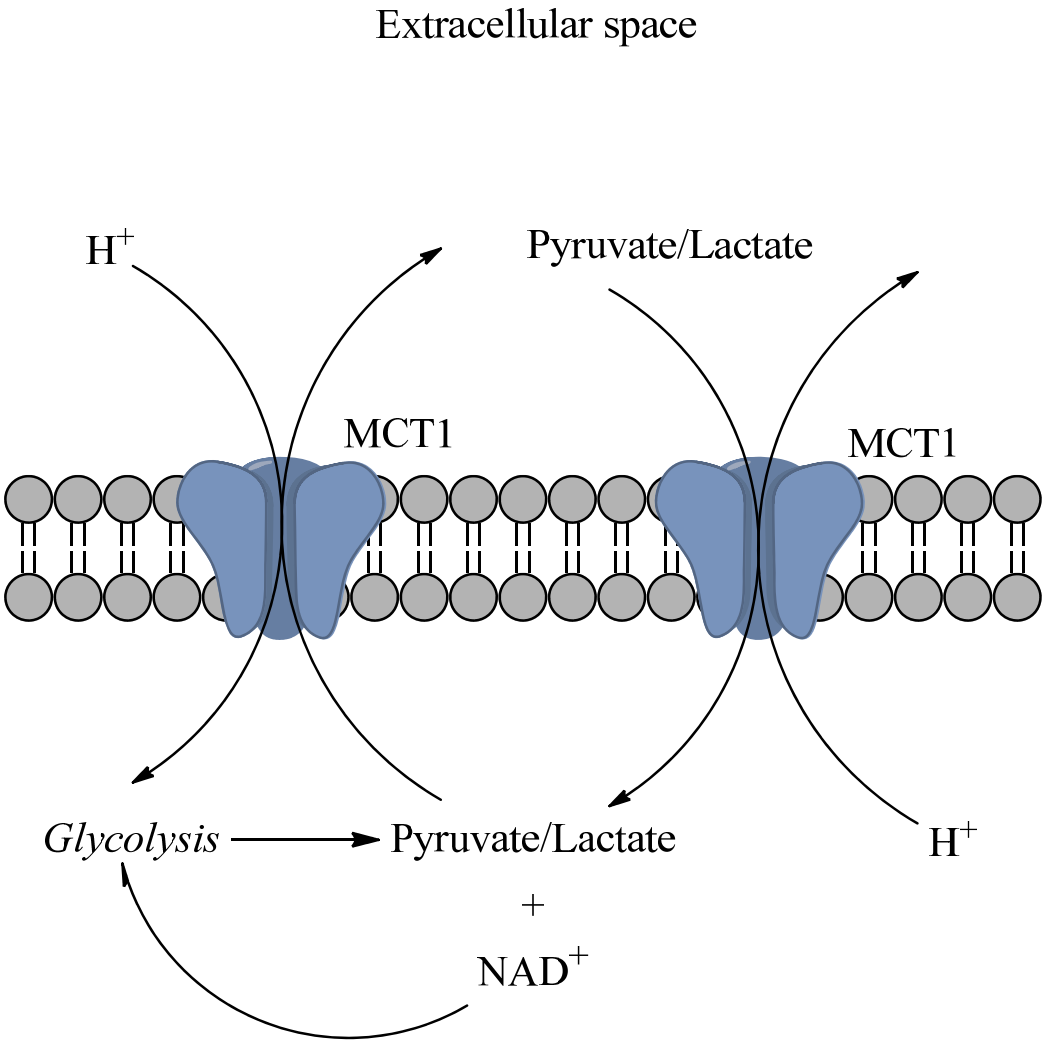

Figure 4.1 – Illustration demonstrating the activity of the proton-coupled monocarboxylate transporter 1 (MCT1). In MCT1 transport, a monocarboxylic acid such as pyruvate or lactate is removed from (left), or brought into the cell (right) by the exchange of one proton (H^+). Pyruvate can be brought into the cell to produce additional lactate, generating additional NAD^+ to further fuel glycolysis. Lactate can also be removed from the cell in order to maintain equilibrium that favors energy production through glycolysis.

4.3 Significance of pyruvate

The monocarboxylic acid pyruvate is the final product following the glycolysis pathway (Figure 1.1). ATP is generated either in the mitochondria from pyruvate through the citric acid cycle or through the repeated conversion of pyruvate into lactate by lactate dehydrogenase in the cytosol, thereby allowing for further occurrences of glycolysis through regeneration of the cofactor NAD^+. Pyruvate has a crucial role in generating specific amino acids (Figure 4.2), as well as preventing cytotoxicity by scavenging peroxides and metal ions, in addition to providing the substrates required to generate ATP.[40-43]

In the work presented here, it was hypothesized that the presence of pyruvate in the media above cultured endothelial and HeLa cells would affect the way that the two cell types metabolize glucose. Extracellular lactate and glucose measurements were performed to determine whether the presence of a 'free' source of energy such as pyruvate would result in the cells consuming and metabolizing glucose at different rates compared to having no pyruvate available.

4.4 Experimental

4.4.1 Preparation of reagents

Unless stated otherwise, all aqueous stock and working solutions were prepared using purified (18.2 MΩ) double-distilled water (DDW). All reagents that were prepared in volumetric glassware were transferred to polypropylene tubes immediately to reduce metal contamination.

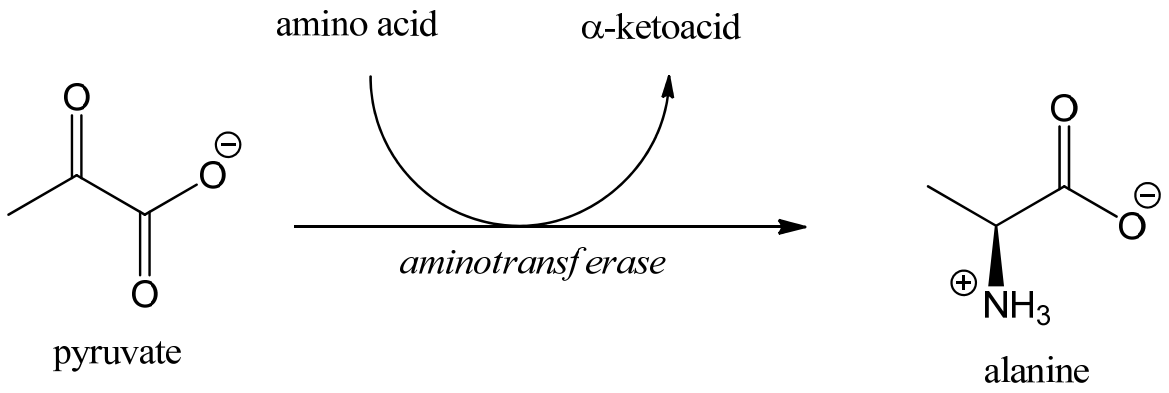

Figure 4.2 – Reaction showing the production of the nonessential amino acid alanine. The aminotransferase enzyme removes the amino group from the amino acid, placing it on pyruvate and ultimately generating alanine. In this case, alanine is used as part of the glucose-alanine cycle to help regenerate glucose in the liver.

50 µg of the pre-packaged 2',7'-bis-(2-carboxyethyl)-5-(and-6)-carboxyfluorescein, acetoxymethyl ester (BCECF AM, Invitrogen) were dissolved in 20 µL of high-quality anhydrous dimethyl sulfoxide (DMSO, Sigma Aldrich) to create a stock concentration of 4.03 mM that was used for the intracellular pH studies. Stock solutions of nigericin and monensin, also used in the intracellular pH studies, were prepared by dissolving 5 mg of both the nigericin sodium salt (Sigma Aldrich) and monensin sodium salt (Sigma Aldrich) in 1 mL of ethanol and 500 µL of high-quality DMSO, respectively. The final stock concentrations of the nigericin and monensin were 6.7 mM and 14.4 mM, respectively. The standards used for the *in situ* calibration were aqueous chloride based solutions containing the following salt (Sigma Aldrich) concentrations (numerical values represent mM concentration); KCl – 130, $MgCl_2$ – 1.0, 4-(2-hydroxyethyl)-1-piperazineethanesulfonic acid (HEPES) – 15.0, 2-(*N*-morpholino) ethanesulfonic acid (MES) – 15.0. The pH of the standards was adjusted by dropwise addition of a 2 M NaOH solution. The pH range of the standards was adjusted to be between 6.0 and 8.0.

The radiolabeled glucose, physiological salt solution (PSS), and the lysis solution used in the intracellular glucose studies were the same as described earlier (2.4.1). Metformin (Sigma Aldrich) was prepared by dissolving 19.8 mg in 500 µL of DMEM, resulting in a 239 mM stock solution for use in the intracellular pH and the lactate release/glucose uptake studies. A 500 mM stock solution of metformin used in the radiolabeled glucose studies was prepared by dissolving 20.7 mg in 250 µL of DDW.

Solutions of AICAR, ACCA, and pyruvate were used in some of the studies measuring lactate and glucose. 75 mM stock solutions of AICAR (Sigma Aldrich) were prepared by dissolving 5 mg in 258 µL of DDW. Stock solutions were stored frozen at -20°C. The MCT inhibitor ACCA stock solution of 0.5 M was prepared by dissolving 10 mg in 105.7 µL of

DMSO and agitated until the solid was completely in solution. The pyruvate (Sigma Aldrich) was supplied directly as a 100 mM sodium pyruvate solution in purified water.

The components and the preparation of the reactants in the extracellular glucose assay were similar to those previously described (3.4.1). The lactate dehydrogenase (LDH) used in the lactic acid assay was obtained as an ammonium sulfate solution (Sigma Aldrich). A glutamate/NaOH buffer was prepared by dissolving 0.422 g L-glutamic acid monosodium salt hydrate (Sigma Aldrich) in 5 mL of DDW. The solution was then adjusted to a pH ~ 8.90 through dropwise addition of a 2 M NaOH solution. A 50 mM nicotinamide dinucleotide (Sigma Aldrich) (NAD^+) stock solution was prepared by dissolving 10.5 mg in 315 µL of DDW immediately before use. The enzyme glutamic-pyruvic transaminase (Sigma Aldrich) (GPT) was prepared by suspending 2.35 mg in 2.35 mL of an enzyme stabilizing 1 mM DL-dithiothreitol (DTT, Sigma Aldrich) solution, resulting in a final enzyme concentration of 1 mg/mL. The stock GPT solutions were stored at -20°C in single use aliquots of 50 µL. The DTT solution was made by dissolving 1.5 mg with 10 mL of DDW.

The compound used to stain the cells was prepared at a concentration of 10 mg/mL. 10 mg of the Hoechst dye 33342 (Invitrogen) were dissolved completely in 1 mL of DMSO. The stock solution was kept at 4°C and thawed as needed.

4.4.2 Endothelial cell culture

The protocols for thawing and culturing the bPAECs obtained from Lonza were described earlier (2.4.3). The only change in the culturing procedures is that the EGM contains the appropriate volume of non-essential amino acids (NEAA) (MIDSCI). The EGM still

contains 7.5% v/v FBS, 2.5% v/v ABS, and penicillin/streptomycin. Cells were grown in 25 or 75 cm^2 tissue culture flasks (MIDSCI) and then subcultured into either 6, 12, or 24-well tissue culture plates. 24 hours before the experiments, the cells were incubated in serum free and NEAA free DMEM or HG DMEM.

4.4.3 HeLa cell culture

Cryogenically frozen HeLa cells were obtained from the laboratory of Dr. Jetze Tepe in the Chemistry Department at Michigan State University. The vial of frozen cells was thawed in a 37°C water bath with the contents immediately transferred to a 75 cm^2 tissue culture flask containing approximately 15 mL of HeLa growth medium (HeLa GM). The HeLa GM consists of 25 mM glucose DMEM supplemented with penicillin/streptomycin, NEAA, and 10% FBS (Atlanta Biologicals, Lawrenceville, GA). The same procedures used to subculture the bPAECs were applied to the HeLa cells when the flasks were full. The cells were then transferred to either 12 or 24-well tissue culture plates and allowed to grow. The HeLa cells were incubated in serum and NEAA free DMEM or HG DMEM 24 hours prior to experimentation as described in the endothelial cell culture.

4.4.4 Intracellular pH measurements – effect of metformin on intracellular pH

The intracellular pH of bPAECs that had been treated with metformin was measured using methods similar to a previous study.[44] Initially, bPAECs were cultured on 24-well tissue

culture plates and allowed to grow until the wells were full. The cells were incubated in either DMEM or HG DMEM containing no serum 24 hours prior to experimentation. The serum free media was then removed, followed by the addition of DMEM or HG DMEM to the wells. After the addition of the DMEM (or HG DMEM), an appropriate volume of the 239 mM metformin stock solution was added that resulted in the desired concentration of metformin. The final volume in each well was 375 μL and the metformin concentrations obtained were 0, 0.5, 1, 2, 5, and 7.5 mM. The bPAECs were allowed to incubate for 24 hours at 37°C.

4.4.4.1 Intracellular pH measurements

Following the 24 hour incubation with metformin, the treatment of cells for pH measurements involved removal of media and rinsing of cells multiple times with serum free DMEM. The 4 μM working solution of the intracellular pH probe BCECF was prepared by diluting 5 μL of the 4 mM stock solution into 5 mL of DMEM or HG DMEM (containing no serum). 250 μL of the working BCECF solution were pipetted on each well of cells (20 wells) with 250 μL of serum free DMEM or HG DMEM pipetted on the additional 4 wells to be treated as 'blanks'. The plates of cells were allowed to incubate for 30 minutes at 37°C. The probe was then removed and the cells were rinsed again with the high chloride buffer solutions described in the 'preparation of reagents'. The chloride buffer (pH 7.40) was kept on the cells for 20 minutes at 37°C, allowing for complete internalization of the BCECF probe. The supernatant was once again removed and replaced with fresh pH 7.40 buffer that was incubated for 15 minutes. The tissue culture plate with the cells was then loaded into the microplate reader and the fluorescence intensities of two different excitation wavelengths were measured consecutively. One fluorescence measurement was obtained using an excitation wavelength of 490 nm and an

emission wavelength at 530 nm, while the other was measured using an excitation wavelength at 440 nm and emission also collected at 530 nm. Ratios of the two fluorescence emission intensities were determined by dividing the emission intensity of the 490 nm excitation wavelength by the emission intensity from the 440 nm excitation wavelength. These ratios were essential in determining the intracellular pH of the bPAECs using a generated 'calibration curve' made *in situ*.

4.4.4.2 *In situ* pH calibration

A calibration curve generated through *in situ* measurements was applied to determine the intracellular pH values of the cells that had been incubated with metformin. While some wells of cells in the 24-well tissue culture plate were treated with metformin, other wells were only treated with DMEM or HG DMEM for the 24 hour incubation. Those wells with no metformin were rinsed with DMEM and the BCECF added in the same way as described above. The BCECF was removed from the cells after the 30 minute incubation at 37°C, after which the cells were rinsed with the chloride buffer. The cells were then incubated for 20 minutes at 37°C in 250 µL of the different pH buffers containing 25 µM nigericin and 10 µM monensin. The solutions were prepared by combining 1.86 µL of the nigericin stock and 0.35 µL of monensin stock in 498 µL of the buffer. The ionophores allow for the equilibration of the extracellular and intracellular pH.

The supernatant was removed after a 20 minute incubation at 37°C and replaced with fresh buffer at the same pH, but without the ionophores. That solution was allowed to incubate for 15 minutes, after which the fluorescence emission intensity at 530 nm was obtained using excitation wavelengths of 490 and 440 nm. The ratio of the two emission intensities was

obtained by dividing the 490 nm intensity by the 440 nm intensity. A calibration curve with the 490/440 emission ratio on the y-axis and the extracellular/intracellular pH on the x-axis was then generated (Figure 4.3).

4.4.5 Liquid scintillation counting in determining metformin's influence on intracellular glucose content

Liquid scintillation counting was utilized to determine the amount of radiolabeled glucose that remained in the endothelial cells after treatment with metformin and ^{14}C-glucose. The protocols used for the intracellular glucose measurements are similar to those described earlier (2.4.6). bPAECs cultured on 6-well tissue culture plates were incubated with serum free DMEM or HG DMEM for 24 hours. The media was replaced with 1.5 mL of DMEM or HG DMEM containing concentrations of metformin ranging from 0 through 7.5 mM that were prepared as described before using the 239 mM stock solution. The cells were then incubated for 24 hours at 37°C.

The cells were rinsed twice with PSS following the 24 hour incubation. 1 mL of PSS that contained 2 μCi/mL C^{14}-glucose was loaded onto the cells, which were incubated an additional 2 hours at 37°C in. The PSS containing the radiolabeled glucose was removed via pipette and discarded. The cells were rinsed multiple times with cold (4°C) PSS and lysed with 1 mL of the alkaline lysis buffer. The buffer was allowed to remain in the wells for 1 hour. 200 μL of the lysate were then transferred to a 96-well microplate followed by 100 μL of the scintillation cocktail. The plate was loaded into the scintillation counter with the luminescence measured and expressed as counts per minute (CPM).

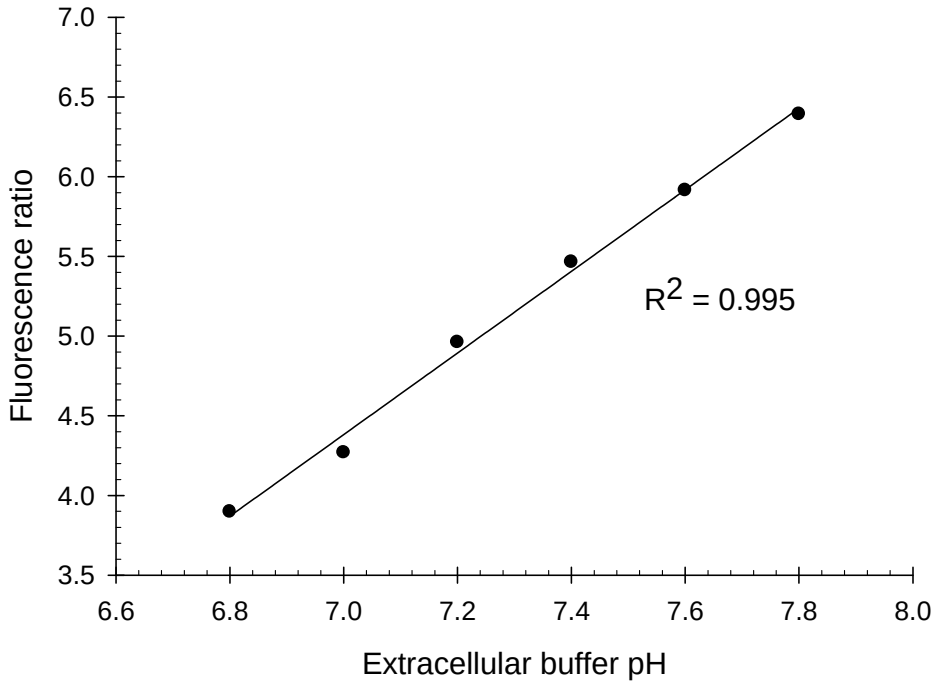

Figure 4.3 – *In situ* calibration curve generated by equilibrating the intracellular pH with that of the surrounding buffer using a previously described nigericin/monensin method. The fluorescence ratio (y-axis) was obtained by measuring the emission intensity obtained from two different excitation wavelengths. This calibration curve was then applied to the ratios obtained from the experimental cells and subsequently used to determine the intracellular pH change in the experimental samples. The curve shown here was one example of the calibration curves generated for the intracellular pH experiments (n = 1).

4.4.6 Determination of the effect of AICAR & metformin on lactate production and glucose consumption of bPAECs

bPAECs were cultured on 12-well tissue culture plates and incubated in either serum free DMEM or HG DMEM 24 hours prior to experimentation. Initially, for the studies examining the effects of AICAR, the media in the wells was removed following the incubation and replaced with 730 μL of DMEM or HG DMEM. The DMEM addition was immediately followed by 20 or 10 μL of the 75 mM AICAR stock solution, resulting in a final concentration of 2 or 1 mM, respectively. 10 or 20 μL of DDW were then added to the 1 and 0 mM AICAR sample well, respectively, in order to ensure that every sample had the same media to water ratio. Those plates were allowed to incubate at 37°C for 24 hours, after which the supernatant was removed and measured for lactate and glucose content.

The initial protocols for the metformin studies were similar to the AICAR protocols. The media in the wells that had been incubating for 24 hours was removed and replaced with 750 μL of DMEM or HGDMEM containing either 0, 1.57, 3.04, 6.08, 15.2, or 22.8 μL of the metformin stock solution; resulting in final concentrations of 0, 0.5, 1, 2, 5, and 7.5 mM, respectively. The endothelial cells were incubated at 37°C for either 18 or 24 hours. The supernatant was removed and measured for the lactate and glucose content.

4.4.7 Inhibition of MCT and the effects on lactate release and glucose uptake

The MCTs on both the bPAECs and HeLa cells were inhibited during incubation with various concentrations of ACCA. The glucose uptake and lactate production of these cells were

measured post-incubation. Cells were grown in 24-well tissue culture plates and incubated with serum free DMEM or HG DMEM 24 hours before the experiment. The media was removed and replaced with 375 μL of DMEM or HG DMEM containing various concentrations of ACCA in DMSO. The ACCA solutions were prepared by adding 7.5, 3.0, 1.5, 0.75, and 0.15 μL of the stock ACCA into 750 μL of DMEM or HG DMEM, resulting in concentrations of 5.0, 2.0, 1.0, 0.5, and 0.1 mM, respectively. DMSO was then added to each sample to bring the total DMSO content to 1% v/v, eliminating any interference that the solvent may generate in the fluorescence based assays. The tissue culture plates containing the cells with the ACCA solutions were incubated at 37°C for either 18 or 24 hours. The supernatant was removed and measured for lactate and glucose at the end of the incubation period.

Identical solutions containing ACCA and DMSO were prepared using DMEM and HG DMEM that had no sodium pyruvate. These solutions were used to observe any influence that pyruvate has on the glucose uptake and metabolism of bPAECs and HeLa cells. The solutions containing pyruvate were prepared by adding 100 μL of the sodium pyruvate stock solution to 10 mL of pyruvate free DMEM or HG DMEM. 100 mL of DDW were added to the pyruvate free DMEM solutions for proper controls. The appropriate volumes of the working ACCA solution were added to the DMEM solutions to prepare the experimental concentrations previously described in the above paragraph. The supernatants were removed with the lactate and glucose levels quantified following an 18 hour incubation.

4.4.8 Extracellular lactate measurements

The enzymatic assay applied to quantitatively determine the lactate in the studies reported here was similar to previously reported lactate assays in the literature, with minor changes in the enzyme concentrations.[45-47] 1 μL of the supernatant above the cells, following incubation with AICAR, metformin, ACCA, or pyruvate, was removed and diluted in 99 μL of DDW in a 96-well, black microplate. Only 0.5 μL of the supernatant were removed and diluted in 99.5 μL of DDW in the same microplate in the metformin studies, due to the elevated measured lactate levels. 100 μL of the enzyme solution were added after all dilutions were prepared. This enzyme solution consisted of a 0.5 M glutamate/NaOH buffer, 5.0 mM NAD^+, 0.7 Units/mL (U/mL) GPT, and 5.0 U/mL LDH. The reaction mechanisms behind the lactate assay are shown in Figure 4.4. 100 μL of the enzyme solution were then added to 99 μL of the L-lactic acid standards ranging from 0 through 100 μM. 1 μL of DMEM containing no glucose or pyruvate was added to the standards so that any interferences caused by the DMEM in the samples were eliminated. 0.5 μL of DMEM were added to the wells during the metformin studies. The fluorescence of the samples and standards was measured using an excitation wavelength of 340 nm and an emission wavelength of 460 nm following a 90 minute incubation at 37°C.

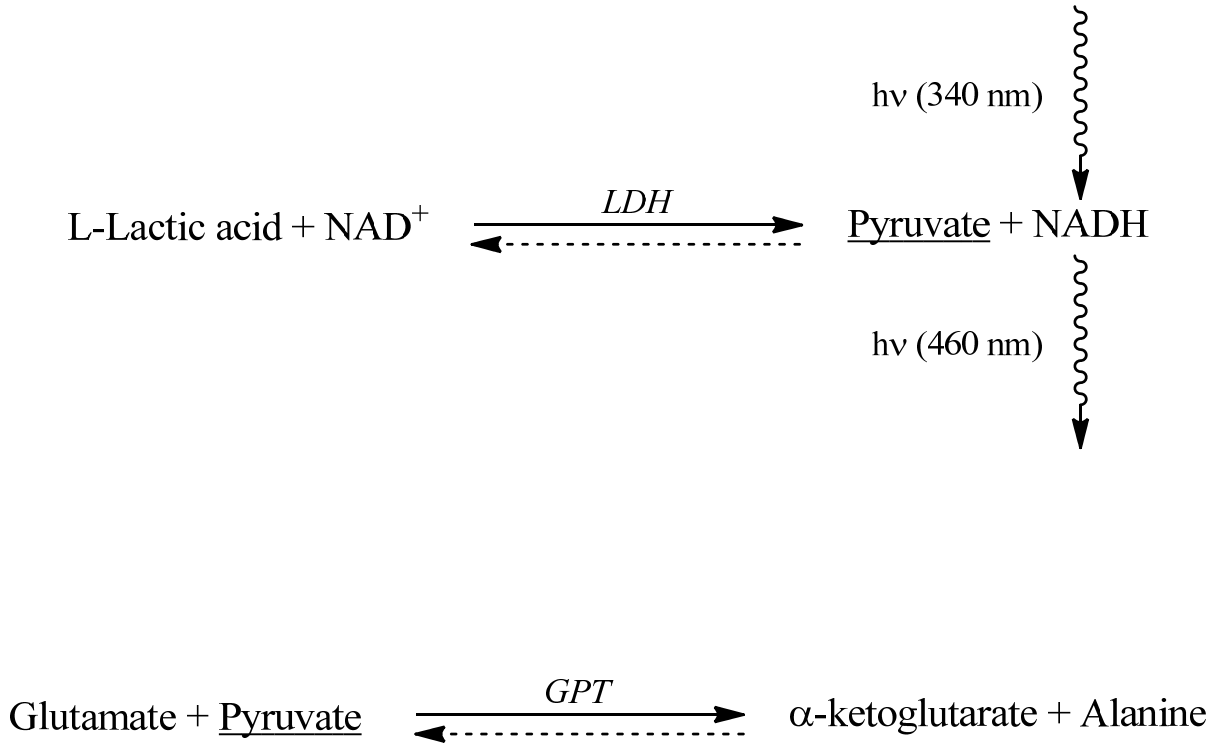

Figure 4.4 – Reaction mechanisms utilized in the lactic acid assay. The glutamic-pyruvic transaminase (GPT) enzyme was added to the enzyme solution due to the presence of pyruvate in the experimental DMEM. GPT utilizes the glutamate from the buffer and the pyruvate that is produced from the oxidation of the L-lactic acid, converting the two molecules into α–ketoglutarate and the amino acid alanine. This conversion of pyruvate by GPT reduced the amount of the molecule that could be reduced back to lactate by lactate dehydrogenase (LDH) and the NADH present.

4.4.9 Glucose consumption measurements

The extracellular glucose assay utilizes the same reaction mechanisms and enzyme solution that were described earlier to measure the glucose uptake by RBCs following treatment with metal-activated C-peptide and metformin (section 3.4.8). 1 μL of the supernatant above the bPAECs or HeLa cells was removed and diluted with 99 μL of DDW in a black, 96-well microplate following the incubation with AICAR, metformin, ACCA, or DMEM +/- pyruvate. The HG DMEM samples were prepared by diluting the supernatant 5-fold by taking 20 μL of the supernatant and adding 80 μL of DMEM containing no glucose. This dilution was performed due to the elevated levels of glucose and the effective range of the assay. 1 μL of the diluted sample was then diluted again with 99 μL of DDW in the 96-well plate. 100 μL of the glucose assay enzyme solution (section 3.4.8) were then added to each well that contained the samples and standards. The samples and the enzyme solution were allowed to incubate for 20 minutes. The fluorescence emission of the samples and standards was collected at 460 nm following an excitation at 340 nm. The DMEM and HG DMEM media were also measured for glucose content, with the HG DMEM diluted 5-fold to match the dilution of the samples. 1 μL of DMEM containing no glucose was added to 99 μL of each glucose standard (0 – 100 μM) to eliminate any effects the DMEM may have on the assay results.

4.4.10 Cell staining and counting

A simple method of staining and manually counting the cells was developed to determine the number of cells on the bottom of the well during the lactate and glucose uptake experiments

for both endothelial and HeLa cells. 20 μL of a 187.5 μg/ml Hoechst 33342 working solution were added to the remaining media in a 12-well tissue culture plate after the supernatant sample was removed for glucose and lactate measurement. 10 μL of the Hoechst dye working solution (5 μg/mL) were added to the supernatant in a 24-well plate to achieve the same final concentration. The working Hoechst solution was prepared by adding 0.5 μL of the stock to 1 mL of DMEM.

The cells were allowed to incubate for 30 minutes at 37°C after the Hoechst dye was administered. The wells were rinsed twice with DMEM followed by the addition of fresh buffer. The fluorescence of each well was then obtained using an Olympus IX71 inverted microscope (Olympus America) set to 20x magnification (Figure 4.5). The Hoechst dye is a fluorescent stain/dye that crosses the cellular membrane and binds to the DNA in the nucleus. The fluorescence images showing the nuclei were obtained using a microscope setup containing a mercury arc lamp light source sent through a 4', 6-diamidino-2-phenylindole (DAPI) filter cube that allows for an excitation wavelength of around 358 nm and an emission wavelength collection of approximately 460 nm.

The images containing the fluorescently stained nuclei of the bPAECs were then analyzed using a Microsuite Biology Suite computer program (Olympus America) with the nuclei manually counted. The average number of cells in each well was determined by combining the number of nuclei in three or four images, measuring the dimensions of the image, and finally extrapolating the average number of cells in each area over the entire surface area of the well. Overlapping cells were consistently counted as the number of nuclei present.

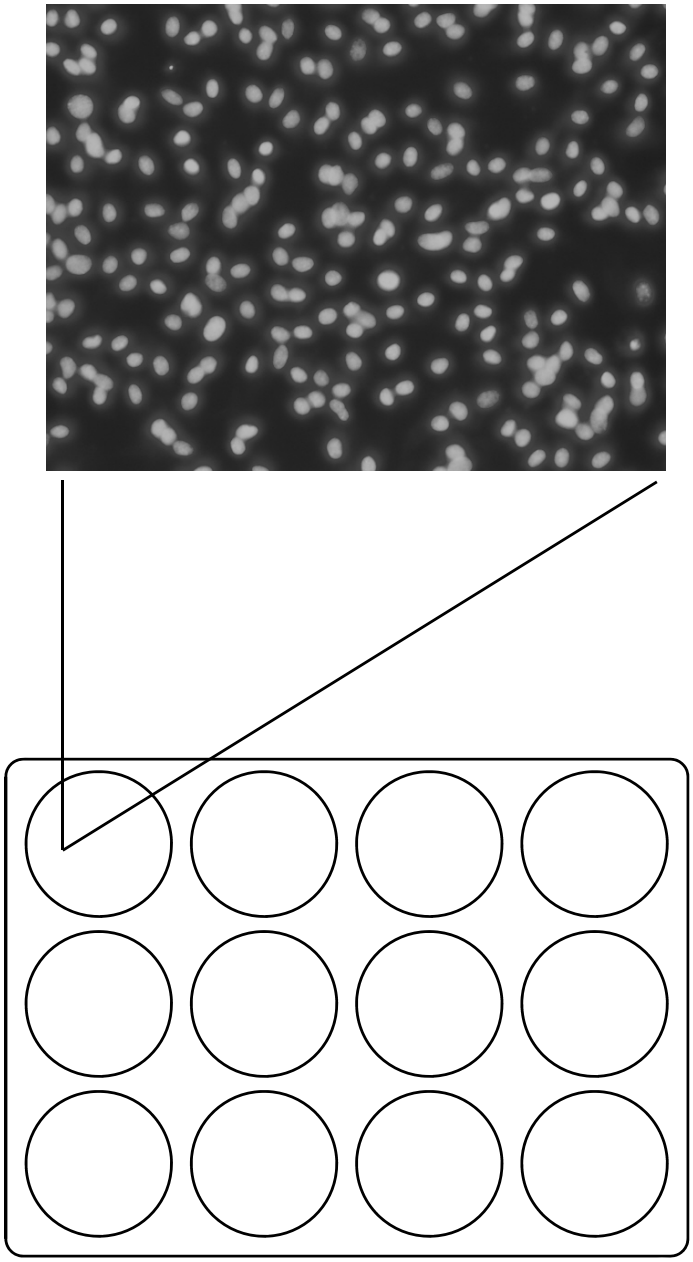

Figure 4.5 – Diagram illustrating the method for determining the cell count in each well. The top image shows the cultured cells (bPAECs specifically) that have been treated with the Hoechst 33342 nuclear dye. The image was obtained from the inverted microscope while exciting the sample with 358 nm and collecting emission intensity at 460 nm. The white areas in the above image represent the nuclei of viable cells. The cells in each area were averaged between 3 and 5 different images and then extrapolated to estimate the total number of cells in each well of the well plate, given that the image dimensions were determined.

4.5 Results

4.5.1 Effect of metformin on the intracellular pH of endothelial cells

The bPAECs were loaded with the intracellular pH probe, BCECF, following a 24 hour incubation with increasing concentrations of metformin,. The intracellular pH of the bPAECs was then determined using a generated *in situ* calibration curve. The intracellular pH of the bPAECs that were incubated with no metformin in the DMEM was 7.05 ± 0.01 (Figure 4.6). Increasing the metformin concentration to 0.5 mM resulted in a non-significant decrease in intracellular pH to 7.03 ± 0.02. When the metformin concentrations were increased to 1, 2, 5, and 7.5 mM, there were significant ($p < 0.01$) decreases in pH as shown in Figure 4.6.

Similar trends in terms of the relative changes in intracellular pH were observed from the bPAECs incubated with metformin and HG DMEM. Both samples gradually decreased the intracellular pH as the metformin concentration was increased. The cells treated with 0 mM metformin were measured to have a basal intracellular pH of 7.06 ± 0.01. Similar to the DMEM samples, there was no change in the intracellular pH following incubation with 0.5 M metformin. The addition of metformin at concentrations between 1 and 7.5 mM resulted in significant ($p < 0.01$) decreases in pH that were similar to the samples incubated in DMEM, also shown in Figure 4.6. The points that are indicated with an (ψ) represent a significant difference between the DMEM and HG DMEM samples containing the same concentration of metformin.

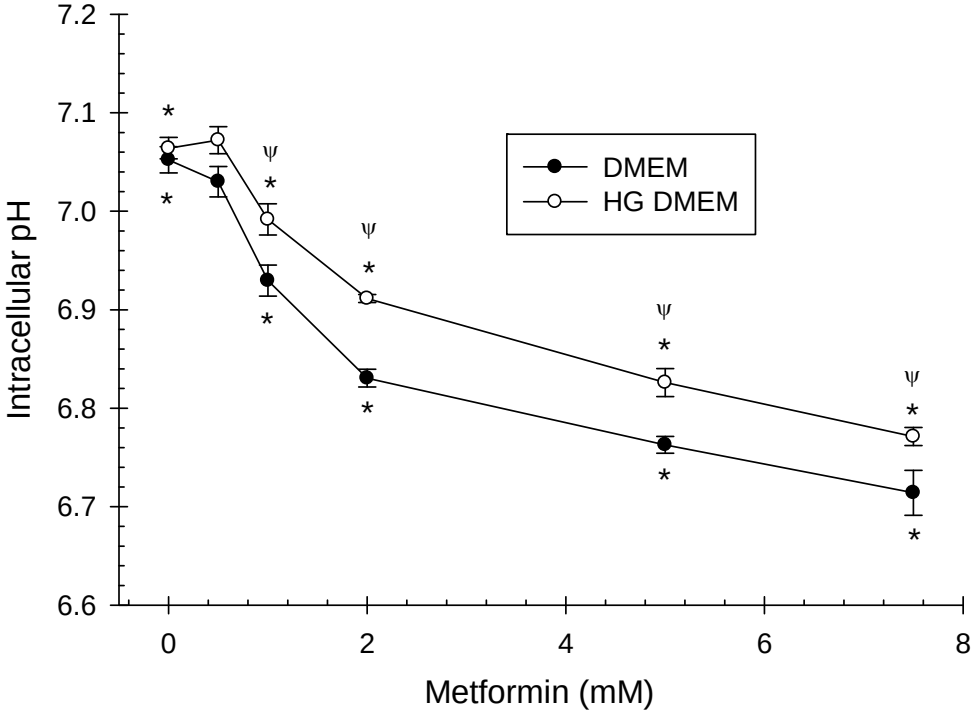

Figure 4.6 – Data representing the intracellular pH change in cultured bPAECs following a 24 hour incubation in varying concentrations of metformin. The intracellular pH values were obtained by comparing the fluorescence ratios to the in situ calibration curve. The points represent the average intracellular pH (n = 5) for the DMEM samples and n = 6 plates for the HG DMEM samples. There are significant changes in intracellular pH when compared to the 0 mM metformin at points indicated with (*$p < 0.05$). The points indicated with (ψ$p < 0.04$)) represent a significant difference between the DMEM and HG DMEM samples. The error bars represent the standard error of the mean.

4.5.2 Intracellular glucose following metformin administration

^{14}C-glucose solutions were administered to bPAECs that had been incubated in DMEM or HG DMEM with varying concentrations of metformin. The intracellular radiolabeled content was measured using liquid scintillation counting. The CPM values of each sample treated with metformin were normalized to the bPAEC sample that contained no metformin. The results of these studies are illustrated in Figure 4.7. There was no change in the intracellular glucose content when the cells were incubated with 0.5 or 1.0 mM metformin. However, there were significant decreases ($p < 0.001$) in the amount of radiolabeled material remaining in the cells as the metformin concentrations were increased from 2.0 through 7.5 mM. 2.0 mM metformin resulted in a normalized value of 0.79 ± 0.04 compared to the untreated cells. 5.0 and 7.5 mM metformin resulted in normalized values of 0.68 ± 0.04 and 0.61 ± 0.05, respectively.

The bPAECs incubated in HG DMEM resulted in similar normalized values to those of the DMEM samples. bPAECs incubated in HG DMEM with 0.5 and 1.0 mM metformin did not result in a significant change in intracellular radiolabeled material with normalized values of 0.96 ± 0.04 and 0.94 ± 0.07, respectively. Concentrations of metformin greater than 1.0 mM resulted in significant changes ($p < 0.005$), as 2.0 mM resulted in a normalized value of 0.77 ± 0.06, 5.0 mM provided a value of 0.64 ± 0.03, and 7.5 mM metformin resulted in a value of 0.568 ± 0.006.

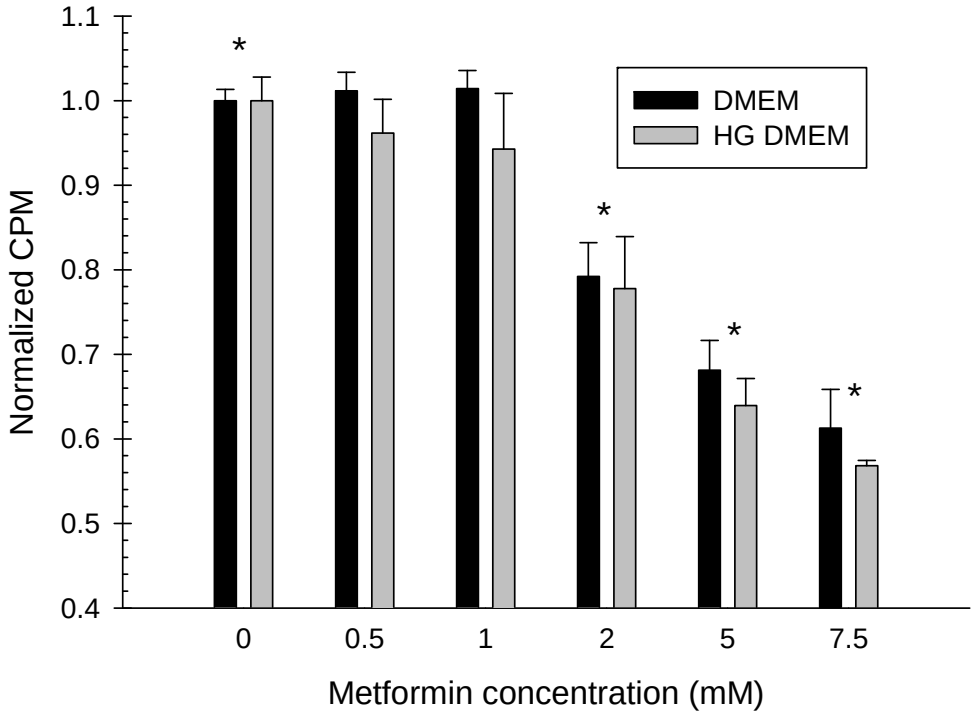

Figure 4.7 – Data representing the intracellular radiolabeled glucose content found in cultured bPAECs following a 24 hour incubation with metformin and either DMEM or HG DMEM. The bPAECs were incubated 2 hours in PSS containing the ^{14}C-glucose, lysed, and CPM values of the lysate obtained using counted using liquid scintillation counting. Each series' (DMEM or HG DMEM) CPM values are normalized to their respective sample containing no metformin. The bars labeled with (*$p < 0.05$) identify a significant difference in the intracellular radiolabeled material when compared to the values of the 0 mM metformin samples. The error bars represent the standard error of the mean for $n = 4$.

4.5.3 Effect of metformin on endothelial lactate production and glucose uptake

4.5.3.1 Lactate release

The results presented here enable the evaluation of the amount of lactate released by each cell, rather than measuring only the concentration of lactate present in the supernatant. The amount of lactate produced was divided by the number of cells in each well determined using the previously described staining and counting method (4.4.10). The molar quantity of lactate in each well was determined by comparing the fluorescence values to the generated L-lactic acid calibration curve and extrapolated considering the total volume of DMEM or HG DMEM applied to the cells in the tissue culture well-plate.

The amount of lactate released per cell is shown in (Figure 4.8). The cells had been incubated for 24 hours in either DMEM or HG DMEM containing metformin ranging in concentrations from 0 through 7.5 mM. It was determined that approximately 5.0 ± 0.2 picomoles (pmol) of lactate were released per cell incubated with 0 mM metformin in DMEM. Significant increases ($p < 0.001$) in released lactate were observed as the concentration of metformin was increased. Incubation of 0.5 mM and 1.0 mM metformin resulted in the release of 7.9 ± 0.5 and 10.9 ± 0.5 pmol lactate from each cell, respectively. Concentrations of metformin ranging between 2 and 7.5 mM resulted in a significant increase ($p < 0.05$) when compared to the 1 mM samples. Cells incubated with 2 mM metformin released 13.1 ± 0.4 pmol/cell, 5 mM metformin resulted in a 13.5 ± 0.4 pmol/cell release, and 7.5 mM metformin caused a release of 14.0 ± 0.5 pmol/cell.

There were similar trends in the lactate released from the bPAECs incubated with HG DMEM and increasing concentrations of metformin. However, the lactate amounts were

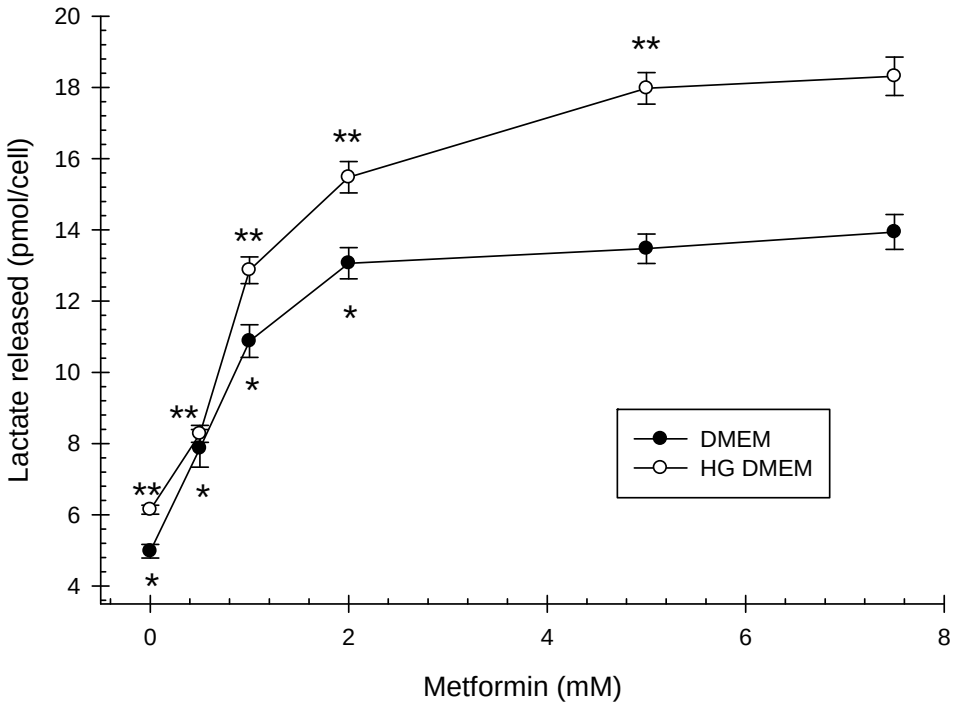

Figure 4.8 – Lactate release from bPAECs incubated with either DMEM or HG DMEM containing varying concentrations of the biguanide metformin. The supernatant was measured for lactate content after a 24 hour incubation. The number of cells present was then quantified, and the lactate released from each cell was determined. The points are the average lactate released from each cell for both DMEM samples. The error bars represent the standard error of the mean with n = 10. Values that were significantly higher than the preceding metformin concentration were indicated with either *$p < 0.05$ or **$p < 0.01$. All metformin concentrations resulted in a significant increase in lactate release when compared to the 0 mM metformin sample.

significantly increased. bPAECs incubated in only HG DMEM with no metformin released 6.1 ± 0.1 pmol of lactate per cell. This value was significantly higher ($p < 0.001$) than that of the lower glucose DMEM incubated cells. Incubation with metformin and HG DMEM resulted in significant increases ($p < 0.001$) for each concentration when compared to the 0 mM metformin sample. Incubation with 0.5 through 7.5 mM metformin resulted in released lactate values of 8.3 ± 0.2, 12.9 ± 0.4, 15.5 ± 0.4, 18.0 ± 0.4, and 18.3 ± 0.5 pmol/cell, respectively. The lactate released from the 0.0, 0.5, 1.0, and 2.0 mM metformin samples were significantly different from each other ($p < 0.001$) while the 5 and 7.5 mM metformin resulted in statistically the same amount of lactate released.

4.5.3.2 Glucose uptake

The amount of glucose consumed was determined indirectly by measuring the amount of glucose in both the supernatant and the DMEM/HG DMEM and subtracting the two values whereas the lactate was determined directly by measuring the lactate in the aliquot of the supernatant via the calibration curve. The metformin induced glucose uptake is shown in Figure 4.9. All values were obtained using the previously described D-glucose calibration curve.

bPAECs consumed approximately 3.42 ± 0.06 pmol of glucose for each cell after they were incubated 24 hours with DMEM with no metformin. There were significant increases ($p < 0.001$) in the amount of glucose taken in by the cells in the presence of metformin. A 24 hour incubation with 0.5 and 1.0 mM metformin resulted in the bPAECs taking in 4.6 ± 0.1 and 5.8 ± 0.1 pmol/cell, respectively. These two values were also significantly different ($p = 0.002$) from each other. The three concentrations of metformin, 2.0, 5.0, and 7.5 mM, were statistically similar to the 1 mM sample while the values of lactate released from the samples containing 2.0

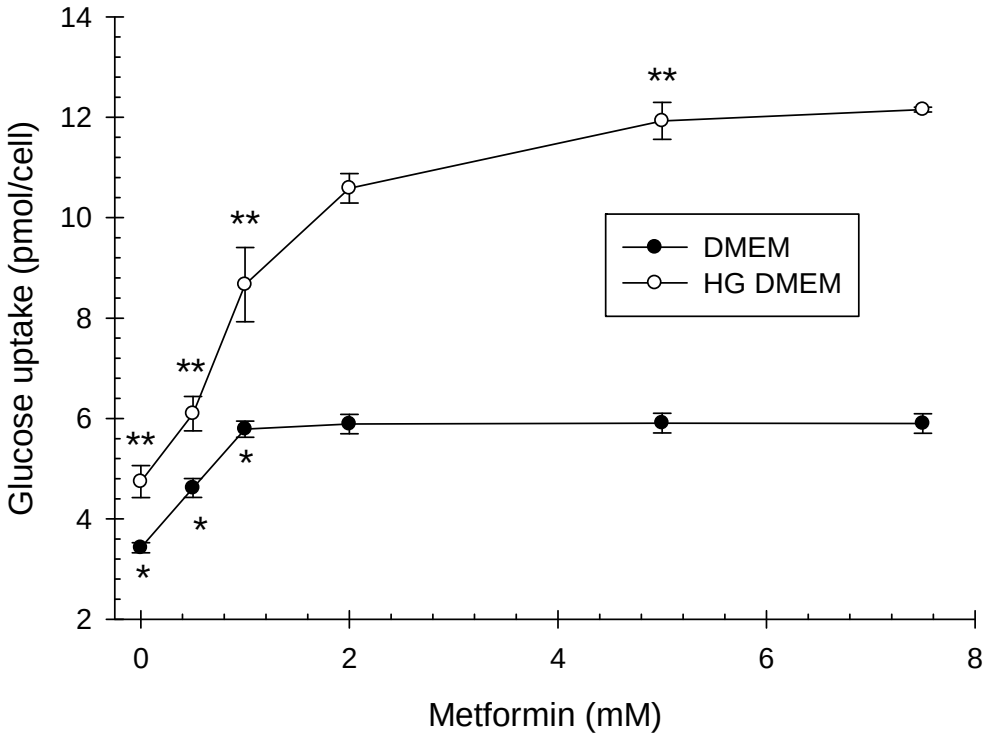

Figure 4.9 – Data showing the glucose uptake by bPAECs following a 24 hour incubation with either DMEM or HG DMEM containing varying concentrations of metformin. The extracellular glucose content was measured using the extracellular glucose assay and then subtracted from the amount of glucose present in the media on top of the cells. The difference indicates the amount of glucose taken in by the bPAECs. The points show the average value of glucose consumed at each metformin concentration. The error bars represent the standard error of the mean (n = 4) for the DMEM samples and n = 5 plates for the HG DMEM samples. Values that were significantly higher than the preceding metformin concentration were indicated with either *$p < 0.01$ or **$p < 0.05$. All metformin concentrations resulted in a significant increase in glucose uptake when compared to the 0 mM metformin sample.

through 7.5 mM metformin were significantly different ($p < 0.001$) than the 1.0 mM metformin samples. 2.0, 5.0, and 7.5 mM metformin all resulted in glucose uptake values of 5.9 ± 0.2 pmol/cell.

The glucose consumed by the bPAECs incubated in HG DMEM and metformin resulted in similar trends as it gradually increased as the DMEM samples did. However, the values at each metformin concentration were higher for the HG DMEM samples. The bPAECs incubated with only HG DMEM for 24 hours (no metformin) consumed 4.7 ± 0.3 pmol/cell. The glucose consumed increased significantly ($p < 0.05$) to 6.1 ± 0.3 and 8.7 ± 0.7 pmol/cell as the metformin concentration was increased to 0.5 and 1.0 mM, respectively. The glucose uptake values at the 0.5 and 1.0 mM metformin concentrations were also significantly ($p < 0.05$) different from each other. The 2 mM metformin concentration sample was statistically similar to the 1 mM sample with a value of 10.6 ± 0.3 pmol/cell. The 5 and 7.5 mM metformin samples were significantly higher ($p < 0.05$) than the 1 mM sample with values of 11.9 ± 0.4 and 12.15 ± 0.05 pmol/cell, respectively.

4.5.4 Effect of AMPK activator AICAR on endothelial glucose metabolism

The bPAEC lactate production and subsequent release along with the glucose consumption were measured following the addition of the AMPK activator AICAR. The cells were incubated in either DMEM or HG DMEM containing 2, 1, or 0 mM AICAR for 24 hours. The protocols for measuring extracellular lactate and glucose consumption were identical to those described earlier (4.4.8 and 4.4.9). The amount of lactate released from the cells was

expressed as the amount released from each individual cell, while the glucose consumed was normalized to the value of the cells that had no AICAR added.

The lactate release results obtained following AICAR administration are illustrated in Figure 4.10. The results show that the cells released lactate at a rate of 5.4 ± 0.2 pmol/cell after a 24 hour incubation in DMEM with no AICAR. The lactate released was significantly lowered ($p < 0.010$) to 4.4 ± 0.1 and 4.2 ± 0.2 pmol/cell, respectively when AICAR was present at concentrations of 1.0 and 2.0 mM. The cells incubated with HG DMEM containing 0 mM AICAR resulted in a 7.0 ± 0.4 pmol/cell rate of lactate release. Incubation of the bPAECs with 1 and 2 mM AICAR resulted in a significant decrease ($p < 0.05$) in lactate release down to 5.7 ± 0.2 and 4.8 ± 0.3 pmol/cell, respectively.

The glucose uptake trend following AICAR administration resembles the trend of the lactate results (Figure 4.11). The glucose uptake by cells incubated with DMEM and no AICAR was normalized to a value of 1.00 ± 0.04. 1 mM AICAR resulted in a significant decrease ($p < 0.001$) in glucose uptake to a normalized value of 0.76 ± 0.03 after 24 hours. 2 mM AICAR resulted in a normalized glucose uptake value of 0.63 ± 0.03 that was lower ($p < 0.03$) than the 1 mM AICAR result. The HG DMEM samples incubated without AICAR were normalized to a value of 1.00 ± 0.09. Samples containing 1 or 2 mM AICAR resulted in significant decreases ($p < 0.03$) in the glucose uptake that were similar to those observed in the DMEM samples. Those normalized values were 0.78 ± 0.07 and 0.63 ± 0.06 for the 1 and 2 mM AICAR samples, respectively.

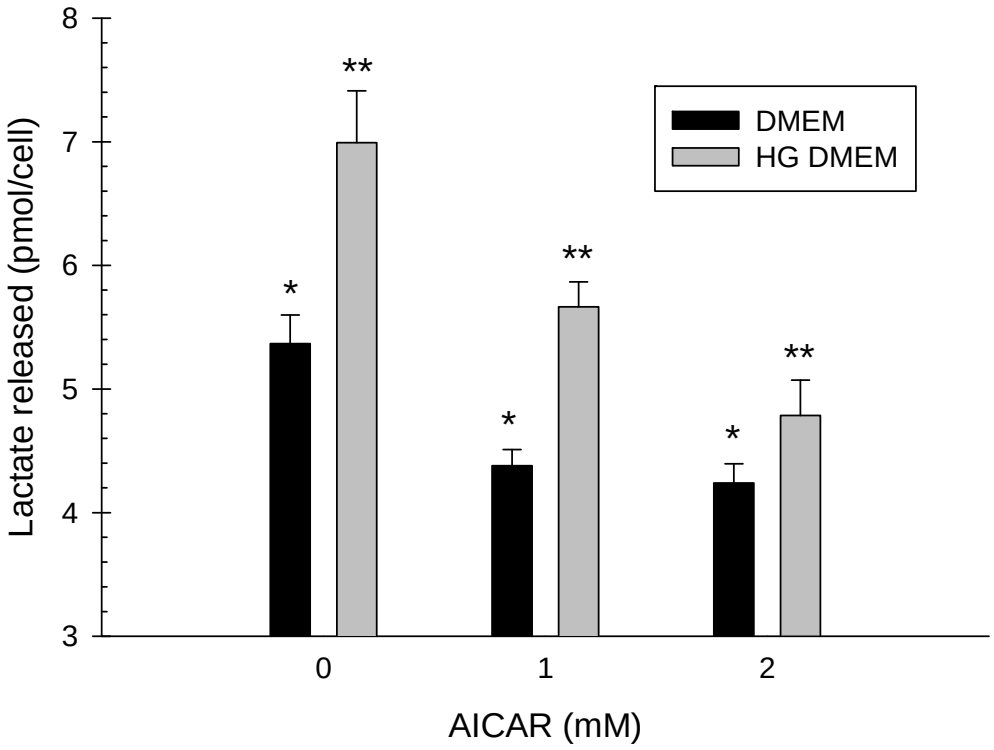

Figure 4.10 – Data showing the lactate production from bPAECs following a 24 hour incubation with the AMP-activated protein kinase (AMPK) activator AICAR. Data bars are expressed as averaged values for n = 4 for DMEM samples and n = 3 for HG DMEM samples. Values are expressed as the amount of lactate released from each cell. The error bars represent the standard error of the mean. Statistically significant differences in the lactate release when compared to the 0 mM AICAR samples are identified with *$p < 0.01$ or **$p < 0.05$.

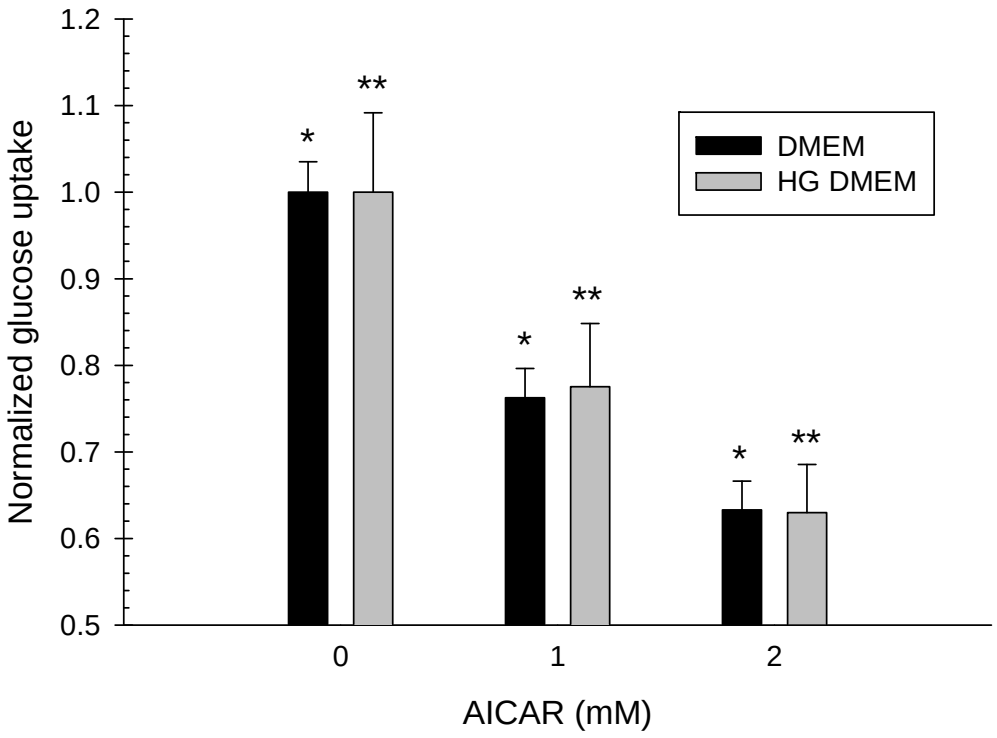

Figure 4.11 – Data illustrating the glucose uptake in bPAECs following administration with the AMPK activator AICAR in either DMEM or HG DMEM. The extracellular glucose was measured and compared to the glucose present in the media with the difference representing the amount of glucose taken in by the bPAECs. The measurements were made following a 24 hour incubation. The glucose uptake values were then normalized to their respective DMEM samples containing no AICAR. Significant differences in the glucose uptake when compared to the 0 mM AICAR samples are indicated with *$p < 0.001$ or **$p < 0.03$. The error bars represent the standard error of the mean for $n = 4$.

4.5.5 Inhibition of MCT with ACCA and the effect it has on glucose metabolism in endothelial and HeLa cells

4.5.5.1 Lactate release

The amount of lactate that was released by both bPAECs and HeLa cells was measured using the previously described lactate assay (4.4.8) following the inhibition of the monocarboxylate transporter (MCT) with varying concentrations of ACCA. The lactate production results are illustrated in Figure 4.12. bPAECs incubated for 18 hours in DMEM that had no ACCA resulted in a release of 3.4 ± 0.2 pmol of lactate from each cell. Concentrations of ACCA between 0.1 and 1.0 mM resulted in significant ($p < 0.01$) increases of lactate released, 4.6 ± 0.1, and 4.20 ± 0.08 pmol/cell, respectively. The lactate released from 2.0 mM was statistically similar to the cells with no ACCA, while the 5.0 mM ACCA samples resulted in a significant decrease ($p < 0.01$) in lactate release with a value of 2.4 ± 0.1 pmol/cell. The bPAECs incubated with identical concentrations of ACCA in HG DMEM, resulted in similar trends in lactate release to the DMEM samples.

Cells incubated in HG DMEM with no ACCA released 4.93 ± 0.02 pmol/cell lactate. This value was significantly higher ($p < 0.001$) than the cells incubated with only DMEM. The 0.1 mM ACCA HG DMEM samples resulted in an increase ($p < 0.02$) of lactate release to a value of 5.4 ± 0.1 pmol/cell. Elevated concentrations of ACCA, 0.5 and 1.0 mM, resulted in no statistical change compared to the 0 mM ACCA samples. The higher concentrations of ACCA administered, 2.0 and 5.0 mM, resulted a decrease ($p < 0.02$) in the amount of lactate released from the bPAECs with values of 4.35 ± 0.04 and 3.22 ± 0.08 pmol/cell, respectively.

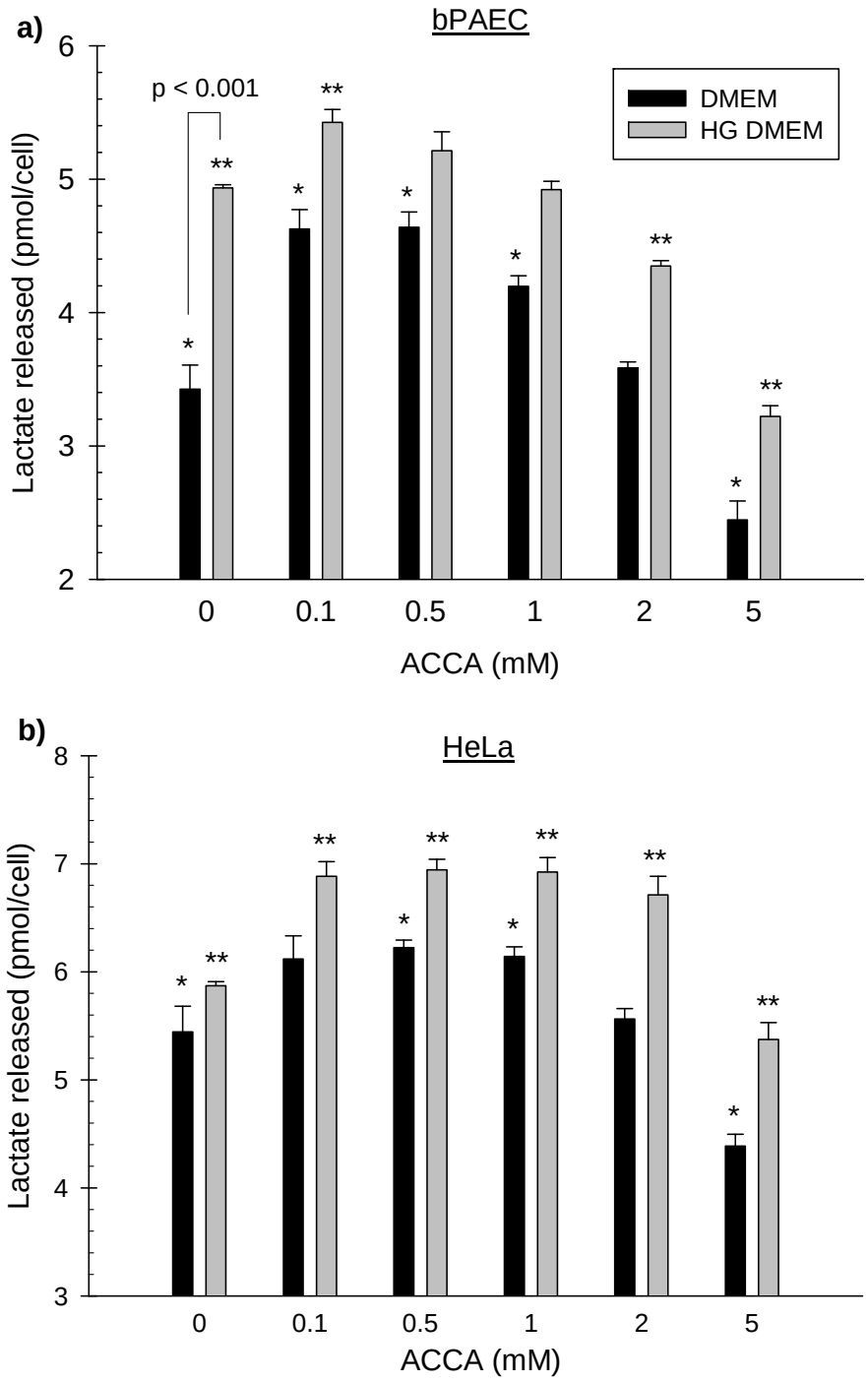

Figure 4.12 – Lactate released from bPAECs (a) and HeLa cells (b) following an 18 hour incubation with varying concentrations of the monocarboxylate transporter (MCT) inhibitor ACCA. The error bars represent the standard error of the mean for n = 4. Statistically significant differences from the 0 mM ACCA samples are indicated with either *$p < 0.05$ for the DMEM samples or **$p < 0.04$ for the HG DMEM samples.

The lactate released from the cultured HeLa cells incubated with ACCA followed similar trends to those of the bPAEC results (Figure 4.12). The samples incubated in DMEM with no ACCA resulted in the release of 5.4 ± 0.2 pmol/cell. There was no observed change in lactate released with an ACCA concentration of 0.1 mM. The samples that were incubated with 0.5 and 1.0 mM ACCA resulted in increased ($p < 0.05$) lactate release values of 6.22 ± 0.07 and 6.14 ± 0.09 pmol/cell, respectively. The 2.0 mM ACCA samples were similar to the 0.0 mM values, while the 5.0 mM ACCA concentration sample resulted in an overall decrease ($p < 0.05$) in the lactate release with an amount of 4.4 ± 0.1 pmol/cell.

The lactate released by the HeLa samples incubated in HG DMEM and ACCA followed a similar trend to the HeLa cells in DMEM. The lactate release from the HeLa cells with no ACCA was similar to the DMEM sample with no ACCA with a value of 5.87 ± 0.04 pmol/cell. Increased ($p < 0.02$) lactate levels were measured from 6.9 ± 0.1 pmol/cell through 6.7 ± 0.2 pmol/cell as the concentration of ACCA was increased from 0.1 to 2.0 mM, respectively. The level of lactate that was released from the HeLa cells incubated with 5.0 mM ACCA was lower ($p < 0.05$) than the sample containing no ACCA, as was the case with the DMEM sample. The value of lactate released by the HeLa cells incubated with HG DMEM and 5.0 mM ACCA was measured to be 5.4 ± 0.2 pmol/cell.

4.5.5.2 Glucose uptake

The glucose uptake by bPAECs and HeLa cells incubated with different concentrations of ACCA was determined by applying the glucose assay described earlier (4.4.9). The glucose uptake values are provided in Figure 4.13. Incubation of bPAECs with DMEM for 18 hours resulted in an uptake of 2.2 ± 0.2 pmol/cell. The addition of each experimental concentration of

ACCA resulted in a significant increase in the amount of glucose taken in by the endothelial cells. 0.1 mM through 2.0 mM ACCA resulted in similar increases in glucose uptake between 3.4 ± 0.2 and 3.08 ± 0.03 pmol/cell, respectively. 5.0 mM ACCA caused an increase in glucose uptake, 2.7 ± 0.2 pmol/cell, compared to the 0.0 mM ACCA samples, but was significantly lower than the glucose uptake at 0.1 mM ACCA.

bPAECs incubated in HG DMEM that contained no ACCA consumed glucose at a rate of 2.3 ± 0.3 pmol/cell. Incubation with ACCA ranging between 0.1 and 1.0 mM resulted in increased glucose uptake to 3.7 ± 0.3 and 4.1 ± 0.2 pmol/cell respectively. Concentrations of ACCA above 1.0 mM did not stimulate an increase in glucose uptake compared to the 0.0 mM ACCA samples.

The glucose transported into HeLa cells with increasing concentrations of ACCA followed trends similar to those of the bPAECs (Figure 4.13). The basal glucose uptake of the HeLa cells in DMEM was 3.5 ± 0.1 pmol/cell. Concentrations of ACCA up to and including 2.0 mM resulted in an increase ($p < 0.01$) of glucose uptake with values of 4.54 ± 0.07 pmol/cell at 0.1 mM, 5.16 ± 0.01 pmol/cell at 1.0 mM, and 5.00 ± 0.04 pmol/cell with 2.0 mM ACCA. 5.0 mM ACCA resulted in the glucose uptake values returning back to near the basal levels at 3.70 ± 0.04 pmol/cell.

4.5.6 Influence of extracellular pyruvate on glucose metabolism of endothelial and HeLa cells

The lactate and glucose assays were applied to monitor the glucose uptake and metabolism into lactate, and how both were affected by the presence or absence of pyruvate.

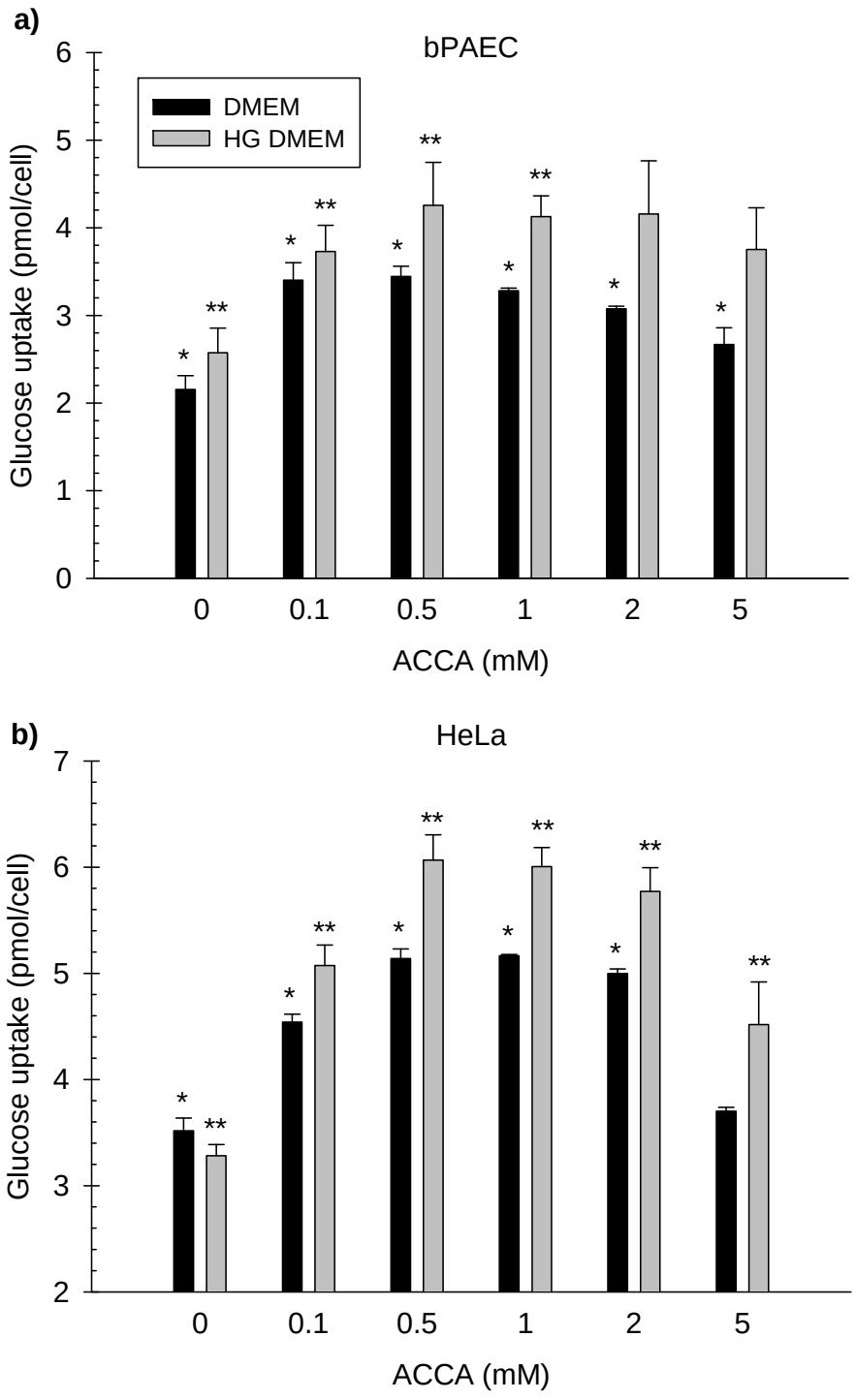

Figure 4.13 – Glucose uptake by bPAECs (a) and HeLa cells (b) following an 18 hour incubation with varying concentrations of the monocarboxylate transporter (MCT) inhibitor ACCA. The error bars represent the standard error of the mean for n = 4. Significant differences in the glucose uptake, when compared to the respective samples containing no ACCA, are indicated with *$p < 0.01$ or **$p < 0.05$ for both cell types.

Both cell types, bPAECs and HeLa cells, were incubated for 18 hours in either DMEM or HG DMEM that either contained or did not contain sodium pyruvate. The lactate release and glucose consumption data are illustrated in Figures 4.14 and 4.15, respectively.

4.5.6.1 Lactate release

bPAECs incubated in DMEM with and without pyruvate released similar levels of lactate at 3.58 ± 0.09 and 3.4 ± 0.2 pmol/cell, respectively. The amount of lactate released was significantly higher ($p < 0.001$) than the corresponding DMEM samples with regards to the when the same bPAECs were incubated with HG DMEM, also without/with pyruvate. The HG DMEM sample with no pyruvate had a lactate release value of 4.7 ± 0.1 pmol/cell, while the HG DMEM sample containing pyruvate resulted in a lactate value of 4.93 ± 0.02 pmol/cell.

HeLa cells incubated in the same DMEM samples that either had, or did not have, pyruvate added to the media resulted in extracellular lactate values that were significantly higher ($p < 0.001$) than their respective bPAEC samples. For instance, the HeLa cells incubated in DMEM without pyruvate resulted in a lactate released value of 5.9 ± 0.1 pmol/cell, while the cells with pyruvate released 5.4 ± 0.2 pmol/cell. There were similar outcomes with the HeLa incubated with HG DMEM with or without pyruvate. Both values were higher than the corresponding bPAEC samples incubated with HG DMEM. The HeLa cells incubated in HG DMEM with no pyruvate resulted in a lactate release of 6.52 ± 0.09 pmol/cell while the samples containing pyruvate was significantly lower ($p < 0.02$) with a value 5.87 ± 0.04 pmol/cell.

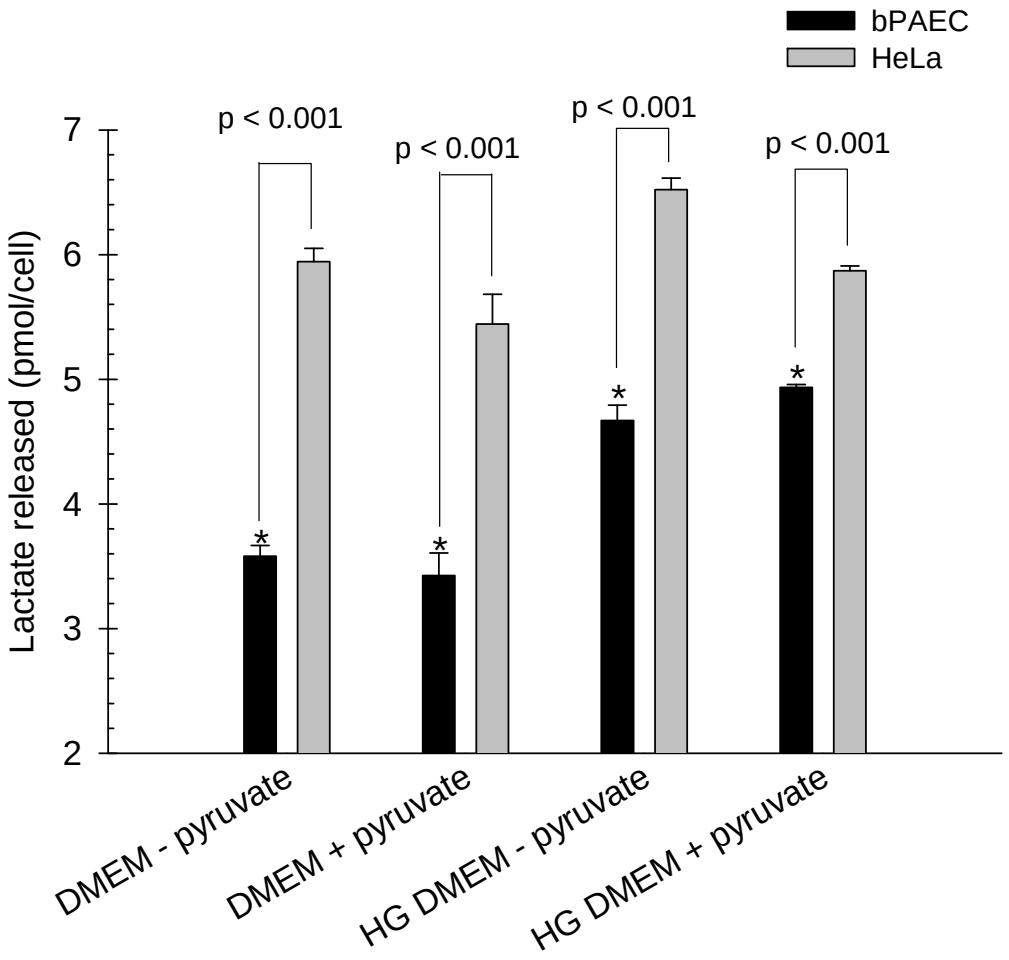

Figure 4.14 – Data illustrating the influence that extracellular pyruvate has on the lactate production of bPAEC (black bars) and HeLa cells (Gray bars). The extracellular lactate was quantified and expressed as the lactate released from each cell following incubation with (+) or without (-) pyruvate in either DMEM or HG DMEM environments. The error bars represent the standard error of the mean for n = 4. The significant differences and corresponding p-values between the bPAEC and HeLa cell lactate release is demonstrated with connecting lines, while the significance between the different bPAEC samples is shown with *$p < 0.001$.

4.5.6.2 Glucose uptake

The bPAECs incubated in DMEM with or without pyruvate transported nearly identical amounts of glucose at 2.2 ± 0.2 and 2.2 ± 0.1 pmol/cell respectively. The glucose taken in by the cells incubated with HG DMEM and no pyruvate was significantly higher ($p < 0.001$) than the DMEM pyruvate free samples with a value of 3.6 ± 0.1 pmol/cell. The HG DMEM sample that had pyruvate present resulted in a glucose uptake measurement of 2.6 ± 0.3 pmol/cell that was statistically equivalent to the DMEM samples that contained pyruvate but lower ($p < 0.02$) than the pyruvate free HG DMEM sample.

The glucose uptake by the HeLa cells has a different trend when compared to the bPAEC results. The samples containing pyruvate resulted in similar values regardless of the extracellular glucose concentration. The DMEM and HG DMEM samples that contained pyruvate resulted in glucose uptake values of 3.5 ± 0.1 and 3.3 ± 0.1 pmol/cell, respectively. The samples that were deprived of the sodium pyruvate resulted in the HeLa cell glucose uptake values that were both significantly higher ($p < 0.01$) than their respective samples that contained pyruvate. The DMEM sample that had no pyruvate resulted in a glucose uptake value of 4.26 ± 0.05 pmol/cell and the HG DMEM sample with no pyruvate had a glucose uptake value of 4.08 ± 0.04 pmol/cell.

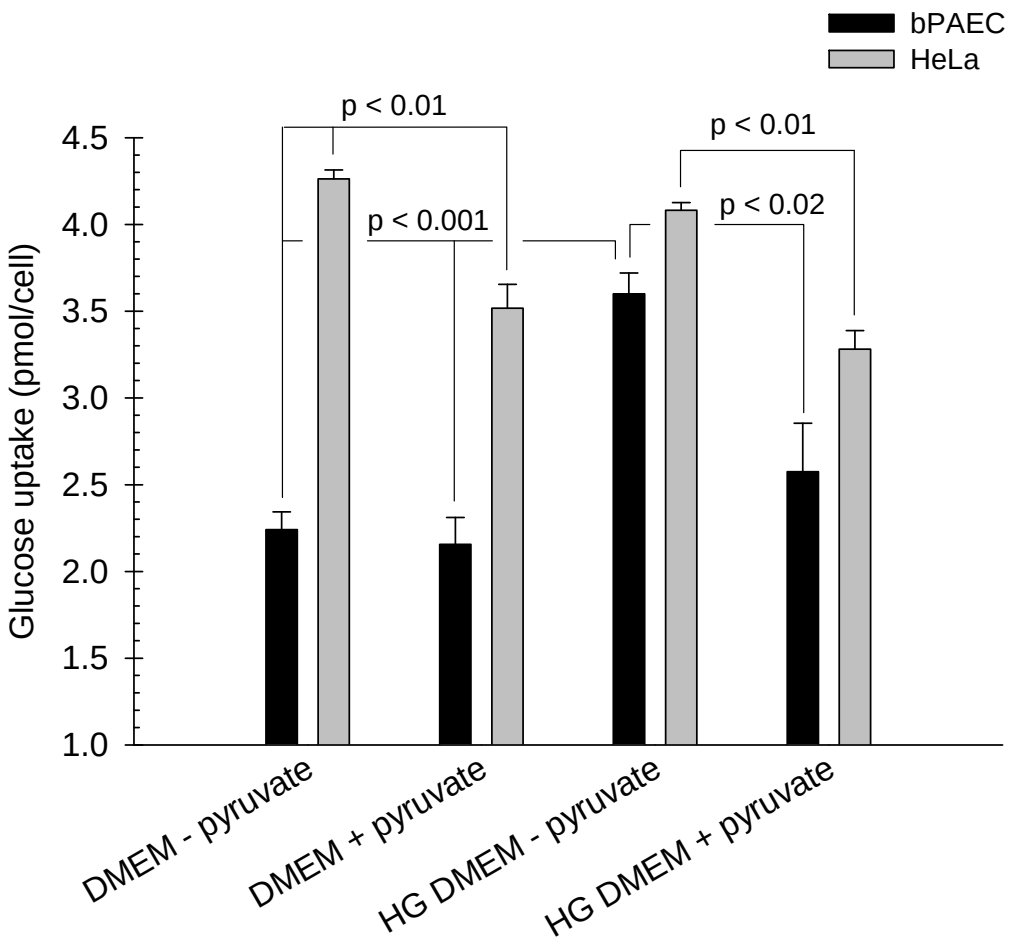

Figure 4.15 – Data illustrating the influence that extracellular pyruvate has on the rates of glucose uptake in bPAECs (black bars) and HeLa cells (gray bars). The extracellular glucose was quantified and subtracted from the glucose in the media, providing the amount of glucose taken in by the cell following incubation with (+) or without (-) pyruvate in either DMEM or HG DMEM environments. The error bars represent the standard error of the mean for n = 4. The significant differences between samples are indicated with connecting lines and accompanied with corresponding (p-values).

4.6 Discussion

Metformin has long been used to treat hyperglycemic conditions found in type 2 diabetics.[48, 49] The mechanism behind metformin's actions remained unknown until recently. Within the last ten years, there have been reports indicating that metformin acts by activating AMPK,[17, 20, 50, 51] one of the significant contributors in regulating cellular energy production and consumption. The metabolic impact of AMPK activation (specifically with metformin and AICAR) on the endothelium metabolism has not been studied extensively, while the activation of AMPK and the metabolic responses that follow have been monitored in multiple different cell types.[18-20]

The metformin induced lactate release from the bPAECs discussed earlier in Chapter 3 needed to be reconsidered and reevaluated. Firstly, the experiments presented in Chapter 3 that examined the lactate release from bPAECs were not considering the idea that there might have been different amounts of cells present in each set of plates. Thereby, different numbers of cells would change the total amount of lactate released into the supernatant (extracellular concentration), while the quantity released from each cell would have remained the same. Therefore, determining the amount of lactate released from each cell, rather than measuring the total lactate, produced a more reproducible set of results. The lactic acid assay enzyme solution was also modified to contain the glutamic-pyruvic transaminase enzyme, as the pyruvate present in the DMEM has the ability to affect the conversion of NAD^+ into NADH.

The results measuring the lactate released from the bPAECs following metformin administration, and applying the modified lactic acid assay, were similar to those found in

studies evaluating heart muscles and metformin treatment.[24] There was an elevated lactate concentration measured extracellularly as the metformin concentration was increased. The elevated lactate levels correlated to an increased glucose uptake as well. Two molecules of pyruvate are produced for each glucose molecule metabolized. At lower concentrations of metformin (0 and 0.5 mM) in the DMEM samples, approximately 2/3 of the glucose taken in was converted into lactate. At the higher concentrations (1 mM and higher), over 90% of the glucose taken in was converted into lactate. At points 2 mM and above, there was more lactate being produced that theoretically could be generated based on the amount of glucose taken in. The later studies show that pyruvate can be utilized rather than glucose for energy production which is used to explain the elevated lactate levels.

The proposed mechanism of metformin's action (AMPK activation and/or mitochondrial inhibition) is different than what is observed following the administration of with other known activators of AMPK such as AICAR. Therefore, it is likely that metformin does not act on AMPK directly.

The findings reported here regarding the AICAR activation of AMPK agree with the earlier reports that indicate AICAR caused a decrease in glucose uptake in human umbilical vein endothelial cells as well as a decreased lactate production.[16] The results were similar even though the two cell types were obtained from different sources (human and bovine). The activation of AMPK via metformin appears to generate an opposite effect metabolically as there are increased glucose uptake and lactate measurements. Metformin appears to cause the endothelial cells to metabolize the increased glucose uptake in more of an anaerobic fashion, that is to say a higher rate of glycolysis. This finding is also supported in multiple reports suggesting that metformin decreases the reactive oxygen species (ROS) generated during oxidative

phorphorylation and the final steps of the electron transport chain (Figure 1.5).[52, 53] The decrease in ROS can be interpreted as a decrease in the oxidative phosphorylation fluxes. The increased glycolytic rates caused by metformin are also supported by the previously discussed risks for developing lactic acidosis for diabetics undergoing metformin therapy.[54-57]

The increased lactate production and subsequent release from the bPAECs treated with metformin led to the hypothesis that the intracellular pH of the cells would decrease. The results obtained by the application of the intracellular pH probe BCECF suggests that the intracellular pH decreases with increasing metformin concentrations and increasing extracellular lactate levels. Such lowering of cytosolic pH due to an increased influx of lactate upon the addition of solutions containing said lactate has been observed in corneal epithelial cells and oocytes.[30, 44] However, the ^{14}C-glucose studies suggest that as the levels of extracellular lactate increase due to increasing metformin concentrations, there is less of the intracellular radiolabeled material that remains inside the cell. This can suggest that at higher concentrations of metformin, more of the glucose is converted anaerobically into lactate and removed from the cell. The removal of each lactate or pyruvate molecule would result in the transport of a proton (H^+) to the intracellular space because the MCT1 is a proton-coupled exchanger. This increased production of lactate, and the influx of H^+ ions would lead to the observed decreased intracellular pH levels for both glucose concentrations.

The difference in intracellular pH changes between the two glucose conditions can be explained by some of the pyruvate results. The intracellular pH measurements of the high glucose samples were slightly higher (less acidic) than the corresponding low glucose samples

with the same metformin concentration. This was interesting because more lactate was produced in the high glucose samples. It was hypothesized that more lactate released would result in an increased proton transfer into the cell, thereby lower intracellular pH. The glucose uptake results by the bPAECs with pyruvate in the media compared to no pyruvate suggests that in high glucose environments, the cells take in pyruvate to provide energy while producing lactate. The transport of pyruvate from the extracellular space into the cell requires the expulsion of H^+ ions, lowering the overall concentration of H^+ in the cell, thereby increasing the pH.

Similar results regarding lactate transport from cells were found to what was reported earlier through inhibition of the MCT by using a-Cyano-4-hydroxycinnamic Acid (ACCA). The studies reported here examined the excretion of lactate while previous studies primarily examined the transport of lactate into the cell, specifically the endothelial cells and HeLa cells,[32, 33, 58] The reported value of ACCA required to decrease lactate uptake into rat muscle is 5 mM.[59] The same 5 mM ACCA used in the studies presented here resulted in the lowest lactate release, compared to all other tested ACCA concentrations, from both the bPAECs and HeLa cells. The decreased value was often significantly lower than the cells containing no ACCA, suggesting that 5 mM may indeed be approaching the concentration for both bPAEC and HeLa cells required to significantly inhibit the transport.

Initially, it was hypothesized that the inhibition of MCT with increasing concentrations of ACCA would result in decreasing values of lactate released from the cells. However, the lactate measurements appeared to be opposite than expected, with values increasing as the ACCA is added. The corresponding glucose uptake measurements suggests that while the lactate release and uptake are inhibited due to the presence of the ACCA, the cells are required to take in more

glucose to compensate for the decreased access to the extracellular lactate or pyruvate that could be used for subsequent energy production.

Certain similarities and differences in the physiologies were observed when comparing the overall glucose metabolism between the two cell types, the non-cancerous bPAECs and the cancerous HeLa cell line. It was hypothesized that the lactate released from the HeLa cells would be greater than the bPAECs as cancer cells tend to undergo elevated rates of glycolysis to fulfill their high energy demands,[60]. The measured lactate release on a per cell basis suggested that very hypothesis. This increased lactate has a correlation with the clinical outcome of a variety of human cancers.[61, 62] It is also thought that the lactate released from cancerous cells can act as signaling molecules to drive angiogenesis in the endothelial cells.[58]

The changes in lactate production under normal and hyperglycemic conditions were somewhat different between the two cell types after measuring the glucose metabolism. The bPAEC studies resulted in a much larger difference in the amount of lactate produced in the normal glucose environment compared to the high glucose environment than was observed in the HeLa cell samples. It has been shown that normal vascular endothelial cells are able to change the prevalence of glucose transporters on their plasma membrane to compensate for the increased glucose uptake, potentially avoiding cellular damage.[63, 64] Not only do the HeLa cells produce lactate at a higher rate, but they produce roughly the same amount of lactate regardless of the extracellular glucose content. These two comparisons can suggest that normal, healthy cells will change how they transport and metabolize glucose based on the sugar levels while the cancerous cells will maintain their elevated rate of glycolysis, presumably to meet their high energy demands.

An additional energy source that was studied in terms of how it affected glucose uptake and metabolism in normal and cancerous cells was pyruvate. The findings of the bPAEC studies demonstrate that the lactate released and the glucose uptake in the DMEM samples was similar whether there was pyruvate present. This suggests that the cells need to produce a certain amount of energy/ATP and will use whatever source of energy is available to them. The results from the high glucose DMEM samples are interesting as it suggests that the bPAECs first will utilize the pyruvate available before the glucose is consumed. The pyruvate is likely the reason for this result given that the amount of lactate released is greater in the high glucose samples containing pyruvate than it is for the normal glucose samples also containing pyruvate while the glucose uptake values are essentially the same. This is also supported in the findings that bPAECs incubated with high glucose DMEM and no pyruvate have a higher influx of glucose compared to the pyruvate containing sample.

The potential dependence on pyruvate supports some of the previously reported studies that evaluate the antioxidant capabilities of pyruvate, especially in hyperglycemic conditions.[40, 41, 43] The extracellular pyruvate can be brought into the cell and used for increased ATP production, while the glucose brought into the cell can be sent through the pentose phosphate pathway, regenerating glutathione levels. The glucose taken in by the cell will have to be used for both generating ATP and regenerating glutathione through the pentose phosphate pathway if the extracellular pyruvate levels are low in combination with a high glucose environment. The shared glucose distribution may not be enough to overcome the oxidative stress put on the cells under hyperglycemic environments.

There were similar results when evaluating the glucose uptake and lactate production from the HeLa cells with or without the presence of pyruvate. There were similar values and

differences in both metabolite measurements, again suggesting that the overall metabolism of the cancerous cells is the same regardless of glucose availability. The HeLa cells in either low or high glucose conditions appeared to consume pyruvate instead of glucose in generating lactate, supporting the ideas that cancer cells may rely heavily on surrounding cells to provide sources of energy other than glucose.[39, 65] The results from the bPAEC studies suggest that under hyperglycemic conditions, normal cells can alter their metabolism to more resemble cancer cells in terms of lactate production and glucose consumption.

In summary, the findings suggest that the endothelial cell metabolism is able to be altered by both metformin addition and by altering the amount of available sources of energy, namely glucose and pyruvate. The presence of metformin appears to result in a decreased intracellular pH through increased lactate production and release from the cell. The studies examining the effect of AICAR on endothelial metabolism suggests that metformin does not act directly on AMPK, but rather stimulates metabolic pathways that can lead to the appearance of the activation of AMPK. Lastly, the studies implementing the ACCA, pyruvate, and hyperglycemic conditions indicate the metabolic similarities that healthy and cancerous cells share under certain conditions. The endothelial and HeLa cells' lactate release was both influenced in similar means after the administration of ACCA. In hyperglycemic conditions, the glucose uptake in the endothelial cells with and without pyruvate resembled the same trend that the cancerous cells exhibited, identifying a priority in the preference of energy generating molecules. Finally, the lactate released from the endothelial cells in hyperglycemic conditions increased to levels that were nearly those of the cancerous cells, suggesting an increase in the anaerobic respiration.

REFERENCES

REFERENCES

1. Hardie, D. G.; Carling, D.; Carlson, M., The AMP-activated/SNF1 protein kinase subfamily: metabolic sensors of the eukaryotic cell? *Annu. Rev. Biochem.* **1998,** 67, 821-855.

2. Kemp, B. E.; Stapleton, D.; Campbell, D. J.; Chen, Z. P.; Murthy, S.; Walter, M.; Gupta, A.; Adams, J. J.; Katsis, F.; van Denderen, B.; Jennings, I. G.; Iseli, T.; Michell, B. J.; Witters, L. A., AMP-activated protein kinase, super metabolic regulator. *Biochem. Soc. Trans.* **2003,** 31, (Pt 1), 162-8.

3. Winder, W. W.; Hardie, D. G., AMP-activated protein kinase, a metabolic master switch: possible roles in type 2 diabetes. *Am. J. Physiol.* **1999,** 277, (1 Pt 1), E1-10.

4. Kemp, B. E.; Mitchelhill, K. I.; Stapleton, D.; Michell, B. J.; Chen, Z. P.; Witters, L. A., Dealing with energy demand: the AMP-activated protein kinase. *Trends Biochem. Sci.* **1999,** 24, (1), 22-5.

5. Hardie, D. G., AMPK and SNF1: Snuffing Out Stress. *Cell Metab.* **2007,** 6, (5), 339-40.

6. Kahn, B. B.; Alquier, T.; Carling, D.; Hardie, D. G., AMP-activated protein kinase: ancient energy gauge provides clues to modern understanding of metabolism. *Cell Metab.* **2005,** 1, (1), 15-25.

7. Ruderman, N. B.; Saha, A. K.; Vavvas, D.; Witters, L. A., Malonyl-CoA, fuel sensing, and insulin resistance. *Am. J. Physiol.* **1999,** 276, (1 Pt 1), E1-E18.

8. Ruderman, N. B.; Cacicedo, J. M.; Itani, S.; Yagihashi, N.; Saha, A. K.; Ye, J. M.; Chen, K.; Zou, M.; Carling, D.; Boden, G.; Cohen, R. A.; Keaney, J.; Kraegen, E. W.; Ido, Y., Malonyl-CoA and AMP-activated protein kinase (AMPK): possible links between insulin resistance in muscle and early endothelial cell damage in diabetes. *Biochem. Soc. Trans.* **2003,** 31, (Pt 1), 202-6.

9. Davies, S. P.; Helps, N. R.; Cohen, P. T.; Hardie, D. G., 5'-AMP inhibits dephosphorylation, as well as promoting phosphorylation, of the AMP-activated protein kinase. Studies using bacterially expressed human protein phosphatase-2C alpha and native bovine protein phosphatase-2AC. *FEBS Lett* **1995,** 377, (3), 421-5.

10. Hawley, S. A.; Davison, M.; Woods, A.; Davies, S. P.; Beri, R. K.; Carling, D.; Hardie, D. G., Characterization of the AMP-activated protein kinase kinase from rat liver and identification of threonine 172 as the major site at which it phosphorylates AMP-activated protein kinase. *J. Biol. Chem.* **1996,** 271, (44), 27879-87.

11. Stein, S. C.; Woods, A.; Jones, N. A.; Davison, M. D.; Carling, D., The regulation of AMP-activated protein kinase by phosphorylation. *Biochem J.* **2000,** 345 Pt 3, 437-43.

12. Hawley, S. A.; Selbert, M. A.; Goldstein, E. G.; Edelman, A. M.; Carling, D.; Hardie, D. G., 5'-AMP activates the AMP-activated protein kinase cascade, and Ca2+/calmodulin activates the calmodulin-dependent protein kinase I cascade, via three independent mechanisms. *J. Biol. Chem.* **1995,** 270, (45), 27186-91.

13. Hardie, D. G., The AMP-activated protein kinase cascade: the key sensor of cellular energy status. *Endocrinology* **2003,** 144, (12), 5179-5183.

14. Hardie, D. G., Regulation of fatty acid synthesis via phosphorylation of acetyl-CoA carboxylase. *Prog. Lipid Res.* **1989,** 28, (2), 117-46.

15. Corton, J. M.; Gillespie, J. G.; Hawley, S. A.; Hardie, D. G., 5-aminoimidazole-4-carboxamide ribonucleoside. A specific method for activating AMP-activated protein kinase in intact cells? *Eur. J. Biochem.* **1995,** 229, (2), 558-65.

16. Dagher, Z.; Ruderman, N.; Tornheim, K.; Ido, Y., The effect of AMP-activated protein kinase and its activator AICAR on the metabolism of human umbilical vein endothelial cells. *Biochem. Biophys. Res. Commun.* **1999,** 265, (1), 112-5.

17. Zhou, G.; Myers, R.; Li, Y.; Chen, Y.; Shen, X.; Fenyk-Melody, J.; Wu, M.; Ventre, J.; Doebber, T.; Fujii, N.; Musi, N.; Hirshman, M. F.; Goodyear, L. J.; Moller, D. E., Role of AMP-activated protein kinase in mechanism of metformin action. *J. Clin. Invest.* **2001,** 108, (8), 1167-74.

18. Zhang, L.; He, H.; Balschi, J. A., Metformin and phenformin activate AMP-activated protein kinase in the heart by increasing cytosolic AMP concentration. *Am. J. Physiol. Heart Circ. Physiol.* **2007,** 293, (1), H457-66.

19. Zakikhani, M.; Dowling, R. J.; Sonenberg, N.; Pollak, M. N., The effects of adiponectin and metformin on prostate and colon neoplasia involve activation of AMP-activated protein kinase. *Cancer Prev Res (Phila)* **2008,** 1, (5), 369-75.

20. Musi, N.; Hirshman, M. F.; Nygren, J.; Svanfeldt, M.; Bavenholm, P.; Rooyackers, O.; Zhou, G.; Williamson, J. M.; Ljunqvist, O.; Efendic, S.; Moller, D. E.; Thorell, A.; Goodyear, L. J., Metformin increases AMP-activated protein kinase activity in skeletal muscle of subjects with type 2 diabetes. *Diabetes* **2002,** 51, (7), 2074-81.

21. Zou, M. H.; Kirkpatrick, S. S.; Davis, B. J.; Nelson, J. S.; Wiles, W. G. t.; Schlattner, U.; Neumann, D.; Brownlee, M.; Freeman, M. B.; Goldman, M. H., Activation of the AMP-activated protein kinase by the anti-diabetic drug metformin in vivo. Role of mitochondrial reactive nitrogen species. *J. Biol. Chem.* **2004,** 279, (42), 43940-51.

22. Fryer, L. G.; Parbu-Patel, A.; Carling, D., The Anti-diabetic drugs rosiglitazone and metformin stimulate AMP-activated protein kinase through distinct signaling pathways. *J. Biol. Chem.* **2002,** 277, (28), 25226-32.

23. Hawley, S. A.; Gadalla, A. E.; Olsen, G. S.; Hardie, D. G., The antidiabetic drug metformin activates the AMP-activated protein kinase cascade via an adenine nucleotide-independent mechanism. *Diabetes* **2002,** 51, (8), 2420-5.

24. An, D.; Kewalramani, G.; Chan, J. K.; Qi, D.; Ghosh, S.; Pulinilkunnil, T.; Abrahani, A.; Innis, S. M.; Rodrigues, B., Metformin influences cardiomyocyte cell death by pathways that are dependent and independent of caspase-3. *Diabetologia* **2006,** 49, (9), 2174-84.

25. Morris, M. E.; Felmlee, M. A., Overview of the proton-coupled MCT (SLC16A) family of transporters: characterization, function and role in the transport of the drug of abuse gamma-hydroxybutyric acid. *AAPS J* **2008,** 10, (2), 311-21.

26. Halestrap, A. P.; Price, N. T., The proton-linked monocarboxylate transporter (MCT) family: structure, function and regulation. *Biochem J.* **1999,** 343 Pt 2, 281-99.

27. Jackson, V. N.; Halestrap, A. P., The kinetics, substrate, and inhibitor specificity of the monocarboxylate (lactate) transporter of rat liver cells determined using the fluorescent intracellular pH indicator, 2',7'-bis(carboxyethyl)-5(6)-carboxyfluorescein. *J. Biol. Chem.* **1996,** 271, (2), 861-8.

28. Price, N. T.; Jackson, V. N.; Halestrap, A. P., Cloning and sequencing of four new mammalian monocarboxylate transporter (MCT) homologues confirms the existence of a transporter family with an ancient past. *Biochem J.* **1998,** 329 (Pt 2), 321-8.

29. Poole, R. C.; Halestrap, A. P., Transport of lactate and other monocarboxylates across mammalian plasma membranes. *Am. J. Physiol.* **1993,** 264, (4 Pt 1), C761-82.

30. Broer, S.; Schneider, H. P.; Broer, A.; Rahman, B.; Hamprecht, B.; Deitmer, J. W., Characterization of the monocarboxylate transporter 1 expressed in Xenopus laevis oocytes by changes in cytosolic pH. *Biochem J.* **1998,** 333 (Pt 1), 167-74.

31. Halestrap, A. P.; Denton, R. M., Specific inhibition of pyruvate transport in rat liver mitochondria and human erythrocytes by alpha-cyano-4-hydroxycinnamate. *Biochem J.* **1974,** 138, (2), 313-6.

32. Cheeti, S.; Warrier, B. K.; Lee, C. H., The role of monocarboxylate transporters in uptake of lactic acid in HeLa cells. *Int. J. Pharm.* **2006,** 325, (1-2), 48-54.

33. Cheeti, S.; Lee, C. H., The involvement of intracellular calcium in the MCT-mediated uptake of lactic acid by HeLa cells. *Mol. Pharm.* **2010,** 7, (1), 169-76.

34. Pinheiro, C.; Reis, R. M.; Ricardo, S.; Longatto-Filho, A.; Schmitt, F.; Baltazar, F., Expression of monocarboxylate transporters 1, 2, and 4 in human tumours and their association with CD147 and CD44. *J. Biomed. Biotechnol.* **2010,** 2010, 427694.

35. Izumi, H.; Torigoe, T.; Ishiguchi, H.; Uramoto, H.; Yoshida, Y.; Tanabe, M.; Ise, T.; Murakami, T.; Yoshida, T.; Nomoto, M.; Kohno, K., Cellular pH regulators: potentially

promising molecular targets for cancer chemotherapy. *Cancer Treat. Rev.* **2003,** 29, (6), 541-9.

36. Wahl, M. L.; Owen, J. A.; Burd, R.; Herlands, R. A.; Nogami, S. S.; Rodeck, U.; Berd, D.; Leeper, D. B.; Owen, C. S., Regulation of intracellular pH in human melanoma: potential therapeutic implications. *Mol. Cancer Ther.* **2002,** 1, (8), 617-28.

37. Gatenby, R. A.; Gillies, R. J., Why do cancers have high aerobic glycolysis? *Nature Rev. Cancer* **2004,** 4, (11), 891-899.

38. Fang, J. S.; Gillies, R. D.; Gatenby, R. A., Adaptation to hypoxia and acidosis in carcinogenesis and tumor progression. *Semin. Cancer Biol.* **2008,** 18, (5), 330-7.

39. Koukourakis, M. I.; Giatromanolaki, A.; Harris, A. L.; Sivridis, E., Comparison of metabolic pathways between cancer cells and stromal cells in colorectal carcinomas: a metabolic survival role for tumor-associated stroma. *Cancer Res.* **2006,** 66, (2), 632-7.

40. Chung, S. J.; Lee, S. H.; Lee, Y. J.; Park, H. S.; Bunger, R.; Kang, Y. H., Pyruvate protection against endothelial cytotoxicity induced by blockade of glucose uptake. *J. Biochem. Mol. Biol.* **2004,** 37, (2), 239-45.

41. Herz, H.; Blake, D. R.; Grootveld, M., Multicomponent investigations of the hydrogen peroxide- and hydroxyl radical-scavenging antioxidant capacities of biofluids: the roles of endogenous pyruvate and lactate. Relevance to inflammatory joint diseases. *Free Radic. Res.* **1997,** 26, (1), 19-35.

42. Kang, Y. H.; Park, S. H.; Lee, Y. J.; Kang, J. S.; Kang, I. J.; Shin, H. K.; Park, J. H.; Bunger, R., Antioxidant alpha-keto-carboxylate pyruvate protects low-density lipoprotein and atherogenic macrophages. *Free Radic. Res.* **2002,** 36, (8), 905-14.

43. Kashiwagi, A.; Nishio, Y.; Asahina, T.; Ikebuchi, M.; Harada, N.; Tanaka, Y.; Takahara, N.; Taki, H.; Obata, T.; Hidaka, H.; Saeki, Y.; Kikkawa, R., Pyruvate improves deleterious effects of high glucose on activation of pentose phosphate pathway and glutathione redox cycle in endothelial cells. *Diabetes* **1997,** 46, (12), 2088-95.

44. Grant, R. L.; Acosta, D., Ratiometric measurement of intracellular pH of cultured cells with BCECF in a fluorescence multi-well plate reader. *In Vitro Cell Dev. Biol. Anim.* **1997,** 33, (4), 256-60.

45. Liddell, J. R.; Zwingmann, C.; Schmidt, M. M.; Thiessen, A.; Leibfritz, D.; Robinson, S. R.; Dringen, R., Sustained hydrogen peroxide stress decreases lactate production by cultured astrocytes. *J. Neurosci. Res.* **2009,** 87, (12), 2696-708.

46. Dringen, R.; Hamprecht, B., Differences in glycogen metabolism in astroglia-rich primary cultures and sorbitol-selected astroglial cultures derived from mouse brain. *Glia* **1993,** 8, (3), 143-9.

47. Dringen, R.; Gebhardt, R.; Hamprecht, B., Glycogen in astrocytes: possible function as lactate supply for neighboring cells. *Brain Res.* **1993,** 623, (2), 208-14.

48. Effect of intensive blood-glucose control with metformin on complications in overweight patients with type 2 diabetes (UKPDS 34). UK Prospective Diabetes Study (UKPDS) Group. *Lancet* **1998,** 352, (9131), 854-65.

49. Abbasi, F.; Chu, J. W.; McLaughlin, T.; Lamendola, C.; Leary, E. T.; Reaven, G. M., Effect of metformin treatment on multiple cardiovascular disease risk factors in patients with type 2 diabetes mellitus. *Metabolism* **2004,** 53, (2), 159-64.

50. McCarty, M. F., Chronic activation of AMP-activated kinase as a strategy for slowing aging. *Med. Hypotheses* **2004,** 63, (2), 334-9.

51. Xie, Z.; Dong, Y.; Scholz, R.; Neumann, D.; Zou, M. H., Phosphorylation of LKB1 at serine 428 by protein kinase C-zeta is required for metformin-enhanced activation of the AMP-activated protein kinase in endothelial cells. *Circulation* **2008,** 117, (7), 952-62.

52. Kukidome, D.; Nishikawa, T.; Sonoda, K.; Imoto, K.; Fujisawa, K.; Yano, M.; Motoshima, H.; Taguchi, T.; Matsumura, T.; Araki, E., Activation of AMP-activated protein kinase reduces hyperglycemia-induced mitochondrial reactive oxygen species production and promotes mitochondrial biogenesis in human umbilical vein endothelial cells. *Diabetes* **2006,** 55, (1), 120-7.

53. Ouslimani, N.; Peynet, J.; Bonnefont-Rousselot, D.; Therond, P.; Legrand, A.; Beaudeux, J. L., Metformin decreases intracellular production of reactive oxygen species in aortic endothelial cells. *Metabolism* **2005,** 54, (6), 829-34.

54. Audia, P.; Feinfeld, D. A.; Dubrow, A.; Winchester, J. F., Metformin-induced lactic acidosis and acute pancreatitis precipitated by diuretic, celecoxib, and candesartan-associated acute kidney dysfunction. *Clin. Toxicol. (Phila)* **2008,** 46, (2), 164-6.

55. Bodmer, M.; Meier, C.; Krahenbuhl, S.; Jick, S. S.; Meier, C. R., Metformin, sulfonylureas, or other antidiabetes drugs and the risk of lactic acidosis or hypoglycemia: a nested case-control analysis. *Diabetes Care* **2008,** 31, (11), 2086-2091.

56. Almirall, J.; Briculle, M.; Gonzalez-Clemente, J.-M., Metformin-associated lactic acidosis in type 2 diabetes mellitus: incidence and presentation in common clinical practice. *Nephrol. Dial. Transplant* **2008,** 23, (7), 2436-2438.

57. Runge, S.; Mayerle, J.; Warnke, C.; Robinson, D.; Roser, M.; Felix, S. B.; Friesecke, S., Metformin-associated lactic acidosis in patients with renal impairment solely due to drug accumulation? *Diabetes Obes. Metab.* **2008,** 10, (1), 91-93.

58. Vegran, F.; Boidot, R.; Michiels, C.; Sonveaux, P.; Feron, O., Lactate influx through the endothelial cell monocarboxylate transporter MCT1 supports an NF-kappaB/IL-8 pathway that drives tumor angiogenesis. *Cancer Res.* **2011,** 71, (7), 2550-60.

59. Watt, P. W.; MacLennan, P. A.; Hundal, H. S.; Kuret, C. M.; Rennie, M. J., L(+)-lactate transport in perfused rat skeletal muscle: kinetic characteristics and sensitivity to pH and transport inhibitors. *Biochim. Biophys. Acta* **1988,** 944, (2), 213-22.

60. DeBerardinis, R. J.; Lum, J. J.; Hatzivassiliou, G.; Thompson, C. B., The biology of cancer: metabolic reprogramming fuels cell growth and proliferation. *Cell Metabolism* **2008,** 7, (1), 11-20.

61. Walenta, S.; Schroeder, T.; Mueller-Klieser, W., Lactate in solid malignant tumors: potential basis of a metabolic classification in clinical oncology. *Curr. Med. Chem.* **2004,** 11, (16), 2195-204.

62. Brizel, D. M.; Schroeder, T.; Scher, R. L.; Walenta, S.; Clough, R. W.; Dewhirst, M. W.; Mueller-Klieser, W., Elevated tumor lactate concentrations predict for an increased risk of metastases in head-and-neck cancer. *Int. J. Radiat. Oncol. Biol. Phys.* **2001,** 51, (2), 349-53.

63. Alpert, E.; Gruzman, A.; Riahi, Y.; Blejter, R.; Aharoni, P.; Weisinger, G.; Eckel, J.; Kaiser, N.; Sasson, S., Delayed autoregulation of glucose transport in vascular endothelial cells. *Diabetologia* **2005,** 48, (4), 752-5.

64. Alpert, E.; Gruzman, A.; Totary, H.; Kaiser, N.; Reich, R.; Sasson, S., A natural protective mechanism against hyperglycaemia in vascular endothelial and smooth-muscle cells: role of glucose and 12-hydroxyeicosatetraenoic acid. *Biochem. J.* **2002,** 362, (Pt 2), 413-22.

65. De Wever, O.; Mareel, M., Role of tissue stroma in cancer cell invasion. *J. Pathol.* **2003,** 200, (4), 429-47.

CHAPTER 5: OVERALL CONCLUSIONS AND FUTURE DIRECTIONS

5.1 Conclusions

5.1.1 C-peptide studies

The biomolecule C-peptide was believed to have one significant contribution *in vivo* upon its initial discovery, namely facilitating the folding of the insulin molecule into the proper alignment, after which the C-peptide is cleaved from the insulin molecule and released into the bloodstream. More recent studies have identified C-peptide as a potential therapeutic treatment for those who have type 1 diabetes, with the experimental results indicating improved blood flow, glucose utilization, and nerve function.[1-3] The overall mechanisms behind the improvements in certain complications associated with diabetes, upon the administration of C-peptide, remained largely unexplained.

Recent work involving C-peptide has reported two significant findings regarding the peptide's physiological benefits. There have been reports identifying C-peptide as a direct stimulator of endothelial (nitric oxide) NO production, which is a known vasodilator.[4, 5] There are also reports from the Spence group that show reproducible results suggesting C-peptide is a significant contributor to red blood cell (RBC) metabolism and determinant in vascular control. Increased glucose uptake and ATP release was observed in both healthy RBCs and RBCs obtained from people with diabetes following treatment with C-peptide. Importantly, these results were only measured when C-peptide was in the presence of certain metals.[6-8] Therefore,

inspired by these previous findings regarding C-peptide, the studies discussed earlier in Chapter 2 were designed to observe the effects of metal-activated C-peptide on another vascular cell component, the endothelium.

Endothelial cells primarily utilize the same glucose transporter (GLUT1) that is used by the RBC. Therefore, it was hypothesized that the administration of metal-activated C-peptide would stimulate an increase in glucose uptake into cultured bovine pulmonary artery endothelial cells (bPAECs) that was similar to that observed in the RBCs. It was observed that metal-activated C-peptide stimulated increased glucose transport into the bPAECs. The measurements were performed through the utilization of similar radiolabeled glucose transport protocols used by the Spence group to measure the glucose uptake into the RBC.[6] The results also suggested that the presence of a metal ion, specifically Zn^{2+}, is required for the C-peptide to elicit these effects of increased glucose uptake. This metal-activation of C-peptide is in agreement with the previous findings from the Spence group.[7, 8]

The studies involving C-peptide and insulin in combination agree with other proposed findings that insulin does not have an effect on endothelial glucose transport.[9] The conclusion can be made from these studies and previous findings from the Spence group that metal-activated C-peptide, and not insulin, is a significant contributor to glucose clearance in multiple essential cell types that are found in the vasculature, specifically the RBC and endothelial cells. The studies presented here also suggest that under hyperglycemic conditions, such as those found in diabetes, metal-activated C-peptide interacts less with the endothelial cells and therefore has less of an influence on the glucose uptake.

Previous studies have identified C-peptide as both a direct and indirect stimulus of endothelial NO production, specifically in aortic endothelial cells.[4, 5] It was initially hypothesized that the same metal-activation property stimulates endothelial glucose transport needs to be present in order for C-peptide to stimulate endothelial NO production. However, the results obtained indicate that metal-activated C-peptide does not elicit a direct response in pulmonary artery endothelial cells similar to that which was observed in the aortic endothelial cells. It was demonstrated by Paul Vogel in the Spence Lab at Michigan State University that RBCs treated with metal-activated C-peptide resulted in an increase in bPAEC NO production by combining microfluidic techniques and the findings that C-peptide causes an increased ATP release from the RBCs. These findings suggest that the process by which C-peptide stimulates NO production in the pulmonary artery is RBC mediated.

Summarily, the C-peptide studies presented here promote metal-activated C-peptide as a potential therapeutic treatment for people with type 1 diabetes. The studies reported here indicate that metal-activated C-peptide at physiological or supraphysiological concentrations can potentially reduce blood glucose levels by stimulating an increased glucose uptake into the pulmonary artery endothelial cells, independent of the presence of insulin. It has also been shown to indirectly stimulate the production of the vasodilator NO from the pulmonary artery endothelial cells, through RBC-derived ATP, a known stimulus of endothelial NO.

5.1.2 Metformin studies

The biguanide metformin has long been administered to people with type 2 diabetes in order to aid in regulating blood sugar levels. The underlying mechanism by which metformin acts and reduces blood sugar levels has remained a mystery, similar to C-peptide treatment. There is also an identified risk of developing a potentially fatal condition known as lactic acidosis in people who take metformin and have renal complications.[10] The fasting plasma lactate levels are shown to be increased in people who have type 2 diabetes and take metformin.[11] Studies were performed to identify a potential mechanism explaining metformin's role in this increased lactate production from both the RBC and endothelial cell.

Results show that RBCs incubated in hyperglycemic conditions resulted in less C-peptide interacting with the cells when compared to the C-peptide interacting with RBCs incubated with normal glucose levels, as measured using an ELISA for C-peptide. The addition of metformin to RBC samples in both normal and high glucose environments resulted in increased levels of C-peptide interacting with the RBC. This increased interaction of C-peptide helps explain the increased ATP levels that were released from the metformin treated RBCs obtained from subjects with diabetes.[8] The results showed both increased glucose uptake and lactate release in RBCs that were treated with both metformin and metal-activated C-peptide. The results suggest that metformin facilitates increased interaction of the C-peptide with the RBCs incubated in hyperglycemic conditions, resulting in increased glucose uptake and elevated lactate production and release into the surrounding area. Such a finding illustrates metformin's ability to decrease blood glucose levels found in type 2 diabetes in the presence of metal-activated C-peptide, while

providing evidence of why there is an increased risk for lactic acidosis in people undergoing metformin therapy.

Initial studies examining endothelial cells and metformin suggest that the addition of metformin directly influences the glucose uptake into cultured cells without influencing the GLUT abundance.[12] The findings presented here supported the idea that metformin does cause an increase in glucose transport into endothelial cells indirectly through utilizing a fluorescence based glucose assay while the earlier studies applied the use of radiolabeled glucose to track glucose uptake. However, the previous studies did not examine the outcome of the increased glucose intake.[7, 8]

It was hypothesized that there would also be an increase in lactate production following metformin administration due to the increased glucose consumption by the endothelial cells. It was thought that there would be results with endothelial cells similar to those with RBCs treated with metformin and C-peptide, as there was increased glucose uptake demonstrated earlier by the bPAECs following incubation with metal-activated C-peptide. However, the findings indicated that there was only an increase in lactate production that was dependent on the metformin concentration. This indicates that metformin results in the endothelial cells to take in more glucose, potentially contributing to the observed *in vivo* effect of reducing blood sugar levels in people with type 2 diabetes, while again contributing to the potential risk of developing lactic acidosis due to the increased lactate production.

The increased lactate production by the endothelial cells following metformin administration led to the notion that the intracellular pH would decrease as more lactate was produced. The decreased intracellular pH caused by metformin was confirmed using the BCECF intracellular probe. However, the findings of the ^{14}C-glucose studies suggest that there is less of

the lactate remaining in the cells at higher concentrations of metformin. The intracellular pH studies combined with the ^{14}C-glucose findings suggest that metformin causes a decrease in intracellular pH by increasing lactate production and release that results in an accumulation of protons (H^+). The proton accumulation can be contributed to the proton-coupled mechanism by which the monocarboxylate transporter (MCT1) transports lactate out of the cell.

The mechanism behind metformin's *in vivo* glucose lowering capabilities remained unknown for some time until recent studies have speculated that the drug works through AMP-activated protein kinase (AMPK) activation. AMPK is an important regulator of cellular energy and is activated by increased AMP/ATP ratios. AMPK activation would presumably result in the cell generating ATP through enhanced glycolysis or glucose oxidation rates. The addition of the well established AMPK activator AICAR on endothelial cells in these reported experiments caused a decrease in glucose uptake and lactate production while earlier studies identified increased glucose oxidation (aerobic respiration).[13] These two findings support each other in the activation of AMPK by AICAR, however they do not support the metformin induced AMPK activation hypothesis as metformin caused increases in glucose uptake and lactate production and release. Therefore, it can be concluded that while metformin is suggested to act via AMPK activation, the mechanism behind the activation is significantly different than that of AICAR.

Overall, an expanded contribution that metformin has in regulating blood glucose levels in people with type 2 diabetes has been demonstrated, while also suggesting how metformin treatment can potentially lead to the development of lactic acidosis. The molecule appears to have similar effects on both the RBC and endothelial cell in terms of glucose consumption and lactate production, however the mechanisms appear somewhat different. Metformin does not

appear to act on the RBC by itself. Instead, metal-activated C-peptide combined with metformin stimulated an increase in glucose uptake accompanied by increased lactate release when compared to metal-activated C-peptide alone. This is suggested to be accomplished through increased interactions of the C-peptide with the RBC that is aided by metformin. Conversely, metformin works independently of C-peptide on the endothelium, stimulated both glucose uptake and lactate release in a concentration dependent manner. This mechanism is believed to be stimulated by AMPK activation.

5.1.3 Hyperglycemia studies and comparison between the two cell types

Over 90 years ago, Otto Warburg made the discovery that cancer cells performed higher rates of glycolysis for energy production, even when there was sufficient oxygen present.[14] This metabolic anomaly is appropriately termed aerobic glycolysis or the 'Warburg effect'. Recently, the Warburg effect has received increased attention as the unique metabolism of cancers has become a primary focus of the diagnosis and treatment of the condition.[15-17] This abnormal glucose metabolism, in combination with the observed increased risk to develop cancer for people that have type 2 diabetes or elevated blood glucose levels were the contributing factors to develop the studies presented earlier that evaluated and compared the glucose metabolism of healthy endothelial cells to that of cancerous HeLa cells in normal and hyperglycemic environments.

The changes that occur in healthy endothelial cells indicative of anaerobic respiration have not been directly compared to cancerous cells, even though there have been studies that have examined increased reactive oxygen species in endothelial cells as a result of

hyperglycemic conditions.[18, 19] The lactate production from the endothelial cells in these reported studies was always significantly higher in the high glucose environments than the production in normal glucose conditions. The HeLa cells produced higher lactate levels than the endothelial cells. However, the lactate production was similar whether the HeLa cells were exposed to normal or high glucose levels. These findings are significant in multiple regards. First, it suggests that the glucose metabolism of cancerous cells is independent of the extracellular glucose surroundings. The cancerous cells constantly maintain an elevated glycolytic flux while healthy cells alter the metabolism based on available glucose. Second, the findings demonstrate that the healthy endothelial cells produce a higher level of lactate following exposure to high glucose conditions. This is also observed without a significantly increased glucose uptake. This increased lactate production, while not as high as the HeLa cell production, does appear to indicate that the endothelial cells perform elevated rates of glycolysis in high glucose conditions that are similar to the cancer cell line.

There were other similarities between the two cell types. One of those similarities was observed when the protein responsible for transporting the lactate from the cell, MCT1, was inhibited by ACCA. The lactate production and glucose uptake were measured. It appeared that lower concentrations of ACCA resulted in elevated lactate productions caused by increased glucose uptake. The highest ACCA concentrations measured also had similar effects on both cell lines. The lactate produced in the samples with the highest ACCA concentration was lower than the amount generated from the cells with no ACCA. The glucose uptake was increased in the bPAECs incubated with the highest ACCA concentrations, most likely due to the cell's inability to release the produced lactic acid and take in extracellular pyruvate or lactate for energy production. These studies not only identify comparisons between the two cell types in

terms of how the lactate release is affected following MCT inhibition, but also demonstrate how the glucose uptake can be altered by inhibiting the release of a metabolic byproduct.

Another metabolic byproduct that appears to have a significant role in glucose uptake and metabolism is pyruvate. It is understood that pyruvate is the end product of glycolysis and the initial reactant of oxidative phosphorylation. There are also findings that exogenous pyruvate regulates oxidative stress,[20] but the mechanism is not entirely understood. The findings observed in these studies suggest that pyruvate can regulate the glucose transport into both the healthy endothelial cells and the cancerous HeLa cells. There was no statistical difference in the amount of lactate generated in either the low or high glucose samples of the HeLa cells, thereby suggesting that the cancer cells have unaltered metabolic rates. The endothelial cells again had a significantly higher lactate release from the high glucose samples, but no change was observed regardless of whether or not pyruvate was present.

It is not until the glucose studies were evaluated that the metabolic influences by pyruvate is explained. There was more glucose taken in by the HeLa cell samples that did not contain pyruvate compared to those that did have it. With the endothelial cells, only the high glucose samples exhibited an effect on glucose transport from the lack of pyruvate. The glucose uptake was nearly that of the HeLa cells. Summarily, regarding the pyruvate studies, it was suggested that cancerous cells do rely on the pyruvate for their energy production, as they produced the same lactate levels but consumed different quantities of glucose. This can be significant as cancer cells can ‘feed’ off of the metabolites released from surrounding cells. The endothelial cells do not appear to be affected by pyruvate at normal glucose levels. However, as the glucose concentration increased, the cells appeared to rely more on the exogenous pyruvate for energy, as

more glucose was taken in by the cell to produce the same amount of lactate in the private free samples that was produced in the samples containing pyruvate.

5.1.4 Overall findings

Overall, the research presented here suggests multiple significant findings regarding cellular metabolism under varying conditions found in diabetes and cancer. First, physiologically relevant levels of metal-activated C-peptide directly stimulates glucose uptake into the endothelium. At the same time, the same metal-activated C-peptide indirectly stimulates endothelial NO production via increased ATP release from RBCs. These findings can prove to be significant in the treatment of type 1 diabetes.

The same metal-activated C-peptide effects on RBCs incubated in hyperglycemic conditions similar to those found in type 2 diabetes can be influenced by the anti-diabetic drug metformin. Metformin resulted in increased C-peptide interaction with the RBC, causing increased glucose uptake and subsequent lactate release. These studies do suggest a possible mechanism of action for metformin while identifying a cause for the observed side effect of lactic acidosis. Acting independently on the endothelial cells in the presence of metal-activated C-peptide, metformin results in increased rates of both glucose uptake and lactate release. This increase of glucose uptake and lactate release resulted in the lowering of the intracellular pH of the endothelial cells, likely due to the release of the byproduct through the MCT1.

The last set of studies identified many similarities that healthy endothelial cells share with cancerous HeLa cells in certain conditions. Both cell types were affected similarly when the MCTs were inhibited by ACCA. The hyperglycemic conditions combined with the pyruvate

studies resulted in findings that suggest the priority that both types of cells place on consuming the pyruvate available to them rather than take in and metabolize glucose. Finally, the lactate released from the healthy endothelial cells in hyperglycemic conditions increased to values similar to those observed in the cancerous cells, suggesting that the rate of anaerobic respiration increases in conditions with elevated glucose levels.

5.2 Future directions

5.2.1 C-peptide studies

Earlier metal-activated C-peptide studies demonstrated that there was increased glucose uptake into cultured endothelial cells following the C-peptide administration. The lactate studies did not suggest an increase in lactate production from the endothelial cells with metal-activated C-peptide. Therefore, the ultimate 'fate' of the glucose brought into the cell remains unknown. Multiple other studies have identified an increase in cellular ROS caused by hyperglycemia by utilizing intracellular fluorescent probes specific for measuring free radicals, specifically 5(6)-chloromethyl-2',7'-dichlorodihydrofluorescein diacetate (CM-H_2DCFDA) or dihydroethidium (DHE).[18, 19, 21, 22] Preliminary experiments utilizing another intracellular ROS probe, Mito-HE (MitoSOX red), have provided data demonstrating that endothelial cells incubated with metal-activated C-peptide might have a slightly higher fluorescence intensity compared to the cells without C-peptide. This potentially suggests that C-peptide stimulates increased oxidative phosphorylation. Further evaluation of the ROS produced by C-peptide administration can be

explored by optimizing the technique and applying different probes, as the fluorescence intensities from the Mito-HE appeared relatively low.

Another potential fate of the increased glucose is the conversion into glycogen. As C-peptide is released with insulin, and insulin stimulates glycogen storage in multiple cell types, C-peptide could have a similar function in the endothelium. Assays determining the intracellular glycogen content have been applied to endothelial cells before following insulin administration.[9] Similar experiments that apply C-peptide to endothelial cells can be performed to determine whether the increased intracellular glucose observed in the radiolabeled transport studies is stored in the cell as glycogen.

5.2.2 Metformin studies

Many of the future metformin studies will likely focus on the mechanism behind the drug's interaction with the endothelial cells, and how it causes the increased glucose uptake and lactate release. The studies discussed earlier have identified a mechanism by which metformin interacts with the RBC indirectly through C-peptide. However, only the effect metformin had on the endothelial cells was explored. It is possible that metformin may act on some metabolic regulator other than AMPK as the findings demonstrating that metformin and AICAR, two proposed activators of AMPK, caused such different metabolic changes when administered to the endothelial cells. The increased AMPK activity monitored by previous experiments could potentially be affected by downstream signaling.[23, 24]

The suggestion that metformin does not act by directly activating AMPK arises from some studies that examine metformin as a potential cancer therapeutic agent.[25] Metformin was

shown to act independently of AMPK through activation of downstream enzymes of the AMPK pathway.[26] There were also characteristic effects observed following metformin treatment even in the absence of AMPK and LKB1, which is an upstream kinase activator of AMPK.[27] Additionally, preliminary studies performed that examined the metabolism of HeLa cells treated with metformin resulted in unexplained findings. HeLa cells lack the LKB1/AMPK pathway, therefore activators of AMPK have little effect on the cellular proliferation. However, the preliminary studies identified an increased lactate production and glucose uptake from the HeLa cells after an 18 hour incubation with varying concentrations of metformin (Figure 5.1). Additional studies, possibly focusing on key parts further down the AMPK signaling pathway, should be done to identify a potentially significant finding on how metformin acts metabolically on cells.

Additional studies regarding metformin can focus on other intracellular changes that occur in the endothelium following treatment. The presented studies identified an intracellular pH change following metformin administration. However, additional cell changes or damages were not measured. Future studies can be performed that look specifically at any damage that is done to the endothelial cells' DNA following prolonged exposure to metformin. This damage can be observed through established markers such as 8-hydroxydeoxyguanosine (8-OHdG)[28] or using a gel-electrophoresis technique.[29]

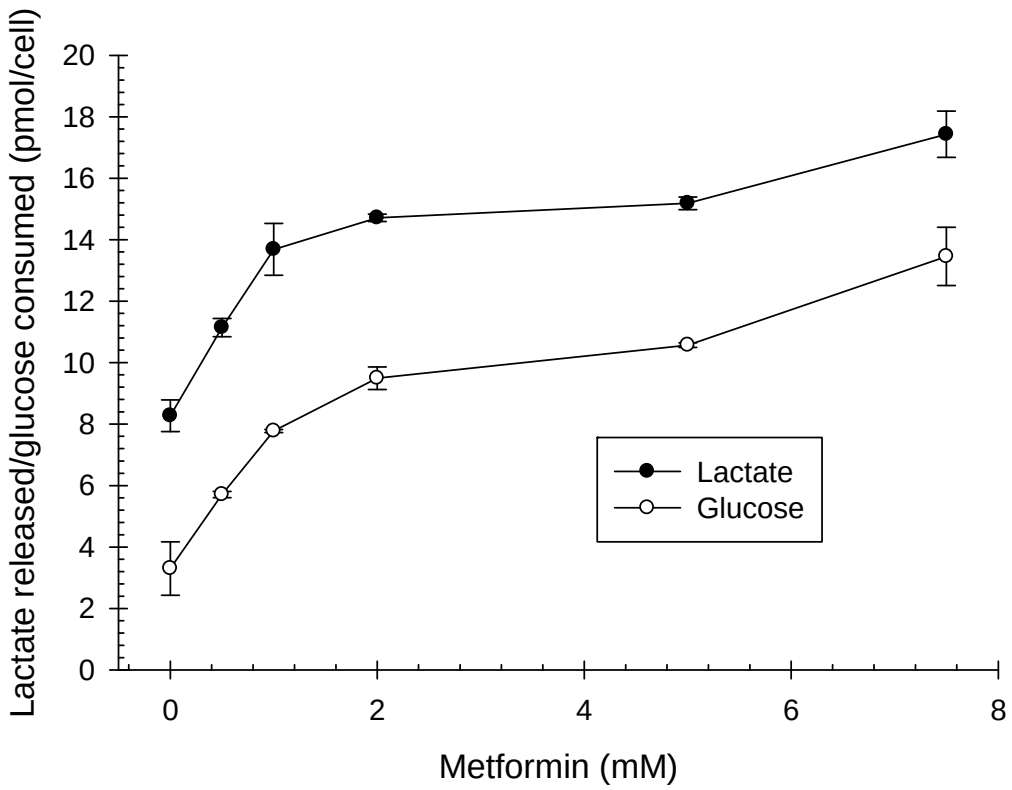

Figure 5.1 – Data illustrating the effect that metformin has on cultured HeLa cells. Following a 24 hour incubation in high glucose DMEM containing various concentrations of metformin, the supernatant was removed and measured for lactate (black) and glucose (white) content. The points represent the average of n = 2 for each concentration of metformin. The error bars represent the standard deviation of those two points.

5.2.3 Hyperglycemia studies

Further studies focusing on the hyperglycemia altered metabolism will likely focus on how the elevated glucose levels cause cancer-like metabolic alterations in normal, healthy cells. One of the initial studies could be first comparing one healthy cell type to a cancerous version of the same cell. There was a direct comparison between the endothelial cells and the HeLa cells in the presented studies. These cells are similar, however it would be more beneficial to compare healthy liver cells to cancerous liver cells, cells from a healthy pancreas and cells from a cancerous pancreas, etc. The changes in metabolism caused by the altered glucose concentrations are still significant and relevant findings. However, concluding that the HeLa cells produce more lactate than the endothelial cells is not as significant as comparing cancerous cells to healthy cells.

It would be interesting to observe whether the increased lactate produced in hyperglycemic environments can damage the cellular DNA. Previous studies have indicated hyperglycemia as a cause for DNA damage due to the increased superoxides that are produced from elevated rates of oxidative phosphorylation.[30, 31] Studies could be performed that reduce the mitochondrial activity by inhibiting certain parts of the aerobic metabolic pathways, resulting in elevated lactate levels. The DNA damage, if any, could be attributed in most part to the increased glucose levels or the elevated lactate present.

Another potential study could utilize a similar microfluidic device used in previous experiments (Figure 2.7). The goal would be to simulate an entire blood vessel or capillary that is part of, or supplies a specific organ tissue. There could be endothelial cells coating the inside of the channel as done in earlier studies in the Spence group.[32] Blood could then be introduced

and flowed through the channels over the endothelial cells. There would still be the polycarbonate membrane present dividing the channel from the cells. The only difference would be that tissue cells from an organ would be cultured on top of the membrane. A potential diagram of the device is illustrated in Figure 5.2.

Utilizing a device such as this would allow for the administration of certain molecules, drugs, etc. that are thought to have a mechanistic action(s) in the vasculature. Different glucose levels could also be administered. RBCs treated with C-peptide could be pumped through the channel with this setup, thereby allowing for the C-peptide to interact with the endothelium lining the inner walls. The cultured tissue cells on the outer surface can be exposed to similar glucose concentrations and any drugs/molecules present in the channels. They would also be exposed to the lactate and any other metabolic byproduct released by the RBCs and/or the endothelial cells in normal or high glucose conditions. They could even be exposed to metformin and metal-activated C-peptide. The tissue cells can then be measured for DNA damage, or even removed and cultured further using regular tissue culture flasks to observe any growth alterations. Most cancers are believed to be initiated through damaged DNA that results in uncontrolled growth. This device potentially allows for the identification of certain sources of DNA damage caused by other cells that are themselves exposed to specific conditions.

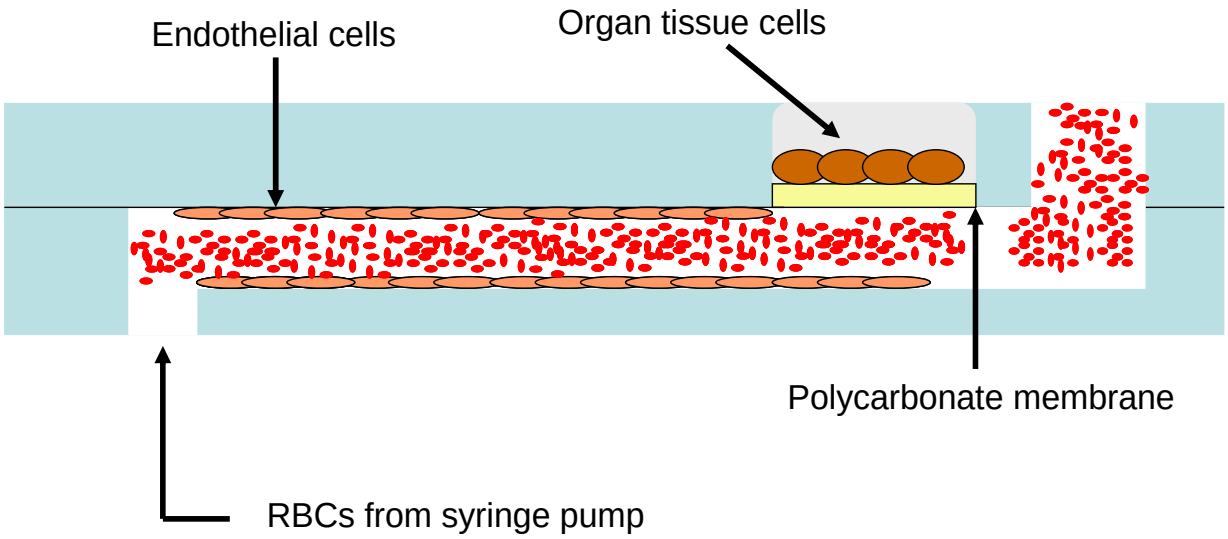

Figure 5.2 – Cross section of the proposed microfluidic device proposed to examine the effects that hyperglycemia and metabolic byproducts can have on the DNA integrity of organ tissue cells. Endothelial cells can be cultured within the channel where RBCs can flow through, thereby simulating a typical blood vessel/artery/capillary. Tissue cells from any specific organ can be cultured on top of the porous polycarbonate membrane, allowing for the interaction with any molecule/byproduct that is released by the endothelial cells or the RBCs in the channel. The tissue cells can be removed and either measured or cultured further.

REFERENCES

REFERENCES

1. Johansson, B. L.; Linde, B.; Wahren, J., Effects of C-peptide on blood flow, capillary diffusion capacity and glucose utilization in the exercising forearm of type 1 (insulin-dependent) diabetic patients. *Diabetologia* **1992,** 35, (12), 1151-8.

2. Sima, A. A. F.; Zhang, W.; Sugimoto, K.; Henry, D.; Li, Z.; Wahren, J.; Grunberger, G., C-peptide prevents and improves chronic Type I diabetic polyneuropathy in the BB/Wor rat. *Diabetologia* **2001,** 44, (7), 889-897.

3. Li, L.; Oshida, Y.; Kusunoki, M.; Yamanouchi, K.; Johansson, B. L.; Wahren, J.; Sato, Y., Rat C peptide I and II stimulate glucose utilization in STZ-induced diabetic rats. *Diabetologia* **1999,** 42, (8), 958-64.

4. Wallerath, T.; Kunt, T.; Forst, T.; Closs, E. I.; Lehmann, R.; Flohr, T.; Gabriel, M.; Schafer, D.; Gopfert, A.; Pfutzner, A.; Beyer, J.; Forstermann, U., Stimulation of endothelial nitric oxide synthase by proinsulin C-peptide. *Nitric Oxide* **2003,** 9, (2), 95-102.

5. Kitamura, T.; Kimura, K.; Makondo, K.; Furuya, D. T.; Suzuki, M.; Yoshida, T.; Saito, M., Proinsulin C-peptide increases nitric oxide production by enhancing mitogen-activated protein-kinase-dependent transcription of endothelial nitric oxide synthase in aortic endothelial cells of Wistar rats. *Diabetologia* **2003,** 46, (12), 1698-705.

6. Medawala, W.; McCahill, P.; Giebink, A.; Meyer, J.; Ku, C. J.; Spence, D. M., A Molecular Level Understanding of Zinc Activation of C-peptide and its Effects on Cellular Communication in the Bloodstream. *Rev. Diabet. Stud.* **2009,** 6, (3), 148-58.

7. Meyer, J. A.; Froelich, J. M.; Reid, G. E.; Karunarathne, W. K.; Spence, D. M., Metal-activated C-peptide facilitates glucose clearance and the release of a nitric oxide stimulus via the GLUT1 transporter. *Diabetologia* **2008,** 51, (1), 175-82.

8. Meyer, J. A.; Subasinghe, W.; Sima, A. A.; Keltner, Z.; Reid, G. E.; Daleke, D.; Spence, D. M., Zinc-activated C-peptide resistance to the type 2 diabetic erythrocyte is associated with hyperglycemia-induced phosphatidylserine externalization and reversed by metformin. *Mol. Biosyst.* **2009,** 5, (10), 1157-62.

9. Artwohl, M.; Brunmair, B.; Fuernsinn, C.; Hoelzenbein, T.; Rainer, G.; Freudenthaler, A.; Porod, E. M.; Huttary, N.; Baumgartner-Parzer, S. M., Insulin does not regulate glucose transport and metabolism in human endothelium. *Eur. J. Clin. Invest.* **2007,** 37, (8), 643-650.

10. Runge, S.; Mayerle, J.; Warnke, C.; Robinson, D.; Roser, M.; Felix, S. B.; Friesecke, S., Metformin-associated lactic acidosis in patients with renal impairment solely due to drug accumulation? *Diabetes Obes. Metab.* **2008,** 10, (1), 91-93.

11. Davis, T. M.; Jackson, D.; Davis, W. A.; Bruce, D. G.; Chubb, P., The relationship between metformin therapy and the fasting plasma lactate in type 2 diabetes: The Fremantle Diabetes Study. *Br. J. Clin. Pharmacol.* **2001,** 52, (2), 137-44.

12. Sasson, S.; Gorowits, N.; Joost, H. G.; King, G. L.; Cerasi, E.; Kaiser, N., Regulation by metformin of the hexose transport system in vascular endothelial and smooth muscle cells. *Br. J. Pharmacol.* **1996,** 117, (6), 1318-24.

13. Dagher, Z.; Ruderman, N.; Tornheim, K.; Ido, Y., The effect of AMP-activated protein kinase and its activator AICAR on the metabolism of human umbilical vein endothelial cells. *Biochem. Biophys. Res. Commun.* **1999,** 265, (1), 112-5.

14. Warburg, O.; Posener, K.; Negelein, E., Metabolism of carcinoma cells. *Biochemische Zeitschrift* **1924,** 152, 309-44.

15. Ristow, M., Oxidative metabolism in cancer growth. *Curr. Opin. Clin. Nutr. Metab.* **2006,** 9, (4), 339-345.

16. Schulz, T. J.; Thierbach, R.; Voigt, A.; Drewes, G.; Mietzner, B.; Steinberg, P.; Pfeiffer, A. F.; Ristow, M., Induction of oxidative metabolism by mitochondrial frataxin inhibits cancer growth: Otto Warburg revisited. *J. Biol. Chem.* **2006,** 281, (2), 977-81.

17. Shaw, R. J., Glucose metabolism and cancer. *Curr. Opin. Cell Biol.* **2006,** 18, (6), 598-608.

18. Ouedraogo, R.; Wu, X.; Xu, S.-Q.; Fuchsel, L.; Motoshima, H.; Mahadev, K.; Hough, K.; Scalia, R.; Goldstein, B. J., Adiponectin suppression of high-glucose-induced reactive oxygen species in vascular endothelial cells. Evidence for involvement of a cAMP signaling pathway. *Diabetes* **2006,** 55, (6), 1840-1846.

19. Quijano, C.; Castro, L.; Peluffo, G.; Valez, V.; Radi, R., Enhanced mitochondrial superoxide in hyperglycemic endothelial cells: direct measurements and formation of hydrogen peroxide and peroxynitrite. *Am. J. Physiol. Heart Circ. Physiol.* **2007,** 293, (6), H3404-14.

20. Chung, S. J.; Lee, S. H.; Lee, Y. J.; Park, H. S.; Bunger, R.; Kang, Y. H., Pyruvate protection against endothelial cytotoxicity induced by blockade of glucose uptake. *J. Biochem. Mol. Biol.* **2004,** 37, (2), 239-45.

21. Ouslimani, N.; Peynet, J.; Bonnefont-Rousselot, D.; Therond, P.; Legrand, A.; Beaudeux, J. L., Metformin decreases intracellular production of reactive oxygen species in aortic endothelial cells. *Metabolism* **2005,** 54, (6), 829-34.

22. Fernandes, R.; Hosoya, K.; Pereira, P., Reactive oxygen species downregulate glucose transport system in retinal endothelial cells. *Am. J. Physiol. Cell Physiol.* **2011,** 300, (4), C927-36.

23. Zou, M. H.; Hou, X. Y.; Shi, C. M.; Kirkpatick, S.; Liu, F.; Goldman, M. H.; Cohen, R. A., Activation of 5'-AMP-activated kinase is mediated through c-Src and phosphoinositide 3-kinase activity during hypoxia-reoxygenation of bovine aortic endothelial cells. Role of peroxynitrite. *J. Biol. Chem.* **2003,** 278, (36), 34003-10.

24. Zou, M. H.; Kirkpatrick, S. S.; Davis, B. J.; Nelson, J. S.; Wiles, W. G. t.; Schlattner, U.; Neumann, D.; Brownlee, M.; Freeman, M. B.; Goldman, M. H., Activation of the AMP-activated protein kinase by the anti-diabetic drug metformin in vivo. Role of mitochondrial reactive nitrogen species. *J. Biol. Chem.* **2004,** 279, (42), 43940-51.

25. Dowling, R. J.; Goodwin, P. J.; Stambolic, V., Understanding the benefit of metformin use in cancer treatment. *BMC Med* **2011,** 9, 33.

26. Kalender, A.; Selvaraj, A.; Kim, S. Y.; Gulati, P.; Brule, S.; Viollet, B.; Kemp, B. E.; Bardeesy, N.; Dennis, P.; Schlager, J. J.; Marette, A.; Kozma, S. C.; Thomas, G., Metformin, independent of AMPK, inhibits mTORC1 in a rag GTPase-dependent manner. *Cell Metab.* **2010,** 11, (5), 390-401.

27. Foretz, M.; Hebrard, S.; Leclerc, J.; Zarrinpashneh, E.; Soty, M.; Mithieux, G.; Sakamoto, K.; Andreelli, F.; Viollet, B., Metformin inhibits hepatic gluconeogenesis in mice independently of the LKB1/AMPK pathway via a decrease in hepatic energy state. *J. Clin. Invest.* **2010,** 120, (7), 2355-69.

28. Wu, L. L.; Chiou, C. C.; Chang, P. Y.; Wu, J. T., Urinary 8-OHdG: a marker of oxidative stress to DNA and a risk factor for cancer, atherosclerosis and diabetics. *Clin. Chim. Acta* **2004,** 339, (1-2), 1-9.

29. Olive, P. L.; Banath, J. P., The comet assay: a method to measure DNA damage in individual cells. *Nat. Protoc.* **2006,** 1, (1), 23-9.

30. Hasty, P.; Campisi, J.; Hoeijmakers, J.; van Steeg, H.; Vijg, J., Aging and genome maintenance: lessons from the mouse? *Science (New York, N.Y.)* **2003,** 299, (5611), 1355-9.

31. Yang, S.; Chintapalli, J.; Sodagum, L.; Baskin, S.; Malhotra, A.; Reiss, K.; Meggs, L. G., Activated IGF-1R inhibits hyperglycemia-induced DNA damage and promotes DNA repair by homologous recombination. *Am. J. Physiol. Renal Physiol.* **2005,** 289, (5), F1144-52.

32. Ku, C. J.; D'Amico Oblak, T.; Spence, D. M., Interactions between multiple cell types in parallel microfluidic channels: monitoring platelet adhesion to an endothelium in the presence of an anti-adhesion drug. *Anal. Chem.* **2008,** 80, (19), 7543-8.